Mechanisms and biogeochemical implications of the mid-Cretaceous global organic carbon burial events

Mechanisms and biogeochemical implications of the mid-Cretaceous global organic carbon burial events

Mechanismen en biogeochemische gevolgen van wereldwijde organische koolstof begravings episodes tijdens het midden Krijt

(Met een samenvatting in het Nederlands)

Proefschrift ter verkrijging van de graad van doctor
aan de Universiteit Utrecht
op gezag van Rector Magnificus, Prof. Dr. W. H. Gispen
ingevolge het besluit van het College voor Promoties
in het openbaar te verdedigen
op maandag 17 september des ochtends te 10.30 uur

Door
Marcel Martinus Maria Kuijpers
geboren op 6 juni 1970, te Hunsel

Aan mijn ouders

Contents

Chapter 1

Introduction and summary

Marcel M. M. Kuypers

1.1 The mid-Cretaceous oceanic anoxic events

The interval spanning the Barremian to Turonian (~125-88 Ma) is known as the mid-Cretaceous 'greenhouse' world [*Barron*, 1983]. As a possible analogue for future climates influenced by anthropogenically enhanced carbon dioxide emissions, the 'greenhouse' climate of the mid-Cretaceous received close attention in the last decades. Both marine and terrestrial proxies indicate that the mid-Cretaceous climate was significantly warmer with a smaller equator-to-pole temperature gradient than the modern climate (Fig. 1) [*Barron*, 1983; *Huber et al.*, 1995].
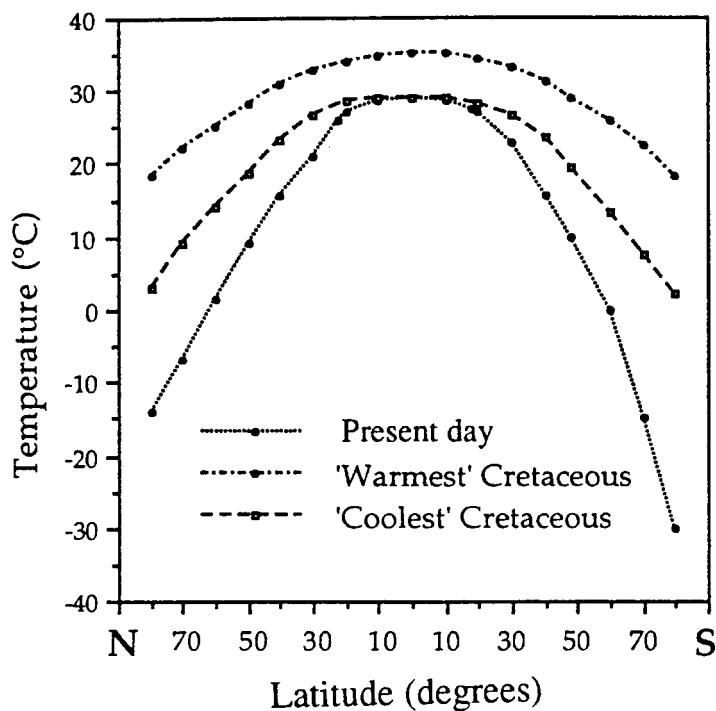
Figure 1. Estimates of latitudinal maximum and minimum temperature gradients for the mid-Cretaceous plotted for comparison against present day mean annual surface temperature [from *Sellwood et al.*, 1994].

It has been suggested that this resulted from an anomalous amount of oceanic volcanism [*Arthur et al.*, 1985; *Larson*, 1991], leading to 3 to 12 times higher atmospheric levels of carbon dioxide during the Cretaceous than at present (Fig. 2) [*Berner*, 1992].
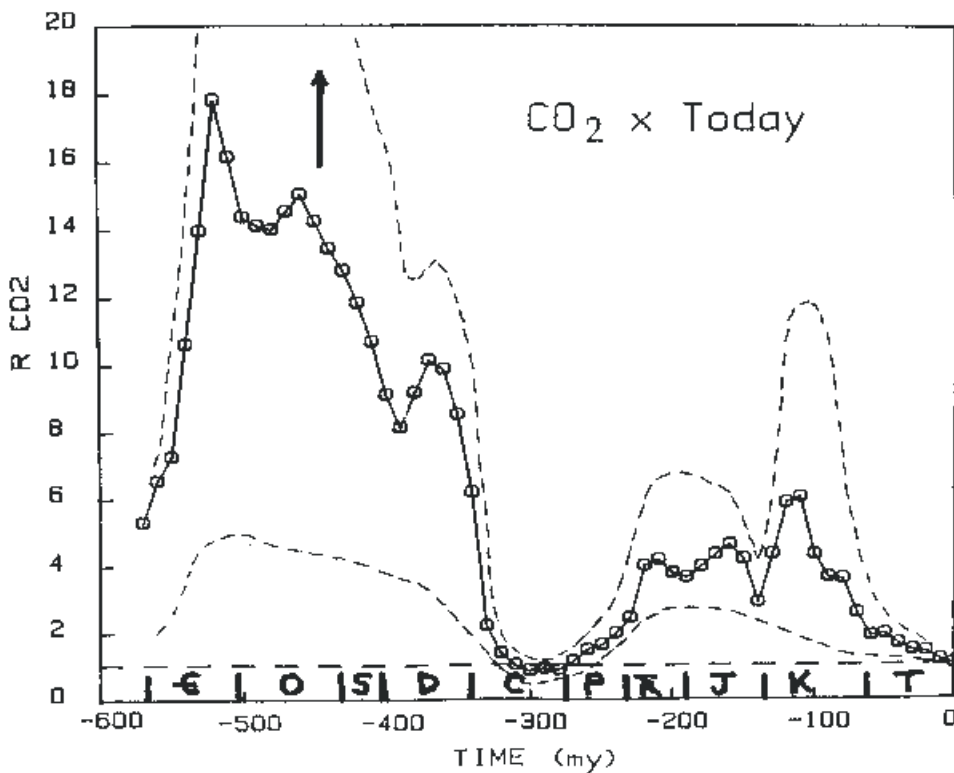
Figure 2. Best estimates of RCO_2 (i.e. the carbon dioxide concentration at a given time normalised to the present day value) vesus time. The arrow denotes that early Paleozoic RCO_2 values may be higher. The dashed lines represent a rough estimate of errors based on sensitivity studies [from *Berner*, 1991].

Burial of organic matter (OM) in the marine realm could have provided a feedback mechanism to the enhanced volcanic outgassing of the mid-Cretaceous. As a result of carbon dioxide exchange between the atmosphere and the ocean, uptake of dissolved inorganic carbon (DIC) during photosynthesis and subsequent export of phytoplanktonic biomass to deeper water and underlying sediment act as a biological carbon dioxide pump. Organic matter (OM) degradation (i.e. respiration) and ocean circulation will eventually return most of this carbon dioxide again to the atmosphere. However, a small amount of OM escapes degradation and is buried in the sediment. This burial of sedimentary OM largely controls the carbon dioxide content of the atmosphere on geological time scales [*Berner*, 1991; *Berner*, 1992].

Oceanic anoxic events (OAEs), episodes of globally enhanced organic carbon (OC) burial rates, may have reduced CO_2 concentrations of the mid-Cretaceous 'greenhouse' atmosphere especially effectively by sequestering large amounts of carbon in the subsurface. Originally the term OAE was introduced to describe the episodic expansion and intensification of the Oxygen Minimum Zone (OMZ), which was proposed to explain the seemingly global distribution of laminated sediments rich (> 1%) in organic carbon (OC) (black shales) in pelagic sequences of Aptian-Albian and Cenomanian/Turonian (C/T) age [*Schlanger and Jenkyns*, 1976]. Since then several other time-bounded envelopes of particularly, perhaps more globally, widespread black shale deposition in marine environments have been identified [*Arthur et al.*, 1987] and a total of five OAEs has been

recognised for the mid-Cretaceous (Fig. 3). In most cases the OAE black shales are devoid of or strongly impoverished in benthic faunas indicating that these sediments were deposited under

Age (My)	Stage	Planktic foraminiferal zonation	Oceanic anoxic event (OAE)
	Turonian		
93.5	Cenomanian	*W. archaeocretacea*	**OAE2 (Bonarelli)***
		R. cushmani	
		R. reicheli	
		R. brotzeni	
98.9	Albian	*R. appenninica*	**OAE1d (Breistroffer)**
		R. ticinensis	
		B. breggiensis	**OAE1c**
		T. primula	
112.2	Aptian	*H. planispira*	**OAE1b (Paquier)***
		T. bejaouaensis	
		H. trocoidea	
		G. algerianus	
		G. ferreolensis	
		L. cabri	**OAE1a (Selli)**
121.0	Barremian	*G. blowi*	

Figure 3. Chrono- and biostratigraphic position of OAEs [modified after *Erbacher et al.*, 1999]. Asterisk (*) denotes OAEs investigated in this thesis.

oxygen-deficient bottom-water conditions [*Summerhayes*, 1987]. The most intensely studied OAEs occurred near the Barremian/Aptian (OAE1a) and Cenomanian/Turonian (C/T OAE or OAE2) transition (Fig. 3). Both OAEs are accompanied by a significant increase in $^{13}C/^{12}C$ ratios for marine carbonates (up to 2.5‰) and organic matter (upto 6‰). This positive excursion in $\delta^{13}C$ values likely resulted from preferential removal of ^{12}C by the globally enhanced burial of ^{13}C

depleted OC into black shales [*Arthur et al.*, 1988]. Positive shifts in $\delta^{13}C$ values of marine carbonate, albeit significantly smaller, may also have been associated with other mid-Cretaceous OAEs [*Erbacher and Thurow*, 1997].

The OAE that occurred near the C/T boundary is the most extensive and has been considered as the type example of the the mid-Cretaceous OAEs [*Wignall*, 1994]. The C/T OAE was accompanied by a marine extinction event that especially affected certain reef building molluscs [i.e., rudists, *Johnson et al.*, 1996; *Philip and Airaud-Crumiere*, 1991], and planktonic foraminifera [*Jarvis et al.*, 1988]. In addition, evidence of a significant decrease in atmospheric CO_2 concentrations during the C/T OAE was provided by the drop in the isotope effect associated with carbon fixation (ε_p) by phytoplankton in the Cretaceous Western Interior Seaway (Fig. 4) of the United States [*Freeman and Hayes*, 1992]. This decline is also documented indirectly by oxygen isotope data, which indicate an 8-13°C cooling at high latitudes during the early Turonian [*Arthur et al.*, 1988; *Jenkyns et al.*, 1994]. Additional indications of global cooling are provided by micropaleontological data, showing an incursion of boreal fauna into low latitude seas [*Kuhnt et al.*, 1986].

1.2 Models for black shale deposition during the mid-Cretaceous OAEs

Two fundamentally different models have been used to explain the enhanced OM burial rate during the OAEs. The *preservational* model is based on decreased OM remineralisation resulting from a decreased oxygen flux. In the modern world's oceans deep ocean circulation is driven by the convective sinking of cold, dense, well-oxygenated water in polar regions (thermohaline circulation). Although enhanced oxygen consumption by OM decomposition and slow downward mixing and diffusion of dissolved oxygen from the surface waters can lead to very oxygen-deficient mid waters (i.e. the OMZs), true anoxic conditions are generally restricted to the sediments and basins isolated from oxygenated deep-sea circulation. However, in the mid-Cretaceous, anoxic water column conditions may have developed more readily as minimal equator-to-pole thermal gradients should have resulted in a decreased formation of oxygenated bottom-waters [*Barron*, 1983]. In addition, a halothermal mode of circulation with the formation of oxygen-poor, warm deep-water in subtropical, net evaporative regions instead of thermohaline circulation has been suggested for the mid-Cretaceous [*Chamberlin*, 1906; *Brass et al.*, 1982; *Hay*, 1988]. This could have resulted in basin-wide oxygen deficiency with the most intense dysoxia/anoxia occurring in the deepest parts of tectonically isolated basins such as the Cretaceous North and South Atlantic (Fig. 4) [*Zimmerman et al.*, 1987; *De Graciansky et al.*, 1984]. The reoccurrence of thinly laminated OM–rich sediments devoid of traces of benthic activity indicates that middle Cretaceous bottom-waters were indeed periodically anoxic [*Summerhayes*, 1987; *Bralower and Thierstein*, 1987]. Sedimentary derivatives (molecular fossils) of a pigment indicative of anoxygenic photosynthetic bacteria recovered from abyssal and shelf sites indicate that anoxic conditions extended even into the photic zone of the southern proto-North Atlantic during the C/T OAE [*Sinninghe Damsté and Köster*, 1998a]. Extensive denitrification in largely anoxic or suboxic mid and deep waters may have led to N_2-fixing cyanobacteria periodically dominating phytoplankton communities during the early to middle Cretaceous [*Rau et al.*, 1987].

The *productivity* model is based on a greatly increased primary productivity that overwhelmed the oxic OM remineralisation potential of the water column. Primary productivity in the modern marine environment is largely controlled by the input of biolimiting nutrients from deeper water into the surface waters. Either enhanced vertical circulation (upwelling), or an enhanced supply of biolimiting nutrients from the terrestrial realm [*Erbacher et al.*, 1996] or from enhanced volcanism [*Sinton and Duncan*, 1997], could have led to increased primary productivity and thus to an expansion and intensification of the OMZs during the OAEs [*Schlanger and Jenkyns*, 1976]. The deposition of OM-rich sediments would have largely been confined to places where the OMZ impinged on the continental margin or other elevated portions of the sea floor, as the deepest places of the basin may have remained oxic. This model has especially been used to explain the OM-rich deposits in the Cretaceous Pacific Ocean [*Schlanger and Jenkyns*, 1976; *Thiede and van Andel*, 1977].

1.3 Biomarkers as tracers of environmental changes during the mid-Cretaceous OAEs

Unlike certain dinoflagellates, diatoms and calcareous algae, many other common pelagic algae and bacteria (e.g. cyanobacteria) do not leave behind microscopically identifiable fossilised remains in the sedimentary record. Instead, taxon specific biochemicals (i.e. biomarkers), such as membrane lipids and pigments or molecular fossils of these compounds formed upon diagenesis, can provide information about their relative abundance in ancient marine environments. Hence these biomarkers can reveal valuable insight concerning the environmental conditions during sediment deposition [*Peters and Moldowan*, 1993; *De Leeuw et al.*, 1995].

For example, Sinninghe Damsté and Köster [*Sinninghe Damsté and Köster*, 1998a] recovered molecular fossils (i.e. sulfur (S)-bound isorenieratane) of a pigment indicative of anoxygenic photosynthetic bacteria from C/T OAE abyssal and shelf sediments of the southern part of the North Atlantic Ocean. S-bound isorenieratane is formed in anoxic sediments upon sulfurisation of the polyunsaturated pigment isorenieratene in the presence of reduced inorganic S species [*Sinninghe Damsté et al.*, 1993; *Koopmans et al.*, 1996]. The pigment isorenieratene is exclusively produced by the brown strains of green sulfur bacteria [*Imhoff*, 1995], which require sunlight penetrating the euxinic part (i.e. containing reduced inorganic sulfur species) of an aquatic environment (Fig. 5) [*van Gemerden and Mas*, 1995]. Currently, these phototrophic bacteria are restricted to a few isolated euxinic basins in the marine realm such as the Black Sea. In such environments they thrive near the hydrogen sulfide/oxygen interface (i.e. chemocline) at depths of up to 150 m, where light levels are less than 1% of surface irradiance, and utilise reduced inorganic sulfur species as electron donors during photosynthesis [*Repeta et al.*, 1989; *van Gemerden and Mas*, 1995]. Therefore, the occurrence of S-bound isorenieratane in the C/T black shales indicates that anoxic conditions periodically reached up into the photic zone of the southern proto-North Atlantic during the C/T OAE [*Sinninghe Damsté and Köster*, 1998a].

The stable carbon isotopic composition of biomarkers can provide additional information concerning the paleoenvironment [e.g. *Kohnen et al.*, 1992; *Hayes et al.*, 1987; *Schouten et al.*, 2000; *Hayes et al.*, 1989; *Freeman and Hayes*, 1992; *Jasper et al.*, 1994; *Schoell et al.*, 1994; *Pagani et al.*, 1999]. The isotope effect associated with carbon fixation (ε_p) by primary producers

causes OC to be depleted in ^{13}C relative to the inorganic carbon source (i.e. DIC/atmospheric CO_2). $\delta^{13}C$ values of fresh OM of primary producers are determined by the stable carbon isotopic composition of the carbon source and ε_p. Heterotrophy, selective preservation, and diagenetic alteration can severely affect the stable carbon isotopic signature of bulk sedimentary OC, while the $\delta^{13}C$ values of biomarkers are largely unaffected [*Grice et al.*, 1998; *Hayes et al.*, 1989; *Freeman and Hayes*, 1992; *Sinninghe Damsté et al.*, 1998]. Therefore, compound-specific stable carbon isotope analysis is particularly useful in stable carbon isotope stratigraphy in settings where carbonate is absent or diagenetically affected. For example, the sharp increase in ^{13}C/^{12}C ratios that is observed worldwide for marine carbonates and OM at the C/T boundary [*Scholle and Arthur*, 1980; *Arthur et al.*, 1988] has been shown to be a powerful tool in high resolution correlation [*Gale et al.*, 1993; *Hasegawa*, 1997]. This positive excursion in $\delta^{13}C$ values reflects a change in the global atmospheric-oceanic pool of inorganic carbon resulting from a global increase in the burial rate of ^{13}C-depleted OC during the C/T OAE [*Arthur et al.*, 1988]. The use of molecular fossils that are specific for primary producers instead of bulk OM for stable carbon isotope stratigraphy greatly reduces the effect of heterotrophy, preservation, and diagenetic alteration on the carbon isotopic signature of OC [*Grice et al.*, 1998; *Hayes et al.*, 1989; *Freeman and Hayes*, 1992; *Sinninghe Damsté et al.*, 1998].
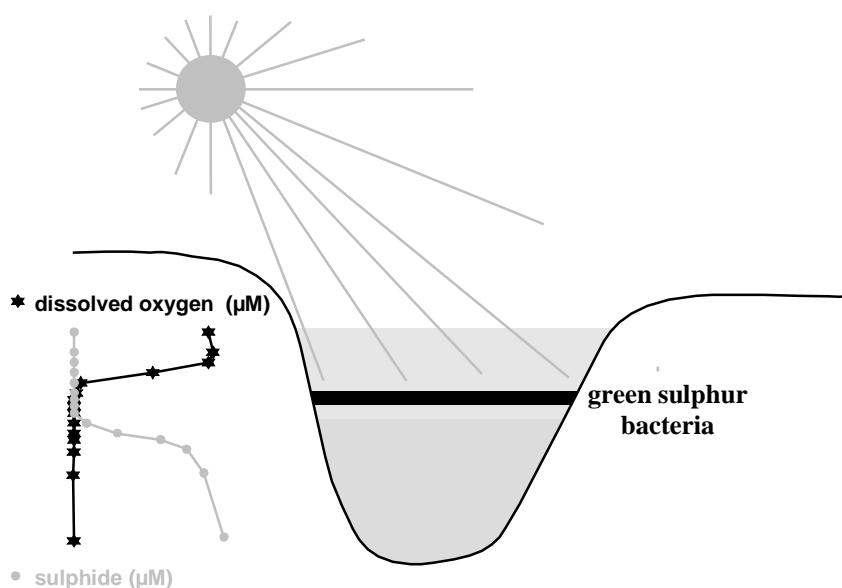
Figure 5. The habitat of green sulfur bacteria with euxinic conditions in the photic zone.

Shifts in the stable carbon isotopic composition of phytoplanktonic biomarkers can also provide important insight into changes in environmental conditions under which photosynthetic carbon fixation occurs. ε_p values for marine phytoplankton shows a pronounced dependence on CO_2 concentration [*Rau et al.*, 1989]. Therefore, the drop in atmospheric CO_2 concentrations resulting from enhanced OC burial rate during the C/T OAE [*Arthur et al.*, 1988; *Freeman and Hayes*, 1992;

Kuypers et al., 1999] should be reflected in the stable carbon isotopic composition of phytoplanktonic OC. Most terrestrial plants do not show the pronounced dependence of ε_p values on pCO$_2$ that is observed for marine phytoplankton [*Freeman and Hayes*, 1992] due to their ability to regulate the amount of CO$_2$ entering the leaf by adjusting the stomatal density of the leaves [*Farquhar et al.*, 1989; *White et al.*, 1994]. Thus, ε_p values of terrestrial higher plants do vary with humidity [*Farquhar et al.*, 1989; *White et al.*, 1994], but with the exception of extreme environments, such changes are expected to cause only minimal isotopic variability. Therefore, δ^{13}C values of biomarkers of terrestrial plants are expected to increase by only ~ 2.5‰ in response to the changes in δ^{13}C values of atmospheric/oceanic CO$_2$ during the C/T OAE [*Scholle and Arthur*, 1980; *Arthur et al.*, 1988; *Jenkyns et al.*, 1994].

In addition, δ^{13}C values of biomarkers can also provide information about the pathway of carbon fixation used by the organism. Carbon fixation in green sulfur bacteria occurs via the reverse tricarboxylic acid (TCA) cycle [*Sirevåg et al.*, 1977; *Van der Meer et al.*, 1998] instead of the Calvin cycle that is used by algae, cyanobacteria and higher plants. The degree of carbon-isotope fractionation during carbon assimilation is much smaller for the reverse TCA cycle than for the Calvin cycle such that green sulfur bacterial lipids are typically enriched in ^{13}C by 10-15‰ relative to algal or cyanobacterial lipids [*Sinninghe Damsté et al.*, 1993; *Koopmans et al.*, 1996]. This isotopic difference is of great help in the recognition of diagenetic products of isorenieratene, indicative of photic zone anoxia.

1.4 Scope and framework of the thesis

The OAE that occurred near the C/T boundary is the most extensive and as such has been considered as the type example of the mid-Cretaceous OAEs [*Wignall*, 1994]. One of the main sites of carbon burial during the C/T OAE was the proto-North Atlantic Ocean, where up to 80 m thick black shales [*Kuhnt et al.*, 1990], which can contain more than 40% organic carbon [*Herbin et al.*, 1986], were deposited basin-wide. The main part of this thesis (Part I) focuses on the causes and consequences of enhanced OM burial in the proto-North Atlantic Ocean during the C/T OAE. Another objective is to determine if the apparent similarities between black shales such as enrichment in OC, lamination, absence of or impoverished benthic faunas, ^{13}C-enrichment of inorganic and/or organic carbon indicate a common cause for the mid-Cretaceous OAEs (Part II). Therefore, the early Albian (~112 My) OAE1b black shales were investigated using the same techniques as for the C/T black shales and the results from both studies were compared.

In Chapter 2 direct evidence is provided for a dramatic decline in pCO$_2$ during the C/T OAE occurring in only ~ 60 ky. The observed carbon isotopic shift of up to 16‰ for individual leaf wax components extracted from sediments from an abyssal site in the southern North Atlantic Ocean suggests a sudden change in plant communities of the north African continent. Specifically this suggests that plants using the C$_3$-type photosynthetic pathway were succeeded by plants using the C$_4$-type pathway. Because C$_4$ plants can outcompete C$_3$ plants only at pCO$_2$ levels below 500 p.p.m.v. [*Cerling et al.*, 1997], the observed change indicates a far larger reduction in C/T CO$_2$-levels (40-80%) than previously [*Freeman and Hayes*, 1992] suggested. The 6‰ excursion in δ^{13}C

values that is observed for molecular fossils of marine phytoplankton is consistent with this large reduction.

In Chapter 3 the C/T sections of three sites along a northeast-southwest transect from Morocco to French Guyana (Fig. 4) were correlated by stable carbon isotope stratigraphy using the characteristic ^{13}C excursion in both bulk OM and molecular fossils of algal chlorophyll and steroids. Carbon isotope stratigraphy was also used to calculate the increase in carbon accumulation rates at these sites of different palaeobathymetric setting during the C/T OAE. To test whether enhanced OM preservation resulted from reduced oxygen supply or enhanced productivity caused the increase in carbon burial in the proto-North Atlantic we reconstructed: 1) Chemocline variations using redox sensitive trace metals and molecular fossils from pigments exclusively produced by bacteria that require both light and free hydrogen sulfide; and 2) Variations in primary productivity using Ba/Al ratios and ^{13}C/^{12}C ratios for molecular fossils of algal chlorophyll and steroids. It is shown that enhanced productivity led to increased organic carbon burial in an euxinic North Atlantic basin during the C/T OAE. We propose that increased upwelling of nutrient-rich, proto-Atlantic deep water, resulting from the tectonically induced formation of a deep water connection between the North and South Atlantic basins enhanced primary productivity during the C/T OAE.

In Chapter 4 the C/T sections of two sites from the northwestern part of the proto-North Atlantic (Fig. 4) were correlated by stable carbon isotope stratigraphy using the characteristic ^{13}C excursion in both bulk OM and molecular fossils of algal chlorophyll. The C/T intervals at these sites show high amplitude, short-term cyclic variations in TOC content with the more pronounced changes in TOC content being accompanied by changes in lithology from green (TOC < 1%) to black claystones (TOC > 1%). We show that these cyclic variations reflect changes in the contribution of marine OM. Sedimentation rates obtained from the isotope stratigraphy and spectral analyses indicate that these changes were predominately precession controlled. To test whether enhanced marine OM preservation resulted from reduced oxygen supply or enhanced productivity caused this precession controlled variation in TOC contents we reconstructed: 1) Chemocline variations using redox sensitive trace metals and molecular fossils from pigments exclusively produced by bacteria that require both light and free hydrogen sulfide; and 2) Variations in primary productivity using Ba/Al ratios, abundance of biogenic silica and ^{13}C/^{12}C ratios for molecular fossils of algal chlorophyll. It is shown that periodically increased primary productivity led to euxinic conditions in the water column of the northwestern proto-North Atlantic. These euxinic conditions, which sometimes extended to at least the base of the photic zone (<150 m), led to enhanced preservation of marine OM resulting in the deposition of OM-rich black claystones. In addition, we show that the trend of continually increasing TOC content and HI values of the black claystones up section that is observed at these sites, most likely resulted from both enhanced preservation due to increased anoxia and increased production of marine OM during the C/T OAE.

In Chapter 5 the role and significance of N_2-fixing cyanobacteria in the increase in OM burial at four proto-North Atlantic sites of different palaeobathymetric setting was determined using nitrogen isotope measurements and molecular fossils of cyanobacterial membrane lipids. The ^{15}N-depletion of OM-rich marine sediments ($\delta^{15}N$ = -2-0 ‰) typical for newly fixed N_2 and the abundance of cyanobacterial membrane lipids indicate that N_2 fixation supplied the additional nutrient N required to increase primary productivity in the proto-North Atlantic during the C/T OAE.

In Chapters 6 and 7 the source for both soluble and insoluble OM of the early Albian OAE 1b black shales of the Ocean Drilling Program (ODP) site 1049C (North Atlantic Ocean off the coast of Florida) and the Ravel section of the Southeast France Basin (SEFB) were determined using optical, chemical, stable carbon and nitrogen isotopic analyses. It is generally believed that these OAEs were caused either by decreased remineralisation or increased production of phytoplanktonic OM. Here we show that enhanced organic carbon (OC) burial during the early Albian OAE1b (~112 My) was caused by a different process. Isoprenoidal tetraether membrane lipids and free isoprenoids, diagnostic for marine planktonic archaea and archaea in general, respectively, are abundantly present in these black shales. In fact, combined biogeochemical and stable carbon isotopic analyses indicate that black shales from this period contain up to 80% of OC derived from archaea. Although there are apparent similarities (distinct lamination, ^{13}C-enrichment of OC) between the black shales of OAE1b and the C/T OAE, our detailed molecular work shows that the origin of the OM (archaeal versus phytoplanktonic) and causes for ^{13}C-enrichment of OC are completely different.

1.5 References

Arthur, M. A., W. A. Dean, and L. M. Pratt, Geochemical and climatic effects of increased marine organic carbon burial at the Cenomanian/Turonian boundary, *Nature*, 335, 714-717, 1988.

Arthur, M. A., W. E. Dean, and S. O. Schlanger, Variations in the global carbon cycle during the Cretaceous related to climate, volcanism, and changes in atmospheric CO_2, *American Geophysical Union Monograph*, 32, 504-529, 1985.

Arthur, M. A., S. O. Schlanger , and H. C. Jenkyns, The Cenomanian-Turonian Oceanic anoxid event,II. Palaeoceanographic controls on organic-matter production and preservation, *Geological Society Special Publication*, 26, 401-420, 1987.

Barron, E. J., A warm, equable Cretaceous: the nature of the problem, *Earth-Science Reviews*, 19, 305-338, 1983.

Berner, R. A., A model for atmospheric CO_2 over Phanerozoic time, *American Journal of Science*, 291, 339-376, 1991.

Berner, R. A., Palaeo-CO_2 and climate, *Nature*, 358, 114-114, 1992.

Bralower, T. J. and H. R. Thierstein, Organic carbon and metal accumulation rates in Holocene and mid-Cretaceous sediments: palaeoceanographic significance, *Geological Society Special Publication*, 26, 345-369, 1987.

Brass, G. W., J. R. Southam, and W. H. Peterson, Warm saline bottom water in the ancient ocean, *Nature*, 296, 620-623, 1982.

Cerling, T. C., J. M. Harris, B. J. MacFadden, M. G. Leakey, J. Quade, V. Eisenmann, and J. R. Ehleringer, Global vegetation change through the Miocene/Pliocene boundary, *Nature*, 389, 153-158, 1997.

Chamberlin, T. C., On a possible reversal of deep-sea circulation and its influence on geological climates, *Journal of Geology*, 14, 363-373, 1906.

De Graciansky, P. C., G. Deroo, J. P. Herbin, L. Montadert, C. Müller, A. Schaaf, and J. Sigal, Ocean -wide stagnation episode in the late Cretaceous, *Nature*, 308, 346-349, 1984.

De Leeuw, J. W., N. L. Frewin, P. F. Bergen, J. S. Sinninghe Damsté, and M. E. Collison, Organic carbon as a palaeoenvironmental indicator in the marine realm, in *Marine Palaeoenvironmental Analysis from Fossils*, edited by D. W. J. Bosence and P. A. Allison, pp. 43-71, Geological Society, London, 1995.

Erbacher, J., C. Hemleben, B. T. Huber, and M. Markey, Correlating environmental changes during early Albian oceanic anoxic event 1B using benthic foraminiferal paleoecology, *Mar. Micropal.*, 38, 7-28, 1999.

Erbacher, J. and J. Thurow, Influence of oceanic anoxic events on the evolution of mid-Cretaceous radiolaria in the North Atlantic and western Tethys, *Mar. Micropal.*, 30, 139-158, 1997.

Erbacher, J., J. W. Thurow, and R. Littke, Evolution patterns of radiolaria and organic matter variations: A new approach to identify sea-level changes in mid-Cretaceous pelagic environments, *Geology*, 24, 499-502, 1996.

Farquhar, G. D., J. R. Ehleringer, and K. T. Hubick, Carbon isotope discrimination and photosynthesis, in *Annual Review of Plant Physiology and Plant Molecular Biology. vol 40*, edited by W. R. Briggs, R. L. Jones, and V. Walbot, pp. 503-537, Annual Reviews Inc., Palo Alto, 1989.

Freeman, K. H. and J. M. Hayes, Fractionation of carbon isotopes by phytoplankton and estimates of ancient CO_2 levels., *Global Biochemical Cycles*, 6, 185-198, 1992.

Gale, A. S., H. C. Jenkyns, W. J. Kennedy, and R. M. Corfield, Chemostratigraphy versus biostratigraphy: data from around the Cenomanian-Turonian boundary, *Journal of the Geological Society, London*, 150, 29-32, 1993.

Grice, K., W. M. Klein Breteler, S. Schouten, V. Grossi, J. W. De Leeuw, and J. S. Sinninghe Damste, Effects of zooplankton herbivory on biomarker proxy records, *Palaeoceanography*, 13, 686-693, 1998.

Hasegawa, T., Cenomanian-Turonian carbon isotope events recorded in terrestrial organic matter from northern Japan, *Pal. Geo, Pal. Clim, Pal. Ecol.*, 130, 251-273, 1997.

Hay, W. W., Paleoceanography: a review for the GSA Centennial, *Geological Society of America Bulletin*, 100, 1934-1956, 1988.

Hayes, J. M., B. N. Popp, R. Takigiku, and M. W. Johnson, An isotopic study of biochemical relationships between carbonates and organic carbon in the Greenhorn formation, *Geochim. Cosmochim. Acta*, 53, 2961-2972, 1989.

Hayes, J. M., R. Takigiku, R. Ocampo, H. J. Callot, and P. Albrecht , Isotopic compositions and probable origins of organic molecules in the Eocene Messel shale, *Nature*, 329, 48-51, 1987.

Herbin, J. P., L. Montadert, C. Müller, R. Gomez, J. W. Thurow, and J. Wiedmann, Organic-rich sedimentation at the Cenomanian-Turonian boundery in oceanic and coastal basins in the North Atlantic and Tethys, *Geological Society Special Publication*, 21, 389-422, 1986.

Huber, B. T., D. A. Hodell, and C. P. Hamilton, Middle-Late Cretaceous climate of the southern high latitudes: Stable isotope evidence for minimal equator-to-pole thermal gradient, *GSA Bulletin*, 107, 1164-1191, 1995.

Imhoff, J. F., Taxonomy and physiology of phototrophic purple bacteria and green sulfur bacteria, in *Anoxygenic photosynthetic bacteria*, edited by R. E. Blankenship, M. T. Madigan, and C. E. Bauer, pp. 1-15, Kluwer Academic Publishers, Dordrecht, 1995.

Jarvis, I., G. A. Carson, M. K. E. Cooper, M. B. Hart, P. N. Leary, B. A. Tocher, D. Horne, and A. Rosenfeld, Microfossil assemblages and the Cenomanian-Turonian (late Cretaceous) oceanic anoxic event, *Cretaceous Research*, 9, 3-103, 1988.

Jasper, J. P., J. M. Hayes, A. C. Mix, and F. G. Prahl, Photosynthetic fractionation of ^{13}C and concentrations of dissolved CO_2 in the central equatorial Pacific during the last 255,000 years, *Palaeoceanography*, 9, 781-798, 1994.

Jenkyns, H. C., A. S. Gale, and R. M. Corfield, Carbon- and oxygen- isotope stratigraphy of the English Chalk and Italian Scaglia and its palaeoclimatic significance, *Geol.Mag.*, 131, 1-34, 1994.

Johnson, C. C., E. J. Barron, E. G. Kauffman, M. A. Arthur, P. J. Fawcett, and M. K. Yasuda, Middle Cretaceous reef collapse linked to ocean heat transport, *Geology*, 24, 376-380, 1996.

Kohnen, M. E. L., S. Schouten, J. S. Sinninghe Damsté, J. W. De Leeuw, D. A. Merritt, and J. M. Hayes, Recognition of paleobiochemicals by a combined molecular sulfur and isotope geochemical approach, *Science*, 256, 358-362, 1992.

Koopmans, M. P., J. Köster, H. M. E. Van Kaam-Peters, F. Kenig, S. Schouten, W. A. Hartgers, J. W. De Leeuw, and J. S. Sinninghe Damsté, Diagenetic and catagenetic products of isorenieratene : Molecular indicators for photic zone anoxia, *Geochim. Cosmochim. Acta*, 60, 4467-4496, 1996.

Kuhnt, W., J. P. Herbin, J. W. Thurow, and J. Wiedmann, Distribution of Cenomanian-Turonian organic facies in the western Mediterranean and along the Adjacent Atlantic Margin, *AAPG Stud. in Geol.*, 30, 133-160, 1990.

Kuhnt, W., J. W. Thurow, J. Wiedmann, and J. P. Herbin, Oceanic anoxic conditions around the Cenomanian/Turonian boundary and the response of the biota, *Mitt. Geol. -Paläeont. Inst. Univ. Hamburg*, 60, 205-246, 1986.

Kuypers, M. M. M., R. D. Pancost, and J. S. Sinninghe Damsté, A large and abrupt fall in atmospheric CO_2 concentration during Cretaceous times., *Nature*, 399, 342-345, 1999.

Larson, R. L., Geological consequences of superplumes, *Geology*, 963-966, 1991.

Pagani, M., M. A. Arthur, and K. H. Freeman, Miocene evolution of atmospheric carbon dioxide, *Palaeoceanography*, 14, 273-292, 1999.

Peters, K. E. and J. M. Moldowan, The Biomarker Guide, pp. 1-363, Prentice Hall, Englewood Cliffs, 1993.

Philip, J. M. and C. Airaud-Crumiere, The demise of the rudist-bearing carbonate platforms at the Cenomanian/Turonian boundary: a global control, *Coral Reefs*, 10, 115-125, 1991.

Rau, G. H., M. A. Arthur, and W. A. Dean, $^{15}N/^{14}N$ variations in Cretaceous Atlantic sedimentary sequences: implications for past changes in marine nitrogen biogeochemistry, *Earth and Planetary Science Letters*, 82, 269-279, 1987.

Rau, G. H., T. Takahashi, and D. J. Des Marais, Latitudinal variations in plankton $\delta^{13}C$: implications for CO_2 and productivity in past oceans, *Nature*, 341, 516-518, 1989.

Repeta, D. J., D. J. Simpson, B. B. Jorgensen, and H. W. Jannasch, Evidence for anoxygenic photosynthesis from the distribution of bacterio-chlorophylls in the Black Sea, *Nature*, 342, 69-72, 1989.

Schlanger , S. O. and H. C. Jenkyns, Cretaceous oceanoc anoxic events: causes and consequences, *Geologie en mijnbouw*, 55, 179-184, 1976.

Schoell, M., S. Schouten, J. S. Sinninghe Damsté, J. W. De Leeuw, and R. E. Summons, A molecular organic carbon isotope record of Miocene climate changes, *Science*, 263, 1122-1125, 1994.

Scholle, P. A. and M. A. Arthur, Carbon-isotope fluctuations in Cretaceous pelagic limestones: potential stratigraphic and petroleum exploration tool, *AAPG Bulletin*, 64, 67-87, 1980.

Schouten, S., H. M. E. Van Kaam-Peters, W. I. C. Rijpstra, M. Schoell, and J. S. Sinninghe Damsté, Effects of an oceanic anoxic event on the stable carbon isotopic composition of early Toarcian carbon, *American Journal of Science*, 300, 1-22, 2000.

Scotese, C. R. and J. Golonka, Paleogeographic Atlas, University of Texas, Arlington, 1992.

Sellwood, B. W., G. D. Price, and P. J. Valdes, Cooler estimates of Cretaceous temperatures, *Nature*, 370, 453-455, 1994.

Sinninghe Damsté, J. S., M. D. Kok, J. Köster, and S. Schouten, Sulfurized carbohydrates: and important sedimentary sink for organic carbon?, *Earth and Planetary Science Letters*, 164, 7-13, 1998.

Sinninghe Damsté, J. S. and J. Köster, A euxinic southern North Atlantic Ocean during the Cenomanian/Turonian oceanic anoxic event, *Earth and Planetary Science Letters*, 158, 165-173, 1998a.

Sinninghe Damsté, J. S., S. G. Wakeham, M. E. L. Kohnen, J. M. Hayes, and J. W. De Leeuw, A 6,000-year sedimentary molecular record of chemocline excursions in the Black Sea, *Nature*, 362, 827-829, 1993.

Sinton, C. W. and R. A. Duncan, Potential link between ocean plateau volcanism and global ocean anoxia at the Cenomanian-Turonian boundary, *Economic Geology*, 92, 838-842, 1997.

Sirevåg, R., B. B. Buchanan, J. A. Berry, and J. H. Troughton, Mechanism of CO_2 fixation in bacterial photosynthesis studied by the carbon isotope fractionation technique., *Arch. Microbiol.*, 112, 35-38, 1977.

Summerhayes, C. P., Organic-rich Cretaceous sediments from the North Atlantic, *Geological Society Special Publication*, 26, 301-316, 1987.

Thiede, J. and T. J. V. van Andel, The paleoenvironment of anaerobic sediments in the late Mesozoic South Atlantic Ocean, *Earth and Planetary Science Letters*, 33, 301-309, 1977.

Van der Meer, M. T. J., S. Schouten, and J. S. Sinninghe Damsté, The effect of the reversed tricarboxylic acid cycle on the ^{13}C contents of bacterial lipids, *Org. Geochem.*, 28, 527-533, 1998.

van Gemerden, H. and J. Mas, Ecology of phototrophic sulfur bacteria, in *Anoxygenic photosynthetic bacteria*, edited by R. E. Blankenship, M. T. Madigan, and C. E. Bauer, pp. 49-85, Kluwer Academic Publishers, Dordrecht, 1995.

White, J. W. C., P. Ciais, R. A. Figge, R. Kenny, and V. Markgraf, A high-resolution record of atmospheric CO_2 content from carbon isotopes in peat, *Nature*, 367, 153-156, 1994.

Wignall, P. B., Mudstone lithofacies in the Kimmeridge Clay Formation, Wessex Basin,Southern England: Implications for the origin and controls of the distribution of mudstone- discussion, *Journal of Sedimentary Research*, A64, 927-929, 1994.

Zimmerman, H. B., A. Boersma, and F. W. McCoy, Carbonaceous sediments and palaeoenvironment of the Cretaceous South Atlantic Ocean, *Geological Society Special Publication*, 26, 271-286, 1987.

Chapter 2

A large and abrupt fall in atmospheric CO_2 concentrations during Cretaceous times

Marcel M.M. Kuypers, Richard D. Pancost, Jaap S. Sinninghe Damsté

Abstract.

Marine carbonates and organic matter (OM) show a sharp increase in their $^{13}C/^{12}C$ isotope ratios at the Cenomanian/Turonian (C/T) boundary [*Scholle and Arthur*, 1980; *Arthur et al.*, 1988] in the Cretaceous period. This isotopic shift resulted from an increase in the rate of sedimentary burial of ^{13}C-depleted organic carbon in response to the C/T 'oceanic anoxic event' [*Arthur et al.*, 1988]. The enhanced burial rate should have led to a significant drop in the atmospheric CO_2 concentration, which could explain the apparent climatic cooling of early Turonian times [*Arthur et al.*, 1988; *Jenkyns et al.*, 1994; *Kuhnt et al.*, 1986]. Here we present stable carbon isotope data for specific compounds from terrestrial leaves and marine phytoplankton, and quantify the abruptness and magnitude of the atmospheric CO_2 concentration change. Isotope shifts in leaf-wax components extracted from abyssal sediments in the northeastern tropical Atlantic Ocean–the components are wind-delivered from Africa–indicate a sudden change in plant communities of the north African continent. Specifically, the data suggest that plants using the C_3-type photosynthetic pathway were succeeded by plants using the C_4-type pathway. If C_4 plants can outcompete C_3 plants only at atmospheric CO_2 concentrations below 500 p.p.m.v. [*Cerling et al.*, 1997], the observed vegetation change indicates a far larger reduction in C/T CO_2 concentration–some 40-80%–than previously suggested [*Freeman and Hayes*, 1992]. The isotopic excursion in the marine phytoplankton compounds is consistent with this estimate. We infer that this dramatic fall in the atmospheric CO_2 concentration was abrupt, occurring in just 60,000 years.

2.1 Introduction

The middle-late Cretaceous climate has been described as a 'greenhouse climate' with minimal Equator-to-pole thermal gradients [*Barron*, 1983]. It has been suggested that this climate condition resulted from extensive periods of volcanic outgassing [*Arthur et al.*, 1985; *Larson*, 1991] leading to increased atmospheric concentrations of the greenhouse gas carbon dioxide (estimates of the partial pressure of CO_2 (pCO_2) vary between 3 and 12 times modern (pre-industrial) values [*Berner*, 1992], that is, 900-3,300 p.p.m.v.). However, the widespread burial of organic matter in black shales during the C/T 'oceanic anoxic event' (OAE) probably led to a significant reduction of pCO_2 [*Arthur et al.*, 1988]. Such a decrease is suggested by the drop in the isotope effect associated with carbon fixation (ε_p) by phytoplankton in the Cretaceous Western Interior Seaway of North America [*Freeman and Hayes*, 1992]. This decline is also documented indirectly by oxygen isotope data, which indicate an 8-13 °C cooling at high latitudes during the early Turonian [*Arthur et al.*, 1988; *Jenkyns et al.*, 1994]. Additional indications of global cooling are provided by micropaleontological data, showing an incursion of boreal fauna into low latitude seas [*Kuhnt et al.*, 1986].

2.2 Methods

2.2.1 Bulk analyses. Total Organic Carbon (TOC) contents were determined by a LECO C/S analyser. The $\delta^{13}C$ values (±0.1‰) ($\delta^{13}C = [(^{13}C/^{12}C)_{sample}/(^{13}C/^{12}C)_{standard}]-1$; the Pee Dee belemnite standard (PDB) has been used) were measured on bulk sediments using automated on-line combustion after removal of the inorganic carbonates with diluted HCl.

2.2.2 Compound specific analyses. The powdered samples (15-30 g) were Soxhlet extracted for ~24 h to obtain the total lipid fraction. An aliquot (~250 mg) of the total extract was separated into an apolar and a polar fraction using column chromatography. $AgNO_3$ column chromatography and urea adduction were used to obtain *n*-alkane fractions. The hydrocarbons that were released from the polar fraction by Raney nickel desulphurisation and subsequent hydrogenation were isolated using column chromatography. Samples were analysed by gas chromatography-mass spectrometry (GC-MS) for identification. Compound-specific $\delta^{13}C$ analyses were performed using GC-isotope ratio mass spectrometry (GC-IRMS). The $\delta^{13}C$ values for individual compounds are the means of duplicate runs ($\sigma = ±0.3$ to 0.6) expressed versus PDB.

2.3 Results and discussion

Here we present the results of a compound-specific carbon isotope study of C/T sediments deposited in the southern part of the North Atlantic Ocean off the coast of northwest Africa (Deep Sea Drilling Project (DSDP) site 367, close to the equator). The laminated black shales consist of a mixture of terrigenous silicates and clay minerals [*Mélières*, 1978], high amounts of organic matter

(up to 50 wt%) and some biogenic carbonate. The thermally immature organic matter is almost exclusively of marine origin, as revealed by the Rock Eval hydrogen indices [*Herbin et al.*, 1986] and the extremely low abundance of lignin pyrolysis products generated from the kerogen. The saturated hydrocarbon fractions consist mainly of short-chain *n*-alkanes (with no obvious odd-over-even carbon number predominance), isoprenoids of bacterial/algal origin, and long-chain *n*-alkanes with a strong odd-over-even carbon number predominance (Carbon Preference Index CPI = 2.7-5.1) derived from leaf waxes of higher plants [*Eglinton and Hamilton*, 1967]. An important mode of transport of leaf-wax *n*-alkanes is via wind, as indicated by the high relative amounts of leaf-wax components in aeolian dust collected at remote ocean sites [*Gagosian et al.*, 1981]; consequently, they are common constituents of extractable organic matter of recent and ancient abyssal plane sediments [*Farrington and Tripp*, 1977]. Taking into account the prevailing wind direction, the most likely candidate for the origin of these wind-transported terrestrial *n*-alkanes is the nearby north African continent. Often, the generation of *n*-alkanes from other sources during dia- and catagenesis makes carbon-isotope analyses of the leaf-wax lipids impossible. In the C/T sediments described here the leaf-wax components are still relatively abundant in the hydrocarbon biomarker fraction due to the fact that most marine biomarkers were transformed to sulphur-bound components during early diagenesis [*Kohnen et al.*, 1991].
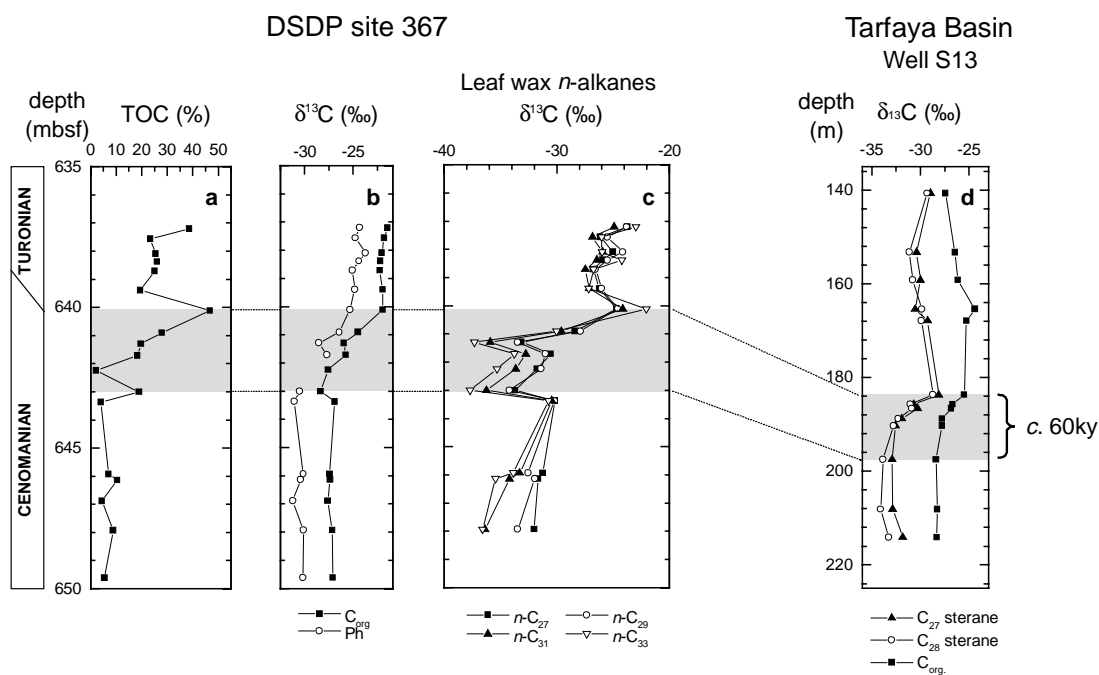

Figure 1 Bulk and biomarker data of the investigated sites; the stratigraphy is also shown. **a-c**, Data from DSDP site 367. **(a)** Total organic carbon (TOC) content; **(b)** and **(c)** carbon isotope values (in ‰ vs. PDB) of C_{org}, and S-bound phytane (Ph) derived from phytoplanktonic chlorophyll **(b)**, leaf-wax components **(c)**. **(d)** Data from shelf sediments from well S13 of the Tarfaya basin; carbon isotope values of C_{org} and free steranes (C_{27} sterane (5α-cholestane) and C_{28} sterane (5α-24-methyl-cholestane)) derived from marine algae. The time difference (estimated at ~60 kyr) between the onset of the $\delta^{13}C_{org}$ excursion and the first maximum carbon isotope- value for organic matter is indicated as a grey shaded area in the graphs. At site 367 carbonate carbon is absent, due to deposition below the carbonate compesation

depth, but carbonate $\delta^{13}C$ values for the Tarfaya shelf sediments, although affected by diagenesis, indicate a 2.5‰ excursion (W. Kuhnt, personal communication).

The isotopic compositions of the terrestrial *n*-alkanes show a remarkable shift coincident with the positive isotope-ratio excursion observed here for organic carbon ($\delta^{13}C_{org}$; Fig. 1b) and worldwide [*Scholle and Arthur*, 1980; *Arthur et al.*, 1988; *Jenkyns et al.*, 1994] for marine carbonates (~2.5‰). Most terrestrial plants do not show the pronounced dependence of ε_p values on pCO_2 that is observed for marine phytoplankton [*Freeman and Hayes*, 1992]; this results from the ability of plants to regulate the amount of CO_2 that enters their leaves by adjusting the stomatal density of the leaves [*Farquhar et al.*, 1989; *White et al.*, 1994]. ε_p values of terrestrial higher plants can vary with humidity [*Farquhar et al.*, 1989; *White et al.*, 1994] but, with the exception of extreme environments, such changes are expected to cause only minimal isotopic variability. Therefore, leaf wax *n*-alkanes are expected to increase by only ~2.5‰ in response to the changes in $\delta^{13}C$ values of atmospheric/oceanic CO_2 during the C/T OAE [*Scholle and Arthur*, 1980; *Arthur et al.*, 1988; *Jenkyns et al.*, 1994]. However, for the leaf wax *n*-alkanes a far larger shift (of 10 to 16‰) is observed (Fig. 1c). The magnitude of the isotopic shift of the sedimentary *n*-alkanes is consistent with a change in the source of these leaf wax lipids from C_3- to C_4-type plants. The carbon isotope effect differs between the two photosynthetic pathways, such that $\delta^{13}C$ values for bulk plant material range from -22‰ to -30‰ for C_3 and -10‰ to -14‰ for C_4 [*Street-Perrot et al.*, 1997]. The *n*-alkanes are typically depleted in ^{13}C relative to the bulk material by 6 and 10‰, respectively [*Collister et al.*, 1994].

In the lower part of the studied section (until 641.29 m) *n*-alkane isotopic values (-38 to -30‰) are typical for a predominately C_3-type origin and become depleted in ^{13}C with increasing carbon number (Fig. 2). This latter trend has been previously observed for C_3 plants [*Collister et al.*, 1994] and for sediment samples dominated by detritus derived from such plants [*Rieley et al.*, 1991]. In the upper part of the section, *n*-alkanes exhibit $\delta^{13}C$ values (-22 to -27‰) that are indicative of mainly C_4-type input or a mixture of C_3-type and C_4-type leaf-wax lipids. In marked contrast to the C_3-dominated *n*-alkane samples, $\delta^{13}C$ values of the individual leaf-wax components in these samples are nearly constant with increasing chain length (Fig. 2), which is consistent with what has been observed for C_4 plants [*Collister et al.*, 1994]. The different trends of $\delta^{13}C$ values versus carbon number for samples dominated by C_3-type and C_4-type plants results in a larger carbon-isotope shift for longer *n*-alkanes (Fig. 2).

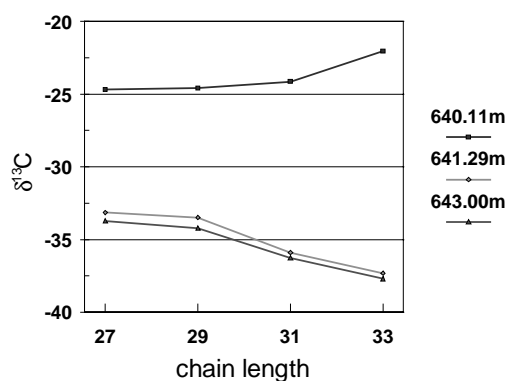**Figure 2** $\delta^{13}C$ values of leaf lipids versus chain length. The $\delta^{13}C$ values of the individual leaf-wax components for a sample before (643.00 m), during (641.29 m) and at the first maximum of (640.11 m) the $\delta^{13}C_{org}$ excursion indicate the rapid shift in the source of these higher plant lipids from C_3- to C_4-

Direct evidence (that is, plant remains) for the presence of C_4-type photosynthesis in the fossil record is scarce, due to the absence of readily fossilized woody parts in most plants using the C_4 system. Instead, the $^{13}C/^{12}C$ ratios of tooth enamel of herbivorous animals, of palaeosol carbonate, and of terrestrial-derived organic matter have been used as tracers for ecosystems dominated by C_3-type and C_4-type plants, and suggest that the C_4-type system did not represent an important part of the terrestrial ecosystem until the late Miocene [*Cerling et al.*, 1997]. However, on basis of palaeo pCO_2 reconstructions, it was proposed that a C_4-type pathway could have evolved independently during the Carboniferous-Permian glaciation and subsequently disappeared in the Mesozoic [*Cerling et al.*, 1997], while other authors [*Spicer*, 1989; *Bocherens et al.*, 1994] suggest that C_4-type photosynthesis could have evolved earlier than the late Miocene. Carbon-isotope measurements provide additional evidence for the presence of C_4-type plant remains in pre-Miocene sediments. Such examples include Carboniferous calcified root mats [*Wright and Vanstone*, 1991], a late Cretaceous lignite sample [*Bocherens et al.*, 1994], collagen from dinosaur bones [*Bocherens et al.*, 1994], and *n*-alkanes in extracts from the Eocene Green River Formation [*Collister et al.*, 1994]. But until now, evidence for a CO_2-driven shift from a C_3-type to a C_4-type dominated ecosystem has not been observed for sediments older than late Tertiary.

The dominant photosynthetic pathway for a given ecosystem (C_3 or C_4) depends on both pCO_2 and temperature [Fig. 3, *Ehleringer et al.*, 1997; *Collatz et al.*, 1998]. Plants using the C_4 photosynthetic pathway use an active CO_2-concentrating mechanism that provides them with an advantage over C_3 plants at low CO_2 levels and high temperatures. But at higher CO_2 levels the C_4 pathway becomes less advantageous, due to the higher energy demand for the concentrating mechanism. Consistent with this, a 10‰ shift in $\delta^{13}C$ values was reported for *n*-alkanes in Pleistocene high-altitude lake sediments and attributed to a change from C_3 to C_4 plants resulting from lower pCO_2 levels during glacial times [*Street-Perrot et al.*, 1997]. Assuming that equatorial temperatures were comparable to present-day temperatures, as is suggested by oxygen-isotope data for the Cenomanian [*Sellwood et al.*, 1994], and a similar response to CO_2 partial pressure for Cretaceous C_3-type/C_4-type plants, pCO_2 during the C/T OAE would have been no more than twice that of the modern (pre-industrial) atmosphere. In fact, Cerling *et al.* [1997] suggested that the C_4 photosynthetic pathway would not be present at atmospheric CO_2 levels of more than 500 p.p.m.v. Assuming that CO_2 levels for the middle Cretaceous ranged from 3 to 12 times modern values [*Berner*, 1992], this suggests that pCO_2 decreased by 40-80%.

In addition to low pCO_2, aridity can also lead to a competitive advantage for C_4 plants [*Bird and Cali*, 1998], as low humidity will lead to stomatal closure and a decreased intercellular CO_2 level [*Collatz et al.*, 1998]. But at the high pCO_2 levels suggested for the Cretaceous, C_3-type plants will predominate independent of the level of humidity [*Cerling et al.*, 1997; *Ehleringer et al.*, 1997]. Increased aridity of the north African continent could have facilitated an increase in C_4-type vegetation during the C/T OAE when pCO_2 was significantly lower (that is, below 500 p.p.m.v.). The presence of both marine and terrestrial biomarkers in sediments from this section provides an opportunity to compare the timing and nature of the carbon isotope excursion on land and in the marine environment. ε_p values for marine phytoplankton show a pronounced dependence

on CO_2 concentration: therefore a drop in CO_2 levels should be reflected in their $\delta^{13}C$ values. For the Western Interior Seaway of North America, a geoporphyrin fraction was used to calculate a 1.5‰ decrease in ε_p values during the C/T OAE [*Hayes et al.*, 1989], and this was subsequently interpreted as a ~20% reduction in pCO_2 levels [*Freeman and Hayes*, 1992]. In sharp contrast, at site 367 the 6‰ increase in the $\delta^{13}C$ values for sulphur-bound phytane derived from algal chlorophyll (Fig. 1b) records a 3.5‰ decrease in ε_p values, assuming a 2.5‰ excursion for inorganic carbon [*Scholle and Arthur*, 1980; *Arthur et al.*, 1988; *Jenkyns et al.*, 1994]. This larger decrease in ε_p values is also suggested by the 5-6‰ increase in $\delta^{13}C$ values observed for a multitude of phytoplanktonic biomarkers from two other North Atlantic C/T sites (that is, the Tarfaya Atlantic coastal basin (Morocco; Fig. 1d) and DSDP site 144 off the coast of northern South America (M.M.M.K. et al., unpublished results)). It is difficult to determine which marine site best records the global pCO_2 change during the C/T OAE, as physiological and environmental variables other than pCO_2 can affect ε_p values for marine phototrophs. However, the larger decrease in ε_p values observed for these three North Atlantic sites is consistent with the 40-80% decrease in pCO_2 required for a transition from C_3-type to C_4-type plants.
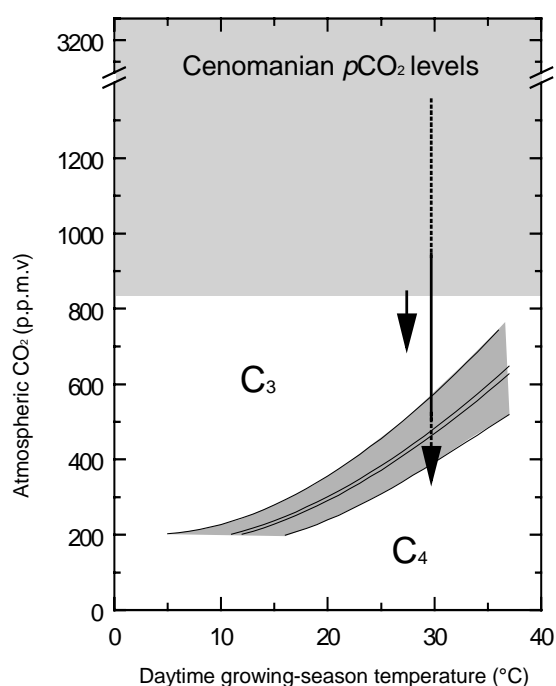

Figure 3 The C_3/C_4 crossover function. This function shows the pCO_2 dependence of the C_3/C_4 crossover temperature [after *Ehleringer et al.*, 1997]. The estimated range of Cenomanian pCO_2 levels is indicated as a grey shaded area. The drop in pCO_2 levels that is observed here (large broken arrow) and the previously [*Freeman and Hayes*, 1992] reported drop (small arrow) for the C/T OAE are shown. It is assumed that equatorial temperatures were comparable to present day values [*Sellwood et al.*, 1994].

There is a difference in timing of the isotope excursion between the marine-derived organic matter and phytane, and the terrestrial *n*-alkanes (Fig. 1). The magnitude of this time lag can be determined if the time difference is known between the onset of the $\delta^{13}C_{org}$ excursion and the first maximum carbon-isotope value for organic matter. As the $\delta^{13}C$ excursion is synchronous for all sites [*Gale et al.*, 1993], data from the expanded C/T section of the Tarfaya basin [*Kuhnt et al.*, 1997; *Kuhnt et al.*, 1990] can be used for this calculation. An accumulation rate of ~12 cm ky^{-1} [*Kuhnt et al.*, 1997] has been derived for these sediments, leading to a calculated duration for this particular excursion interval of ~60 ky (Fig. 1). Assuming a constant accumulation rate, the

difference in timing between the onset of the carbon-isotope excursion of marine markers and the δ^{13}C shift for terrestrial markers is ~30 ky. This difference could be explained by the time needed to reach the low pCO$_2$ values that are favourable for a C$_4$-type pathway through the burial of organic matter.

The enhanced burial of organic matter during the C/T OAE led to a profound decrease in pCO$_2$ [*Arthur et al.*, 1988] allowing the appearance of plants using a CO$_2$-concentrating mechanism (C$_4$-type) in the Cretaceous north African plant community. This shows that in addition to anthropogenic emissions, perturbations of the biogeochemical cycles may have an abrupt and dramatic effect on atmospheric CO$_2$ concentrations.

2.4 References.

Arthur, M. A., W. A. Dean, and L. M. Pratt, Geochemical and climatic effects of increased marine organic carbon burial at the Cenomanian/Turonian boundary, *Nature*, 335, 714-717, 1988.

Arthur, M. A., W. E. Dean, and S. O. Schlanger, Variations in the global carbon cycle during the Cretaceous related to climate, volcanism, and changes in atmospheric CO$_2$, *American Geophysical Union Monograph*, 32, 504-529, 1985.

Barron, E. J., A warm, equable Cretaceous: the nature of the problem, *Earth-Science Reviews*, 19, 305-338, 1983.

Berner, R. A., Palaeo-CO$_2$ and climate, *Nature*, 358, 114-114, 1992.

Bird, M. I. and J. A. Cali, A million-year record of fire in sub-Saharan Africa, *Nature*, 394, 767-769, 1998.

Bocherens, H., E. Friis, A. Mariotti, and K. R. Pedersen, Carbon isotopic abundances in Mesozoic and Cenozoic fossil plants: Palaeoecological implications, *Lethaia*, 26, 347-358, 1994.

Cerling, T. C., J. M. Harris, B. J. MacFadden, M. G. Leakey, J. Quade, V. Eisenmann, and J. R. Ehleringer, Global vegetation change through the Miocene/Pliocene boundary, *Nature*, 389, 153-158, 1997.

Collatz, G., J. A. Berry, and J. S. Clark, Effects of climate and atmospheric CO$_2$ partial pressure on the global distribution of C$_4$ grasses: present, past, and future, *Oecologia*, 114, 441-454, 1998.

Collister, J. W., G. Rieley, B. Stern, G. Eglinton, and B. Fry, Compound-specific δ^{13}C analyses of leaf lipids from plants with differing carbon dioxide metabolisms, *Org.Geochem.*, 21, 619-627, 1994.

Eglinton, G. and R. J. Hamilton, Leaf epicuticular waxes, *Science*, 156, 1322-1335, 1967.

Ehleringer, J. R., T. E. Cerling, and B. R. Helliker, C$_4$ photosynthesis, atmospheric CO$_2$, and climate, *Oecologia*, 112, 285-299, 1997.

Farquhar, G. D., J. R. Ehleringer, and K. T. Hubick, Carbon isotope discrimination and photosynthesis, in *Annual Review of Plant Physiology and Plant Molecular Biology. vol 40*, edited by W. R. Briggs, R. L. Jones, and V. Walbot, pp. 503-537, Annual Reviews Inc., Palo Alto, 1989.

Farrington, J. W. and B. W. Tripp, Hydrocarbons in western North Atlantic surface sediments, *Geochim.Cosmochim.Acta*, 41, 1627-1641, 1977.

Freeman, K. H. and J. M. Hayes, Fractionation of carbon isotopes by phytoplankton and estimates of ancient CO$_2$ levels, *Global Biochemical Cycles*, 6, 185-198, 1992.

Gagosian, R. B., E. T. Peltzer, and O. C. Zafiriou, Atmospheric transport of continentally derived lipids to the tropical North Pacific, *Nature*, 291, 312-314, 1981.

Gale, A. S., H. C. Jenkyns, W. J. Kennedy, and R. M. Corfield, Chemostratigraphy versus biostratigraphy: data from around the Cenomanian-Turonian boundary, *Journal of the Geological Society, London*, 150, 29-32, 1993.

Hayes, J. M., B. N. Popp, R. Takigiku, and M. W. Johnson, An isotopic study of biochemical relationships between carbonates and organic carbon in the Greenhorn formation, *Geochim.Cosmochim.Acta*, 53, 2961-2972, 1989.

Herbin, J. P., L. Montadert, C. Müller, R. Gomez, J. W. Thurow, and J. Wiedmann, Organic-rich sedimentation at the Cenomanian-Turonian boundery in oceanic and coastal basins in the North Atlantic and Tethys, *Geological Society Special Publication*, 21, 389-422, 1986.

Jenkyns, H. C., A. S. Gale, and R. M. Corfield, Carbon- and oxygen- isotope stratigraphy of the English Chalk and Italian Scaglia and its palaeoclimatic significance, *Geol.Mag.*, 131, 1-34, 1994.

Kohnen, M. E. L., J. S. Sinninghe Damsté, and J. W. De Leeuw, Biases from natural sulphurization in palaeoenvironmental reconstruction based on hydrocarbon biomarker distributions, *Nature*, 349, 775-778, 1991.

Kuhnt, W., J. P. Herbin, J. W. Thurow, and J. Wiedmann, Distribution of Cenomanian-Turonian organic facies in the western Mediterranean and along the Adjacent Atlantic Margin, *AAPG Stud.in Geol.*, 30, 133-160, 1990.

Kuhnt, W., A. J. Nederbragt, and L. Leine, Cyclicity of Cenomanian-Turonian organic-carbon-rich sediments in the Tarfaya Atlantic Coastal Basin (Morocco), *Cretaceous Research*, 18, 587-601, 1997.

Kuhnt, W., J. W. Thurow, J. Wiedmann, and J. P. Herbin, Oceanic anoxic conditions around the Cenomanian/Turonian boundary and the response of the biota, *Mitt.Geol.-Paläeont.Inst.Univ.Hamburg*, 60, 205-246, 1986.

Larson, R. L., Geological consequences of superplumes, *Geology*, 963-966, 1991.

Mélières, F., X-ray mineralogy studies, leg 41, Deep Sea Drilling Project, Eastern North Atlantic Ocean, *Initial Reports of the Deep Sea Drilling Project*, 41, 1065-1086, 1978.

Rieley, G., R. P. Collier, D. M. Jones, G. Eglinton, P. A. Eakin, and A. E. Fallick, Sources of sedimentary lipids deduced from stable carbon-isotope analyses of individual compounds, *Nature*, 425-427, 1991.

Scholle, P. A. and M. A. Arthur, Carbon-isotope fluctuations in Cretaceous pelagic limestones: potential stratigraphic and petroleum exploration tool, *AAPG Bulletin*, 64, 67-87, 1980.

Sellwood, B. W., G. D. Price, and P. J. Valdes, Cooler estimates of Cretaceous temperatures, *Nature*, 370, 453-455, 1994.

Spicer, R. A., Physiological characteristics of land plants in relation to environment through time, *Earth-Science*, 80, 321-329, 1989.

Street-Perrot, F. A., Y. Huang, R. A. Perrott, G. Eglinton, P. Barker, L. B. Khelifa, D. D. Harkness, and D. O. Olago, Impact of lower atmospheric carbon dioxide on tropical mountain ecosystems, *Science*, 278, 1422-1426, 1997.

White, J. W. C., P. Ciais, R. A. Figge, R. Kenny, and V. Markgraf, A high-resolution record of atmospheric CO_2 content from carbon isotopes in peat, *Nature*, 367, 153-156, 1994.

Wright, V. P. and S. D. Vanstone, Assessing the carbon dioxide content of ancient atmospheres using palaeocalcretes: theoretical and empirical constraints, *Journal of the Geological Society of London.*, 148, 945-947, 1991.

Chapter 3

Enhanced productivity led to increased organic carbon burial in the euxinic North Atlantic basin during the late Cenomanian oceanic anoxic event

Marcel M.M. Kuypers, Richard D. Pancost, Ivar A. Nijenhuis, Jaap S. Sinninghe Damsté

Abstract.

Three Cenomanian/Turonian (C/T ~93.5 Ma) black shale sections along a northeast-southwest transect in the southern part of the proto-North Atlantic Ocean were correlated by stable carbon isotope stratigraphy using the characteristic excursion in $\delta^{13}C$ values of both bulk organic matter (OM) and molecular fossils of algal chlorophyll and steroids. All three sites show an increase in marine organic carbon (OC) accumulation rates during the C/T Oceanic Anoxic Event (OAE). The occurrence of molecular fossils of anoxygenic photosynthetic green sulfur bacteria, lack of bioturbation and high abundance of redox sensitive trace metals indicates sulfidic conditions, periodically reaching up into the photic zone before as well as during the C/T OAE. During the C/T OAE there was a significant rise of the chemocline as indicated by the increase in concentrations of molecular fossils of green sulfur bacteria and Mo/Al ratios. The presence of molecular fossils of the green strain of green sulfur bacteria indicates that euxinic conditions periodically even occurred at very shallow water depths of 15 m or less during the C/T OAE. However, bottom water conditions did not dramatically change as indicated by more or less constant V/Al and Zn/Al ratios at site 367. This suggests that the increase in OC burial rates resulted from enhanced PP rather than increased anoxia, which is supported by stable carbon isotopic evidence and a large increase in Ba/Al ratios during the C/T OAE. The occurrence of the productivity event during a period of globally enhanced organic carbon burial rates (i.e. the C/T OAE), points to a common cause possibly related to the formation of a deep water connection between North and South Atlantic basins.

3.1 Introduction

The interval spanning the Barremian to Turonian (~125-88 Ma) is known as the mid-Cretaceous 'greenhouse' world [*Barron*, 1983]. Both marine and terrestrial proxies indicate that the mid-Cretaceous climate was significantly warmer with a smaller equator-to-pole temperature gradient than the modern climate. It has been suggested that this resulted from an anomalous amount of oceanic volcanism, leading to 3 to 12 times higher atmospheric levels of carbon dioxide during the Cretaceous than at present [*Berner*, 1992]. The transition from the Cenomanian to the Turonian (C/T) marks a major turning point, with globally dispersed oxygen isotope data indicating that the mid-Cretaceous warming trend ceased at the C/T boundary and was followed by a deterioration at least until the Maastrichtian [*Jenkyns et al.*, 1994]. This long-term cooling was preceded by the global deposition of sediments rich (> 1%) in organic carbon (OC) and devoid of or strongly impoverished in benthic faunas (black shales) [*Schlanger and Jenkyns*, 1976]. An increase in $^{13}C/^{12}C$ ratios for marine carbonates and organic matter at the C/T boundary provides evidence for an increase in the global OC burial rate. This positive excursion in $\delta^{13}C$ values likely resulted from preferential removal of ^{12}C by the enhanced burial of ^{13}C depleted OC as a response to the so-called 'C/T oceanic anoxic event (OAE)' [*Arthur et al.*, 1988]. Originally, the term OAE was introduced to describe the episodic expansion and intensification of the Oxygen Minimum Zone (OMZ), which was proposed to explain the seemingly global distribution of OC-rich sediments in pelagic sequences of Aptian-Albian and C/T age [*Schlanger and Jenkyns*, 1976]. The term OAE has been used by later workers more generally 'as a way of referring to time-bounded envelopes of particularly, perhaps more globally, widespread deposition of OC-rich sediments (black shales) in marine environments' [*Arthur et al.*, 1987]. In accordance with this, the term C/T OAE (i.e. OAE2) will be used in this study for the 300-500 ky period of latest Cenomanian to earliest Turonian age, during which OM burial rates were enhanced. This enhanced OM burial rate led to a significant drop in atmospheric carbon dioxide concentration [*Freeman and Hayes*, 1992; *Arthur et al.*, 1988; *Kuypers et al.*, 1999] and, thereby, could have triggered the early Turonian deterioration of the greenhouse climate.

Two fundamentally different models have been used to explain the enhanced OM burial rate during the C/T OAE. The *preservational* model is based on decreased OM remineralisation resulting from a decreased oxygen flux. In the mid-Cretaceous oceans, anoxic water column conditions may have developed more readily than in the modern world's oceans as minimal equator-to-pole thermal gradients and high sea surface temperatures should have resulted in a decreased formation of oxygenated bottom-waters [*Barron*, 1983]. This could have resulted in basin-wide oxygen deficiency with the most intense dysoxia/anoxia occurring in the deepest parts of tectonically isolated basins such as the Cretaceous North and South Atlantic [*Zimmerman et al.*, 1987; *de Graciansky et al.*, 1984]. The reoccurrence of thinly laminated OM–rich sediments devoid of traces of benthic activity indicates that middle Cretaceous bottom-waters were indeed periodically anoxic [*Summerhayes*, 1987; *Bralower and Thierstein*, 1987]. Sedimentary derivatives (molecular fossils) of a pigment indicative of anoxygenic photosynthetic bacteria recovered from abyssal and shelf sites indicate that anoxic conditions extended even into the photic zone of the southern proto-North Atlantic during the C/T OAE [*Sinninghe Damsté and Köster*, 1998].

The *productivity* model is based on a greatly increased primary productivity that overwhelmed the oxic OM remineralisation potential of the water column. Primary productivity in the modern marine environment is largely controlled by the input of biolimiting nutrients from deeper water into the surface waters. An enhanced supply of biolimiting nutrients could have led to increased PP and thus to an expansion and intensification of the OMZs during the C/T OAE [*Schlanger and Jenkyns*, 1976]. The deposition of OM-rich sediments would have largely been confined to places where the OMZ impinged on the continental margin or other elevated portions of the sea floor, as the deepest places of the basin may have remained oxic. This model has especially been used to explain the OM-rich deposits in the Cretaceous Pacific Ocean [e.g., *Schlanger and Jenkyns*, 1976].

In the proto-North Atlantic Ocean, black shales that can be over 80 m thick [*Kuhnt et al.*, 1990] and that can contain more than 40% OC [*Herbin et al.*, 1986] were deposited basin-wide during the C/T OAE, indicating that this was one of the main sites of carbon burial. This study focuses on the environmental conditions that led to the deposition of the especially well-developed C/T OAE black shales from the southern part of the proto-North Atlantic Ocean [*de Graciansky et al.*, 1984; *Kuhnt et al.*, 1990]. The C/T sections of three sites along a northeast-southwest transect from Morocco to French Guyana (Fig. 1) were correlated by stable carbon isotope stratigraphy using the characteristic ^{13}C excursion in both bulk OM and molecular fossils of algal chlorophyll and steroids. Carbon isotope stratigraphy was also used to calculate the increase in carbon accumulation rates at these sites of different palaeobathymetric setting during the C/T OAE. To test whether enhanced OM preservation resulting from reduced oxygen supply or enhanced productivity caused this increase in carbon burial we reconstructed: 1) Chemocline variations using redox sensitive trace metals and molecular fossils from pigments exclusively produced by bacteria that require both light and free hydrogen sulfide; and 2) Variations in primary productivity using Ba/Al ratios and ^{13}C/^{12}C ratios for molecular fossils of algal chlorophyll and steroids. In addition we discuss the oceanographic consequences of our findings.

3.2. Material and Methods

The samples come from Shell exploration well S13 of the Tarfaya area (Morocco), and Deep Sea Drilling Project (DSDP) holes 144 off the coast of French Guyana (leg 14) and 367 off the coast of Senegal (leg 41). Sediment slices (3-5 cm) were taken from the cores, from which sub-samples were subsequently freeze-dried and powdered in an agate mortar.

Total Organic Carbon (TOC) contents were determined using a CN analyser. The δ^{13}C values ($\pm$0.1‰ versus Vienna Pee Dee belemnite (VPDB)) were measured on bulk sediments, after removal of the inorganic carbonates with diluted HCl, using automated on-line combustion followed by conventional isotope ratio-mass spectrometry. For analyses of the soluble OM powdered samples were Soxhlet extracted for *c.* 24 h to obtain the total extract, which was separated into an apolar and a polar fraction using column chromatography. Hydrocarbons were released from the polar fraction by Raney Nickel desulfurisation and subsequent hydrogenation [*Sinninghe Damsté et al.*, 1993]. Samples were analysed by gas chromatography-mass spectrometry
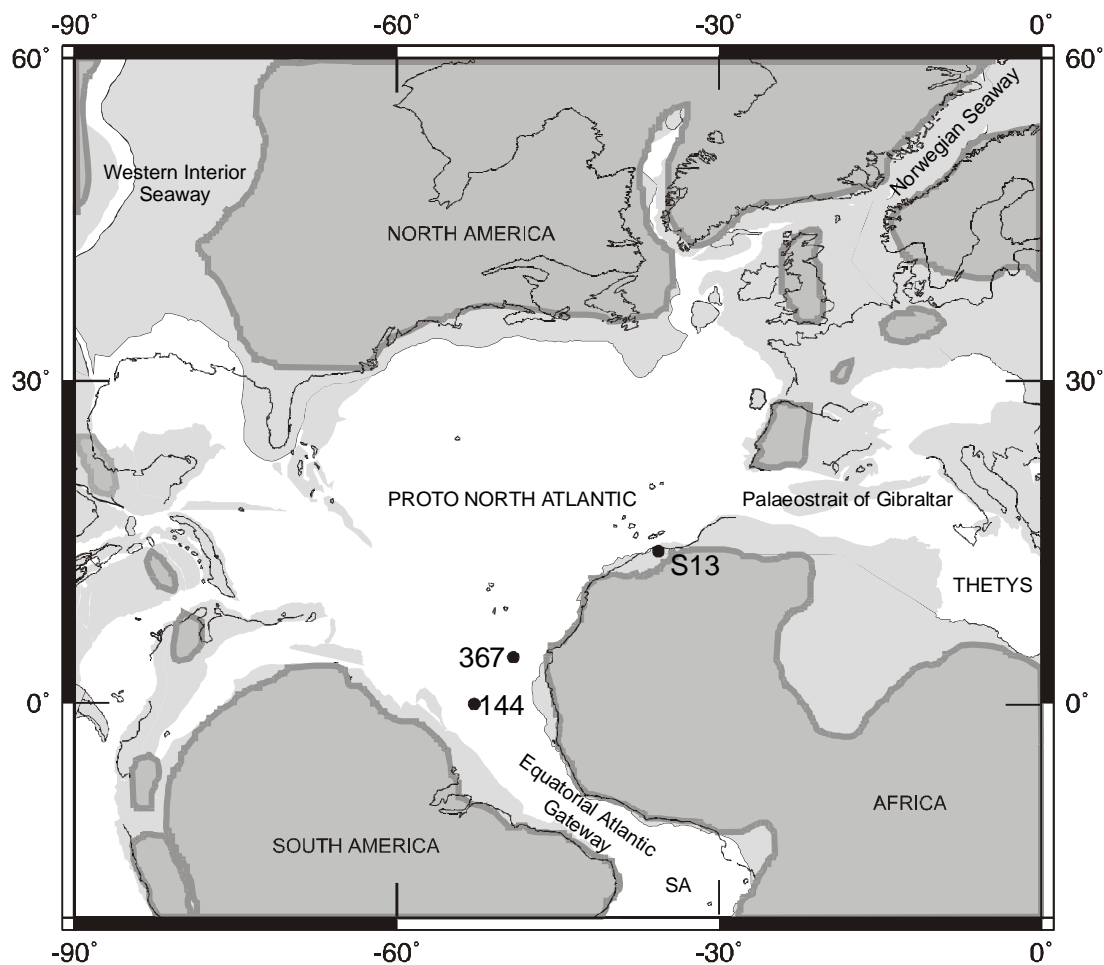
Figure 1. Palaeogeographical map of mid Cretaceous (~94 Ma) North Atlantic showing the position of the three studied cores. Light grey shaded regions represent continental plates (from GEOMAR map generator; www.odsn.de/odsn/services/paleomap/paleomap.html). Dark grey shaded regions represent land [*Scotese and Golonka*, 1992].

(GC-MS) for compound identification. Compound-specific $\delta^{13}C$ analyses were performed using a GC-isotope-ratio-monitoring MS. The $\delta^{13}C$ values for individual compounds are the means of duplicate runs ($\sigma = \pm0.3$ to 0.6) expressed versus VPDB. Pyrolysis (Py)-GC was conducted on a GC equipped with a FID and a cryogenic unit. Samples were pressed onto flattened ferromagnetic wires (Curie temperature of 610°C), which were subsequently inductively heated for 10 s. The desorbed fragments were flushed into the capillary column using helium.

For major, minor and trace element analyses, samples (ca. 125 mg) were digested in 5 ml HF (40%) and 5 ml of a $HClO_4/HNO_3$ mixture at 90 °C. After drying by evaporation at 190 °C, the residue was dissolved in 25 ml 1 M HCl. The resulting solutions were analysed with a Perkin Elmer Optima 3000 inductively coupled plasma atomic emission spectrometer (ICP-AES). The results were checked with international and house standards, and relative standard deviations in duplicate measurements are below 4%.

3.3. Results and Discussion

3.3.1 Stratigraphy and Palaeosetting.

Our study concentrates on the C/T interval roughly between 95 and 93 My before present [*Gradstein et al.*, 1995], which spans two planktic foraminiferal zones of global significance: the late Cenomanian *Rotalipora cushmani* zone and the latest Cenomanian to early Turonian *Whiteinella archaeocretacea* zone (Fig. 2). This interval is particularly well developed in the
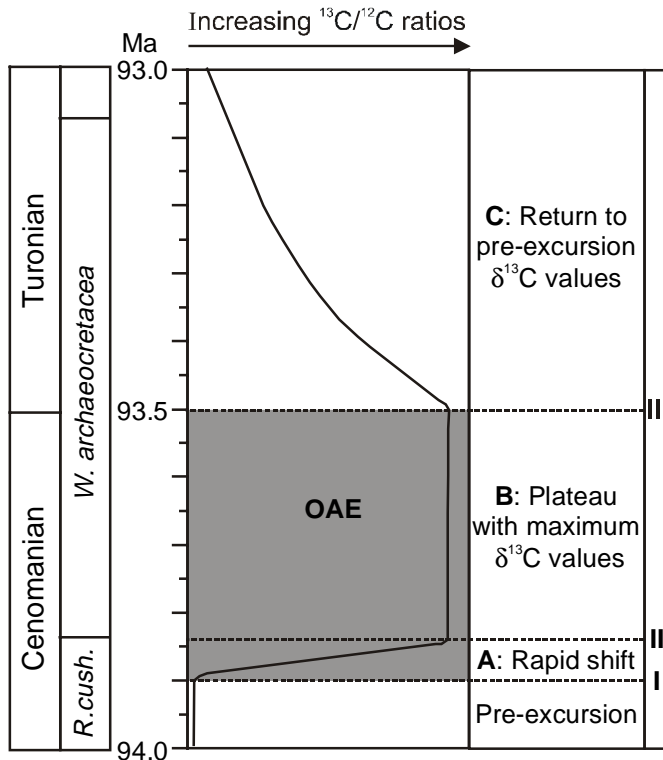

Figure 2. Idealised representation of C/T stable carbon isotope excursion showing the bio-and chronostratigraphic position of the three main phases (modified after [*Gale et al.*, 1993]). Dashed lines with roman numbers show the position of the boundaries between the different phases (pre-excursion, **A**, **B** and **C**) of the isotope excursion

Tarfaya basin (well S13; Morocco), where it reaches a thickness of ~150 m (Fig. 3). The C/T sequence at site S13 consists of OM-rich biogenic carbonates that were deposited in an open shelf sea with a palaeo-water depth at the depocentre (well S13) of 200-300 m [*Kuhnt et al.*, 1990]. Sedimentation rates were as high as 12 cm/ky for the *W. archaeocretacea* zone [*Kuhnt et al.*, 1997] that contains the major part of the C/T OAE.

The black shales that comprise the late Cenomanian sequence at Deep Sea Drilling Program (DSDP) Site 367 (off the coast of north-west Africa) consist of a mixture of terrigenous silicates and clay minerals, high amounts of organic carbon (total organic carbon (TOC) contents up to 50 wt. %) and minor amounts of biogenic carbonate [Herbin et al., 1986]. These sediments were deposited at a water depth of 3700 m. The deposition of such extemely OM-rich sediments at this abyssal site is hard to explain by the expanding OMZ model proposed by *Schlanger and Jenkyns* [1976]. Therefore, it has been suggested that the deeper bottom waters (>3000 m) of the proto North Atlantic were predominately oxic and that a large part of the OC-enrichment of mid-Cretaceous black shales at site 367 resulted from redeposition of sediments deposited where the

OMZ impinged on the seafloor [*Arthur et al.*, 1984]. Indeed, thin tubidites consisting of quartz silt or clayey foraminifer sand do occur but apparently represent only a minor component of the late Cenomanian section [see also *The Shipboard Scientific Party*, 1977]. To the best of our knowledge no direct evidence has so-far been provided for a turbiditic origin of the OM-rich black shales itself [see *Arthur et al.*, 1984 and references therein], and thus, we believe that the deeper bottom waters were predominately anoxic during their deposition (see below).
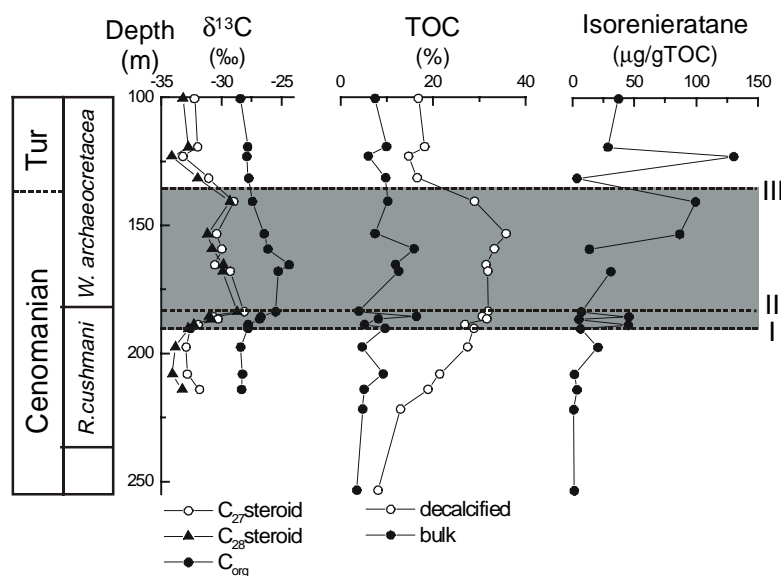

Figure 3. Stratigraphy [*Kuhnt et al.*, 1997], bulk organic carbon and biomarker data of site S13 (Tarfaya basin). Carbon isotope values (in ‰ vs. VPDB) of bulk organic carbon (C_{org}) and free steranes [C_{27} sterane (5α-cholestane) and C_{28} sterane (5α-24-methyl-cholestane)] derived from marine algae, TOC content of the bulk sediment and of the residue obtained after decalcification, and concentration profile of molecular fossil (S-bound isorenieratane) of a pigment of the brown strain of green sulfur bacteria. The dashed lines with Roman numbers show the approximate position of the boundaries between the different phases of the isotope excursion (see also Fig. 2).

At site 144, the southwestern end of the transect, Cenomanian deposits consist of dark laminated carbonaceous cemented limestones and zeolitic calcareous clay [*Hayes et al.*, 1972]. These hemipelagic sediments were deposited on an ancestral Mid-Atlantic ridge at a water depth of ~1300 m [*Berger and von Rad*, 1972].

In sharp contrast to the Tarfaya basin section [*Kuhnt et al.*, 1990], biostratigraphically significant species are largely absent from the middle Cretaceous sediments from sites 144 and 367. Carbon isotope stratigraphy was used instead to constrain the C/T OAE interval and to correlate these abyssal sites with the Moroccan shelf site. The sharp increase in $^{13}C/^{12}C$ ratios that is observed worldwide for marine carbonates and OM at the C/T boundary [*Scholle and Arthur*, 1980; *Arthur et al.*, 1988] has been shown to be a powerful tool in high resolution correlation [e.g. *Gale et al.*, 1993; *Hasegawa*, 1997]. Although this positive excursion in δ^{13}C values consists of several spikes and nudges [*Gale et al.*, 1993], three main phases can be recognised (A to C; schematically depicted in Fig. 2). Phase A is a rapid increase in $^{13}C/^{12}C$ ratios (i.e. rapid shift) that occurred during the latest

part of the *Rotalipora cushmani* zone [*Gale et al.*, 1993; *Kuhnt et al.*, 1990]. This is followed by a plateau with maximum $\delta^{13}C$ values (phase B) mainly during the early part of the *Whiteinella archaeocretacea* zone. Finally, there is a gradual return to pre-excursion $\delta^{13}C$ values (phase C) during the early Turonian. The three boundaries (I to III) between the different phases of the isotope excursion and the pre-excursion conditions are of particular stratigraphic significance. The positive excursion in $\delta^{13}C$ values reflects a change in the global atmospheric-oceanic pool of inorganic carbon resulting from a global increase in the burial rate of ^{13}C-depleted OC [*Arthur et al.*, 1988]. By definition the C/T OAE is the main phase of enhanced carbon burial rates and, therefore, should be coeval with the interval between boundaries I and III (phases A and B, indicated as a grey shaded area in Fig. 2).

The use of molecular fossils that are specific for primary producers instead of bulk OM for stable carbon isotope stratigraphy greatly reduces the effect of heterotrophy, preservation, and diagenetic alteration on the carbon isotopic signature of OC [*Hayes et al.*, 1989; *Freeman and Hayes*, 1992; *Sinninghe Damsté et al.*, 1998]. At site S13 of the Tarfaya basin the stable carbon isotopic compositions of two steranes (5α-cholestane, 24-methyl-5α-cholestane) were used to define the C/T OAE (Fig. 3). These steranes derive from C_{27} and C_{28} sterols, predominantly biosynthesised by marine algae [*Volkman*, 1986]. Their $\delta^{13}C$ values record changes in the stable carbon isotopic composition of algae (Fig. 3). Therefore, the interval from the base of the stable carbon isotopic excursion (I) until the onset of declining $\delta^{13}C$ values (III) for these steranes (indicated as a grey shaded area in Fig. 3) should correlate to the C/T OAE. Milankovitch-derived sedimentation rates (12 cm/ky) previously reported for the *Whiteinella archaeocretacea* zone of site S13 [*Kuhnt et al.*, 1997] were used to calculate a duration of ~400 ky for the C/T OAE. By analogy phase A of the isotope excursion (Fig. 2), was estimated to be ~60 ky [*Kuypers et al.*, 1999]. Although the sample resolution introduces a significant margin of error, the ~400 ky for the C/T OAE is in good agreement with data from Western Europe [*Gale*, 1995] indicating ~350 ky (17 precession cycles) for the same interval. In addition a duration of ~400 ky has recently been reported for the Tunesian Bahloul formation [*Caron et al.*, 1999], which approximately coincides with phases A and B of the C/T isotope excursion [*Nederbragt et al.*, 1998]. In sharp contrast, the $\delta^{13}C$ profile for bulk OC at site S13 (Fig. 3) suggests a significantly shorter duration (~250 ky) for the C/T OAE. This illustrates the benefits of using molecular fossils specific for primary producers instead of bulk OM for stable carbon isotope stratigraphy.

At sites 144 and 367 sulfur (S)-bound phytane (Figs. 4 and 5), which mainly derives from the phytol moiety of phytoplanktonic chlorophyll [*Kohnen et al.*, 1992], was used instead of the more specific algal steranes for carbon isotope stratigraphy because of the low abundance of the latter at these sites. The $\delta^{13}C$ profiles for S-bound phytane (i.e. Ph) at sites 144 and 367 both show the rapid shift in $^{13}C/^{12}C$ ratios that marks phase A (Figs. 4 and 5). The offset of ~3‰ between $\delta^{13}C$ profiles for bulk OC and the molecular fossils of chlorophyll is well within the range reported for extant algae [*Schouten et al.*, 1998]. Assuming that the excursions in $\delta^{13}C$ values at all sites are synchronous [*Gale et al.*, 1993], data from site S13 were used to calculate an average sedimentation rate for phase A of site 367 (~3.5 cm/ky). Coring gaps obscuring the later part of phase A and the whole of phase B do not allow the calculation of sedimentation rates at site 144. Similarly a coring

gap obscuring the later part of phase B at site 367 does not allow an average sedimentation rate to be calculated for the whole C/T OAE.
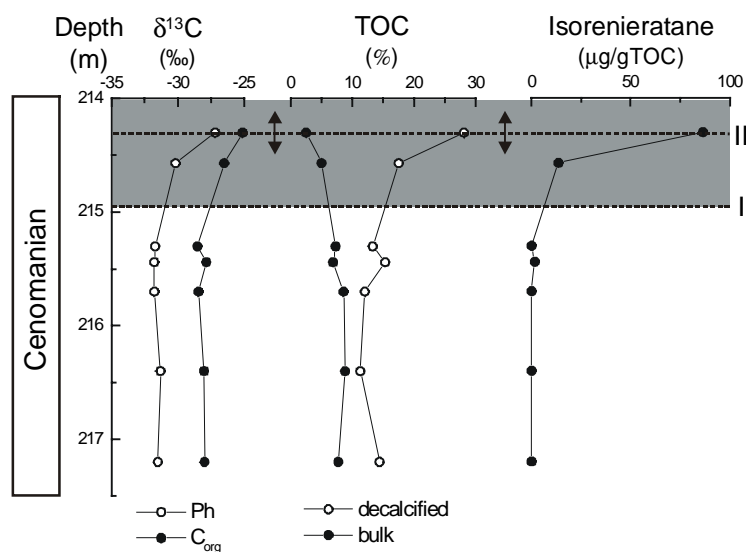

Figure 4. Stratigraphy, bulk organic carbon and biomarker data of site 144. Carbon isotope values (in ‰ vs. VPDB) of C_{org}, S-bound phytane (Ph) derived from phytoplanktonic chlorophyll, TOC content of the bulk sediment and of the residue obtained after decalcification, and concentration profile of molecular fossil (S-bound isorenieratane) of a pigment of the brown strain of green sulfur bacteria. The dashed lines with Roman numbers show the approximate position of the boundaries between the different phases of the isotope excursion (see also Fig. 2) and B indicates the sample containing benthic foraminifera.

The grey shaded areas (Figs. 4 and 5) most likely represent only a part of the total C/T OAE interval present at sites 144 and 367. However, the beginning of the rapid shift in $^{13}C/^{12}C$ ratios (earlier part of phase A) was recovered at all three sites (Figs. 3, 4 and 5) allowing a direct comparison of the changes in OC accumulation rates that occurred during the onset of the C/T OAE.

3.3.2 Organic Carbon Accumulation Rates and Organic Matter Sources

The C/T sediments of site S13 contain high amounts of OC with maximum total organic carbon (TOC) values of ~16% (Fig. 3). During the C/T OAE the average TOC content is significantly higher (~10%) than before (~5%) or after (~8%) (Fig. 3). Superimposed on these long-term trends are high-amplitude, short-term variations in TOC content throughout the investigated section. Previously reported cyclic variation in TOC content for C/T sediments from the Tarfaya basin [*Kuhnt et al.*, 1990] was attributed to fluctuations in the productivity of calcifying organisms and thus, carbonate flux [*Kuhnt et al.*, 1997]. The TOC contents for the residues obtained after decalcification (=TOC$_{decalcified}$) were determined in order to obtain a TOC record that is independent of these cyclic variations in carbonate flux, and which thereby better reflects relative changes in OC accumulation rate during the C/T OAE. The TOC$_{decalcified}$ record shows an increase followed by a decrease, with maximum values within the C/T OAE interval (Fig. 3).

At site 144 the TOC content for the bulk sediment shows a decrease during the C/T OAE (Fig. 4), which co-occurs with an increase in carbonate content reflected by a change from carbonaceous marl to carbonaceous limestone. The negative correlation between TOC and carbonate content may suggest depositional dilution of OC by an increased carbonate flux [*Ricken*, 1993]. The TOC$_{decalcified}$ record (Fig. 4) shows an increase during the C/T OAE for this site.
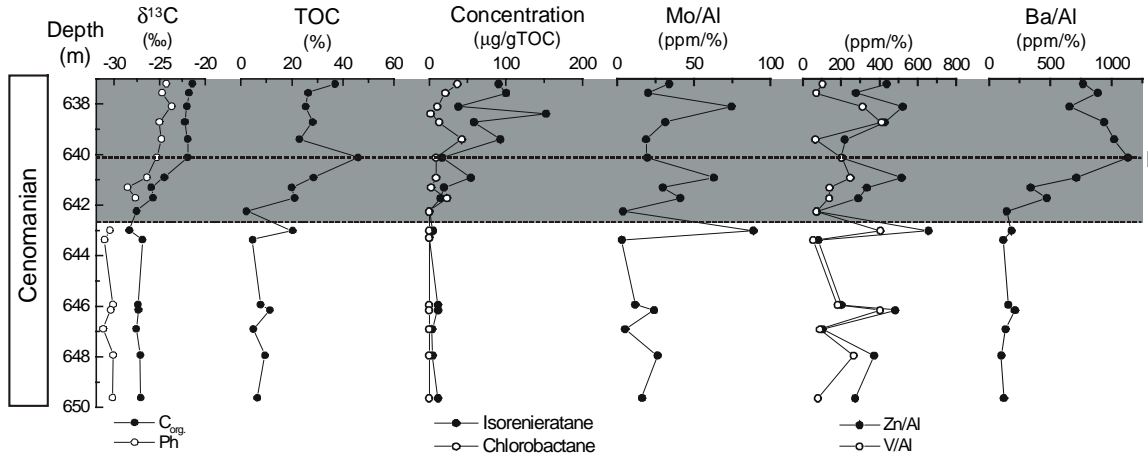

Figure 5. Stratigraphy, bulk organic carbon, biomarker, and trace metal data of site 367. Carbon isotope values (in ‰ vs. VPDB) of C$_{org}$, S-bound phytane (Ph) derived from phytoplanktonic chlorophyll, TOC content of the bulk sediment, concentration profiles of the molecular fossils S-bound isorenieratane and S-bound chlorobactene of green sulfur bacteria derived from members of the brown-and green-strain respectively, redox sensitive trace metals (Mo, Zn and V) normalised to Al, and the productivity proxy Ba/Al. The dashed lines with Roman numbers show the approximate position of the boundaries between the different phases of the isotope excursion (see also Fig. 2).

Extremely high OC contents (maximum TOC = 46%) exceeding the range for most if not all Holocene open ocean sediments below ~2000 m, characterise the Cenomanian sediments of site 367 (Fig. 5). Depositional dilution of OC by carbonate is insignificant for these sediments due to deposition below the carbonate compensation depth (CCD). During the C/T OAE the average TOC content is significantly higher (~25%) than before (~9%) (Fig. 5) suggesting that if sedimentation rates were constant OC accumulation rates increased significantly.

Assuming constant sedimentation rates, the average OC accumulation rates before and during the C/T OAE were determined for sites S13 and 367 using the TOC contents of the bulk (i.e. non decalcified) sediments. Prior to the C/T OAE, OC mass accumulation rates (OC MAR) for site S13 (9 gC·m^{-2}·y^{-1}) and site 367 (3 gC·m^{-2}·y^{-1}) are comparable to data for Holocene sites (Table 1) characterised by suboxic to anoxic bottom waters, high primary productivity (PP) (140-280 gC·m^{-2}·y^{-1}) and high bulk sediment mass accumulation rates (125-150 g·m^{-2}·y^{-1}). Only the OC MAR for the extremely productive (PP~400-500 gC·m^{-2}·y^{-1}) Peruvian shelf is significantly higher. These values are also of the same order of magnitude as reported for Mediterranean Pliocene sapropels [i.e. 0.4-6.7 gC·m^{-2}·y^{-1}; *Nijenhuis and de Lange*, 2000], which are considered younger analogues of black shales [e.g. *Thomson et al.*, 1995].

During the C/T OAE, OC accumulation rates at sites S13 and 367 (9 and 26 gC·m^{-2}·y^{-1}, respectively) were approximately three times greater than prior to the OAE. These values exceed

those determined for most modern marine settings (Table 1) and are comparable to sites characterised by both high productivity and a high preservation potential (e.g. the Peruvian shelf). The OC accumulation rates are comparable to those determined for the OC rich interval of the *W. archaeocretacea* zone (~C/T OAE) of site CM10 off the coast of Senegal but significantly higher than values determined for the same interval of European (e.g. Gubbio) and northern North Atlantic (ODP Site 641A) sites [Table 1; *Kuhnt et al.*, 1990], confirming that the southern proto-North Atlantic was one of the main locations of OC burial during the C/T OAE.

Microscopic screening of the decalcified and sieved (>10 μm) samples reveals that the OM from both shelf (well S13) and deep sea sites (sites 144 and 367) is almost exclusively amorphous with rare vascular plant remains and pollen. High Rock Eval hydrogen indices (HI) [*Herbin et al.*, 1986; *Kuhnt et al.*, 1990] and the low abundance of lignin pyrolysis products generated from the kerogen indicate a marine origin for the thermally immature OM before, during and after the C/T OAE. This is supported by the low abundance (site 367) or even absence (sites S13 and 144) of molecular fossils of unambiguous terrestrial origin (e.g. leaf-wax lipids and oleananes) in the extractable OMHence the increase in OC accumulation rates observed at all three sites resulted from enhanced marine OM burial during the C/T OAE. At site S13 and site 367 this increase in OC accumulation rates could have been as large as 17 and 6 $gC \cdot m^{-2} \cdot y^{-1}$, respectively. The question that remains is: did this increase in the marine OC accumulation rates mainly result from increased preservation under anoxic conditions or from increased primary productivity?

3.3.3 Water Column Redox Proxies

3.3.3.1 Molecular fossils of anoxygenic photosynthetic bacteria. Anoxic conditions periodically reached up into the photic zone as indicated by the abundance of molecular fossils (i.e. S-bound isorenieratane showing the typical 10-15‰ ^{13}C enrichment relative to algal lipids [e.g. *Sinninghe Damsté et al.*, 1993]) indicative of anoxygenic photosynthetic bacteria at sites S13, 144 and 367 (Figs. 3, 4 and 5). This is in good agreement with earlier findings of *Sinninghe Damsté and Köster* [1998]. S-bound isorenieratane is formed in anoxic sediments upon sulfurisation of the polyunsaturated pigment isorenieratene in the presence of reduced inorganic S species [*Sinninghe Damsté et al.*, 1993;]. Carotenoids such as isorenieratene are generally labile compounds [*Sinninghe Damsté and Koopmans*, 1997] that do not survive transport over long distances, clearly indicating a local marine rather than allochthonous source for S-bound isorenieratane. The pigment isorenieratene is exclusively produced by the brown strain of green sulfur bacteria [*Imhoff*, 1995], which require sunlight penetrating the euxinic part (e.g. containing reduced inorganic sulfur species) of an aquatic environment [*van Gemerden and Mas*, 1995]. Currently, these phototrophic bacteria are restricted to a few isolated euxinic basins in the marine realm such as the Black Sea. In such environments they thrive near the hydrogen sulfide/oxygen interface (i.e. chemocline) at depths of up to 150 m, where light levels are less than 1% of surface irradiance [*van Gemerden and Mas*, 1995].

Molecular fossils of isorenieratene were also found in sediments predating the isotope excursion albeit in much lower concentrations, indicating that sulfide-containing water periodically penetrated the photic zone before the actual onset of the C/T OAE (Figs. 3, 4 and 5). While S-bound

isorenieratane is present throughout the interval proceeding the C/T OAE at site S13 and site 367, it was only found in one sample of the same interval at site 144 (Fig. 4). This indicates that sulfide-containing water penetrated the photic zone more frequently at the southeastern side than at the southwestern side of the proto-North Atlantic Ocean, possibly reflecting a shallower average position of the chemocline (i.e. nearer to the photic zone). High amplitude short-term fluctuations in S-bound isorenieratane concentrations occur during the C/T OAE at both site S13 and site 367, although the amplitude is more pronounced at the former site (Figs. 3 and 5). The more pronounced fluctuations at site S13 could represent a sampling artefact as sample sizes are similar (~5 cm) but sedimentation rates significantly lower at site 367. As a result S-bound isorenieratane concentrations at site S13 (Fig. 3) represent an average over a much shorter time scale (~400 years) than at site 367 (Fig. 5) (~1400 years) possibly leading to a less 'smoothed' S-bound isorenieratane record at the former site. Fluctuations in S-bound isorenieratane concentrations could have resulted from changes in anoxygenic productivity. In accordance with the latter, fluctuations in the abundances of isorenieratene and its molecular fossils extracted from Holocene Black Sea sediments were attributed to changes in anoxygenic productivity related to fluctuations in the position of the chemocline [*Repeta*, 1993; *Sinninghe Damsté et al.*, 1993]. The abundance of phototrophic sulfur bacteria in modern settings not only increases and decreases as euxinic conditions rise into or drop below the photic zone, respectively, but also shows a strong positive correlation with light intensity [*van Gemerden and Mas*, 1995]. Therefore, the short-term variations and pronounced long-term increases in S-bound isorenieratane concentrations during the C/T OAE could be produced by either the chemocline penetrating the photic zone at a similar depth but over considerably longer time scales or by relatively short excursions to much shallower depths.

The occurrence of molecular fossils of the pigment chlorobactene (i.e. S-bound chlorobactane) in the OAE sediments of sites 144 and 367 (Figs. 4 and 5) and their absence prior to the OAE interval indicates a rise of the chemoline to shallower depths during the C/T OAE. Chlorobactene is exclusively produced by the green coloured strain of green sulfur bacteria [*Imhoff*, 1995], which thrives at a shallower depth (less than 15 m) than the brown strain since it requires a higher light intensity [*van Gemerden and Mas*, 1995]. Assuming a similar light dependence for these phototrophic sulfur bacteria during the mid-Cretaceous, the occurrence of S-bound chlorobactane indicates that the upper 15 m of the photic zone of the southern proto-North Atlantic periodically contained sulfide during the C/T OAE.

3.3.3.2 Trace metals. Further information on water column redox conditions can be gained from elements (e.g. Mo, Ni and Zn) that precipitate as sulfides under euxinic conditions and certain elements (e.g. Mo and V) that are immobilised under reducing conditions. Sediments underlying a euxinic water column are often characterised by a strong enrichment of these trace metals [e.g. *Arthur et al.*, 1990; *Calvert and Pedersen*, 1993]. In accordance with this, very high trace metal concentrations were previously reported for mid Cretaceous black shales of site 367 [*Brumsack and Thurow*, 1986] and were attributed to enhanced trace metal scavenging in a euxinic water column. The average trace metal concentrations reported here for C/T sediments (table 1) are in good agreement with the data from *Brumsack and Thurow* [1986].

To evaluate the variations in redox conditions, the abundances of Mo, V and Zn have been normalised to aluminium (Al) (Fig. 5). The Mo/Al, V/Al and Zn/Al profiles show strong fluctuations that could result from changes in detrital (i.e. clay minerals) sedimentation rate, the scavenging capacity of sediment and water column, and/or the trace metal abundance in the seawater. Enhanced Mo/Al ratios during the C/T OAE could have resulted from enhanced scavenging related to shoaling of the chemocline. Relatively high Zn/Al and V/Al values occur both before and during the OAE. The lack of a clear increase in V/Al and Zn/Al ratios during the C/T OAE indicates that bottom water redox conditions did not change dramatically.

3.3.3.3 Synthesis of redox proxies.

The occurrence of molecular fossils of pigments from green sulfur bacteria at sites S13, 144 and 367 indicates that the photic (<150 m) zone of the southern proto-North Atlantic Ocean periodically contained sulfide already before the C/T OAE. The deposition of predominately laminated sediments devoid of or strongly impoverished in benthic faunas at sites S13 and 144 [*Berger and von Rad*, 1972; *Kuhnt et al.*, 1990] suggests that these anoxic conditions periodically extended to at least 1300 m water depth. Arthur et al. [1984] suggested that the deeper bottom waters (>3000 m) of the proto North Atlantic were predominately oxic. This is contradicted by other workers who have described the 367 black shales from this interval as laminated and deposited under dysoxic/anoxic conditions [e.g. *Bralower and Thierstein*, 1987; *Sinninghe Damsté and Köster*, 1998]. In any case, the abundance of elements that precipitate as sulfides under euxinic conditions or that are immobilised under reducing conditions throughout the investigated interval of site 367 strongly suggests that the deeper bottom waters were anoxic for extended times [see also *Brumsack and Thurow*, 1986; *Arthur et al.*, 1990]. Consistent with this, very high TOC contents (up to 50%) and hydrogen indices [550-850 mg hydrocarbons/g TOC; *Herbin et al.*, 1986], the abundance of sulfur-bound compounds as well as the high preservation factors for OC are indicative of anoxic conditions during deposition of the sediments [see also *Herbin et al.*, 1986 and *Sinninghe Damsté and Köster*, 1998].

During the C/T OAE there was a significant rise of the chemocline as indicated by the increased concentrations of molecular fossils of green sulfur bacteria. Molecular fossils of the green strain of green sulfur bacteria (DSDP Site 144 and 367) indicate that euxinic conditions periodically even occurred above 15 m during the C/T OAE.

Decreased degradation of OM resulting from anoxic bottom water conditions would have contributed to a high OC preservation in the southern proto-North Atlantic both prior to and during the C/T OAE. Thus shoaling of the chemocline during the C/T OAE probalby did not enhance OM preservation significantly since it apparently only marginally affected the exposure to oxygen. This suggests that the observed increase in OC burial rates during the C/T OAE did not result from increased preservation.

Table 1. Age, water depth, total organic carbon content (TOC), bulk sediment (bulk) and organic carbon (OC) mass accumulation rates (MAR), average concentrations of redox sensitive trace metals (Mo, Ni, V and Zn), average concentration of Ba, export productivity (EP) and primary productivity of site S13, site 367 and a selection of Holocene [*van der Weijden et al.*, 1999; *Arthur et al.*, 1994; *Brumsack and Thurow*, 1986; *Bralower and Thierstein*, 1987], Tertiary [*Passier et al.*, 1999] and mid Cretaceous [*Kuhnt et al.*, 1990; *Thurow et al.*, 1988] sites. Grey shading indicates Holocene sites with oxygen deficient bottom waters.

Site	Age (Myr)	Water depth (m)	Av. TOC (wt%)	Bulk MAR (g m^{-2}yr^{-1})	OC MAR (g m^{-2}yr^{-1})	Av. Mo (p.p.m.)	Av. Ni (p.p.m.)	Av. V (p.p.m.)	Av. Zn (p.p.m.)	Av. Ba (p.p.m.)	EP (gCm^{-2}yr^{-1})	PP (gCm^{-2}yr^{-1})
Cretaceous and Tertiary sites												
Tarfaya S13	~94 (before OAE)	300	5	254	9	n.d.	n.d.	n.d.	n.d.	n.d.	n.d.	n.d.
Tarfaya S13	~94 (during OAE	300	10	254	26	n.d.	n.d.	n.d.	n.d.	n.d.	n.d.	n.d.
DSDP site 367	~94 (before OAE)	3700	8.5	40	3	125	205	1728	1193	875	13	71
DSDP site 367	~94 (during OAE)	3700	24.6	40	9	92	380	912	513	2052	80	179
Senegal CM10	~94 (during OAE)	300	7	476	33	n.d.	n.d.	n.d.	n.d.	n.d.	n.d.	n.d.
Italy Gubbio	~94 (during OAE)	1500	12	0.7	0.1	n.d.	n.d.	n.d.	n.d.	n.d.	n.d.	n.d.
ODP site 641A	~94 (during OAE)	3500	10	0.7	0.1	1950	464	968	6866	1219	n.d.	n.d.
ODP site 969	2.943 (sapropel)	2201	17.7	40	7.1	407	299	1937	123	1316	16	n.d.
Holocene sites												
Arabian Sea	0-0.004	~2000	1	86	0.8	n.d.	n.d.	n.d.	n.d.	n.d.	~70	140-280
Central Pacific	0-0.01	5000-5700	0.3	1.5	0.004	n.d.	210	117	165	n.d.	n.d	50
North Atlantic	0-0.01	2000-3000	0.01-1	1.7-86	0.02-1.7	n.d	n.d	n.d	n.d	n.d.	n.d.	75-230
Arabian Sea	0-0.004	495	4	245	10	n.d.	n.d.	n.d.	n.d.	n.d.	~70	140-280
Arabian Sea	0-0.004	~1000	5.5	124	6.1	n.d.	n.d.	n.d.	n.d.	n.d.	~70	140-280
Black Sea	0-0.003	~2100	5.8	83	4.8	29	75	106	81	n.d.	n.d.	150-240
Black Sea	0-0.003	400-750	1.8	165	3.1					n.d.	n.d.	150-240
Cariaco Trench	0-0.007	892	5.5	180	9.9	n.d.	n.d.	n.d.	n.d.	n.d.	n.d.	170
Peru Shelf	0-0.001	150-400	16.9	248	39	n.d	n.d.	n.d.	n.d.	n.d.	n.d.	400-500

3.3.4 Productivity Proxies

3.3.4.1 Sedimentary Barium. Sedimentary Ba is generally considered as an indicator for palaeoproductivity since it originates from barite formed in decaying phytoplanktonic OM [*Dymond et al.*, 1992; *Francois et al.*, 1995]. Such barite formation has been shown to occur in the well-oxygenated open ocean [*Dymond et al.*, 1992; *Francois et al.*, 1995] as well as in the suboxic to anoxic waters of OMZs and euxinic basins [*Falkner et al.*, 1993; *Dean et al.*, 1997]. Prior to the C/T OAE the average Ba concentration at site 367 is comparable to data reported for C/T sediments and some Pliocene sapropels (Table 1). The five fold increase in Ba/Al ratios indicates enhanced export productivity during the C/T OAE (Fig. 5).

Assuming that the mechanism for Ba enrichment in decaying OM during the Cretaceous was similar to that proposed for more recent settings [*Bishop*, 1988], we estimated productivity before and during the C/T OAE from Ba accumulation rates. Since under suboxic to anoxic diagenetic conditions Ba preservation may be reduced [*Dymond et al.*, 1992; *Falkner et al.*, 1993; *Francois et al.*, 1995; *McManus and et al.*, 1998], the productivity values obtained here could represent underestimates of the absolute values. The amount of OC (in $gC \cdot m^{-2} \cdot y^{-1}$) that is transported out of the photic zone (the export productivity, EP) was calculated, using equations proposed by *Francois et al.* [1995] and *Dymond et al.* [1992]. For a thorough discussion of this method see *Nijenhuis and de Lange* [2000]. The concentration of biogenic Ba was calculated using the Al content of the individual samples and assuming a detrital Ba/Al ratio of $6.1 \cdot 10^{-3}$ [*Dehairs et al.*, 2000]. Export productivity was calculated assuming a constant sedimentation rate of 3.5 cm/ky throughout the interval and using an average dry bulk density of $1.14 \ g \cdot cm^{-2} \cdot ky^{-1}$ [*Hayes et al.*, 1972]. The calculated EP prior to the C/T OAE is comparable to data for the Pliocene sapropels but considerably lower than for modern high productivity sites like the Arabian Sea (Table 1). During the C/T OAE the average EP value is five times higher than prior to the OAE and comparable to the Arabian Sea value.

In the modern ocean nitrate and phosphate formed upon remineralisation of particulate OM (POM) below the photic zone play a key role in sustaining primary productivity (=new production). Assuming this was also the case in the Cretaceous and the amount of nitrogen and phosphorus entering the photic zone was equal to the amount of nitrogen and phosphorus transported out (EP~new production), primary productivity (PP) was calculated from the EP values for site 367 using the equation of *Eppley and Peterson* [1979]:

Total production = (New production/ 0.0025)$^{1/2}$

The calculated average PP (Table 1) of 70 $gC \cdot m^{-2} \cdot y^{-1}$ before the C/T OAE is comparable to the low PP sites of the modern North Atlantic and Central pacific (Table 1). However, a significantly higher average PP of 180 $gC \cdot m^{-2} \cdot y^{-1}$ is calculated during the OAE, which is comparable to the high PP of the modern Arabian Sea and Black Sea. The calculated nearly threefold increase in PP (~100 $gC \cdot m^{-2} \cdot y^{-1}$) is large enough to explain the observed increase in OC accumulation rate at Site 367 during the C/T OAE. As a consequence, preservation factors (PF= OC accumulation rate divided by the

PP) for OC before and during the C/T OAE are identical (both ~5‰). This PF is comparable to what was previously suggested [*Bralower and Thierstein*, 1987] for mid-Cretaceous Black shales, and the maximum PF reported for the euxinic Holocene Black Sea [*Arthur et al.*, 1994] and is consistent with anoxic water column conditions during as well as before the C/T OAE.

3.3.4.2 Stable carbon isotopes. The degree of photosynthetic carbon fractionation (ε_p) for marine phytoplankon shows a strong negative correlation with both growth rate and cell size [e.g. *Laws et al.*, 1995; *Popp et al.*, 1998] therefore an increase in PP should be reflected in $\delta^{13}C$ values of phytoplankton-derived organic matter.]. However, ε_p values for marine phytoplankton also shows a pronounced dependence on CO_2 concentration [*Rau et al.*, 1989]. Therefore, the drop in atmospheric CO_2 concentrations resulting from enhanced OC burial rate during the C/T OAE [*Arthur et al.*, 1988; *Freeman and Hayes*, 1992; *Kuypers et al.*, 1999] should likewise be reflected in the stable carbon isotopic composition of phytoplanktonic OC.

To assess whether there is any carbon isotopic evidence for enhanced PP in the southern proto-North Atlantic during the C/T OAE changes in ε_p values for phytoplankton were determined. $\delta^{13}C$ values for inorganic carbon, which are needed to calculate ε_p, could not directly be determined due to diagenetic alteration (S13 and site 144) or absence of carbonate carbon (site 367). Since enhanced OC burial during the C/T OAE should have affected the stable carbon isotopic composition of inorganic carbon globally in a similar way, data from other sites with better preserved carbonate records are used instead. Such globally dispersed sites indicate that the positive excursion in marine carbonate $\delta^{13}C$ values was ~2.5‰ [e.g. *Arthur et al.*, 1988; *Jenkyns et al.*, 1994]. However, shoaling of the chemocline discussed previously could have introduced ^{13}C depleted recycled inorganic carbon into the photic zone causing smaller increases in $\delta^{13}C$ values for inorganic carbon in the southern proto-North Atlantic. Therefore, the estimated shift of 2.5 ‰ for inorganic carbon is likely a maximum value, and estimated shifts in ε_p are interpreted as minimum values. Assuming a 2.5‰ excursion for inorganic carbon, the 6‰ increase in the $\delta^{13}C$ values for S-bound phytane at site 367 (Figs. 5) records a 3.5‰ decrease in ε_p values. A slightly smaller decrease in ε_p values is suggested by the 5‰ increase in $\delta^{13}C$ values observed for steranes at site S13 (Figs. 3). Coring gaps probably obscure the later part of phase A of the carbon isotope excursion at site 144. The 2‰ decrease in ε_p values that was calculated from the 4.5‰ increase in $\delta^{13}C$ values for S-bound phytane at site 144 (Fig. 5) could therefore be larger. A significantly smaller decrease in ε_p (< 2‰) is indicated by the 4-4.5‰ increase in $\delta^{13}C$ values for S-bound phytane at site 603B [*Kuypers et al.*, unpublished results]. For the Cretaceous Western Interior Seaway (North America) geoporphyrin fractions were used to calculate a 1.5‰ decrease in ε_p values during the C/T OAE [*Hayes et al.*, 1989], and subsequently interpreted as a *c.* 20% reduction in atmospheric CO_2 concentration [*Freeman and Hayes*, 1992]. The shift in ε_p values has only been directly measured for the Cretaceous Western Interior Seaway; nonetheless, the shift in $\delta^{13}C$ values for the geoporphyrin fractions is smaller than for any other OC record, be it bulk or molecular fossils of phytoplanktic origin. This prompted us [*Kuypers* et al., 1999] to suggest that the drop in CO_2 concentrations could have been larger than the 20% suggested by Freeman and Hayes [1992]. However, sites 367 and S13 both exhibit shifts in $\delta^{13}C$ values larger than reported for any other

site indicating significantly larger ε_p shifts -and these are likely minimum estimates. Thus, although we can not determine the absolute effect of either decreased CO_2 concentrations or enhanced algal growth rate/average cell size on the OC isotope records, it seems likely that an increase in PP accounts for the larger shift in $\delta^{13}C$ values for molecular fossils of phytoplanktic origin at sites 367 and S13. This is entirely consistent with the increase in Ba/Al ratios for site 367 and the fact that these two sites experienced a dramatic increase in OC MAR while bottom water redox conditions did not change.

3.4. Palaeoceanographic Implications

The combined redox proxies indicate that the southern part of the proto-North Atlantic Ocean was already periodically euxinic from the bottom to at least the base of the photic (<150 m) zone before the C/T OAE. This is in good agreement with the results obtained from model simulations for the Albian and early Cenomanian proto-North Atlantic Ocean circulation [*Poulsen*, 1999] and probably resulted from a combination of overall sluggish circulation (possibly halothermal instead of thermohaline) and the tectonically isolated nature of the proto-North Atlantic (Fig. 1). Sedimentological and geochemical data from the proto-North Atlantic indicate that anoxic conditions persisted in the southern and southeastern part, while the northern and northeastern part was oxic during most of the Albian to late Cenomanian [*de Graciansky et al.*, 1984]. Conditions in the northwestern part were more versatile with alternating oxic and anoxic periods. The coexistence of oxic and anoxic conditions in the proto-North Atlantic could have resulted from a barrier restricting deep water exchange between the southeastern and northwestern part of the basin [*de Graciansky et al.*, 1984]. Enhanced PP as a result of wind driven upwelling in the equatorial region [*Handoh et al.*, 1999] could have further diminished the oxygen content of the southern part of the proto-North Atlantic Ocean.

During the C/T OAE there was a significant shoaling of the chemocline as indicated by the large increase in the concentrations of molecular fossils of green sulfur bacteria. The occurrence of molecular fossils of pigments specific for the green strain of green sulfur bacteria even indicates that the upper part of the photic zone (<15 m) periodically contained sulfide during the C/T OAE. However, the increase (up to 17 gC·m^{-2}·y^{-1}) in OC accumulation rates at shallow (~300 m; site S13), intermittent (~1300 m; site 144) and deep (3700 m; site 367) water settings probably cannot be attributed to enhanced preservation as our trace metal data suggests there was no major change in bottom water redox conditions.

There is evidence (e.g. enhanced Ba accumulation rates, significantly larger shifts in $\delta^{13}C$ values for OC of phytoplanktic origin than in any other Cretaceous marine realm) for enhanced PP during the C/T OAE in the southern proto-North Atlantic. The increase in PP (~100 gC·m^{-2}·y^{-1}) is large enough to explain the observed increase in OC accumulation rate at site 367 during the C/T OAE. In the modern ocean enhanced PP is closely linked with intensified upwelling of intermediate waters into the photic zone. In accordance with this it has been suggested that fertilisation of the surface waters by upwelling stimulated primary productivity leading to the widespread deposition of OC-rich sediments during the C/T OAE [e.g. *Arthur et al.*, 1987; *Parrish*, 1995]. Enhanced upwelling on a global scale has been attributed to either the initiation of a deep connection between

the proto-North and South Atlantic basins [*Tucholke and Vogt*, 1979; *Summerhayes*, 1987] or the increased formation of warm, saline deep water as a result of a world wide transgression [*Arthur et al.*, 1987].

As alternatives to enhanced upwelling, enhanced volcanism [*Sinton and Duncan*, 1997] and leaching of flooded coastal lowlands [*Erbacher et al.*, 1996] have been suggested as sources for biolimiting nutrients during the C/T OAE. Introduction of hydrothermal Fe to the surface waters could have produced large-scale plankton blooms, but only in basins where Fe was biolimiting. This was probably not the case for the small Atlantic basins where sufficient Fe could be supplied by riverine or aeolian input from the surrounding land [*Sinton and Duncan*, 1997]. Leaching of nutrients from flooded coastal areas could have enhanced PP in the southern proto-North Atlantic. Oxygen utilisation resulting from mineralisation of enhanced OM input could even have facilitated shoaling of the chemocline. However, it is hard to imagine how enhanced PP on its own could lead to euxinic conditions in the generally well mixed upper 15 m of the water column. Thus, we conclude that the co-occurrence of enhanced PP and shoaling of the chemocline in the southern part of the proto-North Atlantic was caused by enhanced upwelling providing new nutrients and sulfide-containing water to the photic zone. The enhanced production of warm, saline deep water could have led to enhanced upwelling and thereby explain the observed changes in the southern proto-North Atlantic during the C/T OAE. It is generally assumed that the rate of production of warm, saline deep water was proportional to the area of shelf flooding and that maximum flooding occurred during the C/T OAE [*Arthur et al.*, 1987]. However, according to *Haq et al.* [1987] the maximum sea level high stand occurred during the early/middle Turonian rather than late Cenomanian, which would argue against a world wide transgression being the ultimate driving force for the C/T OAE.

Alternatively, influx of dense saline water from a different ocean basin could have caused the inferred upwelling. Evidence for the establishment of a deep water connection between the proto-North and South Atlantic basins through the Equatorial Atlantic Gateway may come from the widespread hiatus in the open ocean sediment record of the South Atlantic, which was attributed to an erosional event near the C/T transition [*Zimmerman et al.*, 1987]. A similar unconformity has been recognised through much of the North Atlantic and western Tethyan Seaway [*de Graciansky et al.*, 1984]. In addition, the sedimentary record of the Equatorial Atlantic Gateway has provided evidence for erosive deep water currents, and this has been attributed to the formation of a deep connection between proto-North and South Atlantic basins during the late Cenomanian [*Wagner and Pletsch*, 1999]. There is also evidence from Nd isotopes for invigorated exchange of water between the Atlantic basins and the Pacific at approximately the same time [*Stille et al.*, 1996]. The influx into the proto-North Atlantic of large amounts of highly saline, old, oxygen deficient water from the South Atlantic would have displaced deep water towards the surface [*Tucholke and Vogt*, 1979; *Summerhayes*, 1987]. As a more or less stagnant anoxic basin possibly with a partly estuarine-like circulation [*Arthur et al.*, 1987; *Thierstein and Berger*, 1979], the proto-North Atlantic could have acted as a nutrient trap [*Summerhayes*, 1987] comparable to the Holocene Black Sea and Cariaco Trench that contain high levels of dissolved nutrients such as ammonium and phosphorus [*Sarmiento et al.*, 1988; *Fry et al.*, 1991]. Thus, water brought to the surface as a consequence of the influx of South Atlantic dense water was likely extremely nutrient-rich, such

that upwelling could have globally enhanced PP and caused OC burial to increase; this would have persisted until nutrients from the proto-North Atlantic and the South Atlantic were depleted. Eventually, oxygenated deep water from the eastern Southern Ocean could have entered the proto-North Atlantic during the Turonian [*Poulsen*, 1999] ending the deposition of OC rich sediments.

3.5 References

Arthur, M. A., W. A. Dean, E. D. Neff, B. J. Hay, J. King, and G. Jones, Varve calibration records of carbonate and organic carbon accumulation over the last 2000 years in the Black Sea, *Global Biochem. Cycles*, 8, 195-217, 1994.

Arthur, M. A., W. A. Dean, and L. M. Pratt, Geochemical and climatic effects of increased marine organic carbon burial at the Cenomanian/Turonian boundary, *Nature*, 335, 714-717, 1988.

Arthur, M. A., W. E. Dean, and D. A. V. Stow, Models for the deposition of Mesozoic-Cenozoic fine-grained organic-carbon-rich sediment in the deep sea, in *Fine-grained sediments*, edited by D. A. V. Stow and D. Piper, pp. 527-562, Geol. Soc. Lond. Spec. Publ., London, 1984.

Arthur, M. A., H. C. Jenkyns, H.-J. Brumsack, and S. O. Schlanger , Stratigraphy, geochemistry, and paleoceanography of organic carbon-rich cretaceous sequences, *Cretaceous Resources, Events and Rhythms*, 75-119, 1990.

Arthur, M. A., S. O. Schlanger , and H. C. Jenkyns, The Cenomanian-Turonian Oceanic anoxic event. II. Palaeoceanographic controls on organic-matter production and preservation, *Geol. Society Spec. Publ.*, 26, 401-420, 1987.

Barron, E. J., A warm, equable Cretaceous: the nature of the problem, *Earth-Science Reviews*, 19, 305-338, 1983.

Berger, W. H. and U. von Rad, Cretaceous and Cenozoic sediments from the Atlantic Ocean, *Initial Reports of the Deep Sea Drilling Project*, 14, 787-954, 1972.

Berner, R. A., Palaeo-CO_2 and climate, *Nature*, 358, 114-114, 1992.

Bishop, J. K. B., The barite-opal-organic carbon association in oceanic particulate matter, *Nature*, 332, 341-343, 1988.

Bralower, T. J. and H. R. Thierstein, Organic carbon and metal accumulation rates in Holocene and mid-Cretaceous sediments: palaeoceanographic significance, *Geological Society Special Publication*, 26, 345-369, 1987.

Brumsack, H. J. and J. W. Thurow, The geochemical facies of black shales from the Cenomanian/Turonian boundary event (CTBE), *Mitt.Geol.-Paläeont.Inst.Univ.Hamburg*, 60, 247-265, 1986.

Calvert, S. E. and T. F. Pedersen, Geochemistry of recent oxic and anoxic marine sediments: Implications for the geological record, *Mar. Geol.*, 113, 67-88, 1993.

Caron, M., F. Robazynski, F. Amedro, F. Baudin, Deconinck J.F., P. Hochhuli, K. von Salis-Perch Nielsen, and N. Tribovillard, Estimation de la durée de l'événement anoxique global au passage Cénomanien/Turonien. Approche cyclostratigraphique dans la formation Bahloul en Tunisie centrale, *Bull. Soc. Géol. France*, 170, 144-160, 1999.

de Graciansky, P. C., G. Deroo, J. P. Herbin, L. Montadert, C. Müller, A. Schaaf, and J. Sigal, Ocean -wide stagnation episode in the late Cretaceous, *Nature*, 308, 346-349, 1984.

Dean, W. E., J. V. Gardner, and D. Z. Piper, Inorganic geochemical indicators of glacial-interglacial changes in productivity and anoxia on the California continental margin, *Geochim. Cosmochim. Acta*, 61, 4507-4518, 1997.

Dehairs, F., N. Fagel, A. N. Antia, R. Peinert, M. Elskens, and L. Goeyens, Export production in the Bay of Biscay as estimated from barium-barite in settling material: a comparison with new production, *Deep Sea Res. I*, 47, 583-601, 2000.

Dymond, J., E. Suess, and M. Lyle, Barium in deep-sea sediment: A geochemical proxy for paleoproductivity, *Paleoceanography*, 7, 163-181, 1992.

Eppley, R. W. and B. J. Peterson, Particulate organic matter flux and planktonic new production in the deep ocean, *Nature*, 282, 677-680, 1979.

Erbacher, J., J. W. Thurow, and R. Littke, Evolution patterns of radiolaria and organic matter variations: A new approach to identify sea-level changes in mid-Cretaceous pelagic environments, *Geology*, 24, 499-502, 1996.

Falkner, K. K., G. P. Klinkhammer, T. S. Bowers, J. F. Todd, B. l. Lewis, W. M. Landing, and J. M. Edmond, The behavior of barium in anoxic marine waters, *Geochim. Cosmochim. Acta*, 57, 537-554, 1993.

Francois, R., S. Honjo, S. J. Manganini, and G. E. Ravizza, Biogenic barium fluxes to the deep sea: Implications for paleoproductivity reconstruction, *Global Biochem. Cycles*, 9, 289-303, 1995.

Freeman, K. H. and J. M. Hayes, Fractionation of carbon isotopes by phytoplankton and estimates of ancient CO_2 levels, *Global Biochem. Cycles*, 6, 185-198, 1992.

Fry, B., H. W. Jannasch, S. J. Molyneaux, C. O. Wirsen, J. A. Muramoto, and S. King, Stable isotope studies of carbon, nitrogen and sulfur cycles in the Black Sea and the Cariaco Trench, *Deep Sea Res.*, 38, 1003-1019, 1991.

Gale, A. S., Cyclostratigraphy and the correlation of the Cenomanian Stage in Western Europe, *Geological Society Special Publication*, 85, 177-197, 1995.

Gale, A. S., H. C. Jenkyns, W. J. Kennedy, and R. M. Corfield, Chemostratigraphy versus biostratigraphy: data from around the Cenomanian-Turonian boundary, *J. Geol.l Soc., London*, 150, 29-32, 1993.

Gradstein, F., F. P. Agterberg, J. G. Ogg, J. Hardenbol, P. van Veen, J. Thierry, and H. Huang, A Triassic, Jurassic, and Cretaceous time scale, *SEPM Special Publications*, 54, 95-126, 1995.

Handoh, I. C., G. R. Bigg, E. J. W. Jones, and M. Inoue, An ocean modeling study of the Cenomanian Atlantic: equatorial paleo-upwelling, organic-rich sediments and the consequences for a connection between the proto-North and South Atlantic, *Geophys. Res. Lett.*, 26, 223-226, 1999.

Haq, B. U., J. Hardenbol, and P. R. Vail, Chronology of fluctuating sea levels since the Triassic, *Science*, 235, 1156-1167, 1987.

Hasegawa, T., Cenomanian-Turonian carbon isotope events recorded in terrestrial organic matter from northern Japan, *Palaeogeograph. Palaeoclimatol. Palaeoecol.*, 130, 251-273, 1997.

Hayes, D. E. and et al., Sites 143 and 144, *Initial Reports of the Deep Sea Drilling Project*, 14, 283-338, 1972.

Hayes, J. M., B. N. Popp, R. Takigiku, and M. W. Johnson, An isotopic study of biochemical relationships between carbonates and organic carbon in the Greenhorn formation, *Geochim. Cosmochim. Acta*, 53, 2961-2972, 1989.

Herbin, J. P., L. Montadert, C. Müller, R. Gomez, J. W. Thurow, and J. Wiedmann, Organic-rich sedimentation at the Cenomanian-Turonian boundery in oceanic and coastal basins in the North Atlantic and Tethys, *Geol. Soc. Spec. Publ.*, 21, 389-422, 1986.

Imhoff, J. F., Taxonomy and physiology of phototrophic purple bacteria and green sulfur bacteria, in *Anoxygenic photosynthetic bacteria*, edited by R. E. Blankenship, M. T. Madigan, and C. E. Bauer, pp. 1-15, Kluwer Academic Publishers, Dordrecht, 1995.

Jenkyns, H. C., A. S. Gale, and R. M. Corfield, Carbon- and oxygen- isotope stratigraphy of the English Chalk and Italian Scaglia and its palaeoclimatic significance, *Geol.Mag.*, 131, 1-34, 1994.

Kohnen, M. E. L., S. Schouten, J. S. Sinninghe Damsté, J. W. De Leeuw, D. A. Merritt, and J. M. Hayes, Recognition of paleobiochemicals by a combined molecular sulfur and isotope geochemical approach, *Science*, 256, 358-362, 1992.

Kuhnt, W., J. P. Herbin, J. W. Thurow, and J. Wiedmann, Distribution of Cenomanian-Turonian organic facies in the western Mediterranean and along the Adjacent Atlantic Margin, *AAPG Stud. Geol.*, 30, 133-160, 1990.

Kuhnt, W., A. J. Nederbragt, and L. Leine, Cyclicity of Cenomanian-Turonian organic-carbon-rich sediments in the Tarfaya Atlantic Coastal Basin (Morocco), *Cret. Res.*, 18, 587-601, 1997.

Kuypers, M. M. M., R. D. Pancost, and J. S. Sinninghe Damsté, A large and abrupt fall in atmospheric CO_2 concentration during Cretaceous times, *Nature*, 399, 342-345, 1999.

Laws, E. A., B. N. Popp, R. R. Bidigare, M. C. Kennicutt, and S. A. Macko, Dependence of phytoplankton carbon isotopic composition on growth rate and $(CO_2)_{aq}$: Theoretical considerations and experimental results, *Geochim. Cosmochim. Acta*, 59, 1131-1138, 1995.

McManus, J. and et al., Geochemistry of barium in marine sediments: Implications for its use as a paleoproxy, *Geochim. Cosmochim. Acta*, 62, 3453-3473, 1998.

Nederbragt, A. J., R. N. Erlich, B. W. Fouke, and G. M. Ganssen, Plalaeoecology of the biserial planktonic foraminifer *Heterohelix moremani* (Cushman) in the late Albian to middle Turonian Circum-North Atlantic, *Palaeogeograph. Palaeoclimatol. Palaeoecol.*, 144, 115-133, 1998.

Nijenhuis, I. A. and G. J. de Lange, Geochemical constraints on Pliocene sapropel formation in the eastern Mediterranean, *Mar. Geol.*, 163, 41-63, 2000.

Parrish, J. T., Paleogeography of C_{org}-rich rocks and the preservation versus production controversy, in *Paleogeography, paleoclimate and source rocks*, edited by A. Y. Huc, pp. 1-20, American Association of Petroleum Geologists, USA, 1995.

Passier, H. F., H. J. Bosch, I. A. Nijenhuis, L. L. Lourens, M. E. Bottcher, A. Leenders, J. S. Sinninghe Damsté, G. J. de Lange, and J. W. De Leeuw, Sulphidic Mediterranean surface waters during Pliocene sapropel formation, *Nature*, 397, 146-149, 1999.

Popp, B. N., E. A. Laws, R. R. Bridigare, J. E. Dore, K. L. Hanson, and S. G. Wakeham, Effect of phytoplankton cell geometry on carbon isotopic fractionation., *Geochim. Cosmochim. Acta*, 62, 69-77, 1998.

Poulsen, C. J., The mid-Cretaceous ocean circulation and its impact on Greenhouse Climate dynamics, Ph.D. thesis, Pennsylvania State University, Pennsylvania, 1999.

Rau, G. H., T. Takahashi, and D. J. Des Marais, Latitudinal variations in plankton $\delta^{13}C$: implications for CO_2 and productivity in past oceans, *Nature*, 341, 516-518, 1989.

Repeta, D. J., A high resolution historical record of Holocene anoxygenic primary production in the Black Sea, *Geochim. Cosmochim. Acta*, 57, 4337-4342, 1993.

Ricken, W., Sedimentation as a three-component system, *Lecture Notes in Earth Sciences*, 51, 1-211, 1993.

Sarmiento, J. L., T. Herbert, and J. R. Toggweiler, Mediterranean nutrient balance and episodes of anoxia, *Global Biogeochem. Cycles*, 2, 427-444, 1988.

Schlanger , S. O. and H. C. Jenkyns, Cretaceous oceanoc anoxic events: causes and consequences, *Geologie Mijnbouw*, 55, 179-184, 1976.

Schouten, S., W. C. M. Klein Breteler, P. Blokker, N. Schogt, W. I. C. Rijpstra, K. Grice, M. Baas, and J. S. Sinninghe Damsté, Biosynthetic effects on the stable carbon isotopic composition of algal lipids: Implications for deciphering the carbon isotopic biomarker record, *Geochim. Cosmochim. Acta*, 62, 1397-1406, 1998.

Scotese, C. R. and J. Golonka, Paleogeographic Atlas, University of Texas, Arlington, 1992.

Sinninghe Damsté, J. S., M. D. Kok, J. Köster, and S. Schouten, Sulfurized carbohydrates: and important sedimentary sink for organic carbon?, *Earth Planet. Sci. Lett.*, 164, 7-13, 1998.

Sinninghe Damsté, J. S. and M. P. Koopmans, The fate of carotenoids in sediments: An overview, *Pure Appl. Chem.*, 69, 2067-2074, 1997.

Sinninghe Damsté, J. S. and J. Köster, A euxinic southern North Atlantic Ocean during the Cenomanian/Turonian oceanic anoxic event, *Earth Planet. Sci. Lett.*, 158, 165-173, 1998.

Sinninghe Damsté, J. S., S. G. Wakeham, M. E. L. Kohnen, J. M. Hayes, and J. W. de Leeuw, A 6,000-year sedimentary molecular record of chemocline excursions in the Black Sea, *Nature*, 362, 827-829, 1993.

Sinton, C. W. and R. A. Duncan, Potential link between ocean plateau volcanism and global ocean anoxia at the Cenomanian-Turonian boundary, *Economic Geol.*, 92, 838-842, 1997.

Stille, P., M. Steinmann, and S. R. Riggs, Nd isotope evidence for the evolution of the paleocurrents in the Atlantic and Tethys Oceans during the past 180 Ma, *Earth Planet. Sci. Lett.*, 144, 9-19, 1996.

Summerhayes, C. P., Organic-rich Cretaceous sediments from the North Atlantic, *Geol. Soc. Spec. Publ.*, 26, 301-316, 1987.

The Shipboard Scientific Party, Site 367: Cape Verde Basin, *Initial Reports of the Deep Sea Drilling Project*, 41, 163-232, 1977.

Thierstein, H. R. and W. H. Berger, Injection events in earth history, *Nature*, 276, 461-466, 1979.

Thomson, J., N. C. Higgs, T. R. S. Wilson, I. W. Croudace, G. J. de Lange, and P. J. M. van Santvoort, Redistribution and geochemical behaviour of redox-sensitive elements around S1, the most recent eastern Mediterranean sapropel, *Geochim. Cosmochim. Acta*, 59, 3487-3501, 1995.

Thurow, J. W., M. Moullade, H. J. Brumsack, E. Masure, J. Taugourdou, and K. Dunham, The Cenomanian-Turonian Boundary Event (CTBE) at Leg 103/Hole 641A, *Proceedings of the Ocean Drilling Program, Scientific Results*, 103, 587-634, 1988.

Tucholke, B. E. and P. R. Vogt, Western North Atlantic: sedimentary evolution and aspects of tectonic history, *Initial Reports of the Deep Sea Drilling Project*, 43, 791-825, 1979.

van der Weijden, C. H., G. J. Reichart, and H. J. Visser, Enhanced preservation of organic matter in sediments deposited within the oxygen minimum zone in the northeastern Arabian Sea, *Deep Sea Res. I*, 46, 807-830, 1999.

van Gemerden, H. and J. Mas, Ecology of phototrophic sulfur bacteria, in *Anoxygenic photosynthetic bacteria*, edited by R. E. Blankenship, M. T. Madigan, and C. E. Bauer, pp. 49-85, Kluwer Academic Publishers, Dordrecht, 1995.

Volkman, J. K., A review of sterol markers for marine and terrigenous organic matter, *Org. Geochem.*, 9, 83-99, 1986.

Wagner, T. and T. Pletsch, Tectono-sedimentary controls on the Cretaceous black shale deposition along the opening Equatorial Atlantic Gateway (ODP Leg 159), *Geol. Soc. Spec. Publ.*, 153, 241-265, 1999.

Zimmerman, H. B., A. Boersma, and F. W. McCoy, Carbonaceous sediments and palaeoenvironment of the Cretaceous South Atlantic Ocean, *Geol. Soc. Spec. Publ.*, 26, 271-286, 1987.

Chapter 4

Orbital forcing of organic carbon accumulation in the proto-North Atlantic during the Cenomanian/Turonian oceanic anoxic event

Marcel M.M. Kuypers, W. Irene C. Rijpstra, Richard D. Pancost, Ivar A. Nijenhuis, Jaap S. Sinninghe Damsté

Abstract.

The Cenomanian/Turonian intervals at DSDP sites 105 and 603B from the northern part of the proto North Atlantic show high amplitude, short-term cyclic variations in TOC contents. The more pronounced changes in TOC are also reflected by changes in lithology from green claystones (TOC < 1%) to black claystones (TOC > 1%). Although their depositional history was very different, the individual TOC cycles at sites 105 and 603B can be correlated using stable carbon isotope stratigraphy. Sedimentation rates obtained from the isotope stratigraphy and spectral analyses indicate that these cycles were predominately precession controlled. The coinciding variations in HI, OI, $\delta^{13}C_{org}$, and the abundance of marine relative to terrestrial biomarkers as well as the low abundance of lignin pyrolysis products generated from the kerogen of the black claystones indicate that these cyclic variations reflect changes in the contribution of marine OM. The co-occurrence of lamination, enrichment of redox sensitive trace metals and presence of molecular fossils of pigments from green sulfur bacteria indicates that the northern proto-North Atlantic Ocean water column was sometimes euxinic from the bottom to at least the base of the photic zone (<150 m) during the deposition of the black claystones. In contrast, the green claystones are bioturbated, are enriched in Mn, do not show enrichments in redox sensitive trace metals and show biomarker distributions indicative of long oxygen exposure times, indicating more oxic water conditions. At the same time there is evidence (e.g. enhanced Ba/Al ratios, abundance of biogenic silica and significant ^{13}C-enrichment for OC of phytoplanktic origin) for enhanced primary productivity during the deposition of the black claystones. We propose that increased primary productivity periodically overwhelmed the oxic OM remineralisation potential of the bottom waters resulting in the deposition of OM-rich black claystones. Because the amount of oxygen used for OM remineralisation exceeded the amount supplied by diffusion and deep-water circulation the northern proto North Atlantic became euxinic during these periods. Both sites 105 and 603B show trends of continually increasing TOC contents and HI values of the black claystones up section, which most likely resulted from both enhanced preservation due to increased anoxia and increased production of marine OM during the C/T OAE.

4.1 Introduction

During the Cenomanian/Turonian (C/T) transition laminated sediments rich (> 1%) in organic carbon (OC) (black shales) were globally deposited in a variety of paleo-bathymetric settings [*Schlanger and Jenkyns*, 1976]. Evidence for the global nature of this organic carbon burial event is provided by a coinciding increase in $^{13}C/^{12}C$ ratios for marine carbonates and organic matter. This positive excursion in $\delta^{13}C$ values likely resulted from preferential removal of ^{12}C by the enhanced burial of ^{13}C depleted OC as a response to the so-called 'C/T oceanic anoxic event (OAE)' [*Arthur et al.*, 1988]. The widespread deposition of black-shales during the C/T OAE has been attributed to either decreased OM remineralisation resulting from a decreased oxygen flux (preservation model) [*Bralower and Thierstein*, 1987] or increased primary productivity overwhelming the oxic OM remineralisation potential of the water column (productivity model) [*Schlanger and Jenkyns*, 1976]. The preservation model has mainly been applied for tectonically isolated basins such as the Cretaceous North and South Atlantic [*Zimmerman et al.*, 1987; *De Graciansky et al.*, 1984]. Model simulations for the Albian and early Cenomanian ocean circulation [*Poulsen et al.*, 1999]; *Bice*, personal communication] show that especially the proto-North Atlantic was prone to water column anoxia due to a combination of overall sluggish circulation (possibly halothermal instead of thermohaline), high sea surface temperatures and the tectonically isolated nature of the proto-North Atlantic basin (Fig. 1).
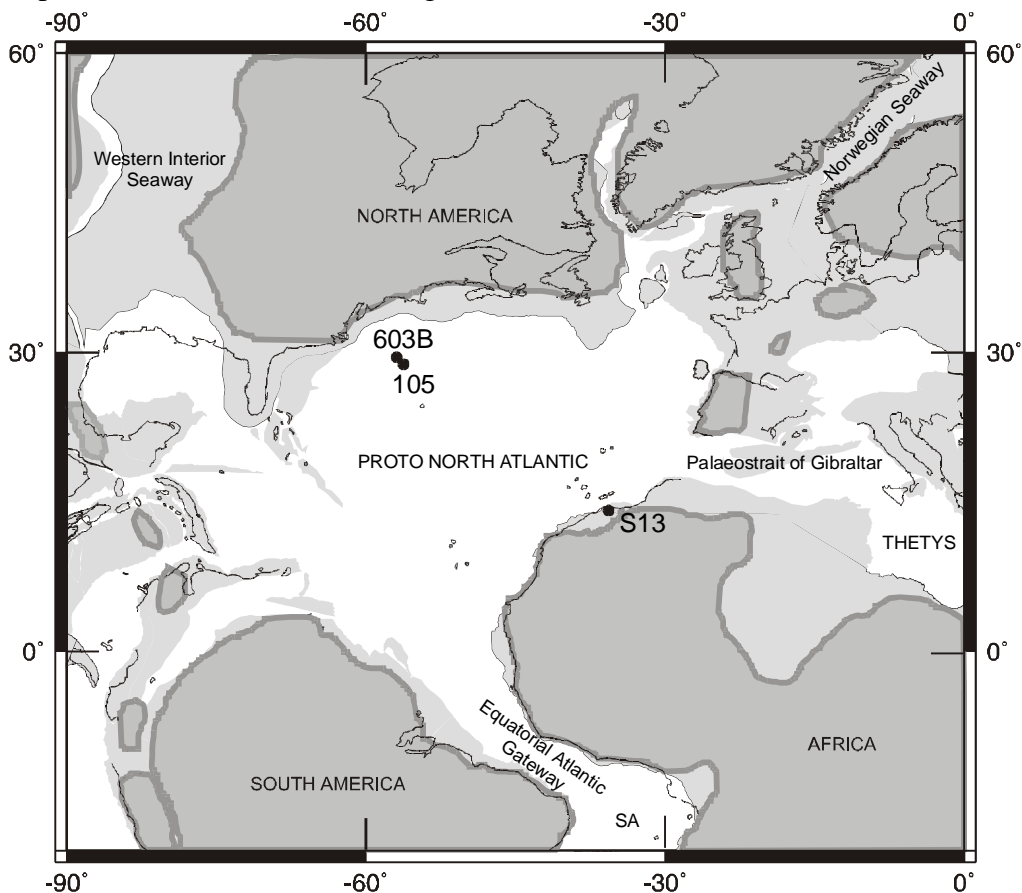

Figure 1. Palaeogeographical map of mid Cretaceous (~94 Ma) North Atlantic showing the position of the four studied cores. Light grey shaded regions represent flooded continental plates (from GEOMAR map generator;

www.odsn.de/odsn/services/paleomap/paleomap.html). Dark grey shaded regions represent land [*Scotese and Golonka*, 1992].

The reoccurrence of thinly laminated OM–rich sediments devoid of traces of benthic activity indicates that proto-North Atlantic bottom-waters were indeed periodically anoxic during the mid Cretaceous [*Summerhayes*, 1987; *Bralower and Thierstein*, 1987]. Sedimentary derivatives (molecular fossils) of a pigment indicative of anoxygenic photosynthetic bacteria recovered from abyssal and shelf sites indicate that anoxic conditions extended even into the photic zone of the southern proto-North Atlantic during the C/T OAE [*Sinninghe Damsté and Köster*, 1998]. Recently we provided evidence (e.g. occurrence of molecular fossils of green sulfur bacteria, lack of bioturbation and high abundance of redox sensitive trace metals) that the southern part of the proto-North Atlantic Ocean was already euxinic up into the photic zone well before the C/T OAE [Kuypers et al., 2000 submitted to Pal.]. Sedimentological and geochemical data from the proto-North Atlantic indicates that anoxic bottom-water conditions persisted in the southern and southeastern part during most of the late Aptian to late Cenomanian [*De Graciansky et al.*, 1987]. However, in the northwestern part conditions were more versatile with alternating oxic and anoxic periods [*De Graciansky et al.*, 1987]. Herbin et al. [*Herbin et al.*, 1987a] showed that the C/T OAE interval at sites 105 and 603B is not a single, homogeneous, black shale layer but rather a condensation of several black claystone layers alternating with thinner levels of green claystone. The coexistence of permanently anoxic conditions in the southern part and alternating oxic and anoxic conditions in the northwestern part of the proto-North Atlantic has been attributed to restricted deep water exchange as a result of a barrier between the southeastern and northwestern part of the basin [*De Graciansky et al.*, 1987]. The diminished oxygen content of the southern part of the proto-North Atlantic Ocean has been suggested to result from enhanced primary productivity (PP) as a result of wind driven upwelling in the equatorial region [*Handoh et al.*, 1999].

Here we provide evidence of precessional forcing in the C/T OAE intervals for these northwestern proto-North Atlantic sites using isotope-stratigraphy and spectral analysis. In addition, changes in geochemical parameters of two green-black-green claystone cycles were studied in high resolution and the results are used together with the data obtained from an overall geochemical analyses for the C/T OAE interval to reconstruct precessional forced chemocline variations and variations in primary productivity.

4.2. Material and methods

4.2.1 Material. The sediment samples used in this study were obtained from the Deep Sea Drilling Project (DSDP) sites 105 (leg 11) and 603B (leg 93) off the coast of North America. One to five cm thick sediment slices were taken from the cores. Sub-samples were taken from these slices and subsequently freeze-dried and powdered in an agate mortar.

4.2.2 Organic matter analyses. Analyses of soluble and insoluble organic matter were performed as described previously by Kuypers et al. [2000; submitted to Paleoceanography]. Briefly, Total Organic Carbon (TOC) contents were determined using a CN analyser. The $\delta^{13}C$ values ($\pm0.1‰$

versus Vienna Pee Dee belemnite (VPDB)) were measured on bulk sediments, after removal of the inorganic carbonates with diluted HCl, using automated on-line combustion followed by conventional isotope ratio-mass spectrometry. For analyses of the soluble OM powdered samples (15 to 30 g) were Soxhlet extracted for c. 24 h to obtain the total extract. The total extract was separated into an apolar and a polar fraction using column chromatography. The hydrocarbons that were released from the polar fraction by Raney Nickel desulfurisation and subsequent hydrogenation [*Sinninghe Damsté et al.*, 1990] were isolated using column chromatography. Samples were analysed by gas chromatography-mass spectrometry (GC-MS) for compound identification. Compound-specific $\delta^{13}C$ analyses were performed using a Finnigan Delta C GC-isotope-ratio-monitoring MS. The $\delta^{13}C$ values for individual compounds are the means of duplicate runs ($\sigma = \pm 0.3$ to 0.6) expressed versus VPDB.

4.2.3 Inorganic analyses. For major, minor and trace element analyses, a 125 mg sample was digested in 5 ml HF (40%) and 5 ml of a $HClO_4/HNO_3$ mixture at 90 °C. After evaporation to dryness on a sand bath at 190°C, the residue was dissolved in 25 ml 1 M HCl. The resulting solutions were analysed with a Perkin Elmer Optima 3000 inductively coupled plasma atomic emission spectrometer (ICP-AES). The results were checked with international and house standards. For all ICP analyses, relative standard deviations in duplicate measurements are below 4%.

X-ray powder diffraction (XRD) was carried out on a home-built (NIOZ, Texel) high accuracy θ-θ diffractometer to determine the mineralogical composition of the sediments. CuKα radiation (40 kv, 40 mA) from a long fine focus tube was applied in combination with variable divergence and antiscatter slits, and an energy dispersive Si/Li detector (Kevex). The measuring slit was set at 0.2 mm and the counting time was 1 sec./0.02°2θ. The samples were Ca exchanged prior to analysis. The samples were measured at 50% relative humidity [*Kühnel and van der Gaast*, 1993] The patterns were corrected for the Lorentz and polarisation factor and for the irradiated specimen volume.

4. 2.4 Spectral analyses. Power spectra for the TOC and HI data from site 603B were obtained by using the AnalySeries 1.0 software. The Blackman-Tukey method was used for the spectral analysis of the high-resolution data set that was reported previously by Herbin et al. [1987]. The data sets were prepared by removing the linear trends of continually increasing TOC contents and HI values of the black claystones up section by determining and subsequently subtracting the linear regression between TOC contents or HI values and depth before using the Fourier technique.

4.3. Results and discussion

4.3.1 Stratigraphy and palaeosetting

Our study concentrates on the sediments of DSDP sites 105 and 603B that have been assigned a late Cenomanian to early Turonian age based on biostratigraphy [*Herbin et al.*, 1987a; *Thurow*, 1988]. Although these sites are only ~125 km apart, their depositional history was very

different with 603B located nearer to the coast and being influenced by coastal oceanic events, whereas Site 105 showed mainly pelagic influences [*Herbin et al.*, 1987a]. Both sites, however, show the OM-enrichment that characterizes C/T sediments worldwide [*Herbin et al.*, 1987a]. The C/T sequences at DSDP sites 105 and 603B consist of an alternation of OM-poor green claystones and OM-rich (TOC 1-25%) black claystones [*Herbin et al.*, 1987a]. Carbonate contents are low (<10%) which suggests that deposition took place below CCD. The hemipelagic sediments of site 603B as well as the pelagic sediments of site 105 were deposited at a water depth of ~4000 m [*Chénet and Francheteau*, 1979].
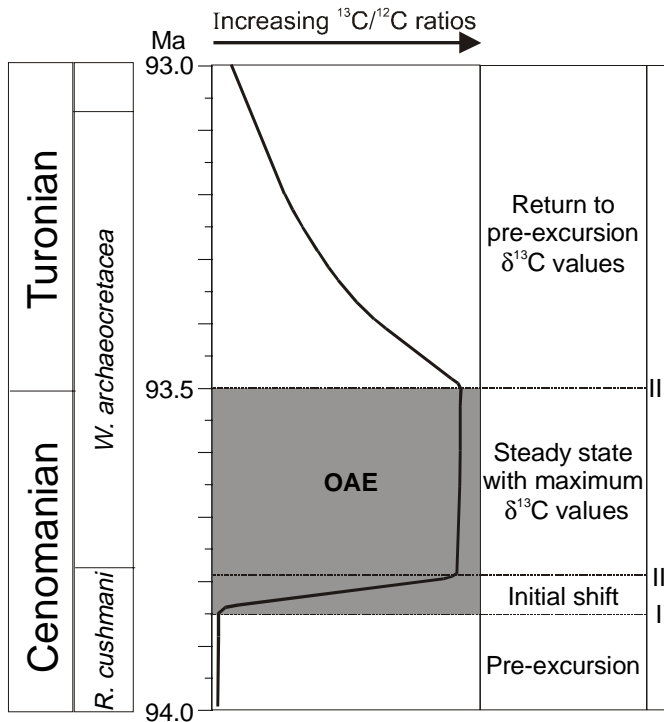
Figure 2. Idealised representation of C/T stable carbon isotope excursion showing the bio-and chronostratigraphic position of the three main phases (modified after [*Gale et al.*, 1993]). Dashed lines with roman numbers show the position of the boundaries between the different phases (pre-excursion, **A**, **B** and **C**) of the isotope excursion

Carbon isotope stratigraphy was used to constrain the C/T OAE interval and to correlate these abyssal sites with the Moroccan shelf site S13, a site with good bio-and chronostratigraphic control [*Kuhnt et al.*, 1997a]. For a more thorough discussion of this method see Kuypers et al. [2000]. The horizontal dotted lines with Roman numbers (I-III) in the idealised representation of C/T stable carbon isotope excursion (Fig. 2) indicate the boundaries between the pre-excursion conditions (i.e. pre-excursion $\delta^{13}C$ values) and the three main phases of the isotope excursion (i.e. rapid positive shift in $\delta^{13}C$ values, plateau with maximum $\delta^{13}C$ values and return to pre-excursion $\delta^{13}C$ values). Of particular stratigraphic significance is boundary II that nearly coincides with the last occurrence of the planktonic foraminifer *Rotalipora cushmani* [*Kuhnt et al.*, 1990] and boundary III, which approximately coincides with the C/T boundary [*Gale et al.*, 1993]. The positive excursion in $\delta^{13}C$ values reflects a change in the global atmospheric-oceanic pool of inorganic carbon resulting from a global increase in the burial rate of ^{13}C-depleted OC [*Arthur et al.*, 1988]. By definition the C/T OAE is the main phase of enhanced carbon burial rates and, therefore, should be coeval with the interval between boundaries I and III (phases A and B, indicated as a grey shaded area in Fig. 2).

Milankovitsch cyclicity-derived sedimentation rates (12 cm/ky) previously reported for the *Whiteinella archaeocretacea* zone of site S13 [*Kuhnt et al.*, 1997b] were used to calculate a duration of ~400 ky for the C/T OAE [Kuypers et al., 2000 submitted to Paleoceanography]. In a similar way phase A of the isotope excursion (Fig. 2), was estimated to be ~60 ky [*Kuypers et al.*, 1999]. Although the sample resolution introduces a significant margin of error, the ~400 ky for the C/T OAE is in good agreement with data from Western Europe [*Gale*, 1995] indicating ~350 ky (17 precession cycles) for the same interval. In addition, a duration of ~400 ky has recently been reported for the Tunesian Bahloul formation [*Caron et al.*, 1999], which approximately coincides with phases A and B of the C/T isotope excursion [*Vonhof*, 1998; *Nederbragt et al.*, 1998].

The use of molecular fossils that are specific for primary producers instead of bulk OM for stable carbon isotope stratigraphy greatly reduces the effect of heterotrophy, preservation, and diagenetic alteration on the carbon isotopic signature of OC [*Hayes et al.*, 1989; *Freeman and Hayes*, 1992; *Sinninghe Damsté et al.*, 1998]. At DSDP site 603B the stable carbon isotopic composition of the acyclic isoprenoid phytane released upon desulfurisation of the polar fraction (e.g. S-bound phytane) was used for carbon isotope stratigraphy (Fig. 3). This S-bound phytane mainly derives from the phytol moiety of phytoplanktonic chlorophyll [*Kohnen et al.*, 1992a] and, thus, reflects the changes in the stable carbon isotopic composition of phytoplankton [*Kohnen et al.*, 1992b]. The δ^{13}C profile for S-bound phytane (i.e. Ph) at DSDP site 603B shows the rapid shift in ^{13}C/^{12}C ratios that marks phase A as well as at least a part of phase B (the plateau with maximum δ^{13}C values) (Fig. 3). The isotopic record of TOC indicates that samples with a TOC < 1% are generally 1-3‰ enriched in ^{13}C relative to adjacent samples with a TOC > 1% (Fig. 3). This indicates that preservation may have affected the bulk OC δ^{13}C record. However, there is a general similarity in trend between the molecular fossil and bulk OC records for the C/T OAE interval (phases A and B) at DSDP site 603B if we exclude the δ^{13}C values of samples with a TOC < 1%. The offset of ~3‰ between δ^{13}C profiles for bulk OC and the molecular fossils of chlorophyll in this interval is well within the range reported for extant algae [*Schouten et al.*, 1998]. This offset is significantly larger (4-5‰) in the pre-excursion interval, which we also attribute to selective preservation (see below). As a consequence, the δ^{13}C excursion is ~1‰ smaller for bulk OC than for S-bound Ph (Fig. 3). The δ^{13}C excursion for bulk OC at DSDP site 105 is comparable in magnitude (~3 ‰) to site 603B (Fig. 4). At DSDP site 105 phase A and part of phase B can be distinguished. Assuming that the excursions in δ^{13}C values at all sites are synchronous [*Gale et al.*, 1993], data from site S13 was used to calculate average sedimentation rates for phase A of DSDP sites 105 and 603B of 1.8 cm/ky and 2.5 cm/ky, respectively. A coring gap obscuring the later part of the phase B (plateau with maximum δ^{13}C values) at DSDP site 603B does not allow an average sedimentation rate to be calculated for the whole C/T OAE. Although no coring gap occurs at DSDP site 105, an average sedimentation rate could not be calculated for the whole C/T OAE because phase C (return to pre-excursion δ^{13}C values) could not be distinguished (Fig. 4). However, assuming a maximum duration of 400 ky for the remainder of the OAE interval we calculated minimum sedimentation rates for DSDP sites 105 and 603B of 0.6 cm/ky and 1.4 cm/ky, respectively.
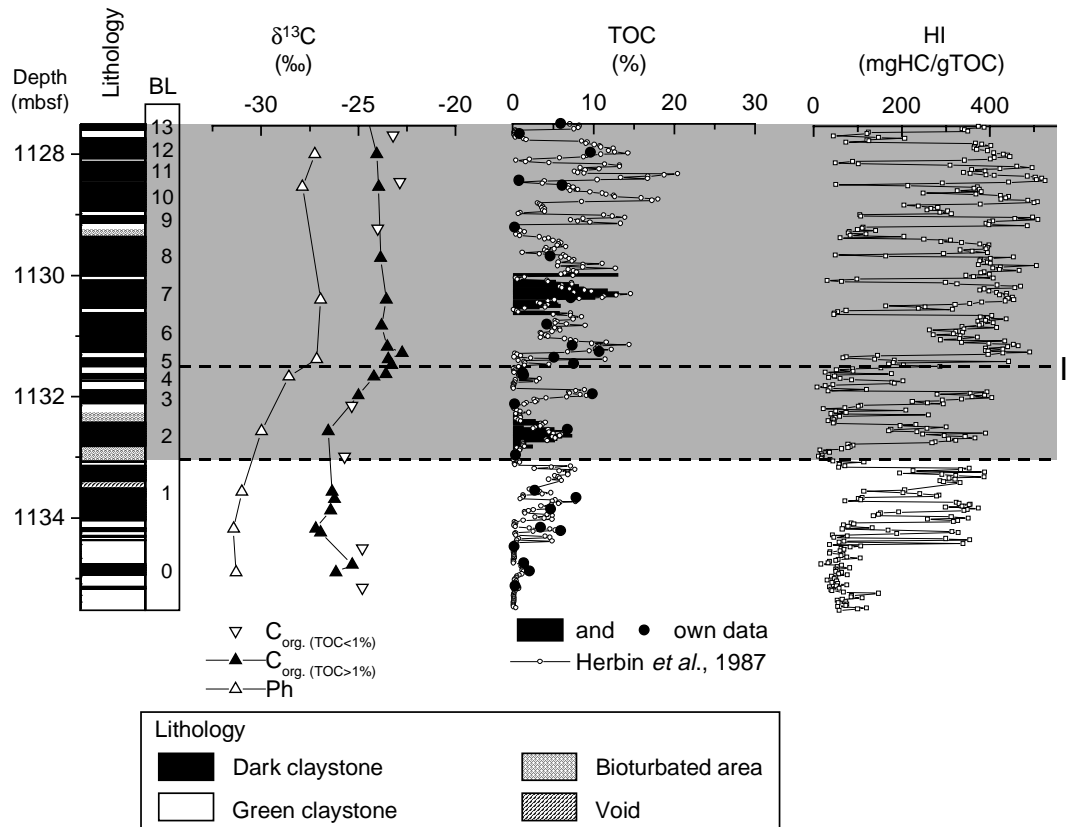
Figure 3. Stratigraphy, biomarker and bulk organic carbon data of DSDP site 603B. Carbon isotope values (in ‰ vs. VPDB) of C_{org}, S-bound phytane (Ph) derived from phytoplanktonic chlorophyll, TOC contents and HI indices of the bulk sediment (own data and data previously reported by Herbin et al. [1987a]). The dashed lines with Roman numbers show the approximate position of the boundaries between the different phases (i.e. rapid positive shift in $\delta^{13}C$ values, plateau with maximum $\delta^{13}C$ values and return to pre-excursion $\delta^{13}C$ values) of the carbon isotope excursion.

4.3.2 Cyclic Variations in Abundance and Source of the Sedimentary OM

4.3.2 1 Cyclic Variations in TOC content and Rock Eval hydrogen and oxygen indices. The late Cenomanian sediments of DSDP sites 105 and 603B contain high amounts of OC with maximum TOC values of ~26% (Figs. 3 and 4). During the C/T OAE the average TOC contents at both sites are significantly higher (5-6%) than before (~2%) (Fig. 3). At both sites this increase in TOC content is accompanied by a significant increase in Rock Eval hydrogen indices (HI) from ~150 mg hydrocarbons/g TOC before to ~270 mg hydrocarbons/g TOC during the C/T OAE [*Herbin et al.*, 1987a]. Superimposed on these long-term trends are high amplitude, short-term cyclic variations in both TOC content and HI values throughout the investigated sections (Fig. 3 and 4). The more pronounced changes in TOC and HI are also reflected by changes in lithology from green claystones, with low TOC and HI values, to black claystones, with high TOC and HI values. HI values are generally <100 mg hydrocarbons/g TOC and oxygen indices (OI) high (OI > 100) for the OM-lean green claystones, which has been attributed to a terrestrial source for the OC [*Herbin et al.*, 1987a]. In sharp contrast, high HI values and low OI values [*Herbin et al.*, 1987a] indicate a predominately marine origin for the thermally immature OM for the OC-rich black claystones. In

order to resolve the sources of the sedimentary OM, both the extractable and insoluble OM were also investigated on a molecular level.
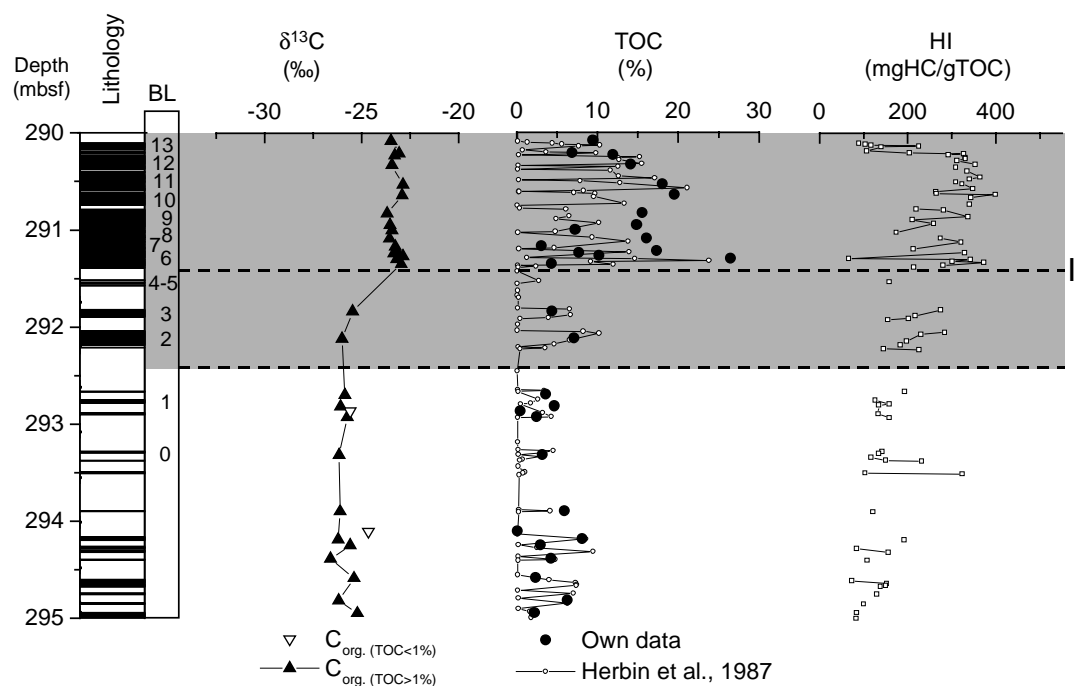

Figure 4. Stratigraphy and bulk organic carbon data of DSDP site 105. Carbon isotope values (in ‰ vs. VPDB) of C_{org}, TOC contents and HI indices of the bulk sediment (own data and data previously reported by Herbin et al. [1987a]). The dashed lines with Roman numbers show the approximate position of the boundaries between the different phases (i.e. rapid positive shift in $\delta^{13}C$ values, plateau with maximum $\delta^{13}C$ values and return to pre-excursion $\delta^{13}C$ values) of the carbon isotope excursion.

4.3.2 2 Cyclic variations in organic matter composition at the molecular level. Only small amounts of total extracts were recovered from the OM-lean sediments outside the black shale interval (1.0 to 2.0 mg/g dry sediment), while higher amounts (4.0 to 8.0 mg/g dry sediment) were recovered from the black shales. The extractable OM was separated into apolar and polar fractions.

The apolar hydrocarbon fractions from the OM-rich black claystones consist mainly of short-chain *n*-alkanes (C_{16}-C_{22}) with no odd-over-even predominance, long-chain (C_{25}-C_{35}) *n*-alkanes with a moderate odd-over-even carbon number predominance (CPI ~1.8), hopanoids, steroids and acyclic isoprenoids (Fig. 5a). Steroids and hopanoids strongly dominate these apolar fractions. In sharp contrast, the apolar fractions from the OM-lean green claystones (Fig. 5b) are strongly dominated by short-chain *n*-alkanes (C_{16}-C_{22}) with no odd-over-even predominance and long-chain (C_{25}-C_{35}) *n*-alkanes with a moderate odd-over-even carbon number predominance (CPI ~1.8). The steroids in the black claystones derive from cholesterol, 24-methyl-cholesterol and 24-ethyl-cholesterol or their unsaturated derivatives, which are predominately biosynthesized by marine algae [*Volkman*, 1986]. However, zooplankton could be a significant source for the C_{27} steroids because cholesterol and its derivatives (C_{27} sterols) are also indirectly formed by dealkylation of ingested C_{28} and C_{29} sterols [*Goad*, 1981] by zooplankton heterotrophically living

on algal biomass. The sedimentary hopanoids are likely diagenetic products of hopanols such as bacteriohopanopolyol derivatives (C_{35}) or diplopterol (hopanes < C_{30}) and may derive from numerous bacterial taxa such as cyanobacteria, heterotrophic bacteria and methanotrophic bacteria [*Rohmer et al.*, 1992]. The odd-over-even predominance (CPI ~1.8) of the *n*-C_{25} to *n*-C_{35} suggests that leaf waxes of terrestrial plants are a significant source for the long-chain *n*-alkanes [*Eglinton and Hamilton*, 1967], while the short-chain *n*-alkanes (C_{16}-C_{22}) with no odd-over-even predominance are non-specific and could derive from a wide variety of algae and bacteria.
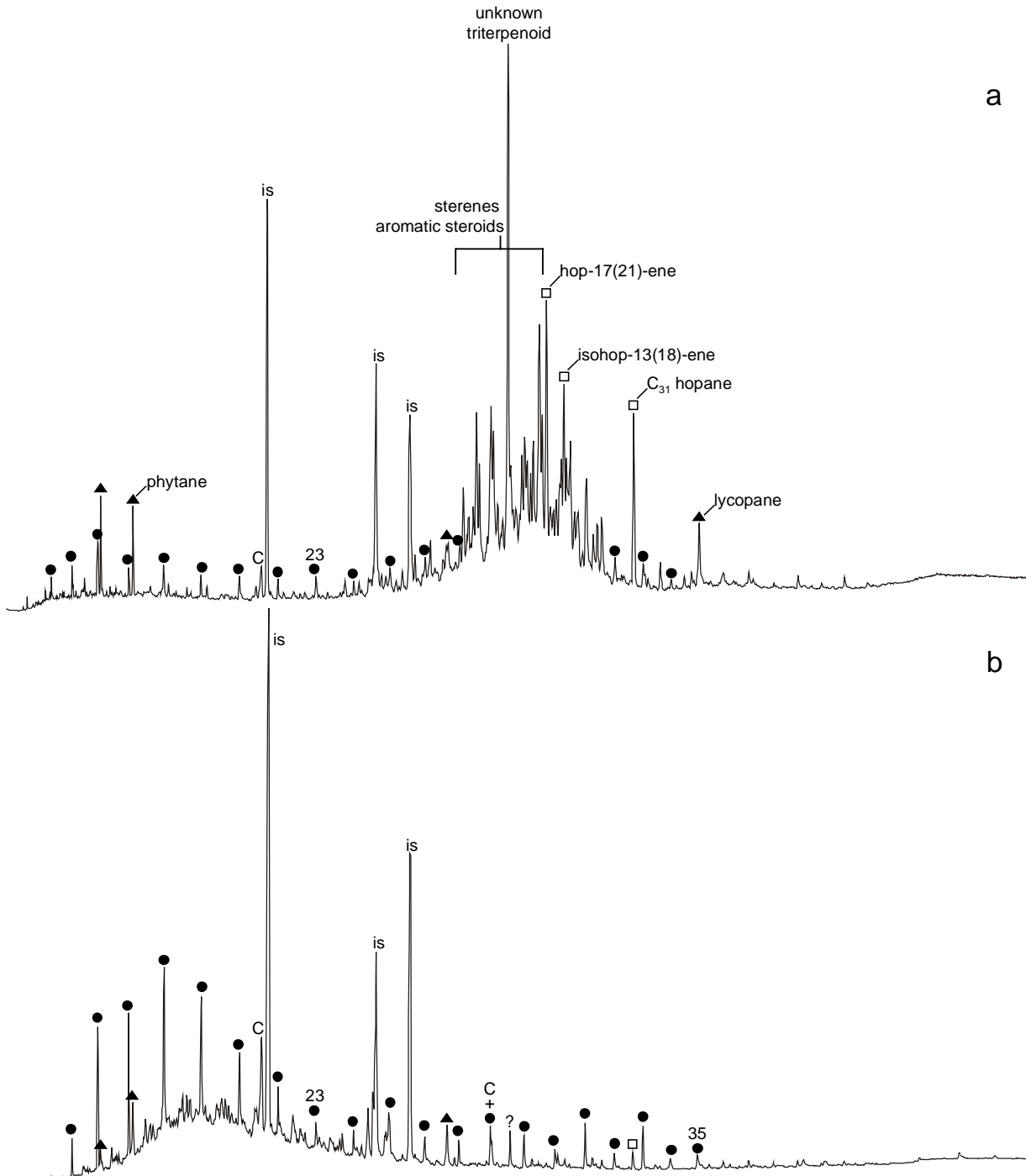
Figure 5. Typical reconstructed total mass chromatogram [i.e. total ion count (TIC)] of apolar fractions of black claystones (**a**), and of green claystones (**b**), of DSDP Site 603B. Filled circles, open squares and filled triangles indicate *n*-alkanes, hopanes and saturated acyclic isoprenoids, respectively. Abbreviations are: is, internal standard; 23, *n*-C_{23}; 35, *n*-C_{35}; C, contaminant; ?, compound of unknown structure.

Since functionalised lipids and carotenoids may become sulfurised during early diagenesis in anoxic, sulfide-rich sediments [*Kok et al.*, 2000], the polar fractions were desulfurised. The apolar fractions obtained after desulfurisation of the polar fractions from the black claystones are mainly dominated by phytane of phytoplanktonic origin and bacterial derived extended (i.e. >C_{30}) hopanoids. These hopanoids are typically dominated by the C_{33} and C_{35} 2-desmethyl-17β,21β(H)-hopanes and their coeluting 2β-methyl-17β,21β(H)-isomers. On average these hopanoids together make up 60 to 80% of the extended hopanes present in the black claystones. The abundance of 2-methylhopanoids relative to desmethylhopanoids indicates that cyanobacteria are an important source of these molecular fossils [*Summons et al.*, 1999; Kuypers et al, in prep]. In contrast, the apolar fractions obtained after desulfurisation of the polar fractions from the green claystones are mainly dominated by *n*-alkanes with no obvious odd-over-even predominance.

In conclusion the low abundance of molecular fossils of unambiguous terrestrial origin (e.g. leaf-wax lipids and oleananes) relative to biomarkers of marine origin (e.g. algal steroids and hopanoids derived from cyanobacteria) supports a predominately marine phytoplanktonic source for the OM of the black claystones. The higher relative abundance of leaf-wax *n*-alkanes on the other hand is in good agreement with a mainly terrestrial source for the OM of the green claystones

Thermal degradation (flash pyrolysis) in combination with gas chromatography was used to investigate the sources of the insoluble OM, representing >90% of the TOC. In accordance with the extremely low (< 100 mg HC/ gTOC) Rock Eval HI indices, no detectable amounts of hydrocarbons were released from the green claystones. Pyrolysis of the decalcified black claystone samples, however, released considerable amounts of hydrocarbons with *n*-alkenes/*n*-alkanes, alkylbenzenes and alkylthiophenes as the main products. These compounds also dominate the pyrolysates from the C/T OAE black shales of the southern part of the proto-North Atlantic [Kuypers et al., unpublished results] and from ancient marine kerogens in general [e.g. *Sinninghe Damsté et al.*, 1989; *Eglinton et al.*, 1990; *Larter and Horsfield*, 1993; *Hartgers et al.*, 1994]. The extremely low abundance of lignin thermal degradation (pyrolysis) products generated from the kerogen supports a predominately marine origin for the OM from the black claystones of DSDP sites 105 and 603B.

4.3.2.3 The effect of cyclic variations in the OM source on $\delta^{13}C_{org}$. There is a significant difference in $\delta^{13}C$ values for bulk OM between adjacent OM-lean green and OM-rich black claystones, with the former being enriched in ^{13}C (up to 2‰) relative to the black claystones (Figs. 3 and 4). In the late Cenomanian interval preceding the isotope excursion, the $\delta^{13}C_{org}$ values even show a moderate negative correlation with TOC (r^2=0.78). This dependence of $\delta^{13}C_{org}$ on TOC (r^2=0.78) is also observed during and after the C/T OAE carbon isotopic excursion after 'detrending' the $\delta^{13}C_{org}$ values for the isotope excursion by substracting the $\delta^{13}C$ values for the marine biomarker S-bound phytane. A similar negative correlation has previously been observed for

$\delta^{13}C_{org}$ and HI for early and middle Cretaceous marine sediments, and was attributed to variations in the relative contribution of refractory terrestrial and marine OM [*Arthur et al.*, 1985]. In modern marine environments $\delta^{13}C$ values for marine OM are commonly more positive than for terrestrial OM. However, during most of the Cretaceous elevated pCO_2 levels resulted in an increase in the isotope effect associated with carbon fixation (ε_p) by phytoplankton, leading to values for marine OM that were generally more negative than for terrestrial OM. The negative correlations between TOC and $\delta^{13}C_{org}$ at sites 105 and 603B, therefore, most likely can be attributed to an increased terrestrial contribution to the green claystones relative to the black claystones.

4.3.3 Sedimentary Cycles and Orbital Forcing

The cyclic variation in TOC content and HI indices of the C/T sediments strongly reminds of the rhythmical bedding related to the Milankovitsch periodicity that is often observed for Pleistocene to Mesozoic sediments [*Berger et al.*, 1992].

The most reliable tests for Milankovitsch forcing in a pre-Pleistocene set of data is the detection of sinusoids with ratios similar to the modern orbital periods [*Park and Herbert*, 1987]. Three distinct peaks are visible at 40, 70 and 200 cm in the power spectrum for the TOC record for site 603B (fig. 6A). The ratio obtained for these wavelengths (1 : 1.8 : 5) corresponds well with the ratio for respectively a ~21 ky precession, a ~40 ky obliquity and a ~100 ky eccentricity signal (1 : 1.9 : 4.8). The best-developed maximum has a wavelength of 40 cm (~21 ky), suggesting that the TOC record is mainly precession controlled. The power spectrum for the HI record of DSDP site 603B shows the same three peaks but there is no particular dominance of the 40 cm cycle (Fig. 6B). Additional evidence for a predominantly precession controlled cyclicity comes from the sedimentation rates for DSDP site 603B. Assuming a minimum sedimentation rate of 1.4 cm/ky for the C/T OAE interval, the maximum duration for the 40 cm cycle is 28 ky, excluding an obliquity (~40 ky) and eccentricity (100 ky) origin.

A minimum of two and a maximum of three cycles in the TOC/HI record between boundaries I and II (~60 kyr) at DSDP site 603B (Fig. 3) is consistent with a precession (~21 kyr) origin. In total ~17 cycles are visible in the TOC and HI record of the C/T section of DSDP site 603B of which not all are expressed as green/black claystone cycles. We attribute this to the TOC content predominately determining the color of the sediment with sediments containing more than 1-2% TOC being black. Because the TOC content remains above 1-2% in some cycles (e.g. black layers (BL) 6 and 8, Fig. 3) only ~14 major black claystones can be recognised (i.e. BL 0-13). Using isotope stratigraphy a comparable number of major black claystones was identified for the same interval at DSDP site 105 (Fig. 4). In fact the ~17 cycles in the TOC record of DSDP site 603B can be correlated with cycles of similar amplitude at DSDP site 105. These cycles are, however, significantly thinner (10-20 cm) than at DSDP Site 603B indicating a lower sedimentation rate at site 105. This is consistent with a two times lower minimum sedimentation rate for the C/T OAE interval obtained by carbon isotope stratigraphy.

We therefore suggest that the high amplitude cyclic variations in TOC content at both DSDP sites 105 and 603B were predominately precession controlled. The coinciding variations in HI, OI, $\delta^{13}C_{org}$, and the abundance of marine relative to terrestrial biomarkers as well as the low abundance

of lignin pyrolysis products generated from the kerogen of the black claystones indicate that these cyclic variations resulted predominantly from changes in the contribution of marine OM. Did the precessional-forced changes in the marine OC accumulation rates of sites 105 and 603B mainly result from increased preservation under anoxic conditions or from increased primary productivity?
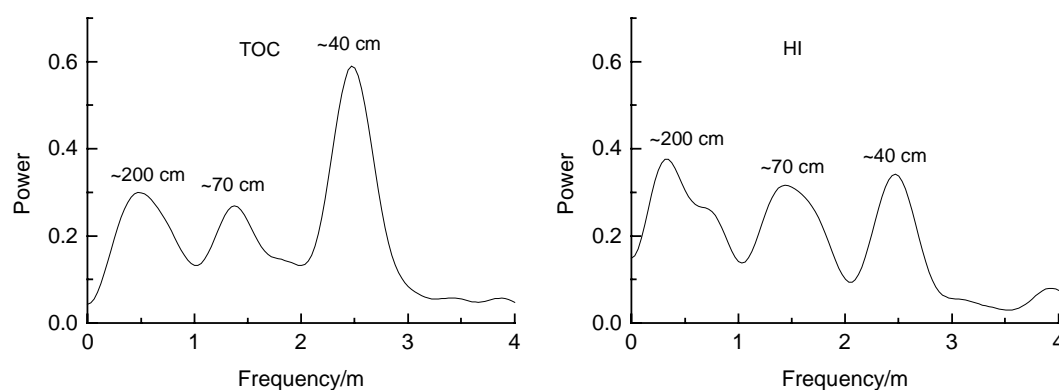

Figure 6. Power spectra of TOC contents (**A**), and HI indices (**B**) of Cenomanian sediments of DSDP site 603B (TOC and HI data from [*Herbin et al.*, 1987a]).

4.3.4 Preservation vs productivity

The presence of precession cycles in the sediment record is often attributed to productivity changes, resulting from climatic changes such as monsoonal intensity. However, the strong variations in HI values and TOC contents of C/T sediments from sites 105 and 603B were attributed to fluctuations in redox conditions of the bottom waters [*Herbin et al.*, 1987a]. To test whether enhanced OM preservation resulting from reduced oxygen supply or enhanced productivity caused this variation in TOC/HI values, two OM-poor green to OM-rich claystone couplets (i.e. the visual expression of the precession cycles) of DSDP site 603B were studied in greater detail (i.e. BL 2 and 7, Fig. 3). The C_{org} (%) data for BL2 and BL7 is comparable to what has been reported by Herbin et al. [1987a] for these particular intervals (Fig. 3).

4.3.4.1 Water Column Redox Proxies. The deposition of laminated sediments and the absence of benthic foraminifers at site 603B indicates predominantly suboxic to anoxic bottomwater conditions during the deposition of both green and black claystones [*Herbin et al.*, 1987a; *Kuhnt*, 1992]. However, the occurrence of thin (10-20 cm) bioturbated layers in the green claystones [Fig. 3; *Herbin et al.*, 1987a] indicates the periodic occurrence of oxic bottom water conditions during the deposition of green claystones.

Further information on water column redox conditions can be gained from chalcophilic elements (e.g. Mo, Ni and Zn) that precipitate as sulfides under euxinic conditions and certain redox sensitive elements (e.g. Mo and V) that are immobilised under reducing conditions [*Nijenhuis and De Lange*, 2000]. In a similar way Mn, which is mobilised under reducing (anoxic) conditions and precipitates as oxyhydroxides under oxic conditions, can provide information about redox

conditions of the bottom waters [*Thomson et al.*, 1995]. To evaluate the variations in redox conditions, the abundances of Mn, Mo, V and Zn have been normalised to aluminium (Al) (Fig. 7). Al is mainly present in clay minerals and although the Al content in clay minerals can vary, normalisation to Al is frequently used [*Calvert and Pedersen*, 1993] to correct for fluctuations in detrital contribution. The low abundance of Mn in BL 2 and 7 relative to the adjacent OM-lean intervals indicates that the OM-rich intervals were deposited under generally more reducing suboxic/anoxic conditions (Fig. 7). The difference in Mn/Al ratios between green and black claystones could have been further enhanced by Mn mobilisation in the reducing anoxic OM rich intervals and subsequent reprecipitation as Mn oxyhydroxides on re-encountering oxygen at the ancient oxidation front [*Thomson et al.*, 1995]. The abundance of Mo/Al, V/Al and Zn/Al (BL 2 and 7; Fig. 7) indicate more reducing anoxic bottom water conditions during the deposition of the black claystones [*Arthur et al.*, 1990; *Calvert and Pedersen*, 1993].

Additional evidence for different redox conditions of the bottom water during the deposition of the green and black claystones, may come from the sedimentary biomarker record. Oxygen exposure time significantly affects the biomarker distribution, with an increasing contribution of more refractory biomarkers like terrestrial *n*-alkanes relative to more labile biomarkers like steroids with increasing exposure to oxygen [*Hoefs et al.*, 2001; *Sinninghe Damsté et al.*, 2001]. The green claystones are dominated by the refractory terrestrial *n*-alkanes, while the labile hopanoids, steroids and lycopane are only present in trace amounts (Fig. 5b). This is indicative of long oxygen exposure times and hence oxygenated bottom waters [*Hoefs et al.*, 2001; *Sinninghe Damsté et al.*, 2001]. The dominance of labile steroids and hopanoids in the apolar fractions of the black claystones (Fig. 5b) on the other hand indicates relatively short oxygen exposure times, which is in good agreement with more anoxic bottom waters.

To investigate whether these anoxic conditions extended into the photic zone, the samples from DSDP Site 603B were checked for fossil derivatives of specific pigments (isorenieratene) of the brown coloured strain of green sulfur bacteria (Chlorobiaceae). These photosynthetic bacteria require both light and H_2S for carbon fixation and are, therefore, indicators for photic zone anoxia. At the present day the habitat for green sulfur bacteria is restricted to a few euxinic basins such as the Black Sea [*Repeta et al.*, 1989; *Sinninghe Damsté et al.*, 1993; *van Gemerden and Mas*, 1995]. Sinninghe Damsté and Köster [1998] showed that during the mid Cretaceous C/T OAE these organisms were also present in the proto North Atlantic Ocean. More recently we showed that green sulfur bacteria were already present in the southern part of the proto North Atlantic well before the C/T OAE [Kuypers et al., 2000 submitted to Paleoceanography]. Molecular fossils of isorenieratene (e.g. isorenieratane) were found in the apolar fraction of several black claystones (BL 0-2, 4, 5, 7, 10, 12) of DSDP site 603B in concentrations of 7-300 ng/g sediment. This indicates that sulfide-containing water sometimes penetrated the photic zone before as well as during the C/T OAE. We calculated accumulation rates for isorenieratane in order to compare the abundance of isorenieratane at site 603B to its abundance in sediments from the southern proto North Atlantic [Kuypers et al, 2001 submitted to Paleoceanography]. Assuming an average duration of ~21 ky for the ~40 cm precession cycles (i.e. an average sedimentation rate of 1.9 cm/ky), accumulation rates of up to 9 μg isorenieratane $m^{-2} \cdot y^{-1}$ were calculated for DSDP site 603B. The accumulation rates obtained for the southern proto North Atlantic are much higher (e.g. up to 1400 and 2600 μg isorenieratane $m^{-2} \cdot y^{-1}$ at

sites S13 and 367, respectively). These differences in isorenieratane accumulation rates could have resulted from significantly higher anoxygenic productivity in the water column of the southern proto North Atlantic. In accordance with this, fluctuations in the abundances of isorenieratene extracted from Holocene Black Sea sediments were attributed to changes in anoxygenic productivity related to fluctuations in the position of the chemocline [*Repeta*, 1993]. The abundance of phototrophic sulfur bacteria in modern settings shows a strong positive correlation with light intensity [*van Gemerden and Mas*, 1995]. Therefore, the 100 to 300 times higher abundance of isorenieratane at sites S13 and 367 relative to site 603B suggests that sulfide-containing water penetrated the photic zone much more frequently and/or at much shallower depths at the southern side than at the northern side of the proto North Atlantic Ocean. In fact the low abundance of isorenieratane at site 603B suggests that sulfide-containing water only occasionally penetrated the photic zone at the northern side of the proto North Atlantic Ocean.

Isorenieratane was found in all investigated samples from within BL7 with highest concentrations in the center of this black claystone while isorenieratane concentrations were below the detection limit in the overlying green claystone (Fig. 7). The latter is in good agreement with the green claystones being deposited under oxic conditions. The apparent positive correlation between TOC content and abundance of isorenieratane within BL7 could indicate that enhanced OM accumulation was accompanied by a rise of the average position of the chemocline (i.e. nearer to the photic zone) during its deposition. This seems to be supported by a co-occurring increase in Mo/Al ratios (Fig. 7).

Intriguingly, small amounts of isorenieratane (21 ng/g sediment) were found in one green claystone of site 603B, which was likely deposited under more oxic conditions. Based upon the available data it can not be excluded that these are not truly autochthonous molecular fossils but were transported over longer distances. Such an allochthonous source was previously suggested for aryl isoprenoids derived of isorenieratene of green sulfur bacteria extracted from North Atlantic deep-sea sediments deposited during 'Heinrich' events [*Rosell-Melee et al.*, 1997].

4.3.4.2 Productivity Proxies. Sedimentary Ba is generally considered as an indicator for palaeoproductivity since it originates from barite formed in decaying phytoplanktonic OM in surface waters [*Dymond et al.*, 1992; *de Lange et al.*, 1994; *Francois et al.*, 1995]. Such barite formation has been shown to occur in the well-oxygenated open ocean [*Dymond et al.*, 1992; *Francois et al.*, 1995] as well as in the suboxic to anoxic waters of OMZs and euxinic basins [*Falkner et al.*, 1993; *Dean et al.*, 1997].

The Ba/Al ratios are significantly higher (1.6 times) in BL 7 than in the adjacent OM-lean green claystones, indicating enhanced export productivity during the deposition of this OM-rich interval (Fig. 7). The Ba/Al ratios within BL 2 are comparable to BL 7 (Fig. 7). However, Ba/Al ratios in the adjacent green claystones are higher than in the green claystones above and below BL7, which could have resulted from bioturbation. The Ba/Al ratios within the black claystones do not show the strong correlation with TOC contents that is generally observed for sapropels but rather shows a topped appearance (Fig. 7). This could indicate that variations in preservation rather than productivity controlled the TOC variations within the black claystones. An alternative explanation is that the Ba/Al record has been affected by remobilisation of barite under reducing conditions.
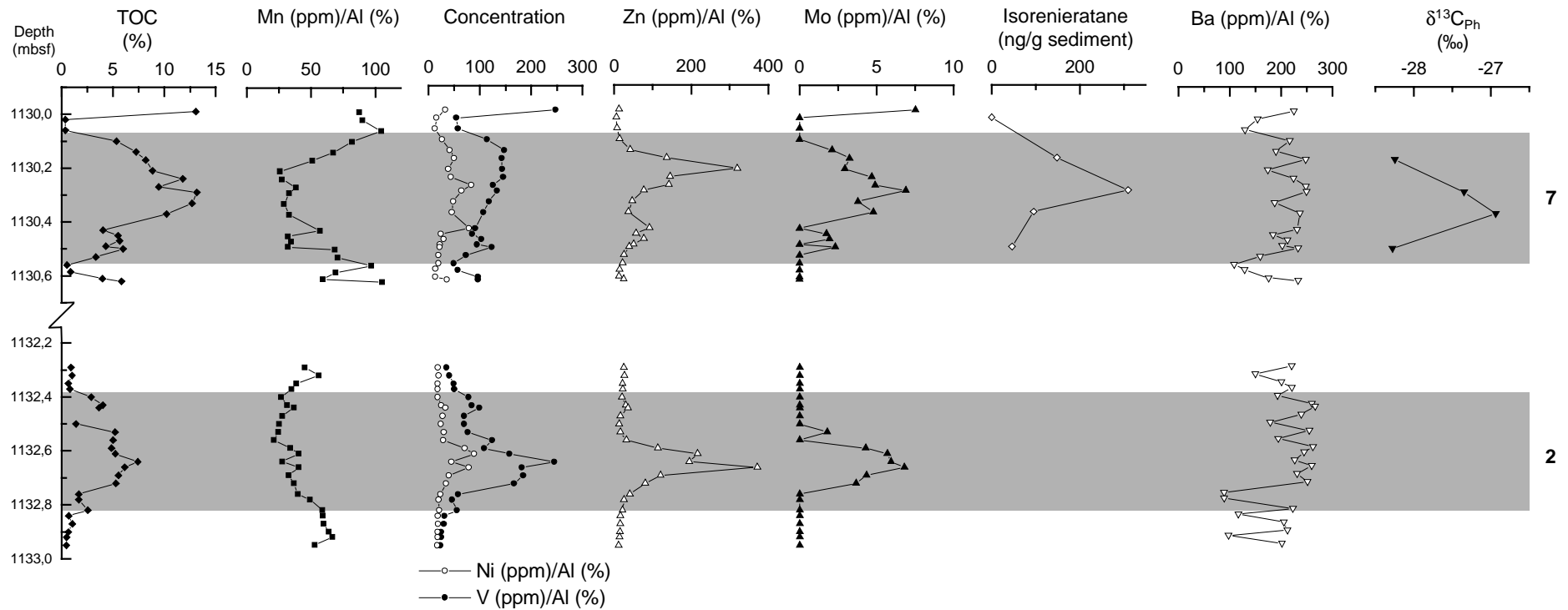
Figure 7. Bulk organic carbon, trace metal and biomarker data of DSDP site 603B. TOC contents of the bulk sediment, concentration profiles of redox sensitive trace metals (Mn, Mo, Zn and V) normalised to Al, concentration profile of the molecular fossil isorenieratane of green sulfur bacteria, concentration profile of the productivity proxy Ba/Al and carbon isotope values (in ‰ vs. VPDB) of S-bound phytane (Ph) derived from phytoplanktonic chlorophyll. The shaded areas show the approximate position of the black claystones BL2 and BL7 (see also Fig. 3). There is no biomarker data (i.e. isorenieratane abundance and $\delta^{13}C$ values for S-bound Ph) available for BL2 and the adjacent green claystones.

Under suboxic to anoxic diagenetic conditions Ba preservation may be reduced [*Dymond et al.*, 1992] leading to an underestimation of the former Ba levels and thus productivity. Additional evidence for a high primary productivity during the deposition of BL 2 and 7 is provided by the mineralogical composition of the black claystones. The black claystones contain abundant opal CT (Fig. 8a), which is a diagenetic product of biogenic opal, while no opal CT was detected in the green claystones (Fig. 8b). Biogenic opal is predominantely produced by diatoms and radiolarians in highly productive surface waters. Because opal easily dissolves upon sedimentation, special conditions (a high sedimentation rate and a high opal flux) are needed for its preservation. Consequently, the presence of opal proves (but the absence of opal does not exclude) high primary productivity. Opal CT is abundantly present and even strongly dominates the mineralogical composition of some of the investigated samples from the center of the black claystones BL 2 and 7.
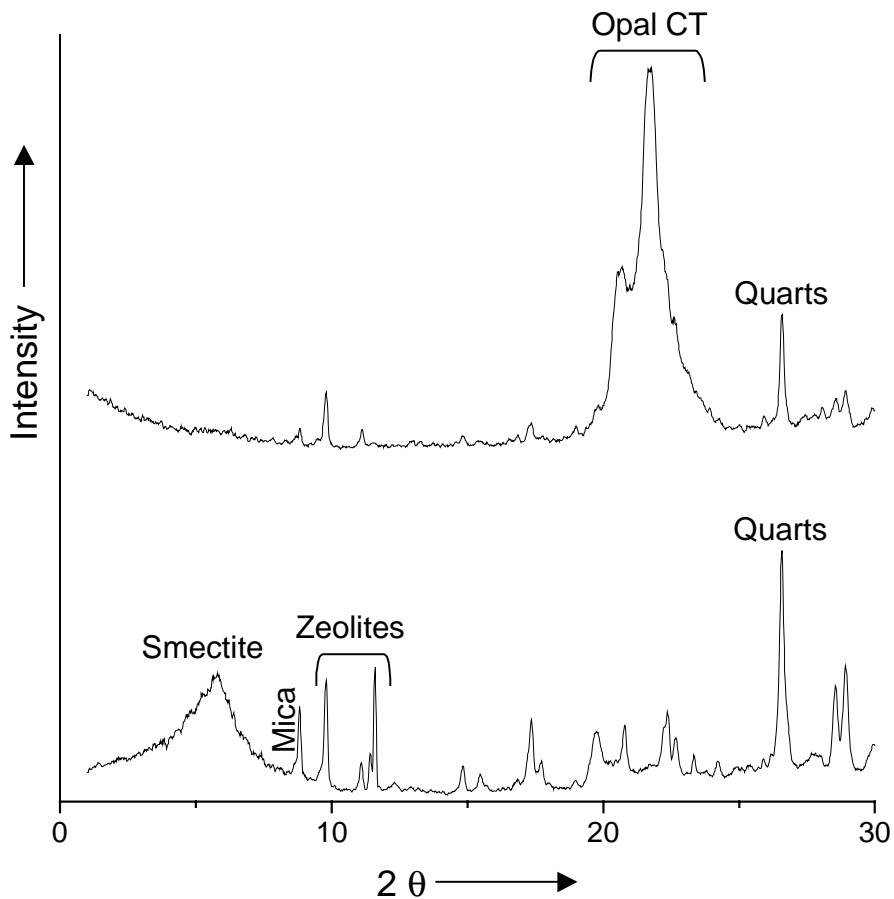

Figure 8. Typical XRD patterns of the centre of the black claystone BL7 (**a**), and of the underlying green claystone (**b**), of DSDP Site 603B. The patterns have been smoothed by a two points moving average.

An increase in productivity could result from changes in either growth rate or average cell size (i.e. carbon content per cell) of the phytoplanktic community. The degree of photosynthetic carbon fractionation (ε_p) for marine phytoplankon shows a strong negative correlation with both growth rate and cell size [*Laws et al.*, 1995; *Pancost et al.*, 1997; *Popp et al.*, 1998; *Burkhardt et*

al., 1999; *Bidigare et al.*, 1999]; therefore an increase in productivity should be reflected in $\delta^{13}C$ values of phytoplankton-derived organic matter. In accordance with this, variations in $\delta^{13}C$ values for bulk marine OC and molecular fossils of phytoplanktonic origin have been attributed to changes in ε_p resulting from changes in productivity [*Pancost et al.*, 1999; *Krishnamurthy et al.*, 2000; *Murphy et al.*, 2000]. $\delta^{13}C$ values for inorganic carbon, which are needed to calculate ε_p, could not directly be determined due to absence of carbonate carbon at DSDP site 603B. Assuming there was no significant change in the in $\delta^{13}C$ values for dissolved inorganic caron during the deposition of BL 7, the increase in $\delta^{13}C$ values for S-bound phytane at DSDP site 603B (Fig. 7) records a ~1‰ decrease in ε_p values. This decrease may have been larger, because shoaling of the chemocline discussed previously could have introduced ^{13}C depleted recycled inorganic carbon into the photic zone. Thus, it seems likely that an increase in productivity accounts for the shift in $\delta^{13}C$ values for the molecular fossil of phytoplanktic origin at site 603B. This is entirely consistent with the high Ba and opal CT levels in BL 7.

4.3.4.3 Synthesis of redox and productivity proxies. The co-occurrence of lamination enrichment of redox sensitive trace metals and presence of molecular fossils of pigments from green sulfur bacteria indicates that the northern proto-North Atlantic Ocean water column was occasionally euxinic from the bottom to at least the base of the photic zone (<150 m) during the deposition of the black claystones (Fig. 7). In contrast, the green claystones are bioturbated, are enriched in Mn, do not show enrichments in redox sensitive trace metals and show biomarker distributions indicative of long oxygen exposure times, indicating more oxic water conditions. At the same time there is evidence (e.g. enhanced Ba/Al ratios, abundance of biogenic silica and significant ^{13}C-enrichment for OC of phytoplanktonic origin) for enhanced primary productivity during the deposition of the black claystones.

We propose that enhanced productivity of OM was an important factor in generating and sustaining euxinic conditions during the deposition of the black claystones. Enhanced primary productivity periodically overwhelmed the oxic OM remineralisation potential of the bottom waters leading to the deposition of OM-rich black claystones. A combination of overall sluggish circulation (possibly halothermal instead of thermohaline) and the tectonically isolated nature of the proto-North Atlantic (Fig. 1) likely facilitated the periodic development of anoxic water column conditions [*Poulsen*, 1999; *Bice*, personal communication]. Because the amount of oxygen used for OM remineralisation exceeded the amount supplied by diffusion and deep water circulation, bottom waters became euxinic. These euxinic conditions occasionally even extended into the photic zone of the proto North Atlantic.

4.3.5. Long-term changes as a result of the C/T OAE

During the C/T OAE the average TOC contents at both sites are significantly higher (5-6%) than before (~2%) (Figs. 3 and 4), while average sedimentation rates at both sites remain approximately the same, indicating a large increase in OC accumulation rates during the C/T OAE. An average sedimentation rate of 1.9 cm/ky was calculated for site 603B, assuming an average

duration of ~21 ky for the ~40 cm precession cycles. In a similar approach an average sedimentation rate of 0.9 cm/ky was calculated for DSDP Site 105. Assuming constant sedimentation rates throughout the investigated sections, the average OC accumulation rates before and during the C/T OAE were determined using the TOC contents of the bulk sediments. Prior to the C/T OAE, the OC mass accumulation rates (OC MAR) for sites 105 (0.2 $gC \cdot m^{-2} \cdot y^{-1}$) and 603B (0.6 $gC \cdot m^{-2} \cdot y^{-1}$) were significantly smaller than the 9 $gC \cdot m^{-2} \cdot y^{-1}$ and 3 $gC \cdot m^{-2} \cdot y^{-1}$ previously determined for the same interval at site S13 and DSDP site 367, respectively [Kuypers et al., 2000 submitted to Paleoceanography]. During the C/T OAE, OC accumulation rates at sites 105 (0.6 $gC \cdot m^{-2} \cdot y^{-1}$) and 603B (1.5 $gC \cdot m^{-2} \cdot y^{-1}$) were approximately three times greater than prior to the OAE but still significantly smaller than for the same interval at sites S13 and 367 (9 and 26 $gC \cdot m^{-2} \cdot y^{-1}$, respectively). This increase in OM accumulation rates at sites 105 and 603B is accompanied by a significant increase in HI values from ~150 mg hydrocarbons/g TOC before to ~270 mg hydrocarbons/g TOC during the C/T OAE [*Herbin et al.*, 1987a]. However, these HI values are still significantly lower than for the same interval at sites S13 and 367 (600-700 mg hydrocarbons/g TOC) [*Herbin et al.*, 1986; *Kuhnt et al.*, 1990] indicating a more refractory nature of the sedimentary OM in the northern part than in the southern part of the proto North Atlantic during the C/T OAE. The sediments from site 603B show a significantly lower abundance of redox sensitive trace metals and molecular fossils of green sulfur bacteria than site 367 [Kuypers et al., 2000 submitted to Paleoceanography], indicating that the more refractory nature of OM resulted from more oxic conditions in the northern part of the proto North Atlantic during the C/T OAE. Previously we attributed the significant increase in marine OC accumulation rates in the southern part of the proto-North Atlantic (sites S13, 144 and 367) to an increase in primary productivity [Kuypers et al., 2000 submitted to Paleoceanography]. As was pointed out by Schlanger *et al.* [1987]; 'the widespread distribution of anoxic sediments deposited synchronously during such a short-lived event indicates that such sediments are not simply the product of coincidental local climatic or basinal water mass characteristics'. Therefore, it is tempting to attribute the increase in OM accumulation rates in the northern part of the proto-North Atlantic (sites 105 and 603B) also to an increase in primary productivity. However, there is only a small increase in average Ba/Al ratios from 140 before to 180 during the C/T OAE at site 603B, suggesting only a small increase in productivity. At the same time average Mo/Al (0 to 4), Ni/Al (14 to 50), V/Al (22 to 125) and Zn/Al (19 to 52) ratios as well as the average concentration of isorenieratane (23 to 65 ng/g sediment) are all significantly enhanced during the C/T OAE, indicating more anoxic conditions. This is in good agreement with the strong reduction in the thickness of the green claystones at both sites 105 and 603B during the C/T OAE. It can, however, not be excluded that the Ba/Al record has been affected by diagenesis as indeed seems to be indicated by the constant Ba/Al ratios within the black claystones and that, therefore, the increase in productivity during the C/T OAE is underestimated. Interestingly, the relative contributions of metals of terrestrial origin like Al (8 % to 5 %), Ti (0.45 % to 0.20 %) and Zr (82 p.p.m. to 56 p.p.m.) are all significantly reduced, which could indicate an enhanced dilution by biogenic opal during the C/T OAE. If so, this would indicate enhanced primary productivity. Additional data is needed to clarify this issue.

In any case the periodic increase in productivity seems to have been more pronounced at site 603B than at site 105, resulting in significantly higher OM accumulation rates at the former site

during the deposition of the black claystones. Lower accumulation rates of biogenic components like opal and OM during deposition of the black claystones may also have led to significantly lower sedimentation rates at site 105. However, at both sites the most OC-rich black claystones as well as the thinnest green claystones occur during phase B of the isotope excursion (i.e. plateau with maximum δ^{13}C values, Figs. 3 and 4). These long-term trends most likely resulted from global environmental changes that occurred during the C/T OAE possibly related to the formation of a deep water connection between North and South Atlantic basins [Kuypers et al., 2000 submitted to Paleoceanography].

4.4. Conclusions

1).   The high amplitude, short-term cyclic variations in TOC content and HI values of the C/T interval at DSDP sites 105 and 603B most likely resulted from precession controlled changes in productivity.

2).   Periodically increased primary productivity led to euxinic conditions in the water column of the northwestern proto North Atlantic.

3).   These anoxic conditions, which sometimes extended to at least the base of the photic zone (<150 m), led to enhanced preservation of marine OM resulting in the deposition of OM-rich black claystones.

4).   The trends at sites 105 and 603B of continually increasing TOC contents and HI values of the black claystones up section most likely resulted from both enhanced preservation due to increased anoxia and increased production of marine OM as a response to the environmental changes during the C/T OAE.

4.5 References

Arthur, M. A., W. A. Dean, and L. M. Pratt, Geochemical and climatic effects of increased marine organic carbon burial at the Cenomanian/Turonian boundary, *Nature*, 335, 714-717, 1988.

Arthur, M. A., W. E. Dean, and G. E. Claypool, Anomalous ^{13}C enrichment in modern marine organic carbon, *Nature*, 315, 216-218, 1985.

Arthur, M. A., H. C. Jenkyns, H. J. Brumsack, and S. O. Schlanger , Stratigraphy, geochemistry, and paleoceanography of organic carbon-rich Cretaceous sequences, *Cretaceous Resources, Events and Rhythms*, 75-119, 1990.

Berger, A., M. F. Loutre, and J. Laskar, Stability of the astronomical frequencies over the earth's history for paleoclimate studies, *Science*, 255, 560-566, 1992.

Bidigare, R. R., K. L. Hanson, K. O. Buesseler, S. G. Wakeham, K. F. Freeman, R. D. Pancost, F. J. Millero, P. A. Steinberg, B. N. Popp, M. Latasa, M. R. Landry, and E. A. Laws, Iron-stimulated changes in ^{13}C fractionation and export by equatorial Pacific phytoplankton: Toward a paleogrowth rate proxy, *Paleoceanography*, 14, 589-595, 1999.

Bralower, T. J. and H. R. Thierstein, Organic carbon and metal accumulation rates in Holocene and mid-Cretaceous sediments: palaeoceanographic significance, *Geological Society Special Publication*, 26, 345-369, 1987.

Burkhardt, S., U. Riebesell, and I. Zondervan, Effects of growth rate, CO_2 concentration, and cell size on the stable carbon isotope fractionation in marine phytoplankton, *Geochim.Cosmochim.Acta*, 63, 3729-3741, 1999.

Calvert, S. E. and T. F. Pedersen, Geochemistry of recent oxic and anoxic marine sediments: Implications for the geological record, *Mar.Geol.*, 113, 67-88, 1993.

Caron, M., F. Robazynski, F. Amedro, F. Baudin, J. F. Deconinck, P. Hochhuli, K. Salis-Perch Nielsen, and N. Tribovillard, Estimation de la durée de l'événement anoxique global au passage Cénomanien/Turonien. Approche cyclostratigraphique dans la formation Bahloul en Tunisie centrale, *Bull.Soc.géol.France*, 170, 144-160, 1999.

Chénet, P. Y. and J. Francheteau, Bathymetric reconstruction method: application to the Central Atlantic Basin between 10ºN and 40ºN, *Initial Reports of the Deep Sea Drilling Project*, 51, 52, 53, 1501-1514, 1979.

De Graciansky, P. C., E. Brosse, G. Deroo, J. P. Herbin, L. Montadert, C. Müller, J. Sigal, and A. Schaaf, Organic-rich sediments and palaeoenvironmental reconstructions of the Cretaceous North Atlantic, in *Marine Petroleum Source Rocks*, edited by J. Brooks and A. J. Fleet, pp. 317-344, Geological Soc. Spec. Plub., .., 1987.

De Graciansky, P. C., G. Deroo, J. P. Herbin, L. Montadert, C. Müller, A. Schaaf, and J. Sigal, Ocean -wide stagnation episode in the late Cretaceous, *Nature*, 308, 346-349, 1984.

de Lange, G. J., B. J. H. van Os, P. A. Pruysers, J. J. Middelburg, D. Castradori, P. J. M. van Santvoort, H. Eggenkamp, and F. G. Prahl, Possible early diagenetic alteration of palaeo proxies, *NATO ASI Ser.I*, 17, 225-258, 1994.

Dean, W. E., J. V. Gardner, and D. Z. Piper, Inorganic geochemical indicators of glacial-interglacial changes in productivity and anoxia on the California continental margin, *Geochim.Cosmochim.Acta*, 61, 4507-4518, 1997.

Dymond, J., E. Suess, and M. Lyle, Barium in deep-sea sediment: A geochemical proxy for paleoproductivity, *Paleoceanography*, 7, 163-181, 1992.

Eglinton, G. and R. J. Hamilton, Leaf epicuticular waxes, *Science*, 156, 1322-1335, 1967.

Eglinton, T. I., J. S. Sinninghe Damsté, M. E. L. Kohnen, and J. W. De Leeuw, Rapid estimation of the organic sulphur content of kerogens, coals and asphaltenes by pyrolysis-gas chromatography, *Fuel*, 69, 1394-1404, 1990.

Falkner, K. K., G. P. Klinkhammer, T. S. Bowers, J. F. Todd, B. Lewis, W. M. Landing, and J. M. Edmond, The behavior of barium in anoxic marine waters, *Geochim.Cosmochim.Acta*, 57, 537-554, 1993.

Francois, R., S. Honjo, S. J. Manganini, and G. E. Ravizza, Biogenic barium fluxes to the deep sea: Implications for paleoproductivity reconstruction, *Global Biochemical Cycles*, 9, 289-303, 1995.

Freeman, K. H. and J. M. Hayes, Fractionation of carbon isotopes by phytoplankton and estimates of ancient CO_2 levels, *Global Biochemical Cycles*, 6, 185-198, 1992.

Gale, A. S., Cyclostratigraphy and the correlation of the Cenomanian Stage in Western Europe, *Geological Society Special Publication*, 85, 177-197, 1995.

Gale, A. S., H. C. Jenkyns, W. J. Kennedy, and R. M. Corfield, Chemostratigraphy versus biostratigraphy: data from around the Cenomanian-Turonian boundary, *Journal of the Geological Society, London*, 150, 29-32, 1993.

Goad, L. J., Sterol biosynthesis and metabolism in marine invertebrates, *Pure Appl.Chem.*, 51, 837-852, 1981.

Handoh, I. C., G. R. Bigg, E. J. W. Jones, and M. Inoue, An ocean modeling study of the Cenomanian Atlantic: equatorial paleo-upwelling, organic-rich sediments and the consequences for a connection between the proto-North and South Atlantic, *Geophysical Research Letters*, 26, 223-226, 1999.

Hartgers, W. A., J. S. Sinninghe Damsté, and J. W. De Leeuw, Geochemical significance of alkylbenzene distribution in flash pyrolysates of kerogens, coals, and asphaltenes, *Geochim.Cosmochim.Acta*, 58, 1759-1775, 1994.

Hayes, J. M., B. N. Popp, R. Takigiku, and M. W. Johnson, An isotopic study of biochemical relationships between carbonates and organic carbon in the Greenhorn formation, *Geochim.Cosmochim.Acta*, 53, 2961-2972, 1989.

Herbin, J. P., E. Masure, and J. Roucaché, Cretaceous formations from the lower continental rise off Cape Hatteras: organic geochemistry , dinoflagelate cysts, and the Cenomanian/Turonian boundary event at sites 603 (Leg 93) and 105 (Leg 11), *Initial Reports of the Deep Sea Drilling Project*, 93, 1139-1160, 1987a.

Hoefs, M. J. L., Rijpstra, I. C., and Sinninghe Damsté, J. S. The influence of oxic degradation on the sedimentary biomarker record I: Evidence from Madeira Abyssal Plain turbidites. Geochimica et Cosmochimica Acta . 2001.
Ref Type: In Press

Kohnen, M. E. L., S. Schouten, J. S. Sinninghe Damsté, J. W. De Leeuw, D. Merritt, and J. M. Hayes, The combined application of organic sulphur and isotope geochemistry to assess multiple sources of palaeobiochemicals with identical carbon skeletons, *Org.Geochem.*, 19, 403-419, 1992a.

Kohnen, M. E. L., S. Schouten, J. S. Sinninghe Damsté, J. W. De Leeuw, D. A. Merritt, and J. M. Hayes, Recognition of paleobiochemicals by a combined molecular sulfur and isotope geochemical approach, *Science*, 256, 358-362, 1992b.

Kok, M. D., W. I. C. Rijpstra, L. Robertson, J. K. Volkman, and J. S. Sinninghe Damsté, Early steroid sulfurisation in surface sediments of a permanently stratified lake (Ace Lake, Antarctica), *Geochim.Cosmochim.Acta*, 64, 1425-1436, 2000.

Krishnamurthy, R. V., P. A. Meyers, and N. A. Lovan, Isotopic evidence of sea-surface freshening, enhanced productivity, and improved organic matter preservation during sapropel deposition in the Tyrrhenian Sea, *Geology*, 28, 263-266, 2000.

Kühnel, R. A., and van der Gaast, S.J., in *Advances in x-ray analysis*; edited by Gilfrich et al., pp. 439-449, Plenum Press, New York, 1993.

Kuhnt, W., Abyssal recolonization by benthic foraminifara after the Cenomanian /Turonian boundary anoxic event in the North Atlantic, *Mar.Micropal.*, 19, 257-274, 1992.

Kuhnt, W., J. P. Herbin, J. W. Thurow, and J. Wiedmann, Distribution of Cenomanian-Turonian organic facies in the western Mediterranean and along the Adjacent Atlantic Margin, *AAPG Stud.in Geol.*, 30, 133-160, 1990.

Kuhnt, W., A. J. Nederbragt, and L. Leine, Cyclicity of Cenomanian-Turonian organic-carbon-rich sediments in the Tarfaya Atlantic Coastal Basin (Morocco), *Cretaceous Research*, 18, 587-601, 1997a.

Kuhnt, W., A. J. Nederbragt, and L. Leine, Cyclicity of Cenomanian-Turonian organic-carbon-rich sediments in the Tarfaya Atlantic Coastal Basin (Morocco), *Cretaceous Research*, 18, 587-601, 1997b.

Kuypers, M. M. M., R. D. Pancost, and J. S. Sinninghe Damsté, A large and abrupt fall in atmospheric CO_2 concentration during Cretaceous times, *Nature*, 399, 342-345, 1999.

Larter, S. R. and B. Horsfield, Determination of structural components of kerogens by the use of analytical pyrolysis methods, in *Organic geochemistry; principles and applications*, edited by M. H. Engel and S. A. Macko, pp. 271-287, Plenum Press, New York, 1993.

Laws, E. A., B. N. Popp, R. R. Bidigare, M. C. Kennicutt , and S. A. Macko, Dependence of phytoplankton carbon isotopic composition on growth rate and($CO_{2)aq}$: Theoretical considerations and experimental results, *Geochim.Cosmochim.Acta*, 59, 1131-1138, 1995.

Murphy, A. E., B. B. Sageman, and D. Hollander, Eutrophication by decoulping of the marine biogeochemical cycles of C, N, and P: A mechanism for the Late Devonian mass extinction, *Geology*, 28, 427-430, 2000.

Nederbragt, A. J., R. N. Erlich, B. W. Fouke, and G. M. Ganssen, Palaeoecology of the biserial planktonic foraminifer *Heterohelix moremani* (Cushman) in the Albian to middle Turonian Circum-North Atlantic, *Pal.Geo, Pal.Clim, Pal.Ecol.*, 144, 115-133, 1998.

Nijenhuis, I. A. and G. J. De Lange, Geochemical constraints on Pliocene sapropel formation in the eastern Mediterranean, *Mar.Geol.*, 163, 41-63, 2000.

Pancost, R. D., Freeman, K. F., Patzkowsky, M. E., Versteegh, G. J. M., and Sinninghe Damsté, J. S. Can changes in phytoplankton growth rates influence the geochemical record of climate change? 31. 1999.
Ref Type: Conference Proceeding

Pancost, R. D., K. H. Freeman, S. G. Wakeham, and C. Y. Robertson, Controls on carbon isotope fractionation by diatoms in the Peru upwelling region, *Geochim.Cosmochim.Acta*, 61, 4983-4991, 1997.

Park, J. and T. D. Herbert, *Journal of Geophysical Research*, 92B, 14027, 1987.

Popp, B. N., E. A. Laws, R. R. Bridigare, J. E. Dore, K. L. Hanson, and S. G. Wakeham, Effect of phytoplankton cell geometry on carbon isotopic fractionation, *Geochim.Cosmochim.Acta*, 62, 69-77, 1998.

Poulsen, C. J., The mid-Cretaceous ocean circulation and its impact on Greenhouse Climate dynamics, Pennsylvania State University, 1999.

Poulsen, C. J., E. J. Barron, and W. H. Peterson, A reinterpretation of mid-Cretaceous shallow marine temperatures through model-data comparison, *Paleoceanography*, 14, 679-697, 1999.

Repeta, D. J., A high resolution historical record of Holocene anoxygenic primary production in the Black Sea, *Geochim.Cosmochim.Acta*, 57, 4337-4342, 1993.

Repeta, D. J., D. J. Simpson, B. B. Jorgensen, and H. W. Jannasch, Evidence for anoxygenic photosynthesis from the distribution of bacterio-chlorophylls in the Black Sea, *Nature*, 342, 69-72, 1989.

Rohmer, M., P. Bisseret, and S. Neunlist., The hopanoids, prokaryotic triterpenoids and precursors of ubiquitous molecular fossils, in *Biological markers in sediments and petroleum*, edited by J. M. Moldowan, P. Albrecht, and R. P. Philp, pp. 1-17, Prentice Hall, New Jersey, 1992.

Rosell-Melee, A., M. A. Maslin, J. R. Maxwell, and P. Schaeffer, Biomarker evidence for "Heinrich" events, *Geochim.Cosmochim.Acta*, 61, 1671-1678, 1997.

Schlanger , S. O., M. A. Arthur, H. C. Jenkyns, and P. A. Scholle, The Cenomanian-Turonian oceanic anoxic event, I .Stratigraphy and distribution of organic carbon-rich beds and the marine d^{13}C excursion, *Geological Society Special Publication*, 26, 371-399, 1987.

Schlanger , S. O. and H. C. Jenkyns, Cretaceous oceanoc anoxic events: causes and consequences, *Geologie en mijnbouw*, 55, 179-184, 1976.

Schouten, S., W. C. M. Klein Breteler, P. Blokker, N. Schogt, W. I. C. Rijpstra, K. Grice, M. Baas, and J. S. Sinninghe Damsté, Biosynthetic effects on the stable carbon isotopic composition of algal lipids: Implications for deciphering the carbon isotopic biomarker record, *Geochim.Cosmochim.Acta*, 62, 1397-1406, 1998.

Scotese, C. R. and J. Golonka, Paleogeographic Atlas, University of Texas, Arlington, 1992.

Sinninghe Damsté, J. S., T. I. Eglinton, J. W. De Leeuw, and P. A. Schenck, Organic sulphur in macromolecular sedimentary organic matter: I. Structure and origin of sulphur-containing moieties in kerogen, asphalthenes and coal as revealed by flash pyrolysis, *Geochim.Cosmochim.Acta*, 53, 873-889, 1989.

Sinninghe Damsté, J. S., M. E. L. Kohnen, and J. W. De Leeuw, Thiophenic biomarkers for palaeoenvironmental assessment and molecular stratigraphy, *Nature*, 345, 609-611, 1990.

Sinninghe Damsté, J. S. and J. Köster, A euxinic southern North Atlantic Ocean during the Cenomanian/Turonian oceanic anoxic event, *Earth and Planetary Science Letters*, 158, 165-173, 1998.

Sinninghe Damsté, J. S., Rijpstra, I. C., and Reichart, G. J. The influence of oxic degradation on the sedimentary biomarker record II. Evidence from Arabian Sea sediments. Geochimica et Cosmochimica Acta . 2001. Ref Type: In Press

Sinninghe Damsté, J. S., S. G. Wakeham, M. E. L. Kohnen, J. M. Hayes, and J. W. De Leeuw, A 6,000-year sedimentary molecular record of chemocline excursions in the Black Sea, *Nature*, 362, 827-829, 1993.

Sinninghe Damsté, J. S., C. M. White, J. B. Green, and J. W. De Leeuw, Organosulfur compounds in sulfur-rich Rasa coal, *Energy and Fuels*, 13, 728-738, 1998.

Summerhayes, C. P., Organic-rich Cretaceous sediments from the North Atlantic, *Geological Society Special Publication*, 26, 301-316, 1987.

Summons, R. E., L. L. Jahnke, J. M. Hope, and G. A. Logan, 2-Methylhopanoids as biomarkers for cyanobacterial oxygenic photosynthesis, *Nature*, 400, 554-557, 1999.

Thomson, J., N. C. Higgs, T. R. S. Wilson, I. W. Croudace, G. J. de Lange, and P. J. M. van Santvoort, Redistribution and geochemical behaviour of redox-sensitive elements around S1, the most recent eastern Mediterranean sapropel, *Geochim.Cosmochim.Acta*, 59, 3487-3501, 1995.

Thurow, J., Cretaceous radiolarians of the North Atlantic Ocean: ODP Leg 103 (Sites 638, 640, and 641) and DSDP Legs 93 (Site 603) and 47B (site 398), *Proceedings of the Ocean Drilling Program, Scientific Results*, 103, 379-418, 1988.

Van Gemerden, H. and J. Mas, Ecology of phototrophic sulfur bacteria, in *Anoxygenic photosynthetic bacteria*, edited by R. E. Blankenship, M. T. Madigan, and C. E. Bauer, pp. 49-85, Kluwer Academic Publishers, Dordrecht, 1995.

Volkman, J. K., A review of sterol markers for marine and terrigenous organic matter, *Org.Geochem.*, 9, 83-99, 1986.

Vonhof, H. B., Synchronous strontium and carbon isotope excursions across the Cenomanian-Turonian Oceanic Anoxic Event, Vrije Universiteit, 1998.

Zimmerman, H. B., A. Boersma, and F. W. McCoy, Carbonaceous sediments and palaeoenvironment of the Cretaceous South Atlantic Ocean, *Geological Society Special Publication*, 26, 271-286, 1987.

Chapter 5

Cyanobacterial N$_2$ fixation fuelled enhanced biological CO$_2$ pumping during a Cretaceous oceanic anoxic event

Marcel M.M. Kuypers, Stefan Schouten, Jaap S. Sinninghe Damsté

Abstract.

The so-called Cenomanian/Turonian oceanic anoxic event (C/T OAE) is characterised by a large global increase in organic matter (OM) burial rates. We investigated the role of N$_2$-fixing cyanobacteria in this increase at four proto-North Atlantic sites of different palaeobathymetric setting using bulk nitrogen isotope measurements and molecular fossils of cyanobacterial membrane lipids. The organic matter rich sediments (black shales) show ^{15}N/^{14}N ratios (δ^{15}N = -2-0 ‰) typical for newly fixed N$_2$, indicating that microbial N$_2$ fixation was the main source of nitrogen for phytoplanktonic growth in the proto-North Atlantic prior to and during the C/T OAE. This agrees well with the abundance of molecular fossils (e.g. 2-methylhopanoids) of cyanobacteria, which are the main N$_2$-fixers in the modern ocean. Extensive N$_2$ fixation was essential to sustain productivity in this dysoxic/anoxic basin, where massive loss of nitrate occurred due to extensive denitrification. We propose that increased upwelling of anoxic, phosphorus (P)-loaded, proto-Atlantic deep water, resulting from the formation of a deep water connection between the North and South Atlantic basins, stimulated cyanobacterial productivity, increasing the amount of N$_2$ fixed by these diazotrophs. This increased nitrogen supply, enhanced phytoplanktonic biomass production and led to a large increase in OM burial during the C/T OAE. The enhanced activity of the 'biological pump' led to a significant drop in atmospheric carbon dioxide concentration during the C/T OAE and, thereby, could have triggered the early Turonian deterioration of the greenhouse climate.

5.1. Introduction

As a result of carbon dioxide exchange between the atmosphere and the ocean, uptake of dissolved inorganic carbon (DIC) during photosynthesis and subsequent export of phytoplanktonic biomass to deeper water and underlying sediment acts as a biological carbon dioxide pump. Organic matter (OM) degradation (i.e. respiration) and ocean circulation will eventually return most of this carbon dioxide back to the atmosphere. However, a small amount of OM escapes degradation and is buried in the sediment. This burial of sedimentary OM largely controls the carbon dioxide content of the atmosphere on geological time scales [*Berner*, 1991; *Berner*, 1992].

In addition to DIC, phytoplankton in the ocean surface waters consumes mainly dissolved nitrogen (N) and phosphorus (P). While DIC will normally not be limiting phytoplanktonic growth as it is present in excessive amounts in the upper mixed layer of the ocean, the availability of nutrient N and P limits the production of phytoplanktonic particulate OM (POM). Riverine input is the only significant source of phosphate, the form of dissolved P that is normally used by phytoplankton, to the ocean [*Jahnke*, 1992; *Mackenzie et al.*, 1993]. Nitrate, nitrite and ammonium are the N compounds (i.e. reactive N) that are generally easily taken up by phytoplankton. An important input of reactive N to the ocean comes via river water, but unlike P, there is also a significant atmospheric input [*Mackenzie et al.*, 1993; *Jaffe*, 1992]. The atomic ratios of C, N and P of POM are similar throughout the marine realm [*Copin-Monteguet and Copin-Monteguet*, 1983; *Toggweiler*, 1993] and on average phytoplanktonic biomass is characterised by a C:N:P ratio of 106:16:1 [*Redfield et al.*, 1963]. In principle C, N and P are released upon remineralisation of POM in similar ratios [*Redfield et al.*, 1963]. These regenerated nutrients can subsequently be used again for the production of POM. To sustain primary productivity the flux of nutrient N and P entering the photic zone needs to be equal to the flux of nutrient N and P exported from it. When photosynthetic production increases relative to remineralisation of POM nutrient N and P will be lost to the sediment and primary productivity will decrease.

In sharp contrast to P, reactive N is not only lost to the sediment but can also be converted to N_2 or N_2O (denitrification) gas, which are much less easily used by phytoplankton. Denitrification is in fact the main sink for reactive N in the marine realm and occurs in suboxic environments, where bacteria use nitrate or nitrite instead of oxygen as an oxidator [*Codispoti and Christensen*, 1985]. In theory this loss of reactive N as a result of denitrification could lead to an ocean-water N:P ratio significantly smaller than the Redfield (i.e. 15-16) ratio and hence a severe limitation of reactive N for phytoplankton growth. In reality ocean-water N:P ratios are only slightly below Redfield ratio. This discrepancy between theory and reality has been attributed to the activities of N_2-fixing organisms (mainly cyanobacteria) in the marine realm [*Tyrrell*, 1999]. These organisms can use the nearly inexhaustible atmospheric reservoir of N_2 as N source but due to the high-energy demand of N_2 fixation they can only outcompete non-N_2-fixing algae, when reactive N concentrations are low relative to P. According to the model proposed by Tyrrell [*Tyrrell*, 1999], there is a negative feedback between reactive N versus P concentrations and the abundance of N_2-fixers. Decreasing N:P ratios as a result of denitrification will lead to an increase in N_2 fixation and subsequent release of reactive N upon remineralisation of their biomass will increase N:P ratios.

Although N$_2$ fixation can fuel up to half of the new production in oligotrophic ocean gyres [*Karl et al.*, 1997], N$_2$-fixers make up a relatively small amount of total phytoplanktonic biomass in the modern ocean [*Tyrrell*, 1999]. However, reduced ocean circulation and extensive denitrification in largely anoxic or suboxic mid and deep waters may have led to N$_2$-fixing cyanobacteria periodically dominating phytoplankton communities during the early to middle Cretaceous [*Rau et al.*, 1987]. Thinly laminated OM–rich sediments devoid of traces of benthic activity (i.e. black shales) that were globally deposited in a variety of paleo-bathymetric settings [*Schlanger and Jenkyns*, 1976] indicate that anoxic waters were particularly widespread during the so-called Cenomanian/Turonian oceanic anoxic event (C/T OAE) [*Summerhayes*, 1987; *Bralower and Thierstein*, 1987]. Sedimentary derivatives (molecular fossils) of a pigment indicative of anoxygenic photosynthetic bacteria recovered from abyssal and shelf sites indicate that anoxic conditions extended even into the photic zone of the southern proto-North Atlantic during the C/T OAE [*Sinninghe Damsté and Köster*, 1998]. At the same time a sharp increase in ^{13}C/^{12}C ratios for marine carbonates and OM provides evidence for a large increase in the global organic carbon (OC) burial rate and a significant drop in atmospheric carbon dioxide concentration during the C/T OAE [*Arthur et al.*, 1988; *Freeman and Hayes*, 1992; Kuypers et al., 1999].

One of the main sites of carbon burial during the C/T OAE was the proto-North Atlantic Ocean, where up to 80 m thick black shales [*Kuhnt et al.*, 1990], which can contain more than 40% organic carbon [*Herbin et al.*, 1986], were deposited basin-wide. Recently, we reported an increase in marine OC accumulation rates at three sites in the southern part of the proto-North Atlantic (Fig. 1; site S13, and DSDP sites 144 and 367), which we attributed to an increase in primary productivity during the C/T OAE [*Kuypers et al.*, 2000 submitted to Paleoceanography]. This increase in primary productivity was accompanied by a significant rise of the chemocline, with euxinic conditions periodically occurring at very shallow water depths of 15 m or less, while bottom water redox conditions did not markedly change (i.e. remained euxinic). An increase in OM accumulation rates, albeit smaller, also occurred at the northern proto-North Atlantic site 603B during the C/T OAE [*Kuypers et al.*, in prep]. Globally enhanced OM burial and thus enhanced burial of organic nitrogen would have increased the phytoplanktonic reactive N demand, while reactive N losses would have been especially high due to extensive denitrification during the C/T OAE. N$_2$-fixing cyanobacteria could have supplied the additional reactive N required to sustain or even increase marine productivity during the C/T OAE.

Here we determine the role and significance of N$_2$-fixing cyanobacteria in the increase of OM burial at four proto-North Atlantic sites (Fig. 1) of different palaeobathymetric settings using nitrogen isotope measurements and cyanobacterial membrane lipids. In addition we discuss the consequences of our findings for the mid-Cretaceous global biogeochemical cycles.
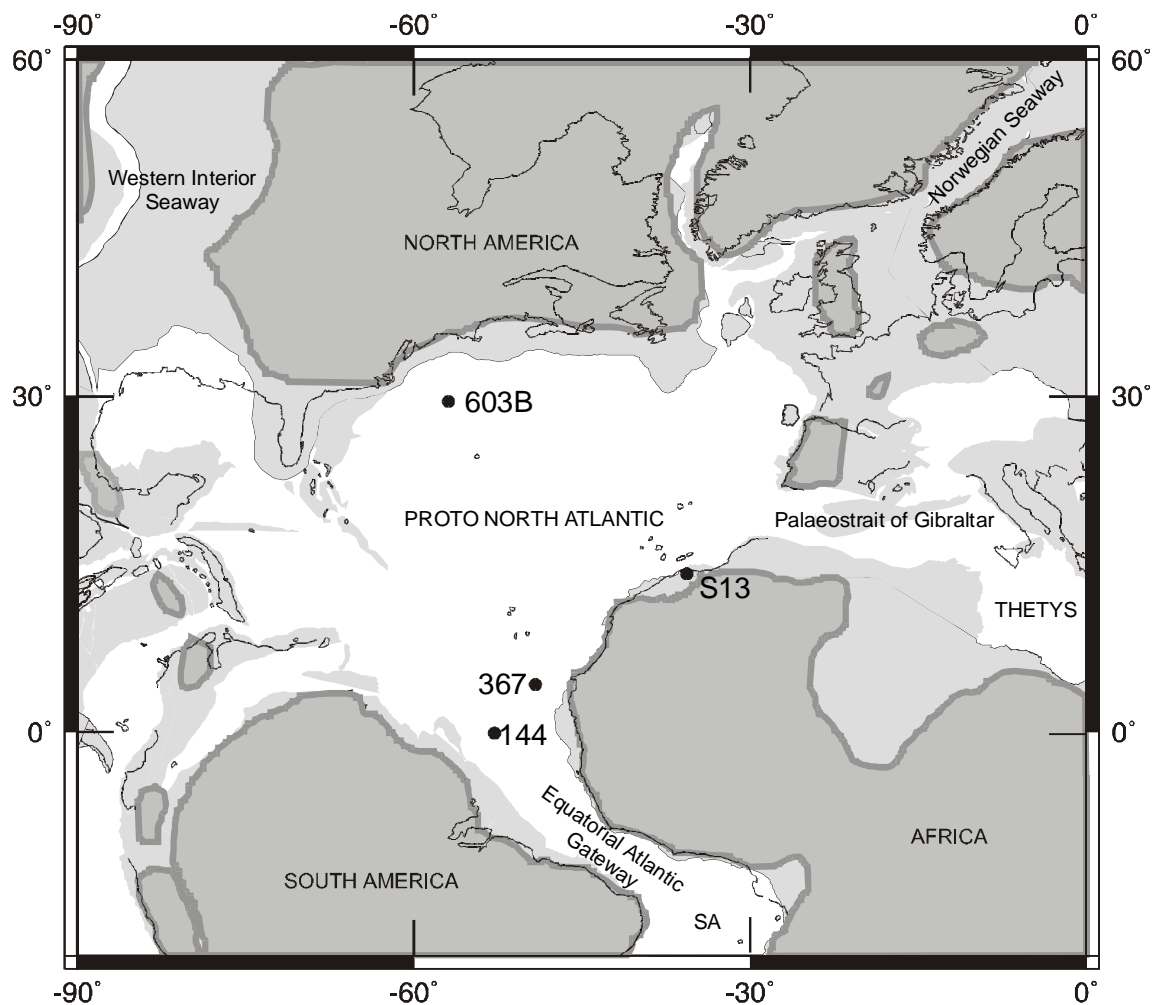
Figure 1. Palaeogeographical map of mid Cretaceous (~94 Ma) North Atlantic showing the position of the four studied cores. Light grey shaded regions represent flooded continental plates (from GEOMAR map generator; www.odsn.de/odsn/services/paleomap/paleomap.html). Dark grey shaded regions represent land [*Scotese and Golonka*, 1992].

5.2. Material and Methods

5.2.1 Material. The sediment samples used in this study were obtained from the Shell exploration well S13 of the Tarfaya area (Morocco), the Deep Sea Drilling Project (DSDP) sites 144 off the coast of French Guyana (leg 14), 367 off the coast of Senegal (leg 41) and 603B off the coast of North America (leg 93). Two to five cm thick sediment slices were taken from the cores. Sub-samples were taken from these slices and subsequently freeze-dried and powdered in an agate mortar.

5.2.2 Stable nitrogen isotopes. The $\delta^{15}N$ values were measured for bulk sediments. The $\delta^{15}N$ measurements were performed using an automated on-line combustion system (Carlo Erba CN analyser 1502 series) followed by conventional isotope ratio-mass spectrometry (Fisons Optima). The $\delta^{15}N$ values for bulk sediments are expressed relative to atmospheric N_2 and have a precision better than 0.2 ‰.

5.2.3 Organic matter analyses. Analyses of soluble and insoluble organic matter were performed as described previously by Kuypers et al. [2000; submitted to Paleoceanography]. Briefly, Total Organic Carbon (TOC) contents were determined using a CN analyser. The δ^{13}C values (±0.1‰ versus Vienna Pee Dee belemnite (VPDB)) were measured on bulk sediments, after removal of the inorganic carbonates with diluted HCl, using automated on-line combustion followed by conventional isotope ratio-mass spectrometry. For analyses of the soluble OM powdered samples (15 to 30 g) were Soxhlet extracted for *c*. 24 h to obtain the total extract. An aliquot (*c*. 250 mg) of the total extract was separated into an apolar and a polar fraction using column chromatography. The hydrocarbons that were released from the polar fraction by Raney Nickel desulfurisation and subsequent hydrogenation [*Sinninghe Damsté et al.*, 1990a] were isolated using column chromatography. Samples were analysed by gas chromatography-mass spectrometry (GC-MS) for compound identification. Compound-specific δ^{13}C analyses were performed using a Finnigan Delta C GC-isotope-ratio-monitoring MS. The δ^{13}C values for individual compounds are the means of duplicate runs ($\sigma = \pm 0.3$ to 0.6) expressed versus VPDB.

5.2.4 Determination of the relative abundance of sulfur-bound 2-methylhopanes. $17\beta,21\beta$(H)-Trishomohopane (C_{33}; **I**) and $17\beta,21\beta$(H)-pentakishomohopane (C_{35}; **II**) are coeluting with 2β-methyl-$17\beta,21\beta$(H)-trishomohopane (C_{34}; **III**) and 2β-methyl-$17\beta,21\beta$(H)-pentakishomohopane (C_{36}; **IV**), respectively. For calculating the abundance of **III** and **IV** relative to the abundance of the coeluting **I** and **II**, respectively, the following equation was used:

% 2-methylhopane $C_n = 100 \cdot x/(x + y)$ [1]

were x = peak area of **III** and y = peak area of **I** for n = 33, and x = peak area of **IV** and y = peak area of **II** for n = 35. The peak areas were obtained by mass chromatography of *m/z* 369 and 383 for $17\beta,21\beta$(H)-hopanes (i.e. **I** and **II**) and 2β-methyl-$17\beta,21\beta$(H)-hopanes (i.e. **III** and **IV**), respectively. This method was used to determine the relative abundance of 2-methylhopanoids in the C/T sediments analysed in this study as well as a suite of GC-MS analyses from other thermally immature Phanerozoic sediments present in the archive of our laboratory.

5.3. Stratigraphy, palaeosetting and organic carbon accumulation rates

Our study concentrates on the C/T interval between 95 and 93 My before present [*Obradovich*, 1993; *Gradstein et al.*, 1994; *Gradstein et al.*, 1995], roughly coinciding with the late Cenomanian *Rotalipora cushmani* zone and the latest Cenomanian to early Turonian *Whiteinella archaeocretacea* zone. This interval reaches a thickness of ~150 m at well S13 of the Tarfaya basin in the southeastern part of the proto North Atlantic Ocean (Fig. 2). The C/T sequence at site S13 consists of an alternation of dark laminated carbonaceous chalks and lighter coloured homogeneous limestones, deposited in an open shelf sea at a palaeo-water depth of 200-300 m [*Einsele and Wiedmann*, 1982; *Thurow and Kuhnt*, 1986; *Kuhnt et al.*, 1990]. The late Cenomanian to early
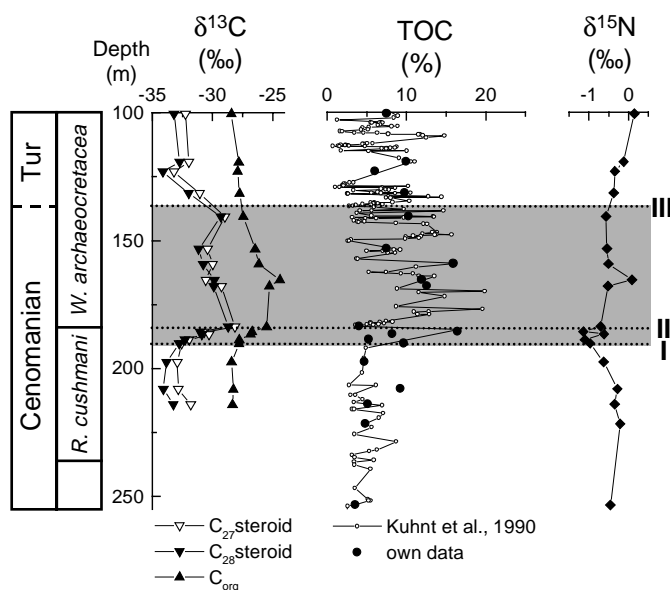
Figure 2. Stratigraphy [*Kuhnt et al.*, 1997], biomarker, bulk organic carbon and nitrogen data of site S13 (Tarfaya basin). Carbon isotope values (in ‰ vs. VPDB) of bulk organic carbon (C_{org}) and free steranes [C_{27} sterane (5α-cholestane) and C_{28} sterane (5α-24-methyl-cholestane)] derived from marine algae, TOC content of the bulk sediment (own data and data previously reported by Kuhnt et al. [*Kuhnt et al.*, 1990]), and nitrogen isotope values (in ‰ vs. atmospheric N_2) of the bulk sediment. The dashed lines with Roman numbers show the approximate position of the boundaries between the different phases (i.e. rapid positive shift in $\delta^{13}C$ values, plateau with maximum $\delta^{13}C$ values and return to pre-excursion $\delta^{13}C$ values) of the carbon isotope excursion.

Turonian sediments of site S13 contain high amounts of marine OC [*Kuhnt et al.*, 1990] with maximum total organic carbon (TOC) values of ~16% (Fig. 2).

At DSDP Site 144, the late Cenomanian deposits consist of dark laminated carbonaceous cemented limestones and zeolitic calcareous clay [*Hayes and et al.*, 1972] containing up to 8% (Fig. 3) marine OC [*Kuypers et al.*, 2000 submitted to Paleoceanography]. These hemipelagic sediments were deposited at a water depth of ~1300 m [*Berger and von Rad*, 1972].

The black shales that make up the late Cenomanian sequence at DSDP Site 367 (off the coast of north-west Africa) consist of a mixture of terrigenous silicates and clay minerals [*Mélières*, 1978] and high amounts of marine [*Herbin et al.*, 1987; *Kuypers et al.*, 2000 submitted to Paleoceanography] organic carbon (total organic carbon (TOC) contents up to 46 wt. %; Fig. 4). These sediments contain only minor amounts of biogenic carbonate due to deposition below the carbonate compensation depth (CCD). A water depth of 3700 m has been estimated for this time interval at DSDP Site 367 [*Chénet and Francheteau*, 1979].

The late Cenomanian sequence at DSDP site 603B consists of an alternation of OM poor green claystones and OM-rich (TOC 1-21%) black claystones [*Herbin et al.*, 1987]. Carbonate contents are very low (<10%), which suggests that deposition took place below CCD. These hemipelagic sediments were deposited at a water depth of ~4000 m [*Chénet and Francheteau*, 1979]. Rock Eval indices are generally low (HI < 100 mg hydrocarbons/g TOC) for the OM-lean green claystones, which has been attributed to a terrestrial source for the OC [*Herbin et al.*, 1987].

In sharp contrast, high Rock Eval hydrogen indices (HI) [*Herbin et al.*, 1987; *Kuhnt et al.*, 1990] and the low abundance of lignin pyrolysis products generated from the kerogen [*Sinninghe Damsté et al.*, unpublished data] indicate a marine origin for the thermally immature OM for the OC-rich black claystones. This is supported by the low abundance of molecular fossils of unambiguous terrestrial origin (e.g. leaf-wax lipids and oleananes) in the extractable OM [Kuypers et al., unpublished data]. The high amplitude short-term cyclic variations in TOC content of these sediments have been attributed to fluctuations in redox conditions of the bottom waters [*Herbin et al.*, 1987].

In sharp contrast to the shelf section from site S13 [*Kuhnt et al.*, 1990], biostratigraphically significant species are largely absent from the middle Cretaceous sediments from DSDP sites 144, 367 and 603B. Instead, the investigated sections of these abyssal sites were correlated with the C/T section of site S13 by stable carbon isotope stratigraphy using the characteristic ^{13}C excursion in both bulk OM and molecular fossils of algal chlorophyll and steroids (Figs. 2-5). For a more thorough discussion of this method see Kuypers et al. [2000]. The horizontal dotted lines with Roman numbers (I-III) in the various plots (Figs. 2-5) indicate the boundaries between the pre-excursion conditions (i.e. pre-excursion δ^{13}C values) and the three main phases of the isotope excursion (i.e. rapid positive shift in δ^{13}C values, plateau with maximum δ^{13}C values and return to pre-excursion δ^{13}C values). Of particular stratigraphic significance is boundary II that nearly coincides with the last occurrence of *R. cushmani* [*Kuhnt et al.*, 1990] and boundary III, which approximately coincides with the C/T boundary [*Gale et al.*, 1993]. The C/T OAE is coeval with the interval between boundaries III and I (indicated as a grey shaded area in Fig. 2). Coring gaps obscure the later part of the first phase of the carbon isotope excursion (rapid positive shift in δ^{13}C values) and whole of the second phase (plateau with maximum δ^{13}C values) at DSDP Site 144, while coring gaps obscure the later part of the second phase at DSDP Sites 367 and 603B. Hence the grey shaded areas (Figs. 3-5) most likely represent only a part of the total C/T OAE interval present at DSDP Sites 144, 367 and 603B. However, the beginning of the rapid shift in δ^{13}C values was recovered at all sites (Figs. 2-5) allowing a direct comparison of the changes in OC accumulation rates that occurred during the onset of the C/T OAE.

Prior to the C/T OAE, OC mass accumulation rates were significantly larger for the southern part of the proto-North Atlantic (~9 and 3 gC·m^{-2}·y^{-1} for S13 and DSDP site 367, respectively), than for the northern part (~0.6 gC·m^{-2}·y^{-1} for site 603B) [*Kuypers et al.*, 2000 submitted to Paleoceanography; *Kuypers et al.*, in prep.]. There is a significant increase in marine OC accumulation rates at all sites during the C/T OAE. At the southern proto-North Atlantic site S13 and DSDP Site 367 this increase in OC accumulation rates could have been as large as 17 and 6 gC·m^{-2}·y^{-1}, respectively [*Kuypers et al.*, 2000 submitted to Paleoceanography], while it was significantly smaller (~1 gC·m^{-2}·y^{-1}) at the northern proto-North Atlantic site 603B [*Kuypers et al.*, in prep.].

5.4. Results and discussion

5.4.1 Proxy records for N$_2$-fixing cyanobacteria

Unlike certain algae such as dinoflagellates, diatoms and calcareous algae, pelagic cyanobacteria do not leave behind microscopically identifiable fossilised remains. Instead, specific cyanobacterial biomarkers, such as the 2-methyl-bacteriohopanepolyol membrane lipids and the pigment zeaxanthin or molecular fossils of these compounds formed upon diagenesis, can provide information about their relative abundance in ancient marine phytoplankton communities [*Summons et al.*, 1999; *Bianchi et al.*, 2000]. The stable nitrogen isotopic composition of sedimentary OM or the sediment itself can provide information about the significance of cyanobacterial N$_2$ fixation in the biogeochemical cycle of ancient marine environments [*Rau et al.*, 1987; *Haug et al.*, 1998; *Sachs and Repeta*, 1999; *Bianchi et al.*, 2000]. Especially a combined biomarker and nitrogen isotopic study can provide important insights in the ecological role of N$_2$-fixing cyanobacteria in ancient marine settings. In addition the stable carbon isotopic composition of phytoplanktic biomarkers can provide important insight into environmental conditions under which photosynthetic carbon fixation occurred. Thus we investigated the abundance of cyanobacterial biomarkers and their stable carbon isotopic composition and the stable nitrogen isotopic composition of the North Atlantic C/T sediments.

5.4.1.1 Stable nitrogen isotopes. The late Cenomanian to early Turonian sediments of site S13 (Tarfaya basin) are ^{15}N-depleted relative to atmospheric N$_2$ with minimum δ^{15}N values of -1.1‰ (Fig. 2). During the C/T OAE the average δ^{15}N value is slightly more depleted in ^{15}N ($\sim$ -0.7‰) than before ($\sim$ -0.4‰) or after ($\sim$ -0.2‰) (Fig. 2). At DSDP Site 144 the δ^{15}N values for the bulk sediment ($\sim$ -1.7‰) are on average even more depleted in ^{15}N than at site S13 (Fig. 3). A similar ^{15}N depletion is also observed for the sediments of DSDP Site 367 (i.e. δ^{15}N$_{average}$ $\sim$ -1.5‰; Fig. 4). During the C/T OAE δ^{15}N values ($\sim$ -1.7‰) are on average slightly more depleted in ^{15}N than before ($\sim$ -1.3‰). At DSDP site 603B we measured δ^{15}N values for two intervals containing an OM-rich/OM-lean cycle (Fig. 5). While the OM-rich intervals of site 603B show similar negative δ^{15}N values ($\sim$ -1.5‰) as sites S13, 144 and 367, the OM-lean intervals are significantly more enriched in ^{15}N (δ^{15}N $\sim$ 1.7‰). At site 603B there is a strong negative correlation between δ^{15}N values and TOC content of the bulk sediment (R^2 = 0.96). In sharp contrast, there is no correlation or only a minor correlation (R^2 = 0.5) between the δ^{15}N values and the TOC contents of the sediment at sites S13, 144 and 367.

It is generally assumed that sedimentary N predominantly derives from organic N compounds (i.e. ON) like proteins. This is supported by the fact that the stable nitrogen isotopic composition of sedimentary N is similar to that of insoluble OM (i.e. kerogen) isolated from the sediment [*Peters et al.*, 1978]. However, degradation can substantially influence the N-isotopic composition of sedimentary OM. Heterotrophic bacteria play a key role in the degradation of phytoplanktonic OM [*Cole et al.*, 1988]. These organisms that use organic carbon as their sole carbon source can use ammonium as reactive N source and as a consequence of their abundance a large fraction of total ammonium uptake in the marine environment has been attributed to bacteria [*Wheeler and Kirchman*, 1986]. Since heterotrophic bacteria grown at high concentrations of NH$_4^+$ can exhibit
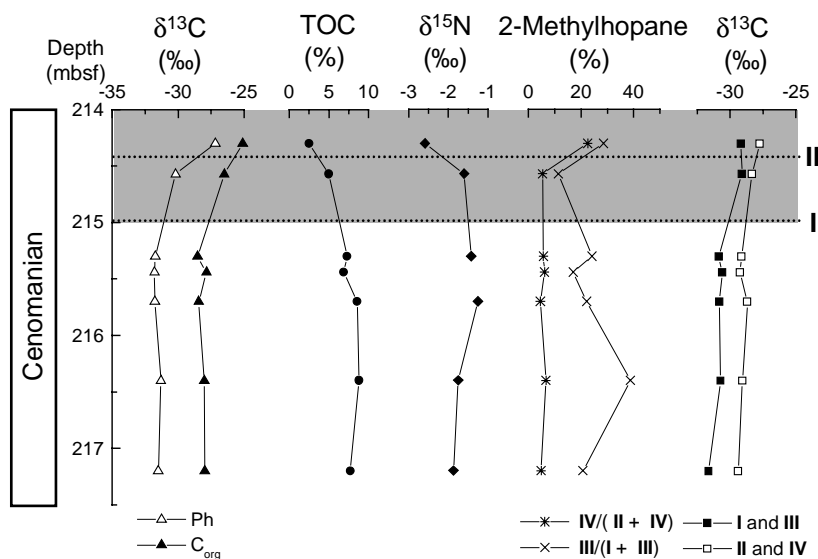
Figure 3. Stratigraphy, biomarker, bulk organic carbon and nitrogen data of DSDP Site 144. Carbon isotope values (in ‰ vs. VPDB) of C_{org}, S-bound phytane (Ph) derived from phytoplanktonic chlorophyll, TOC content of the bulk sediment, nitrogen isotope values (in ‰ vs. atmospheric N_2) of the bulk sediment, the relative abundance of molecular fossils (i.e. S-bound 2-methyl-hopanes) of membrane lipids of cyanobacteria, and the stable carbon isotopic composition of molecular fossils of membrane lipids predominantly of cyanobacterial origin. The dashed lines with Roman numbers show the approximate position of the boundaries between the different phases (i.e. rapid positive shift in $\delta^{13}C$ values, plateau with maximum $\delta^{13}C$ values and return to pre-excursion $\delta^{13}C$ values) of the carbon isotope excursion.

large (up to 27‰) isotopic effects during nitrogen fixation [*Hoch et al.*, 1992] incorporation of large quantities of bacterial biomass could result in ^{15}N depleted sedimentary OM. Protein hydrolyses and subsequent bacterial utilisation of released amino acids or short-chain peptides on the other hand may lead to a significant ^{15}N enrichment of sedimentary OM [*Macko et al.*, 1994 and references therein]. Increases as well as decreases in $\delta^{15}N$ values with water depth have been observed for POM settling through the water column [*Calvert et al.*, 1992 and references therein]. Surface sediments, however, are generally more or less enriched in ^{15}N relative to phytoplankton [*Altabet et al.*, 1999; *Holmes et al.*, 1999]. When bottom waters are well oxygenated or suboxic, sediments are enriched in ^{15}N by 4-6‰ or 2-4‰, respectively, while $\delta^{15}N$ values for recent as well as ancient sediments deposited under anoxic bottom water conditions are within 2‰ of phytoplankton biomass [*Sachs and Repeta*, 1999]. At site 603B bottom water redox conditions may have fluctuated, with OM-poor and OM-rich sediments representing more or less oxic and anoxic conditions, respectively [*Herbin et al.*, 1987; *Kuypers et al.*, in prep.]. While the OM-rich sediments probably preserve the phytoplanktonic nitrogen isotope signature, diagenetic ^{15}N enrichment of decomposing OM in the presence of oxygen could have severely affected the $\delta^{15}N$ values for the OM-poor sediments of site 603B (Fig. 4). In sharp contrast, bottom waters were constantly anoxic in the southern part of the proto-North Atlantic during the entire deposition of the investigated sections (sites S13, 144 and 367), before as well as during the C/T OAE [*Brumsack*, 1986; *Sinninghe Damsté and Köster*, 1998; *Kuypers et al.*, 2000 submitted to Paleoceanography]. Hence the black shales of sites S13, 144 and

367 and the OM-rich intervals of site 603B are expected to preserve the original stable nitrogen isotopic ratios of phytoplanktonic POM.
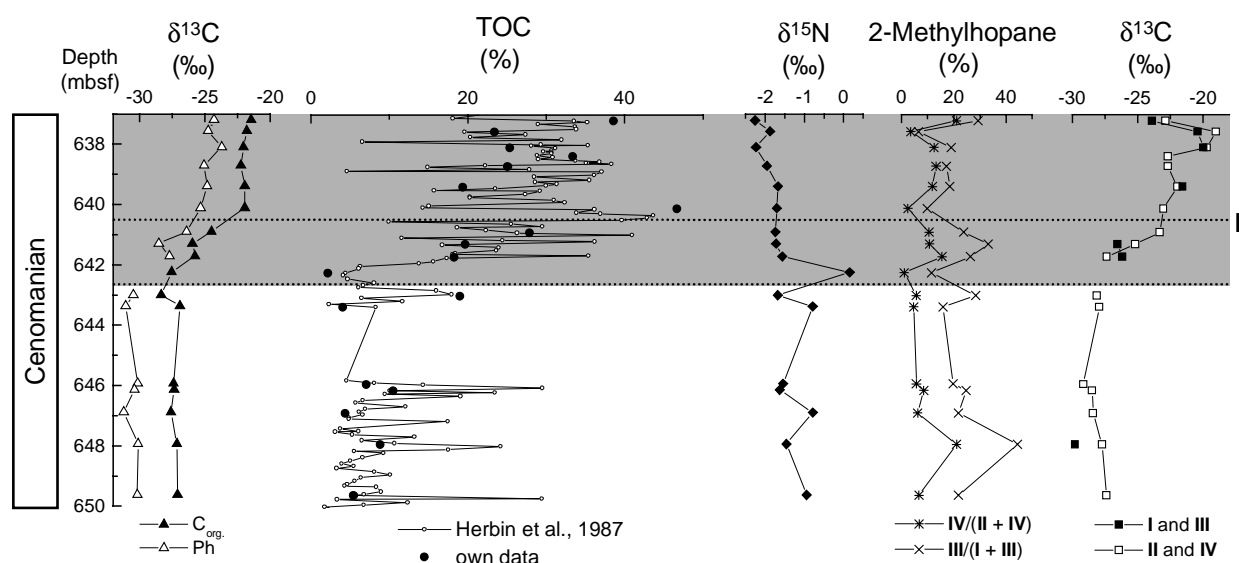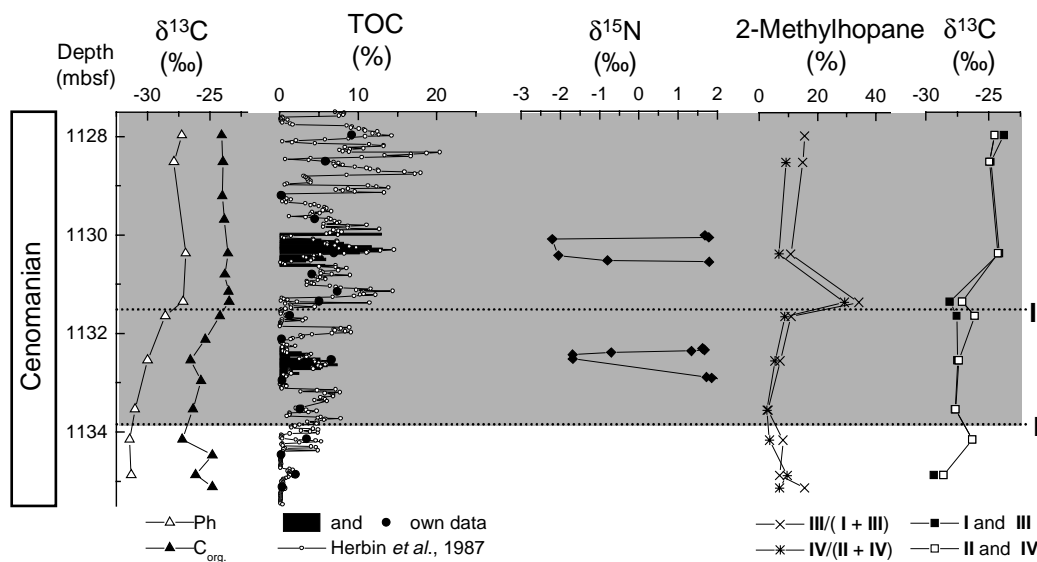

Figure 4. Stratigraphy, biomarker, bulk organic carbon and nitrogen data of DSDP Site 367. Carbon isotope values (in ‰ vs. VPDB) of C_{org}, S-bound phytane (Ph) derived from phytoplanktonic chlorophyll, TOC content of the bulk sediment (own data and data previously reported by Herbin et al. [*Herbin et al.*, 1986]), nitrogen isotope values (in ‰ vs. atmospheric N_2) of the bulk sediment, the relative abundance of molecular fossils (i.e. S-bound 2-methyl-hopanes) of membrane lipids of cyanobacteria, and the stable carbon isotopic composition of molecular fossils of membrane lipids predominantly of cyanobacterial origin. The dashed lines with Roman numbers show the approximate position of the boundaries between the different phases (i.e. rapid positive shift in $\delta^{13}C$ values, plateau with maximum $\delta^{13}C$ values and return to pre-excursion $\delta^{13}C$ values) of the carbon isotope excursion.

The stable nitrogen isotopic composition of POM is a function of the $\delta^{15}N$ value of the nitrogen substrate and the isotopic effect associated with nitrogen fixation [*Altabet and Deuser*, 1985; *Francois et al.*, 1992]. In the modern ocean nitrate formed upon remineralization of POM below the photic zone plays a key role in sustaining primary productivity (=new production). The preferred uptake of ^{14}N by phytoplankton causes a decrease (~5‰) in POM $\delta^{15}N$ values relative to the nitrogen substrate at high nitrate concentrations, while under nitrate-limiting conditions the $\delta^{15}N$ values of source and POM are roughly equal. Hence variations in the $^{15}N/^{14}N$ ratios of sedimentary marine OM have been used to track past changes in relative supply of nitrate to the photic zone [*Altabet et al.*, 1991; *Calvert et al.*, 1992; *Farrell et al.*, 1995]. Since the mean $\delta^{15}N$ value for global deep-water nitrate is 5-6‰ [*Farrell et al.*, 1995], the $\delta^{15}N$ values for extant marine phytoplankton are normally above 0‰. The stable N-isotopic composition of nitrate entering the photic zone is influenced by regional differences in the degree of microbial reduction of nitrate to N_2 and/or N_2O gas under suboxic conditions (i.e. denitrification) [*Altabet et al.*, 1995; *Altabet et al.*, 1999]. Water column denitrification is accompanied by a significant isotopic fractionation (20-40‰) resulting in a substantial enrichments in ^{15}N for the residual nitrate in regions with suboxic intermediate waters (~100-1500 m), such as the Arabian Sea and the Peru upwelling zone [*Altabet et al.*, 1999 and

references therein]. By analogy, substrate nitrate should have been substantially enriched in ^{15}N during the C/T OAE due to overall enhanced oceanic denitrification rates resulting from a significant increase in the ocean area with suboxic to anoxic intermediate waters. Because this would lead to ^{15}N enrichment rather than ^{15}N depletion of the C/T sediments, the negative $\delta^{15}N$ values observed for the OM-rich sediments of sites S13, 144, 367 and the OM-rich sections of site 603B point to a N source other than upwelled nitrate for most of the C/T marine phytoplankton.

Figure 5. Stratigraphy, biomarker, bulk organic carbon and nitrogen data of DSDP Site 603B. Carbon isotope values (in ‰ vs. VPDB) of C_{org}, S-bound phytane (Ph) derived from phytoplanktonic chlorophyll, TOC content of the bulk sediment (own data and data previously reported by Herbin et al. [*Herbin et al.*, 1987]), nitrogen isotope values (in ‰ vs. atmospheric N₂) of the bulk sediment, the relative abundance of molecular fossils (i.e. S-bound 2-methyl-hopanes) of membrane lipids of cyanobacteria, and the stable carbon isotopic composition of molecular fossils of membrane lipids predominantly of cyanobacterial origin. The dashed lines with Roman numbers show the approximate position of the boundaries between the different phases (i.e. rapid positive shift in $\delta^{13}C$ values, plateau with maximum $\delta^{13}C$ values and return to pre-excursion $\delta^{13}C$ values) of the carbon isotope excursion.

Although nitrate is generally the main source for new production in the modern ocean, in some systems such as estuaries [*Waser et al.*, 1998a] and anoxic basins [*Velinsky et al.*, 1991; *Velinsky and Fogel*, 1999] ammonium could be the main source of new nitrogen. This is because ammonium, if present in sufficient amounts, will always be the preferred nitrogen source for phytoplankton [*Waser et al.*, 1998b]. Like the anoxic waters of the Black Sea, Saanich Inlet, and the Nordic Framvaren fjord [*Velinsky et al.*, 1991; *Velinsky and Fogel*, 1999], the euxinic waters of the proto-North Atlantic ocean could have contained large amounts of ammonium. It has been shown that algae grown at high concentrations of ammonium under well-constrained laboratory conditions can exhibit large (up to 25‰) isotopic effects during nitrogen fixation [*Pennock et al.*, 1996; *Waser et al.*, 1998a; *Waser et al.*, 1998b]. In accordance with this, $\delta^{15}N$ values of ~1‰ observed for the POM maximum within the euxinic waters of the Nordic Framvaren fjord were attributed to the isotope effect associated with ammonium uptake by photosynthetic anaerobic purple and green

sulfur bacteria [*Velinsky and Fogel*, 1999]. In the oxic part of the fjords water column $\delta^{15}N$ values for phytoplanktonic PN were significantly more ^{15}N-enriched (~ 4‰), which they attributed to the use of nitrate instead of ammonium. The extremely low ammonium concentrations in the oxic part of the water column were attributed to a combination of intense utilisation by anoxygenic photosynthetic bacteria and extensive microbial ammonium oxidation. Extensive anaerobic photosynthesis by green sulfur bacteria could in principle explain the negative $\delta^{15}N$ values for the C/T sediments from the North Atlantic since molecular fossils of their pigments are abundantly present [*Sinninghe Damsté and Köster*, 1998; *Kuypers et al.*, 2000 submitted to Paleoceanography]. Carbon fixation in green sulfur bacteria occurs via a non-Calvin cycle pathway which results in a strong (10-15‰) enrichment in ^{13}C of their biomass relative to algae or cyanobacteria [*Sirevåg et al.*, 1977; *Van der Meer et al.*, 1998]. Hence a significant contribution of green sulfur bacterial OM to the sediment should also be reflected in the $\delta^{13}C$ values for sedimentary OM. However, $\delta^{13}C$ values for OC are relatively depleted in ^{13}C before as well as during the C/T OAE (Figs. 2-5) indicating that green sulfur bacteria did not significantly contribute to the sedimentary OM.

An alternative and in our view more plausible explanation for the ^{15}N depletion of the OM-rich sediments of sites S13, 144, 367 and in the OM-rich sections of site 603B, is microbial N_2 fixation. N_2 fixation was also invoked by Rigby and Batts [1986] and Rau et al. [1987] to explain the ^{15}N depletion of Cretaceous OM-rich deposits from Australia and the North and South Atlantic, respectively. A $\delta^{15}N$ value of 0‰ for atmospheric N_2 and minor isotopic fractionation during N_2-fixation results in $\delta^{15}N$ values of –3 to 1‰ for OM from extant marine N_2-fixing cyanobacteria [*Minagawa and Wada*, 1986; *Carpenter et al.*, 1997]. This characteristic ^{15}N-depletion of fixed N has been used to determine the contribution of N_2 fixation to the reactive N pool in ancient environments [*Rau et al.*, 1987; *Haug et al.*, 1998; *Sachs and Repeta*, 1999]. $\delta^{15}N$ values are more or less constantly negative throughout the investigated sections of the southern proto-North Atlantic, indicating that N_2 fixation contributed substantially to the reactive N pool before as well as during the C/T OAE [Figs. 1-3].

5.4.1.2 Molecular Fossils of Cyanobacterial Membrane Lipids. Bacteriohopanepolyols (BHPs) are membrane lipids exclusively produced by bacteria. They have been recovered from numerous taxa including cyanobacteria [*Rohmer et al.*, 1992]. Like sterols in eukaryotic membranes, they serve a regulating and rigidifying function and as such BHPs are major constituents of bacterial membranes with concentrations varying between 0.1-3 mg/g cell material (dry weight) [*Rohmer et al.*, 1992]. A high proportion of cultured cyanobacteria and recent microbial mats dominated by cyanobacteria contain in addition to 'regular' BHPs, BHPs methylated at the C2 position (i.e. 2-methyl-BHPs), which are absent or only present in relatively low amounts in other bacteria [*Summons et al.*, 1999]. Both BHPs without a methyl group at the C2 position (i.e. 2-desmethyl BHPs) and 2-methyl-BHPs are rapidly transformed in sediments by a variety of diagenetic reactions like oxidation, dehydration, and subsequent hydrogenation, and/or side chain cleavage [*Köster et al.*, 1997]. Their diagenetic derivatives (i.e. C_{31} to C_{36} hopanoids), however, have been recovered from OC-rich sediments as old as 2,500 My [*Summons et al.*, 1999]. These extended hopanoids are especially abundant in anoxic sediments, as a result of the reaction of BHPs with reduced inorganic

sulfur species [*Sinninghe Damsté et al.*, 1995; *Köster et al.*, 1997] during early diagenesis [*Kok et al.*, 2000; *Werne et al.*, 2000]. This natural sulfurisation reaction often preserves taxon-specific carbon-skeletons (i.e. biomarkers) in the geological record [*De Leeuw and Sinninghe Damsté*, 1989]. In thermally immature euxinic sediments more than 50% of the extractable extended hopanoids are present as sulfur-bound hopanoids, often preserving the biological 17β,21β(H)-conformation [*Sinninghe Damsté et al.*, 1995].

Selective chemical degradation of sulfur-carbon bonds (i.e. desulfurisation) released considerable amounts of extended hopanes from the extractable OM of the C/T sediments from DSDP sites 144, 367 and 603B. These hopanes are typically dominated by the C$_{33}$ and C$_{35}$ 2-desmethyl-17β,21β(H)-hopanes **I** and **II** and their coeluting 2β-methyl-17β,21β(H)-isomers **III** and **IV** (Fig. 6). On average **I-IV** together make up 60 to 80% of the extended hopanes present at the various sites. Desulfurisation of the polar fractions did not release any significant amounts of extended hopanes at the shelf site S13.

Summons et al. [*Summons et al.*, 1999] used the relative abundance of 2-methylhopanes, expressed as the so-called '2-methylhopane index', versus the coeluting 2-desmethylhopanes to determine the ecological importance of cyanobacteria in ancient environments. Similarly, we determined the 2-methylhopane indices for sites 144, 367 and 603B from the relative intensities of coeluting 2-desmethylhopanoids and 2-methylhopanoids. In the remainder of this paper the terms 'C$_{33}$ hopanoids' and 'C$_{35}$ hopanoids' will be used for the coeluting pairs of 2-desmethylhopanoids and 2-methylhopanoids **I+III** and **II+IV** (see TIC in Fig. 6), respectively. At DSDP site 144 average index values are 8% and 23% for C$_{35}$-hopanoids and C$_{33}$-hopanoids, respectively, with maximum values of 40% for C$_{33}$-hopanoids (Fig. 3). Similar average values [10% (C$_{35}$ hopanoids) to 22% (C$_{33}$ hopanoids)] are found at site 367, where maximum index values are slightly higher (44%; Fig. 4). At site 603B the average index value for C$_{33}$ hopanoids is slightly lower (13%) while the average index value for C$_{35}$ hopanoids is comparable (10%) to sites 144 and 367 (Fig. 5). In general, the C$_{33}$ hopanoids released upon desulfurisation contain a significantly higher contribution of 2β-methylhopanoid than the C$_{35}$-hopanoids. The relatively high quantities of C$_{33}$ hopanoids are remarkable since in most cases the hopanoids released upon desulfurisation are dominated by C$_{35}$ hopanoids only [e.g. *De Leeuw and Sinninghe Damsté*, 1990; *Sinninghe Damsté et al.*, 1990b; *Köster et al.*, 1997].

Less than 50% of the investigated cyanobacteria and microbial mats dominated by cyanobacteria contain 2β-methyl-BHPs, while all produce significant quantities of 'regular' 2-desmethyl-BHPs [*Summons et al.*, 1999]. On average 2β-methyl-BHPs make up less than 23% of the total amount of BHPs present in cyanobacteria. Ancient marine environments like their modern analogous probably contained communities consisting of several cyanobacterial taxa. In addition, other bacteria, such as heterotrophic bacteria exclusively producing regular 2-desmethyl-BHPs, will have been abundantly present in the proto-North Atlantic. Therefore, the high average relative abundances (exceeding 20%) of 2β-methylhopanoids at sites 144, 367 and 603B are remarkable. In fact, they exceed nearly all values reported by Summons et al. [1999] for a variety of Phanerozoic settings. The relative abundance of 2β-methylhopanoids for the C/T sediments of DSDP sites 144, 367 and 603B also exceeds nearly all thermally immature euxinic sediments from a variety of up to
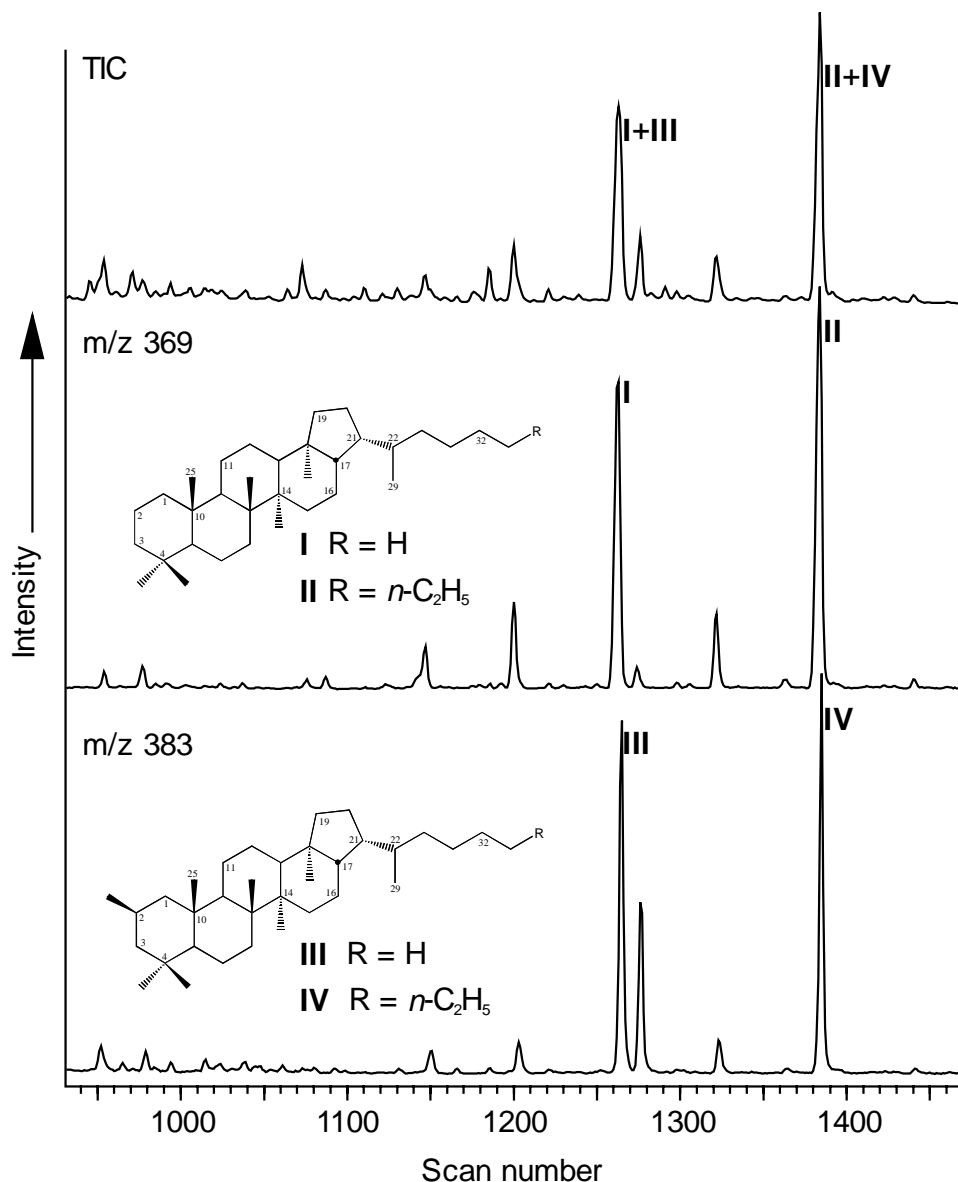
Figure 6. Mass chromatograms of *m/z* 369 and 383 for 17β,21β(H)-hopanes (i.e. **I** and **II**) and 2β-methyl-17β,21β(H)-hopanes (i.e. **III** and **IV**), respectively, and reconstructed total mass chromatogram [i.e. total ion count (TIC)]. The Roman numbers in the TIC indicate the two coeluting pairs of 2-methyl and 2-desmethyl extended hopanes **I**+**III** (C_{33} hopanoids) and **II**+**IV** (C_{35} hopanoids), respectively. 2β-Methyl-17β,21β(H)-trishomohopane (C_{34}; **III**) and 2β-methyl-17β,21β(H)-pentakishomohopane (C_{36}; **IV**), respectively, were identified on basis of relative retention time [*Summons and Jahnke*, 1992]. The stereochemistry of the methyl group at the C2 position in **III** and **IV** is only tentatively identified because 2α– and 2β-methylhopanes have similar retention times in contrast to 3β-methylhopanes [*Summons and Jahnke*, 1992] and can not be distinguished by mass spectrometry. The sulfur-bound hopanoids present in these sediments all still possess the biological 17β,21β(H)-configuration. The stereochemistry at the C17 and C21 positions is much more prone to isomerisation than the stereochemistry of the methyl substituent at the C2 position [*Summons and Jahnke*, 1992; *Van Duin et al.*, 1997]. Since 2β is the biological configuration for 2-methylhopanoids [*Summons et al.*, 1999], we infer that **III** and **IV** are 2β-methyl-hopanes.

200 My old settings that have been investigated in our laboratory (Table 1). In most of these sediments the percentage of 2-methylhopanoids is well below the minimum values for the

bathyal/abyssal proto-North Atlantic C/T sediments. The only noteworthy exception is the Jurassic Calcaires en Plaquettes Formation, where paleoenvironmental reconstructions demonstrated a major contribution of cyanobacteria [*Tribovillard et al.*, 1992; *van Kaam-Peters and Sinninghe Damsté*, 1997]. The high contributions of 2β-methylhopanoids to the C_{33}- and C_{35}-hopanoids from sites 144, 367 and 603B indicate that cyanobacteria were very abundant in the C/T North Atlantic. They were also most likely the main source of regular 2-desmethyl extended hopanes, which are normally believed to derive from a range of bacterial sources [*Rohmer et al.*, 1992] within the marine environment, since the percentage of 2-methylhopanoids is close to the average value of ~23% for a suite of extant cyanobacteria [*Summons et al.*, 1999]. The relatively high abundance of C_{33} hopanoids released upon desulfurisation could indicate that certain cyanobacteria biosynthesise(d) BHPs by carbon-carbon linkage of a D-triose instead of a D-pentose [*Rohmer et al.*, 1992] to the pentacyclic triterpenoid. If so, these C_3 extended hopanoids may prove to be biomarkers that are highly specific for certain (N₂-fixing?) cyanobacteria.

Samples origin	n	Age	Setting	2-Methyl % C_{33} hopanoids	C_{35} hopanoids
C/T sites					
DSDP Site 144 (NA)	7	C/T OAE (~94 My)	Bathyal (~1300 m)	23.3	8.0
DSDP Site 367 (NA)	17	C/T OAE (~94 My)	Abyssal (~3700 m)	21.8	9.5
DSDP Site 603B (NA)	11	C/T OAE (~94 My)	Abyssal (~4000 m)	13.3	10.1
Other Phanerozoic sites					
ODP Site 1084 (Lüderitz Bay, SA)	1	Pleistocene	Coastal upwelling site (1990 m)	0.3	0.1
ODP site 969 (eastern Mediterranean)	1	Pliocene sapropel (2.943 My)	Land-locked silled deep basin	0	0
Perticara Basin (Northern Apennines, Italy)	1	Miocene	Evaporitic basin	n.a.	0
Vena del Gesso basin (Northern Apennines, Italy)	5	Miocene (~5.2 My)	Evaporitic basin	0.3	0.7
Monterey Fm. (Naples Beach, California)	4	Miocene (8-24 My)	Coastal basin (1000-500 m)	0	1.7
Menilite Fm. (Carpathians, Poland)	1	Oligocene (30.5-36 My)	Narrow foreland basin	n.a.	0.4
Ghareb Fm. (Central Jordan)	1	Maastrichtian/ Campanian	Restricted shallow basin	n.a.	0
ODP Site 1049C (Blake Nose, NA)	3	Albian OAE1b (~112 My)	Bathyal (~1000 m)	0	0
Kimmeridge Clay Formation (Kimmeridge Bay, UK)	2	Kimmeridgian	Shelf basin	0	0
Calcaires en Plaquettes Fm. (Orbagnoux, France)	1	Kimmeridgian	Lagoonal microbial mat community	20.3	17.2
Oxford Clay Fm. (Great Britain)	1	Oxfordian	Epicontinental sea	0	1.6
Paris Basin (France)	1	Toarcian	Epicontinental sea	n.a.	0

Table 1. Age, paleosetting including water depth (where available) and average 2-methylhopane indices (2-methyl %) of C_{33}- and C_{35}-hopanoids of DSDP Sites 144, 367, 603B and a selection of [*Brumsack and Thurow*, 1986; *Bralower and Thierstein*, 1987]Tertiary, Cretaceous and Jurassic sites. Abbreviations are NA, North Atlantic; SA, South Atlantic; Fm, formation; My, million years before present; n.a., not applicable.

The extremely low abundance of sulfur-bound (S-bound) extended hopanoids at site S13 can be attributed to a significantly higher thermal maturity of the sedimentary OM at this shelf site than at the abyssal sites 144, 367 and 603B [*Sinninghe Damsté and Köster*, 1998]. Extended unsaturated

hopanoids (i.e. hopenes) released upon thermal degradation of S-bound hopanoids [*Köster et al.*, 1997], are abundantly present in the apolar fractions of site S13. Although no significant amounts of 2-methyl-hopenes were detected at site S13, a substantial cyanobacterial input of hopanoids can not be excluded because only half of the studied cyanobacterial cultures produce 2-methyl-BHPs [*Summons et al.*, 1999].

Since both 2-methyl and 2-desmethyl extended hopanoids coelute upon gas chromatographic analysis only the stable carbon isotopic composition of the pairs of 2-desmethylhopanoids and 2-methylhopanoids **I+III** (i.e. C_{33} hopanoids) and **II+IV** (i.e. C_{35} hopanoids) could be determined. The $\delta^{13}C$ values of C_{33} and C_{35} hopanoids are similar at the bathyal/abyssal sites and only at site 144 there is an minor offset of ~1.5‰ (Figs. 3-5). In addition, the $\delta^{13}C$ values of C_{33} and C_{35} hopanoids co-vary at sites 144, 367 and 603B, which suggests a common source for these hopanoids. There is no correlation between the percentage of 2β-methylhopanoids and the stable carbon isotopic composition of the C_{33} and C_{35} hopanoids (Figs. 3-5). This suggests that the carbon isotopic composition of regular 2-desmethyl and 2-methyl extended hopanoids is similar and co-varies, which is in good agreement with a predominantly cyanobacterial origin of both regular and 2-methyl extended hopanes.

Little is known about the isotopic fractionation by cyanobacteria and all our current knowledge is restricted to one taxon, the unicellular *Synechococcus* [*Popp et al.*, 1998]. Assuming that the factors that control the stable carbon isotopic composition of *Synechococcus* were more or less the same for mid-Cretaceous cyanobacteria, the isotopic composition of cyanobacterial hopanoids prior to and during the C/T OAE can be estimated. It has been shown that, in sharp contrast to algae investigated up to now, the stable isotopic composition of *Synechococcus* is relatively independent of CO_2 concentration and growth rate [*Popp et al.*, 1998]. This has been attributed either to the high cell area to volume ratio for these small organisms [*Popp et al.*, 1998] or to active bicarbonate uptake [*Keller and Morel*, 1999]. The degree of isotope fractionation during carbon fixation (ϵ_p) for *Synechococcus* is 16-18‰ [*Popp et al.*, 1998]. Dissolved inorganic carbon (DIC) was enriched in ^{13}C by 2-3‰ relative to modern values [*Arthur et al.*, 1985; *Hayes et al.*, 1999] during most of the mid-Cretaceous. Assuming ϵ_p for mid-Cretaceous cyanobacteria was also 16-18‰, $\delta^{13}C$ values of cyanobacterial biomass should be –21 to –24‰ before the C/T OAE. If we assume that like the hopanoids of *Synechococcus* cyanobacterial BHPs were depleted by 6-8‰ relative to biomass [*Sakata et al.*, 1997], $\delta^{13}C$ values of cyanobacterial hopanes should be between –27 and –32‰ during the mid-Cretaceous. These theoretical values agree well with the observed $\delta^{13}C$ values of the hopanes prior to the C/T OAE. $\delta^{13}C$ values of DIC increased by 2.5‰ during the C/T OAE [*Jenkyns et al.*, 1994] and a similar increase would be expected for cyanobacteria. However, the hopanes from the C/T OAE interval show a considerably larger increase in $^{13}C/^{12}C$ ratios at sites 367 and 603B during the C/T OAE (Figs. 3-5). This suggests a change in the cyanobacterial community with taxa characterised by a significantly smaller fractionation becoming dominant during the C/T OAE. Intriguingly the extant filamentous N_2-fixing cyanobacterium *Trichodesmium* is significantly more ($\delta^{13}C_{biomass}$ ~ -13‰) ^{13}C-enriched [*Carpenter et al.*, 1997] than would be expected from the results of Popp et al. [1998] for *Synechococcus*. Since *Trichodesmium* was collected from oligotrophic ocean surface waters it seems likely that this ^{13}C-enrichment

resulted from a smaller ε_p for this species rather than 'heavier' DIC values. Thus other cyanobacteria may have an ε_p significantly different from the 16-18‰ determined for *Synechococcus*. The minor shift in $\delta^{13}C$ values of the hopanes could indicate that a change in cyanobacterial community did not occur at DSDP Site 144 but as a result of the general lack of data for the C/T OAE interval a change can also not be excluded.

5.4.2 The proto-North Atlantic N cycle and its implications for the mid-Cretaceous carbon cycle.

There is abundant evidence (i.e. ^{15}N-depletion of OM-rich marine sediments typical for newly fixed N_2 and the abundance of cyanobacterial membrane lipids) that N_2-fixing cyanobacteria played an important role in the N-cycle of the proto-North Atlantic during the C/T. This is in good agreement with the model proposed by Rau et al. [1987], where reduced ocean circulation and extensive denitrification in largely anoxic or suboxic mid and deep waters may have led to N_2 fixation periodically providing an alternate N source for phytoplankton communities during the early to middle Cretaceous. Cyanobacteria are the main N_2-fixers in the marine realm and the abundance of their membrane lipids (e.g. 2-methylhopanoids) in these black shales agrees well with N_2 fixation being the main source of nutrient N for phytoplanktonic growth in the proto-North Atlantic Ocean during this time.

Denitrification in a largely anoxic water column would have removed large quantities of reactive N, decreasing N:P ratios of the seawater. Regeneration of P from sedimenting algal POM is favoured under anoxic conditions and could have further decreased N:P ratios [*Ingall and Jahnke*, 1997; *Van Cappellen and Ingall*, 1994]. Preferential P regeneration relative to OC oxidation is indicated by the extremely high atomic C/P ratios for the OC-rich sediments of sites 367 and 603B [*Kuypers et al.*, in prep.]. Average atomic C/P ratios exceed 400 at both sites, while C/P ratios for fresh marine OM is ~ 106 [*Redfield et al.*, 1963]. Hence, seawater supplied to the photic zone would most likely have contained low concentrations of reactive N relative to P (N/P < Redfield) giving N_2-fixing cyanobacteria a competitive advantage over algae [*Tyrrell*, 1999]. In addition to P the availability of the micronutrient iron (Fe) limits growth of N_2-fixing cyanobacteria as a result of the high dissolved Fe demand of the N_2 fixation mechanism [*Falkowski et al.*, 1998]. Dissolved Fe was probably not biolimiting in the small Atlantic basins where sufficient Fe could be supplied by riverine or aeolian input from the surrounding land [*Sinton and Duncan*, 1997]. Like in the modern Black Sea reduction of iron oxides in the suboxic/anoxic waters even could have led to high dissolved Fe concentrations [*Lewis and Landing*, 1991] in the near-surface waters of the proto-North Atlantic basin. Excretion of N during N_2 fixation and remineralisation of cyanobacterial biomass in the upper part of the water column could have released reactive N for algal growth (Fig. 7). Therefore, even though N_2 fixation by cyanobacteria was the primary source of reactive N for phytoplanktonic growth in the proto-North Atlantic, algae could have contributed significant amounts of OM to the C/T sediments (see below).

5.4.2.1 The significance of N₂-fixing cyanobacteria as a source of sedimentary OM. Based upon the extreme ^{15}N-depletion of the sediment and the amorphous nature of the sedimentary OM, Rau et

al. [1987] suggested that biomass of N_2-fixing cyanobacteria could make up a significant part of early and middle Cretaceous insoluble sedimentary OM. The amorphous nature of the C/T sedimentary OM of sites S13, 144, 367 and 603B in itself does neither support nor exclude a cyanobacterial origin and generally only indicates a marine origin. Although the strong ^{15}N-depletion of the C/T sediments could indicate an important input of cyanobacterial OM, this depletion could also be explained by other processes involving incorporation of newly fixed N_2 in algal biomass. The most direct way of incorporation of newly fixed N_2 in algal biomass occurs in several species of mat-forming pelagic diatoms that harbor the N_2-fixing endosymbiont *Richelia intracellularis*, which provides them with reactive N [*Carpenter et al.*, 1999]. The combined biomass of algal host and cyanobacterial symbiont shows a ^{15}N-depletion typical for newly fixed N_2 (δ^{15}N ~ -1.5‰) [*Carpenter et al.*, 1999]. Blooms of some of these mat-forming diatoms could significantly contribute new N to regions of the ocean that are poor in reactive N [*Carpenter et al.*, 1999]. It has been suggested that these mats could also contribute significant amounts of OM to the sediment [*Kemp et al.*, 1999]. In fact the high OC content of the sapropels of the Mediteranean Sea may be entirely accounted for by sedimenting mat-forming diatoms and their N_2-fixing endosymbionts [*Kemp et al.*, 1999; *Sachs and Repeta*, 1999]. Like the mats itself these sapropels show the ^{15}N depletion typical for newly fixed nitrogen (δ^{15}N ~ -0.1‰) [*Sachs and Repeta*, 1999]. Kemp et al. [1999] proposed that these mat-forming diatoms also contributed significantly to the black shale deposits of the Cretaceous.

An alternative and less direct way of incorporation of newly fixed N_2 in algal biomass is the utilisation of N excreted by living N_2-fixing cyanobacteria. For instance the extant filamentous genus *Trichodesmium*, which is thought to be the most significant N_2-fixer in present-day open-ocean waters [*Carpenter et al.*, 1999 and references therein], releases up to 50% of the fixed N_2 as dissolved N [*Glibert and Bronk*, 1994]. Additional reactive N is released upon degradation of *Trichodesmium* in the upper part of the water column and both processes are a significant source of N for other phytoplankton in some oligotrophic marine settings [*Letelier and Karl*, 1996]. This significantly affects the stable nitrogen isotopic composition of the total phytoplanktonic community in areas where *Trichodesmium* is common [*Minagawa and Wada*, 1986; *Carpenter et al.*, 1997; *Capone et al.*, 1998]. Similar observations were made for the Baltic Sea, where the nitrogen isotopic composition of all size-classes of plankton were strongly affected by the direct or indirect incorporation of ^{15}N-depleted fixed N_2 during blooms of the N_2-fixing *Aphanizomenon sp.* and *Nodularia spumigena* [*Rolff*, 2000]. Therefore, although the sedimentary δ^{15}N signature is strongly affected by cyanobacterial N_2 fixation, algae could still have contributed significantly to the C/T sedimentary OM.

The abundance of molecular fossils of cyanobacterial membrane lipids relative to typical algal biomarkers such as steroids could provide insight into the significance of cyanobacteria as a source of sedimentary OM during the C/T. The extractable OM of the C/T sediments from site S13 contains much more steroids than hopanoids. At DSDP site 144 steroids are also more abundant than hopanoids. However, the extractable OM of the C/T sediments from DSDP site 367 contains much more hopanoids than steroids. There are large differences between sediment samples at DSDP site 603B. Some sediments contain significantly more hopanoids than steroids while other samples are dominated by steroids. The concentration of BHPs in bacterial cells is in the same order of

magnitude as sterols in eukaryotes (e.g. algae) [*Rohmer et al.*, 1992]. Assuming the preservation potential of both membrane components is similar, it seems that at site 367 and for some parts of the C/T sequence of site 603B, cyanobacteria could have significantly contributed to the sedimentary OM. The significant co-variation between the carbon isotopic composition of the extended hopanoids, sulfur-bound Ph and bulk OM also suggests a significant cyanobacterial contribution to the OM at site 367 (Fig. 4). In contrast at sites S13 and 144 and throughout most of the C/T sequence of site 603B, algal-derived OM seems to dominate the sedimentary OM. Here processes involving repackaging of newly fixed N$_2$ in algal biomass must be implied to explain the strong ^{15}N-depletion of the C/T sediments. Interesting in this respect is the fact that some of the C/T black claystones of DSDP site 603B contain large amounts of biogenic silica [*Kuypers et al.*, unpublished results]. Although no recognisable remains were found, diatoms and more specifically mat-forming diatoms containing N$_2$-fixing endosymbionts could be the source of biogenic silica and perhaps a significant part of the OM at this site.

5.4.2.2 Cyanobacterial N$_2$ fixation and the enhanced biological CO$_2$ pumping during the C/T OAE. Both shelf (S13) and abyssal marine sediments (144, 367 and 603B) show a ^{15}N-depletion typical for newly fixed N$_2$ already well before the C/T OAE (Figs. 2-5). We attribute the important role of N$_2$-fixers in the nitrogen cycle of the proto-North Atlantic Ocean prior to the C/T OAE to basin-wide stagnation and anoxia (Fig. 7). Previously we have shown that the southern part of the proto-North Atlantic was euxinic well before the C/T OAE [*Kuypers et al.*, 2000 submitted to Paleoceanography]. The co-occurrence of lamination, enrichment of trace metals and abundance of molecular fossils of pigments from green sulfur bacteria at different palaeo-water depths indicates that the southern proto-North Atlantic Ocean water column was periodically euxinic from the bottom to at least the base of the photic (<150 m) zone prior to as well as during the C/T OAE. Similar conditions may have periodically occurred in the northern part of the proto-North Atlantic as well [*Herbin et al.*, 1987; *Kuypers et al.*, unpublished results].

During the C/T OAE there is a significant increase in marine OC accumulation rates at the sites in the southern part of the proto-North Atlantic (sites S13, 144 and 367), which we have attributed to an increase in primary productivity [*Kuypers et al.*, 2000 submitted to Paleoceanography]. An increase in OM accumulation rates also occurred in the northern proto-North Atlantic (site 603B) during the C/T OAE [*Kuypers et al.*, unpublished results]. In the modern ocean enhanced primary productivity is closely linked with intensified upwelling of intermediate waters into the photic zone. Enhanced upwelling in the proto-North Atlantic has been attributed to the initiation of a deep connection between the proto-North and South Atlantic basins [*Tucholke and Vogt*, 1979; *Summerhayes*, 1981; *Summerhayes*, 1987]. The influx into the proto-North Atlantic of large amounts of highly saline, old, oxygen deficient water from the northern South Atlantic would have displaced deep water towards the surface [*Tucholke and Vogt*, 1979; *Summerhayes*, 1981; *Summerhayes*, 1987]. As a more or less stagnant anoxic basin possibly with a partly estuarine-like circulation [*Arthur et al.*, 1987; *Thierstein and Berger*, 1979], the proto-North Atlantic could have acted as a nutrient trap [*Summerhayes*, 1987] comparable to the Holocene Black Sea and Cariaco Trench that contain relatively high levels of dissolved reactive N and especially P below the chemocline [*Sarmiento et al.*, 1988; *Velinsky et al.*, 1991; *Fry et al.*, 1991].
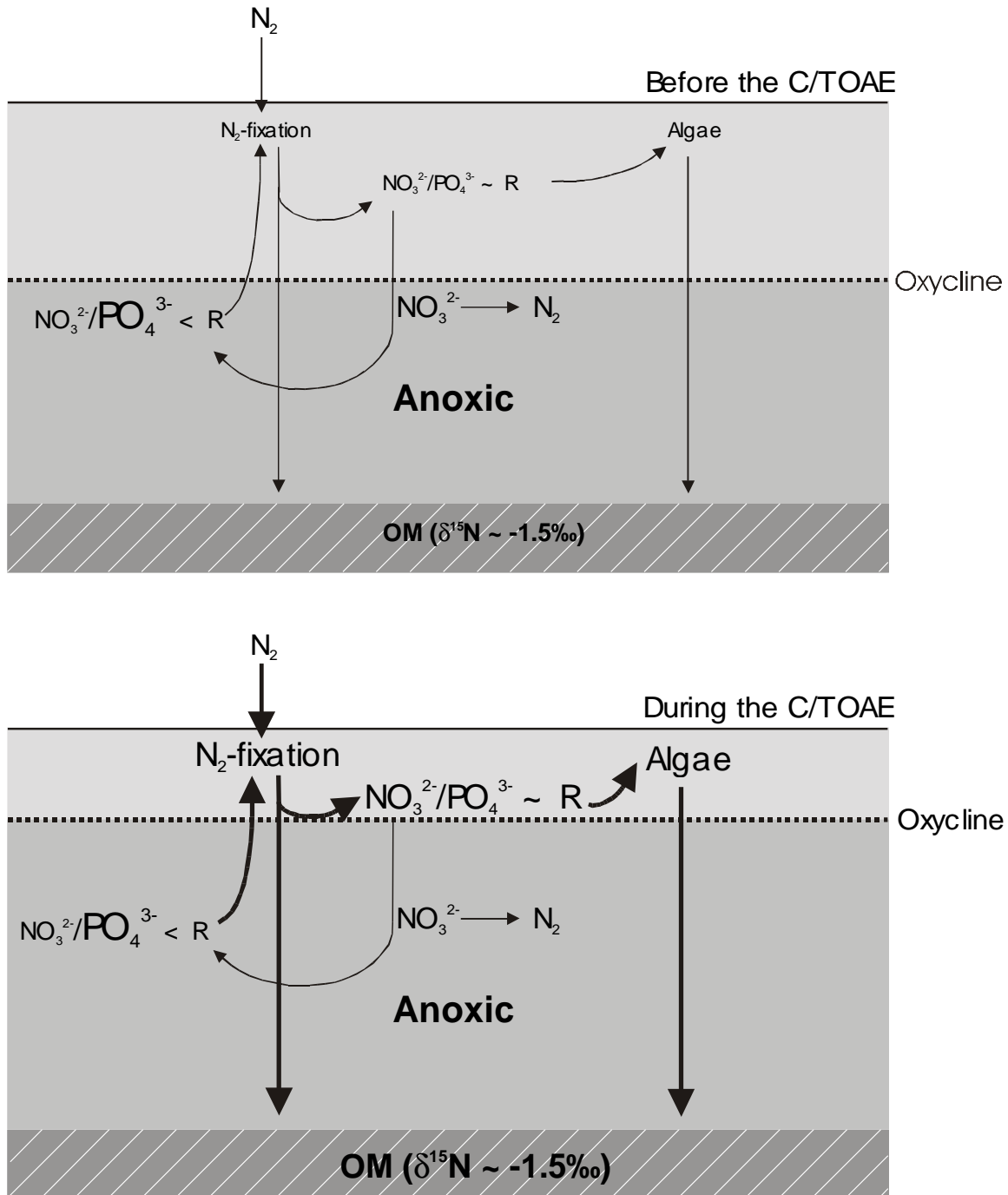
Figure 7. Simplified representation of the nitrogen, phosphorus and carbon cyle in the mid-Cretaceous North Atlantic Ocean before and during the C/T OAE. Abbreviations are R, Redfield ratio for N/P ~ 16; OM, organic matter; NO_3^{2-}, reactive N (mainly nitrate); PO_4^{3-}, phosphate. The arrows indicate fluxes of major nutrients N and P, and phytoplanktonic OM. Increased fluxes of major nutrients N, P and phytoplanktonic OM during the C/T OAE are indicated by the thick black arrows. Enhanced nutrient N and P levels, increased N_2-fixation and increased algal biomass during the C/T OAE are indicated by the larger text font size. The thick dotted line mark the relative depth of the oxycline, which is inferred from the occurrence of specific biomarkers of photosynthetic anoxygenic green sulfur bacteria [Kuypers et al., 2000 submitted to Paleoceanography] .

Thus, water brought to the surface as a consequence of the influx of South Atlantic dense water was likely extremely nutrient-rich but had a deficit of N relative to P (Fig. 7). Neither $\delta^{15}N$ values of the bulk sediments nor the relative abundance of 2-methyl-hopanoids shows a significant change indicating that N₂-fixing cyanobacteria remained the main source of nutrient N during the C/T OAE. However, the shift in $\delta^{13}C$ values for cyanobacterial hopanoids could indicate that there was a change in the composition of the cyanobacterial community. Changes in the composition of the cyanobacterial community have also been observed for modern marine settings like the Baltic Sea, where the blooming filamentous cyanobacterium *Aphanizomenon flos-aquae* is replaced by the shallower dwelling filamentous *Nodularia spumigena* as a response to the shallowing of the upper mixed layer [*Kononen et al.*, 1996]. The increase in primary productivity during the C/T OAE was accompanied by a significant rise of the chemocline, with euxinic conditions in the southern proto-North Atlantic periodically occurring at very shallow water depths of 15 m or less, while bottom water redox conditions did not markedly change (i.e. remained euxinic) [*Kuypers et al., 2000* submitted to Paleoceanography]. This shallowing of the chemocline could have resulted in a competitive advantage for cyanobacteria like the extant *Nodularia* with a tolerance for higher temperatures, higher light intensity as a result of better protective mechanisms against photo-oxidation and/or higher phosphate affinity [*Kononen et al.*, 1996]. Inceased upwelling of anoxic, P-loaded waters would have increased the amount of N₂ fixed by these cyanobacteria fuelling a larger production of phytoplanktonic biomass leading to the observed increase in OC burial. This enhanced activity of the biological pump led to a significant drop in atmospheric carbon dioxide concentration during the C/T OAE [*Freeman and Hayes*, 1992; *Arthur et al.*, 1988; Kuypers et al., 1999] and, thereby, could have triggered the early Turonian deterioration of the greenhouse climate.

5.5 References

Altabet, M. A. and W. G. Deuser, Seasonal variations in natural abundance of ¹⁵N in particles sinking to the deep Sargasso Sea, *Nature*, 315, 218-219, 1985.

Altabet, M. A., W. G. Deuser, S. Honjo, and C. Steinen, Seasonal and depth-related changes in the source of sinking particles in the North Atlantic, *Nature*, 373, 506-509, 1991.

Altabet, M. A., R. Francois, D. W. Murray, and W. L. Prell, Climate-related variations in denitrification in the Arabian Sea from sediment ¹⁵N/¹⁴N ratios, *Nature*, 373, 506-509, 1995.

Altabet, M. A., D. W. Murray, and W. L. Prell, Climatically linked oscillations in Arabian Sea denitrification over the past 1 m.y.: Implications for the marine N cycle, *Palaeoceanography*, 14, 732-743, 1999.

Arthur, M. A., W. A. Dean, and L. M. Pratt, Geochemical and climatic effects of increased marine organic carbon burial at the Cenomanian/Turonian boundary, *Nature*, 335, 714-717, 1988.

Arthur, M. A., W. E. Dean, and G. E. Claypool, Anomalous ¹³C enrichment in modern marine organic carbon, *Nature*, 315, 216-218, 1985.

Arthur, M. A., S. O. Schlanger , and H. C. Jenkyns, The Cenomanian-Turonian Oceanic anoxid event,II. Palaeoceanographic controls on organic-matter production and preservation, *Geological Society Special Publication*, 26, 401-420, 1987.

Berger, W. H. and U. von Rad, Cretaceous and Cenozoic sediments from the Atlantic Ocean, *Initial Reports of the Deep Sea Drilling Project*, 14, 787-954, 1972.

Berner, R. A., A model for atmospheric CO_2 over Phanerozoic time, *American Journal of Science*, 291, 339-376, 1991.

Berner, R. A., Palaeo-CO_2 and climate, *Nature*, 358, 114-114, 1992.

Bianchi, T. S., E. Engelhaupt, P. Westman, T. Andrén, C. Rolff, and R. Elmgren, Cyanobacterial blooms in the Baltic Sea: natural or human-induced?, *Limnology and Oceanography*, 45, 716-726, 2000.

Bralower, T. J. and H. R. Thierstein, Organic carbon and metal accumulation rates in Holocene and mid-Cretaceous sediments: palaeoceanographic significance, *Geological Society Special Publication*, 26, 345-369, 1987.

Brumsack, H.-J., Trace metal accumulation in black shales from the Cenomanian/Turonian boundary event, *Earth-Science*, 8, 337-343, 1986.

Brumsack, H. J. and J. W. Thurow, The geochemical facies of black shales from the Cenomanian/Turonian boundary event (CTBE), *Mitt.Geol.-Paläeont.Inst.Univ.Hamburg*, 60, 247-265, 1986.

Calvert, S. E., B. Nielsen, and M. R. Fontugne, Evidence from nitrogen isotope ratios for enhanced productivity during formation of eastern Mediterranean sapropels, *Nature*, 359, 223-225, 1992.

Capone, D. G., A. Subramaniam, J. P. Montoya, M. Voss, C. Humborg, A. M. Johansen, R. L. Siefert, and E. J. Carpenter, An extensive bloom of the N_2-fixing cyanobacterium *Trichodesmium erythraeum* in the central Arabian Sea, *Marine Ecology Progress Series*, 172, 281-292, 1998.

Carpenter, E. J., H. R. Harvey, B. Fry, and D. G. Capone, Biogeochemical tracers of the marine cyanobacterium *Trichodesmium*, *Deep Sea Research*, 44, 27-38, 1997.

Carpenter, E. J., J. P. Montoya, J. Burns, M. R. Mulholland, A. Subramaniam, and D. G. Capone, Extensive bloom of a N_2-fixing diatom/cyanobacterial association in the tropical Atlantic Ocean, *Marine Ecology Progress Series*, 185, 273-283, 1999.

Chénet, P. Y. and J. Francheteau, Bathymetric reconstruction method: application to the Central Atlantic Basin between 10ºN and 40ºN, *Initial Reports of the Deep Sea Drilling Project*, 51, 52, 53, 1501-1514, 1979.

Codispoti, L. A. and J. P. Christensen, Nitrification, denitrification and nitrous oxide cycling in the eastern tropical south Pacific Ocean, *Mar.Chem.*, 16, 277-300, 1985.

Cole, J. J., S. Findlay, and M. L. Pace, Bacterial production in fresh and saltwater ecosystems: A cross-system overview, *Marine Ecology Progress Series*, 43, 1-10, 1988.

Copin-Monteguet, C. and G. Copin-Monteguet, Stoichiometry of carbon, nitrogen and phosphorus in marine particulate matter, *Deep Sea Research*, 30, 31-46, 1983.

De Leeuw, J. W. and J. S. Sinninghe Damsté, Organic sulfur compounds and other biomarkers as indicators of palaeosalinity: A critical evaluation, *preview*, 1-15, 1989.

De Leeuw, J. W. and J. S. Sinninghe Damsté, Organic sulfur compounds and other biomarkers as indicators of palaeosalinity, *ACS Symposium Series*, 429, 419-443, 1990.

Einsele, G. and J. Wiedmann, Turonian black shales in the Moroccan coastal basins: first upwelling in the Atlantic Ocean?, in *Geology of the North West African continental margin*, edited by v.von Rad et.al., pp. 396-414, Springer, Berlin, 1982.

Falkowski, P. G., R. T. Barber, and V. Smetacek, Biogeochemical controls and feedbacks on ocean primary production, *Science*, 281, 200-206, 1998.

Farrell, J. W., T. F. Pedersen, S. E. Calvert, and B. Nielsen, Glacial-interglacial changes in nutrient utilization in the equatorial Pacific Ocean, *Nature*, 377, 514-517, 1995.

Francois, R., M. A. Altabet, and L. H. Burckle, Glacial to interglacial changes in surface nitrate utilization in the Indian sector of the southern ocean as recorded by sediment $\delta^{15}N$, *Palaeoceanography*, 7, 589-606, 1992.

Freeman, K. H. and J. M. Hayes, Fractionation of carbon isotopes by phytoplankton and estimates of ancient CO_2 levels., *Global Biochemical Cycles*, 6, 185-198, 1992.

Fry, B., H. W. Jannasch, S. J. Molyneaux, C. O. Wirsen, J. A. Muramoto, and S. King, Stable isotope studies of carbon, nitrogen and sulfur cycles in the Black Sea and the Cariaco Trench, *Deep Sea Research*, 38, 1003-1019, 1991.

Gale, A. S., H. C. Jenkyns, W. J. Kennedy, and R. M. Corfield, Chemostratigraphy versus biostratigraphy: data from around the Cenomanian-Turonian boundary, *Journal of the Geological Society, London*, 150, 29-32, 1993.

Glibert, P. M. and D. A. Bronk, Realease of dissolved nitrogen by marine diazotrophic cyanobacteria, *Trichodesmium* spp., *Appl.Environ.Microbiol.*, 60, 3996-4000, 1994.

Gradstein, F., F. P. Agterberg, J. G. Ogg, J. Hardenbol, P. van Veen, J. Thierry, and H. Huang, A Triassic, Jurassic, and Cretaceous time scale, *SEPM Special Publications*, 54, 95-126, 1995.

Gradstein, F., F. P. Agterberg, J. G. Ogg, J. Hardenbol, P. van Veen, J. Thierry, and Z. Huang, A mesozoic time scale, *Journal of Geophysical Research*, 99, 24051-24074, 1994.

Haug, G. H., T. F. Pedersen, D. M. Sigman, S. E. Calvert, B. Nielsen, and B. J. Peterson, Glacial/interglacial variations in production and nitrogen fixation in the Cariaco basin during the last 580 kyr, *Paleoceanography*, 13, 427-432, 1998.

Hayes, D. E. and et al., Sites 143 and 144, *Initial Reports of the Deep Sea Drilling Project*, 14, 283-338, 1972.

Hayes, J. M., H. Strauss, and A. J. Kaufman, The abundance of ^{13}C in marine organic matter and isotopic fractionation in the global biogeochemical cycle of carbon during the past 800 Ma, *Chemical Geology (Isotope Geoscience Section)*, 161, 103-125, 1999.

Herbin, J. P., E. Masure, and J. Roucaché, Cretaceous formations from the lower continental rise off Cape Hatteras: organic geochemistry , dinoflagelate cysts, and the Cenomanian/Turonian boundary event at sites 603 (Leg 93) and 105 (Leg 11), *Initial Reports of the Deep Sea Drilling Project*, 93, 1139-1160, 1987.

Herbin, J. P., L. Montadert, C. Müller, R. Gomez, J. W. Thurow, and J. Wiedmann, Organic-rich sedimentation at the Cenomanian-Turonian boundery in oceanic and coastal basins in the North Atlantic and Tethys, *Geological Society Special Publication*, 21, 389-422, 1986.

Hoch, M. P., M. L. Fogel, and D. L. Kirchman, Isotope fractionation associated with ammonium uptake by a marine bacterium, *Limnology and Oceanography*, 37, 1447-1459, 1992.

Holmes, M. E., C. Eicher, U. Struck, and G. Wefer, Reconstruction of surface ocean nitrate utilization using stable nitrogen isotopes in sinking particles and sediments, in *Use of proxies in paleoceanography: examples from the South Atlantic*, edited by G. Fisher and G. Wefer, pp. 447-468, Springer-Verlag, Berlin, 1999.

Ingall, E. and R. A. Jahnke, Influence of water-column anoxia on the elemental fractionation of carbon and phophorus during sediment diagenesis, *Mar.Geol.*, 139, 219-229, 1997.

Jaffe, D. A., Global Biogeochemical Cycles, pp. 263-284, Academic, London, 1992.

Jahnke, R. A., Global Biogeochemical Cycles, pp. 301-315, Academic, London, 1992.

Jenkyns, H. C., A. S. Gale, and R. M. Corfield, Carbon- and oxygen- isotope stratigraphy of the English Chalk and Italian Scaglia and its palaeoclimatic significance, *Geol.Mag.*, 131, 1-34, 1994.

Karl, D., R. Letelier, L. Tupas, J. Dore, J. Christian, and D. Hebel, The role of nitrogen fixation in biogeochemical cycling in the subtropical North Pacific Ocean, *Nature*, 388, 533-538, 1997.

Keller, K. and F. M. M. Morel, A model of carbon isotopic fractionation and active carbon uptake in phytoplankton, *Marine Ecology Progress Series*, 182, 295-298, 1999.

Kemp, A. E. S., R. B. Pearce, I. Koizumu, J. Pike, and S. J. Rance, The role of mat-forming diatoms in the formation of Mediterranean sapropels, *Nature*, 398, 57-61, 1999.

Kok, M. D., S. Schouten, and J. S. Sinninghe Damsté, Formation of insoluble, nonhydrolyzable, sulfur-rich macromolecules via incorporation of inorganic sulfur species into algal carbohydrates, *Geochim.Cosmochim.Acta*, 64, 2689-2699, 2000.

Kononen, K., J. Kuparinen, K. Mäkelä, J. Laanemets, J. Pavelson, and S. Nõmmann, Inititiation of cyanobacterial blooms in a frontal region at the entrance of the Gulf of Finland, Baltic Sea, *Limn.Ocean.*, 41, 98-112, 1996.

Köster, J., H. M. E. Van Kaam-Peters, G. F. Koopmans, J. W. De Leeuw, and J. S. Sinninghe Damsté, Sulphurisation of homohopanoids: Effects on carbon number distribution, speciation, and 22S/22R epimer ratios, *Geochim.Cosmochim.Acta*, 61, 2431-2452, 1997.

Kuhnt, W., J. P. Herbin, J. W. Thurow, and J. Wiedmann, Distribution of Cenomanian-Turonian organic facies in the western Mediterranean and along the Adjacent Atlantic Margin, *AAPG Stud.in Geol.*, 30, 133-160, 1990.

Kuhnt, W., A. J. Nederbragt, and L. Leine, Cyclicity of Cenomanian-Turonian organic-carbon-rich sediments in the Tarfaya Atlantic Coastal Basin (Morocco), *Cretaceous Research*, 18, 587-601, 1997.

Letelier, R. M. and D. M. Karl, Role of *Trichodesmium* spp. in the productivity of the subtropical North Pacific Ocean, *Marine Ecology Progress Series*, 133, 263-273, 1996.

Lewis, B. l. and W. M. Landing, The biogeochemistry of manganese and iron in the Black Sea, *Deep Sea Research*, 38, Suppl.2, S773-S803, 1991.

Mackenzie, F. T., L. M. Ver, L. M. Sabine, M. Lane, and A. Lerman, Interactions of C, N, P and S Biogeochemical Cycles and Global Change, *NATO ASI Ser.I*, 14, 1-61, 1993.

Macko, S. A., M. H. Engel, and Y. Qian, Early diagenesis and organic matter preservation- a molecular stable carbon isotope perspective, *Chemical Geology*, 114, 365-379, 1994.

Mélières, F., X-ray mineralogy studies, leg 41, Deep Sea Drilling Project, Eastern North Atlantic Ocean, *Initial Reports of the Deep Sea Drilling Project*, 41, 1065-1086, 1978.

Minagawa, M. and E. Wada, Nitrogen isotope ratios of red tide organisms in the East China Sea: a characterization of biological nitrogen fixation, *Mar.Chem.*, 19, 245-259, 1986.

Obradovich, J. D., A Cretaceous Time Scale, *Geological Association of Canada Special Paper*, 39, 379-396, 1993.

Pennock, J. R., D. J. Velinsky, J. D. Ludlam, J. H. Sharp, and M. L. Fogel, Isotopic fractionation of ammonium and nitrate during uptake by *Skeletonema costatum*: implications for δ^{15}N dynamics under bloom conditions, *Limnology and Oceanography*, 41, 451-459, 1996.

Peters, K. E., R. E. Sweeney, and I. R. Kaplan, Correlation of carbon and nitrogen isotope ratios in sedimentary organic matter, *Limnology and Oceanography*, 23, 598-604, 1978.

Popp, B. N., E. A. Laws, R. R. Bridigare, J. E. Dore, K. L. Hanson, and S. G. Wakeham, Effect of phytoplankton cell geometry on carbon isotopic fractionation., *Geochim.Cosmochim.Acta*, 62, 69-77, 1998.

Rau, G. H., M. A. Arthur, and W. A. Dean, ^{15}N/^{14}N variations in Cretaceous Atlantic sedimentary sequences: implications for past changes in marine nitrogen biogeochemistry, *Earth and Planetary Science Letters*, 82, 269-279, 1987.

Redfield, A. C., B. H. Ketchum, and F. A. Richards, The influence of organisms on the composition of sea water, in *The sea, Interscience, Volume 2.*, edited by M. N. Hill, pp. 26-77, Interscience Press, New York, 1963.

Rigby, D. and B. D. Batts, The isotopic composition of nitrogen in Australian coals and oil shales, *Chemical Geology*, 58, 273-282, 1986.

Rohmer, M., P. Bisseret, and S. Neunlist., The hopanoids, prokaryotic triterpenoids and precursors of ubiquitous molecular fossils, in *Biological markers in sediments and petroleum*, edited by J. M. Moldowan, P. Albrecht, and R. P. Philp, pp. 1-17, Prentice Hall, New Jersey, 1992.

Rolff, C., Seasonal variation in δ^{13}C and δ^{15}N of size-fractionated plankton at a coastal station in the northern Baltic proper, *Marine Ecology Progress Series*, 203, 47-65, 2000.

Sachs, J. P. and D. J. Repeta, Oligotrophy and nitrogen fixation during eastern Mediterranean sapropel events, *Science*, 286, 2485-2488, 1999.

Sakata, S., J. M. Hayes, A. R. McTaggart, R. A. Evans, K. J. Leckrone, and R. K. Togasaki, Carbon isotopic fractionation associated with lipid biosynthesis by a cyanobacterium: Relevance for interpretation of biomarker records., *Geochim.Cosmochim.Acta*, 61, 5379-5389, 1997.

Sarmiento, J. L., T. Herbert, and J. R. Toggweiler, Mediterranean nutrient balance and episodes of anoxia, *Global Biogeochemical Cycles*, 2, 427-444, 1988.

Schlanger , S. O. and H. C. Jenkyns, Cretaceous oceanoc anoxic events: causes and consequences, *Geologie en mijnbouw*, 55, 179-184, 1976.

Scotese, C. R. and J. Golonka, Paleogeographic Atlas, University of Texas, Arlington, 1992.

Sinninghe Damsté, J. S., A. C. T. Duin, D. Hollander, M. E. L. Kohnen, and J. W. De Leeuw, Early diagenesis of bacteriohopanepolyol derivatives: Formation of fossil homohopanoids, *Geochim.Cosmochim.Acta*, 59, 5141-5147, 1995.

Sinninghe Damsté, J. S., T. I. Eglinton, and J. W. De Leeuw, Characterisation of sulfur-rich high molecular weight substances by flash pyrolysis and Raney Ni desulfurisation, *ACS Symposium Series*, 429, 486-528, 1990a.

Sinninghe Damsté, J. S., M. E. L. Kohnen, and J. W. De Leeuw, Thiophenic biomarkers for palaeoenvironmental assessment and molecular stratigraphy, *Nature*, 345, 609-611, 1990b.

Sinninghe Damsté, J. S. and J. Köster, A euxinic southern North Atlantic Ocean during the Cenomanian/Turonian oceanic anoxic event, *Earth and Planetary Science Letters*, 158, 165-173, 1998.

Sinton, C. W. and R. A. Duncan, Potential link between ocean plateau volcanism and global ocean anoxia at the Cenomanian-Turonian boundary, *Economic Geology*, 92, 838-842, 1997.

Sirevåg, R., B. B. Buchanan, J. A. Berry, and J. H. Troughton, Mechanism of CO$_2$ fixation in bacterial photosynthesis studied by the carbon isotope fractionation technique., *Arch.Microbiol.*, 112, 35-38, 1977.

Summerhayes, C. P., Organic facies of middle Cretaceous black shales in deep North Atlantic, *AAPG Bulletin*, 65, 2364-2380, 1981.

Summerhayes, C. P., Organic-rich Cretaceous sediments from the North Atlantic, *Geological Society Special Publication*, 26, 301-316, 1987.

Summons, R. E. and L. L. Jahnke, Hopenes and hopanes methylated in ring-A: correlation of the hopanoids from extant methylotrophic bacteria with their fossil analogues, in *Biological markers in sediments and petroleum*, edited by J. M. Moldowan, P. Albrecht, and R. P. Philp, pp. 182-200, Prentice-Hall, New Yersey, 1992.

Summons, R. E., L. L. Jahnke, J. M. Hope, and G. A. Logan, 2-Methylhopanoids as biomarkers for cyanobacterial oxygenic photosynthesis., *Nature*, 400, 554-557, 1999.

Thierstein, H. R. and W. H. Berger, Injection events in earth history, *Nature*, 276, 461-466, 1979.

Thurow, J. W. and W. Kuhnt, Mid-Cretaceous of the Gibraltar Arch Area, *Geological Society Special Publication*, 22, 423-445, 1986.

Toggweiler, J. R., Carbonoverconsumption, *Nature*, 363, 210-211, 1993.

Tribovillard, N., G. E. Gorin, S. Belin, G. Hopfgartner, and R. Pichon, Organic-rich biolaminated facies from a Kimmeridgian lagoonal environment in the French Southern Jura mountains. A way of estimating accumulation rate variations, *Pal.Geo, Pal.Clim, Pal.Ecol.*, 99, 163-177, 1992.

Tucholke, B. E. and P. R. Vogt, Western North Atlantic: sedimentary evolution and aspects of tectonic history, *Initial Reports of the Deep Sea Drilling Project*, 43, 791-825, 1979.

Tyrrell, T., The relative influences of nitrogen and phosphorus on oceanic primary production, *Nature*, 400, 525-531, 1999.

Van Cappellen, P. and E. Ingall, Benthic phosphorus regeneration, net primary production, and ocean anoxia: a model of the coupled marine biogeochemical cycles of carbon and phosphorus, *Paleoceanography*, 9, 677-692, 1994.

Van der Meer, M. T. J., S. Schouten, and J. S. Sinninghe Damsté, The effect of the reversed tricarboxylic acid cycle on the ^{13}C contents of bacterial lipids, *Org.Geochem.*, 28, 527-533, 1998.

Van Duin, A. C. T., J. S. Sinninghe Damsté, G. F. Koopmans, B. Van de Graaf, and J. W. De Leeuw, A kinetic calculation method of homohopanoid maturation: applications in the reconstruction of burial histories of sedimentary basins, *Geochim.Cosmochim.Acta*, 61, 2409-2429, 1997.

van Kaam-Peters, H. M. E. and J. S. Sinninghe Damsté, Characterisation of an extremely organic sulphur-rich, 150 Ma old carbonaceous rock: palaeoenvironmental implications, *Org.Geochem.*, 27, 371-397, 1997.

Velinsky, D. J. and M. L. Fogel, Cycling of dissolved and particulate nitrogen and carbon in the Framvaren Fjord, Norway: stable isotopic variations, *Mar.Chem.*, 67, 161-180, 1999.

Velinsky, D. J., M. L. Fogel, J. F. Todd, and B. M. Tebo, Isotopic fractionation of dissolved ammonium at the oxygen-hydrogen sulfide interface in anoxic waters, *Geophysical Research Letters*, 18, 649-652, 1991.

Waser, N. A. D., P. J. Harrison, B. Nielsen, S. E. Calvert, and D. H. Turpin, Nitrogen isotope frationation during the uptake and assimilation of nitrate, nitrite, ammonium, and urea by a marine diatom, *Limnology and Oceanography*, 43, 215-224, 1998a.

Waser, N. A. D., K. Yin, Z. Yu, K. Tada, P. J. Harrison, D. H. Turpin, and S. E. Calvert, Nitrogen isotope fractionation during nitrate, ammonium and urea uptake by marine diatoms and coccolithophores under various conditions of N availability, *Marine Ecology Progress Series*, 169, 29-41, 1998b.

Werne, J. P., D. J. Hollander, T. W. Lyons, and L. C. Peterson, Climate-induced variation in productivity and planktonic ecosystem structure from the Younger Dryas to Holocene in the Cariaco Basin, Venezuela, *Palaeoceanography*, 15, 19-29, 2000.

Wheeler, P. A. and D. L. Kirchman, Utilization of inorganic and organic nitrogen by bacteria in marine systems, *Limn.Ocean.*, 31, 998-1009, 1986.

Chapter 6

Massive expansion of marine Archaea during a mid-Cretaceous oceanic anoxic event

Marcel M.M. Kuypers, Peter Blokker, Jochen Erbacher, Hanno Kinkel, Richard D. Pancost, Stefan Schouten, Jaap S. Sinninghe Damsté

Abstract

Biogeochemical and stable carbon isotopic analysis of black shale sequences deposited during an Albian oceanic anoxic event (~112 Myr) indicate that up to 80 wt. % of sedimentary organic carbon is derived from marine, non-thermophilic archaea. The ^{13}C content of archaeal molecular fossils indicates that these archaea were living chemoautotrophically. Their massive expansion may have been a response to the strong stratification of the ocean during this anoxic event. In fact, the sedimentary record of archaeal membrane lipids suggests that this anoxic event actually marks a moment in Earth history at which certain hyperthermophilic archaea adapted to low-temperature environment.

6.1 Introduction

The mid-Cretaceous was a period of exceptional oceanic volcanic activity. Evidence of this igneous activity is provided by the presence of large oceanic plateau, including the Ontong Java, Kerguelen and Caribbean Plateau, which have been dated at 125-88 Myr (*1*). Enhanced volcanic outgassing of CO_2 could have caused the mid-Cretaceous 'greenhouse' climate (*2*), with its minimal equator-to-pole temperature difference. In contrast, episodic oceanic anoxic events (OAEs) may have effectively reduced CO_2 concentrations during brief periods by sequestering carbon in the subsurface (*3*, *4*). The widespread deposition of black-shales during the OAEs has been attributed either to decreased organic matter (OM) remineralisation resulting from a decreased oxygen flux (*5*) or to increased primary productivity overwhelming the oxic OM remineralisation potential of the water column (*6*). The increase in organic carbon (OC) accumulation rates during the OAEs in these two basically different models is attributed to enhanced burial of marine OM, which is typically of phytoplanktonic origin. Here we determined the source for both soluble and insoluble OM of the early Albian OAE 1b black shales of the Ocean Drilling Program site 1049C (North Atlantic Ocean off the coast of Florida: 30°08'N, 76°06'W) and the Ravel section of the Southeast France Basin (44°06'N, 6°28'E) using optical, chemical, and stable carbon isotopic analyses, and show that the sources of OM for this OAE are fundamentally different from other OAEs.

6.2 Results and discussion

The upper Aptian-lower Albian sequence of site 1049C consists of marls and calcareous marls characterised by a low (< 0.1 wt%) OC content interrupted by an OC-rich (up to 6 wt%; Fig. 1A) black shale interval. This black shale interval (grey shaded area; Fig. 1) has been identified as the local expression of OAE 1b (*7*). The bulk OC shows a sharp increase in its ^{13}C-content during the OAE1b (Fig. 1B). Similar increases in $\delta^{13}C$ values observed for marine carbonates and OM from other mid Cretaceous OAEs have been attributed to an increase in the ^{13}C content of the oceanic/atmospheric pool of inorganic carbon as a result of globally enhanced OC burial rates (*3*). However, the stable carbon isotopic composition of picked planktonic and benthic foraminifers (*7*) indicate that there was no significant increase in $\delta^{13}C$ values for inorganic carbon during the OAE1b at site 1049C.

To resolve the origin of the increase in $\delta^{13}C$ values for bulk OC ($\delta^{13}C_{org.}$) we first analysed the extractable OM. The saturated hydrocarbon fractions of the black shales contain long-chain (C_{25}-C_{31}) *n*-alkanes that are largely derived from leaf waxes of terrestrial plants, some bacterial hopanoids and acyclic isoprenoids. Remarkably, the acyclic isoprenoid, 2,6,15,19-tetramethylicosane [TMI (**I**), Fig. 1] is the most abundant component of the saturated hydrocarbon fraction. So far, TMI has only been found in the contemporaneous (*7*) OAE1b black shale of the Ravel section in France (*8*). TMI (**I**) is structurally closely related to 2,6,10,15,19-pentamethylicosane (PMI) (**II**), a compound of known archaeal origin (*9*), which was also present in the saturated hydrocarbon fraction. Further evidence for archaeal compounds was found on

treating the polar fraction from the black shale interval with HI/LiAlH$_4$ to cleave ether bonds. The released fractions were dominated by acyclic (**a**), monocyclic (**b**), bicyclic (**c**) and tricyclic (**d**)
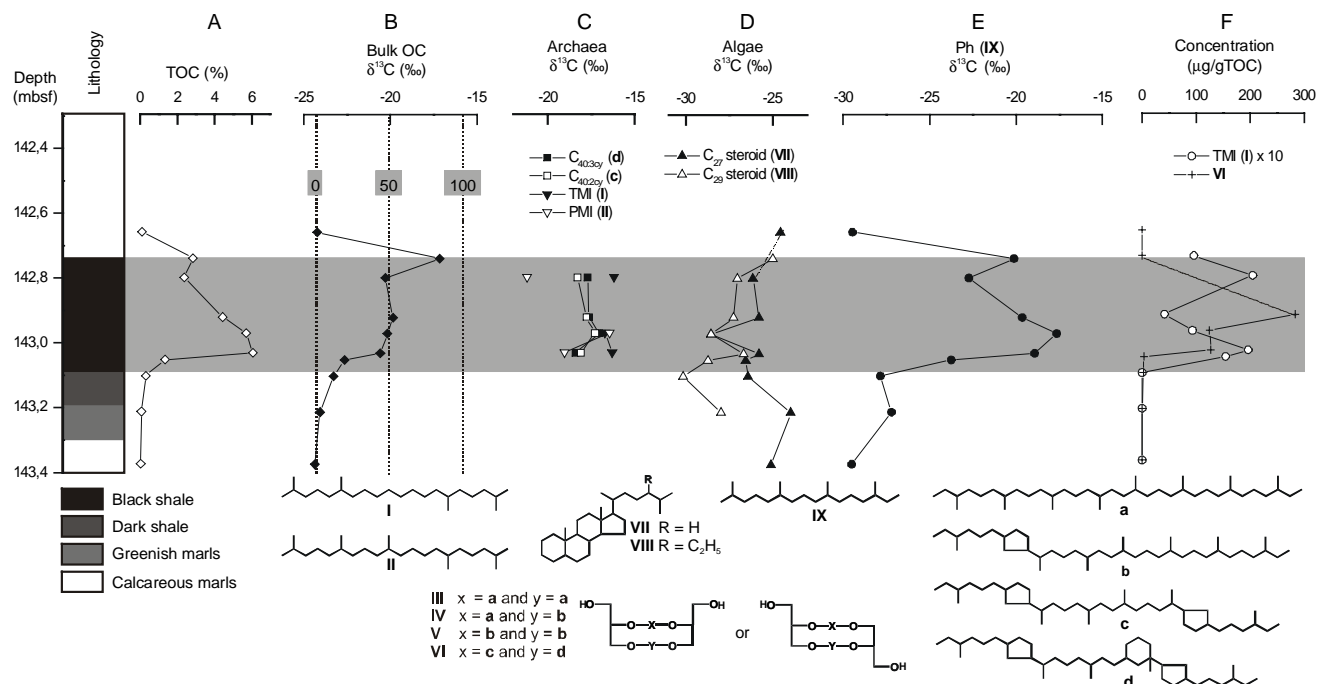

Figure 1 Stratigraphy, bulk and biomarker data of Ocean Drilling Project site 1049C. TOC content (**A**), and carbon isotope values (in ‰ vs. VPDB) of bulk OC (**B**), bi- (C$_{40:2cy}$) and tricyclic (C$_{40:3cy}$) biphytanes, PMI (**II**) and TMI (**I**) derived from archaea (**C**), oxygen-bound steranes [cholestane (**VII**) and 24-ethyl-cholestane (**VIII**)] mainly derived from marine algae (**D**), and oxygen-bound phytane (**IX**) derived either from the isotopically 'light' (^{12}C-rich) phytol side-chain (**VI**) of algal and cyanobacterial chlorophyll or the isotopically 'heavy' (^{13}C-rich) archaeal membrane lipids (**E**), and concentrations (µg/gTOC) of GDGT **VI** and TMI derived from archaea (**F**) of late Aptian/early Albian abyssal sediments from site 1049C (*28*). In all graphs the centre of the bullet corresponds to the top of the ~2 cm thick sediment samples. The OAE1b black shale interval has been indicated as a grey shaded area in the graphs. Dotted lines in graph (**B**) indicate estimated contributions (in %) of archaeal derived insoluble OM to TOC as discussed in text. Relevant structures are indicated.

biphytanes (C$_{40}$ isoprenoids), which are also exclusively found in archaea (*10, 11*). In addition, a recently developed HPLC/MS technique (*12*) revealed the presence of four (**III-VI**) intact isoprenoid glycerol dialkyl glycerol tetraethers (GDGTs) in the black shale interval. GDGTs are the main constituents of archaeal membranes (*11*) and **IV-V** are characteristic of the archaeal lineage Crenarchaeota (*10, 13*), which includes the hyperthermophilic archaea which thrive at temperatures >60°C. In contrast, **VI** is highly diagnostic for their non-thermophilic relatives (*11, 14-16*), and the dominance of this compound (representing 60% of total GDGTs) indicates an important input of non-thermophilic crenarchaeota. To the best of our knowledge this is the earliest fossil evidence for marine non-hyperthermophilic crenarchaeota, extending their geological record by more than 60 million years (*14*).

The δ^{13}C values of components of unambiguous archaeal origin such as **II**, **c** and **d** and the related **I** are significantly enriched in ^{13}C relative to algal steroids **VII-VIII** (Fig. 1C-D), bacterial derived hopanes and the leaf-wax *n*-alkanes *n*-C$_{29}$ and *n*-C$_{31}$ from higher plants (*17*). Cholestane

(**VII**) and 24-ethyl-cholestane (**VIII**), released after HI/LiAlH$_4$ treatment, derive from C$_{27}$ and C$_{29}$ sterols, predominantly biosynthesised by marine algae (*18*). Their δ^{13}C values record changes in the stable carbon isotopic composition of algae (Fig. 1C). The offset of >10‰ between the δ^{13}C values for TMI/PMI and the algal biomarkers (Figs. 1C-D) is in agreement with our earlier observations for the OAE1b black shales of the Ravel section in France (*8*).

While archaeal lipids are abundant in the OC-rich OAE1b black shales, they are largely absent in the adjacent sediments (Fig. 1F). This suggests a significantly increased archaeal contribution to the sedimentary OM during OAE1b. Evidence for an increase in the relative contribution of archaeal biomass is also provided by the ~12‰ shift in δ^{13}C values for the isoprenoid phytane (**IX**) released from the polar fractions upon HI/LiAlH$_4$ treatment (Fig. 1E). Phytane (**IX**) derives either from the isotopically 'light' (^{12}C-rich) phytol side-chain of algal and cyanobacterial chlorophyll or the isotopically 'heavy' (^{13}C-rich) archaeal membrane lipids such as archaeol. Before and after the black shale interval, δ^{13}C values for phytane (**IX**) are comparable to those of steranes, consistent with an algal origin, whereas in the black shale interval it is enriched by up to 12‰, indicating a predominant archaeal origin. There is no coinciding positive shift in δ^{13}C values for the algal steranes (Fig. 1D). Therefore, the sharp increase in δ^{13}C values for phytane (**IX**) indicates a change in the relative contribution from algal and archaeal OM sources during the OAE1b. An increase in the relative contribution of ^{13}C enriched archaeal biomass to the OM deposited during OAE1b could thus also explain the shift in δ^{13}C values for bulk OC (Fig. 1B).

To determine the archaeal contribution to the bulk OM, the insoluble OM, representing >95% of the bulk OM, was also investigated. Thin laminae of amorphous OM (as revealed by scanning electron microscopy) that occur throughout the black shale make up a significant part of the OM. This OM cannot be hydrolysed either by strong acid or base, and shows the enrichment in ^{13}C (δ^{13}C = -15.5‰) typical of archaeal lipids. Both thermal (flash pyrolysis) and chemical degradation (RuO$_4$ oxidation) of this amorphous OM almost exclusively (>95%) releases molecules with acyclic isoprenoidal carbon skeleton. These isoprenoids were also abundant in the flash pyrolysates of the OAE1b black shale of the Ravel section (*8, 19*). The weighted average of the δ^{13}C values of the chemically released isoprenoids (δ^{13}C = -14‰) from the black shale is in good agreement with the bulk isotopic composition of the OC from the laminae, indicating that these are the main components of this polymeric OM. The distribution of chemical degradation products indicates that the polymer consists of monomers with essentially two different carbon skeletons: TMI (**I**) and PMI (**II**) linked together by ether-bonds [Kuypers et al., unpublished results]. This strongly suggests that the positive shift in δ^{13}C$_{org.}$ (Fig. 1B) indeed results from an increased contribution of ^{13}C enriched archaeal-derived OC during OAE1b.

The relative contribution of archaeal polymer to the OC can be estimated from δ^{13}C$_{org.}$ using a two end-member mixing model and assuming that the δ^{13}C value (~ -24‰) for bulk sedimentary OC before the OAE1b represents the non-archaeal endmember and δ^{13}C = -15.5‰ for the archaeal endmember. There is on average a very large (~50 wt%) and sometimes even a predominant (~80 wt%) contribution of archaeal OC in the black shale interval (Fig. 1B). A significant contribution (up to 40 wt%) of archaeal OC is also found for the OAE1b black shales in France using the stable carbon isotopic composition of *n*-alkanes and isoprenoids obtained after off-line pyrolysis of the

bulk OM (*19*) as algal and archaeal endmembers, respectively. Although prokaryotes can constitute more than 70 wt% of carbon biomass in the upper ocean (*20*) and their biomarkers are abundantly present in the sediment (*21*), evidence for a substantial (>10 %) prokaryotic contribution to Phanerozoic OC-rich sediments is generally lacking (*22*). Therefore, the domination of OM derived from archaea during OAE1b is both unexpected and unprecedented, indicating that this was a unique time in Earth history. Certainly, it reveals that enhanced OM deposition during OAE1b was caused by a different mechanism than has been invoked for other OAEs.

The diversity of archaeal lipids recovered from the OAE1b black shales suggests that they derive from a multitude of archaeal species. However, the specific ^{13}C enrichment of these lipids indicates a common 'heavy' (^{13}C-rich) carbon source for the archaea and/or a common pathway of carbon-fixation with a reduced ^{13}C fractionation effect compared to the Calvin cycle used by algae, cyanobacteria and higher plants. The large enrichment (up to 12 ‰) in ^{13}C/^{12}C ratios between the algal biomarkers and the archaeal molecular fossils suggest that archaea were not living heterotrophically on photoautotrophic biomass. Hence it seems likely that the archaea present during OAE1b were autotrophs and used a chemical energy source for carbon fixation. The ecological niche of these chemoautotrophic archaea in the mid-Cretaceous ocean is not clear.

The abundance of GDGT **VI** in the OAE1b black shales can be interpreted, however, to suggest that at least some of these archaea were thriving in the marine water column. In the present-day ocean GDGT **VI** is abundantly present in marine particulate OM and surface sediments (*11*, *16*), which is consistent with the fact that planktonic representatives of the marine crenarchaeota comprise as much as 20% of the picoplankton (*23*). Compound-specific radiocarbon analyses of biphytanes **c** and **d** derived from **VI** indicate that these archaea are not feeding on phytoplanktonic biomass but rather use 'old' ^{14}C-depleted dissolved inorganic carbon from well below the photic zone in the water column (*24*). Furthermore, these components show a significant ^{13}C enrichment (4-5‰) relative to algal steroids (*14*), indicating that planktonic crenarchaeota, like related hyperthermophiles (*25*), may use a non-Calvin cycle pathway of carbon assimilation with a smaller degree of carbon-isotope fractionation during carbon assimilation. The offset between δ^{13}C values for the biphytane **d** derived from **VI** in present-day marine particulate OM (-20 to –23‰) (*14*) and in OAE1b sediments (-17 to –18‰) can be explained by the enrichment of dissolved inorganic carbon in ^{13}C by 2-3‰ relative to modern values during the mid-Cretaceous (*2*). The remainder of the larger (3-7‰) enrichment of biphytane **d** relative to algal steroids can probably be accounted for by enhanced carbon isotope fractionation by algae during the mid-Cretaceous due to enhanced CO_2 availability (*26*). Carbon isotopic evidence thus suggests that the mid-Cretaceous crenarchaeota producing GDGT **VI** used similar biochemical pathways as their present-day representatives.

The massive expansion of marine, non-thermophilic archaea during the mid-Cretaceous OAE1b is unprecedented and could actually mark a moment in geological history at which certain hyperthermophilic archaea adapted to low-temperature environments. Older sediments of comparable thermal maturity do not contain the characteristic GDGT **VI**, whereas this GDGT is commonly found in black shales younger than Albian (*11*, *14*). On the other hand, TMI (**I**) and macromolecular OM composed thereof has so far only been reported for this time interval. This suggests that at least two distinct groups of marine, non-thermophilic archaea existed, of which one has thrived for the past 112 Myr, whereas the other (TMI-producing) group seems to become

extinct after OAE1b when environmental conditions became less favourable. Prolonged (millions of years) periods of enhanced hydrothermal activity (*1*) would have significantly altered the ocean chemistry during the mid-Cretaceous, providing the necessary reduced compounds to sustain a large community of chemoautotrophic archaea. In fact, the Cretaceous strontium isotope record indicates maximum ocean-ridge crustal production during the Aptian-early Albian stages (*27*). In addition, the pronounced water column stratification and anoxic conditions that are characteristic for OAE1b (*7*) may have assisted in the development of a diverse community of marine, chemoautotrophic, non-thermophilic archaea.

6.3 References and Notes

1. R. L. Larson, *Geology* **19**, 547 (1991).
2. M. A. Arthur, W. E. Dean, S. O. Schlanger, *Amer. Geophys. Union Monogr.* **32**, 504 (1985).
3. M. A. Arthur, W. A. Dean, L. M. Pratt, *Nature* **335**, 714 (1988).
4. M. M. M. Kuypers, R. D. Pancost, J. S. Sinninghe Damsté, *Nature* **399**, 342 (1999).
5. T. J. Bralower and H. R. Thierstein, *Geol. Soc. Spec. Publ.* **26**, 345 (1987).
6. S. O. Schlanger and H. C. Jenkyns, *Geol. Mijnb.* **55**, 179 (1976).
7. J. Erbacher, B. T. Huber, R. D. Norris, M. Markey *Nature* **409**, 325 (2001).
8. A. Vink, S. Schouten, S. Sephton, J. S. Sinninghe Damsté, *Geochim. Cosmochim. Acta* **62**, 965 (1998).
9. S. Schouten, M. J. E. C. van der Maarel, R. Huber, J. S. Sinninghe Damsté, *Org. Geochem.* **26**, 409 (1997).
10. M. De Rosa and A. Gambacorta, *Prog. Lipid Res.* **27**, 153 (1988).
11. S. Schouten, E. C. Hopmans, R. D. Pancost, J. S. Sinninghe Damsté, *Proc. Nat. Acad. Sci. USA* **97**, 14421 (2000).
12. E. C. Hopmans, S. Schouten, R. D. Pancost, M. T. J. van der Meer, J. S. Sinninghe Damsté, *Rapid. Commun. Mass Spectrom.* **14**, 585 (2000).
13. K. O. Stetter, in *Extremophiles: Microbial Life in Extreme Environments*, K. Horikoshi and W. D. Grant, Eds. (Wiley-Liss, Inc., New York, 1998), Chap. 1.
14. M. J. L. Hoefs et al., *Appl. Environ. Microbiol.* **63**, 3090 (1997).
15. E. F. DeLong et al., *Appl. Environ. Microbiol.* **64**, 1133 (1998).
16. Recent direct HPLC-MS analyses of a uni-archaeal culture of the non-thermophilic crenarchaeotum *Cenarchaeum symbiosum* (kindly provided by Dr. E.F. DeLong) and marine particles from the marine water column have indicated that **VI** is one of the most abundant lipids present (Schouten, Hopmans and Sinninghe Damsté, unpublished results).
17. For supplementary material is available see appendix
18. J. K. Volkman, *Org. Geochem.* **9**, 83-99 (1986).
19. I. M. Höld, S. Schouten, H. M. E. van Kaam-Peters, J. S. Sinninghe Damsté, *Org. Geochem.* **28**, 179 (1998).
20. J. A. Fuhrman, T. D. Sleeter, C. A. Carlson, L. M. Proctor, *Mar. Ecol. Progr. Ser.* **57**, 207 (1989).
21. G. Ourisson and P. Albrecht, *Acc. Chem. Res.* **25**, 398 (1992).
22. J. S. Sinninghe Damsté and S. Schouten, *Org. Geochem.* **26**, 517 (1997).
23. M. B. Karner, E. F. DeLong, D. M. Karl, *Nature* **409**, 507 (2001).
24. A. Pearson, T. I. Eglinton, A. P. McNichol, B. C. Benitez-Nelson, J.M. Hayes, Geochim. Cosmochim. Acta, in press.
25. M. T. J. van der Meer, S. Schouten, W. I. C Rijpstra, G. Fuchs., J. S. Sinninghe Damsté, FEMS Microbiol. Lett., in press.
26. M. A. Arthur, W. E. Dean, G. E. Claypool, *Nature* **315**, 216 (1985).
27. T. J. Bralower, P. D. Fullager, C. K. Paull, G. S. Dwyer, R. M. Leckie *GSA Bull.* **109**, 1421 (1997).
28. Total Organic Carbon (TOC) contents were determined using a CN analyser. The $\delta^{13}C$ values (± 0.1‰) ($\delta^{13}C = [(R_{sample}/R_{standard} - 1) \cdot 1{,}000]$, where R is $^{13}C/^{12}C$ and the standard the Vienna Pee Dee belemnite) were measured

on bulk sediments after removal of the inorganic carbonates with diluted HCl using automated on-line combustion followed by conventional isotope ratio-mass spectrometry. The powdered samples (15 to 30 g) were Soxhlet extracted for *c*. 24 h to obtain the total lipid fraction. The total extracts were separated into apolar and polar fractions using column chromatography. The hydrocarbons that were released from the polar fraction by HI/LiAlH$_4$ and subsequent hydrogenation were isolated using column chromatography. Samples were analysed by GC-mass spectrometry (GC-MS) for identification. Compound-specific $\delta^{13}C$ analyses were performed using GC-isotope-ratio-monitoring MS. The $\delta^{13}C$ values for individual compounds are the means of duplicate runs ($\delta^{13}C = \pm 0.3$ to 0.6) expressed versus VPDB. HPLC/MS analyses were performed as previously described (*12*). Macromolecular material was isolated from the decalcified and extracted sediments by density centrifugation (at 3700 r.p.m. for 5 min) using pure dichloromethane (floating fraction). Fourier transform infrared spectroscopy (frequency range of 400 cm^{-1} to 4000 cm^{-1}) was performed on 2 mg of dry macromolecular material pressed into KBr pellets. The extract obtained after RuO$_4$ degradation of ~5 mg of isolated macromolecular material was derivatised with BF$_3$/methanol prior to analysis. Curie-point flash pyrolysis (10 s; 610°C) was performed with a pyrolysis unit connected to a gas chromatograph.

Appendix

Source organism	Biochemical Precursor	C skeleton	Mode	$\delta^{13}C$ (‰)
Higher plants	*n*-C$_{27}$	*n*-C$_{27}$	Free	-27.7 to –28.9
	n-C$_{31}$	*n*-C$_{31}$	Free	-27.7 to –28.0
Algae/higher plants	24-ethyl-cholesterols	C$_{29}$ sterane (**VIII**)	Alc.	-25.1 to –30.2
Algae	24-methyl-cholesterols	C$_{28}$ sterane	Alc.	-27.0 to –29.2
Algae/zooplankton	Sterols	C$_{27}$ sterane (**VII**)	Alc.	-23.9 to –28.5
Algae/cyanobact.	Chlorophyll	Phytane (**IX**)	Alc.	-27.2 to –29.5
Heterotr./cyanobact.	Bacteriohopanepolyols	C$_{29}$ hopane	Free	-23.7 to –24.9
	Bacteriohopanepolyols	C$_{31}$ hopane	Free	-26.1 to –27.0
Archaea/bacteria	Squalane/squalene	Squalane	Free	-17.6 to –23.4
Archaea	GDGTs (**III, IV**)	C$_{40:1cycl.}$ (**b**)	E-bd/alc.	-17.6 to –20.0
	GDGTs (**V**)	C$_{40:2cycl.}$ (**c**)	E-bd/alc.	-17.1 to –18.4
	GDGTs (**VI**)	C$_{40:3cycl.}$ (**d**)	E-bd/alc.	-17.3 to –18.3
	Archaeol	Phytane (**IX**)	E-bd.	-17.7
	PMI (**II**)/unsat. PMI	PMI (**II**)	Free	-16.5 to –21.2
	Unknown	TMI (**I**)	Free	-16.2 to –16.7
	Funct. TMI/PMI	TMI/PMI	E-bd	-13.1 to –15.0

Source organisms, inferred biochemical precursor, isotopic composition and mode of occurrence of C skeletons encountered in the sediment. Carbon skeletons are shown in Fig. 1. Carbon skeletons occur in the following modes: free hydrocarbons (free), macromolecularly S-bound moiety (S-bd), alcohols (Alc.) and ether-bound moiety (E-bd). The range of measured stable carbon isotopic values for individual components is indicated. Abbreviations are isopr., isoprenoid alkanes; 1cycl., mono cyclic; Funct., functionalised; unsat., unsaturated; Heterotr., heterotrophic bacteria; cyanobact., cyanobacteria.

Chapter 7

Archaeal remains dominate marine organic matter from the early Albian oceanic anoxic event 1b

Marcel M.M. Kuypers, Peter Blokker, Ellen C. Hopmans, Hanno Kinkel, Richard D. Pancost, Stefan Schouten, Jaap S. Sinninghe Damsté

Abstract

The sources for both soluble and insoluble organic matter of the so-called early Albian (~112 Myr) 'oceanic anoxic event (OAE) 1b' black shales of the Ocean Drilling Program (ODP) site 1049C (North Atlantic Ocean off the coast of Florida) and the Ravel section of the Southeast France Basin (SEFB) were determined using optical, chemical, stable carbon and nitrogen isotopic analyses. Archaea-derived isoprenoidal tetraether membrane lipids and free and macromolecularly bound isoprenoid alkanes are abundant in these black shales. More specifically, the presence of certain ether lipids (bi/tricyclic biphytane tetraethers) indicates an important contribution of representatives of marine planktonic archaea. The large difference (up to 12 ‰) in $^{13}C/^{12}C$ ratios between algal biomarkers and the much more abundant planktonic archaea-derived biomarkers indicates that the latter were living chemoautotrophically, possibly using ammonium as an energy source. This offset in $^{13}C/^{12}C$ ratios was used to estimate that up to ~40% of the organic matter of the SEFB and up to ~80% of the organic matter of ODP site 1049C preserved in the black shales is derived from archaea. Furthermore, it is shown that, even though there are apparent similarities (high OC content, distinct lamination, ^{13}C-enrichment of organic carbon) between the black shales of OAE1b and the Cenomanian/Turonian (C/T ~ 94 Myr) OAE, the origin of the organic matter (archaeal versus phytoplanktonic) and causes for ^{13}C-enrichment of OC are completely different.

7.1. Introduction

Extensive oceanic volcanism is thought to have led to 3 to 12 times higher atmospheric levels of carbon dioxide during the mid-Cretaceous (~125-88My) than at present [*Arthur et al.*, 1985a; *Larson*, 1991; *Berner*, 1992]. This could have caused the mid-Cretaceous 'greenhouse' climate with its warm temperatures and small equator-to-pole temperature gradient [*Barron*, 1983]. Oceanic anoxic events (OAEs), episodes of globally enhanced organic carbon (OC) burial rates, may have effectively reduced CO_2 concentrations of the mid-Cretaceous 'greenhouse' atmosphere by sequestering carbon in the subsurface.

Originally the term OAE was introduced to describe the episodic expansion and intensification of the Oxygen Minimum Zone (OMZ), which was proposed to explain the seemingly global distribution of laminated OC-rich (> 1%) sediments (black shales) in pelagic sequences of Aptian-Albian and Cenomanian/Turonian (C/T) age [*Schlanger and Jenkyns*, 1976]. Since then several other time-bounded envelopes of particularly, perhaps more globally, widespread black shale deposition in marine environments have been identified [*Arthur et al.*, 1987] and a total of five OAEs have been recognised for the mid-Cretaceous. In most cases the OAE black shales are devoid of or strongly impoverished in benthic faunas indicating that these sediments were deposited under oxygen-deficient bottom-water conditions [*Summerhayes*, 1987]. The most intensely studied OAEs occurred near the Barremian/Aptian (OAE1a) and C/T (C/T OAE or OAE2) transition. Both OAEs are accompanied by a significant increase in $^{13}C/^{12}C$ ratios for marine carbonates (up to 2.5‰) and organic matter (up to 6‰). These positive excursions in $\delta^{13}C$ values reflect changes in the global atmospheric-oceanic pool of inorganic carbon resulting from a global increase in the burial rate of ^{13}C-depleted OC [*Arthur et al.*, 1988]. Positive shifts in $\delta^{13}C$ values of marine carbonate, albeit it significantly smaller, may also have been associated with other mid- Cretaceous OAEs [*Erbacher and Thurow*, 1997].

There are apparent similarities between OAE black shales such as enrichment in OC, lamination, absence of or impoverished benthic faunas, ^{13}C-enrichment of inorganic and/or organic carbon. To investigate if this also implies that organic matter (OM) in various OAE black shales has a similar origin, we studied early Albian (~112 My) OAE1b black shales and compared the results with our earlier findings for the C/T OAE [Kuypers et al., submitted]. So far, knowledge about the community of organisms contributing OM to these black shales is mainly restricted to visual identification of microfossils such as pollen or dinoflagellate cysts and ignores organisms that do not leave behind microscopically readily identifiable fossilised remains such as bacteria. In fact, the visually identifiable fraction generally makes up only a small part of the total OM present and most OM in these OC-rich sediments is amorphous. Lipids and pigments or their fossilised remains (biomarkers) and their stable carbon isotopic composition [e.g. *Freeman et al.*, 1990] can give important information on the sources of the extractable OM. In a similar way, the analyses of products released upon thermal and chemical degradation can reveal important insights into the sources of insoluble OM [e.g. *Blokker et al.*, 2000].

Here we use detailed molecular and compound-specific carbon isotope measurements, thermal (flash pyrolysis), and chemical degradation (RuO_4 oxidation) techniques to determine the sources of both soluble and insoluble OM of OAE1b black shales from the Ravel section of the Southeast

France Basin (SEFB) and Ocean Drilling Program (ODP) site 1049C (North Atlantic Ocean off the coast of Florida) (Fig.1) and show that the sources of OM for this OAE are fundamentally different from the C/T OAE.

Figure 1. Palaeogeographic reconstruction for the late Aptian (120 Myr ago) showing the position of the two studied sections. Modified after Erbacher et al. [2001].

7.2. Material and Methods

7.2.1 Geological setting. The upper Aptian-lower Albian at the SEFB consists of a monotonous sequence of dark, fine-grained, marly sediments. The laminated black shales of the Niveau Paquier (the local expression of the OAE1b) consist of a mixture of biogenic carbonate, clay minerals, silt-sized quarts and abundant OM [*Tribovillard and Gorin*, 1991].

The upper Aptian-lower Albian sequence of ODP site 1049C consists of marls and calcareous marls characterised by a low OC content interrupted by an OC-rich black shale interval [*Shipboard Scientific Party*, 1998]. This black shale interval (indicated as a grey shaded/black area in Fig. 2) has been identified as the local expression of OAE 1b [*Erbacher et al.*, 1999; *Erbacher et al.*, 2001].

7.2.2 Samples. The samples used in this study were taken from the Ravel section of the Southeast France Basin (SEFB) and Ocean Drilling Program (ODP) Hole 1049C off the coast of northern Florida (leg 171B). Two to three cm thick sediment slices were taken from core 12 section 3 recovered from 142.3-143.8 meters below seafloor at ODP Site 1049C. Sub-samples were taken from the slices and subsequently freeze-dried and powdered in an agate mortar. Five samples were analysed from the Ravel section of the SEFB [Vink et al., 1998].

7.2.3 Bulk Analyses. Total Organic Carbon (TOC) and Total Nitrogen (N_{tot}) contents were determined with a Carlo Erba CN analyser 1502 series. The $\delta^{15}N$ measurements were performed using an automated on-line combustion system (Carlo Erba CN analyser 1502 series) followed by conventional isotope ratio-mass spectrometry (Fisons optima; [*Fry et al.*, 1992]). The $\delta^{15}N$ values for bulk sediments are expressed relative to atmospheric N_2, with a precision better than 0.2 ‰. To measure the $\delta^{13}C$ values ($\delta^{13}C = [(^{13}C/^{12}C)_{sample}/(^{13}C/^{12}C)_{standard}]-1$) of OC, inorganic carbon was removed from the bulk sediments with 2 M HCl (12 h at 60°C). Subsequently, the sediments were rinsed three times with demineralised water to remove $CaCl_2$ and dried in a stove (12 h at 60°C). The $\delta^{13}C$ measurements were performed using an automated on-line combustion system (Carlo Erba CN analyser 1502 series) followed by conventional isotope ratio-mass spectrometry (Fisons optima). The $\delta^{13}C$ values for OC are expressed versus the VPDB standard, with a standard deviation for duplicate runs of ± 0.1‰.

Small sub-samples were decalcified with 2 M HCl and subsequently sieved (10 μm mesh) for microscopic screening.

7.2.4 Extraction and fractionation of extractable organic matter. The powdered samples (10 to 20 g) of ODP Site 1049C were Soxhlet extracted with a dichloromethane (DCM)/methanol (7.5:1, v/v) mixture for 24 h to obtain the total lipid fraction. Total lipid fractions, to which a mixture of four standards was added for quantitative analyses [*Kohnen et al.*, 1990], were separated into apolar and polar fractions using a column (20 x 2 cm; column volume (V_0) =35 ml) packed with alumina (activated for 2.5 h at 150 °C) eluted with hexane/DCM (9:1, v/v; 150 ml) and methanol/DCM (1:1, v/v; 150 ml), respectively. The apolar fractions were further separated by column chromatography on $AgNO_3$-impregnated silica, with hexane as eluent (to remove unsaturated compounds) to obtain relatively simple fractions for isotope-ratio-monitoring gas chromatography-mass spectrometry (irm-GC-MS). Portions of the polar fractions were silylated using bis(trimethyl-silyl)trifluoro-acetamide (BSTFA)/pyridine and analysed by gas chromatography (GC) and GC-mass spectrometry (GC-MS).

Aliquots of the polar fractions were treated with HI/LiAlH$_4$ as described previously [*Hoefs et al.*, 1997]. Briefly, the fractions were refluxed in a solution of 56 wt% HI in water for 1 h and the released alkyl iodides were isolated using column chromatography (alumina as stationary phase, hexane/DCM (9:1, v/v) as eluent). Subsequently, the alkyl iodides were treated with LiAlH$_4$ in 1,4-dioxane for 1 h to convert them into hydrocarbons. The hydrocarbons were hydrogenated under a hydrogen-atmosphere for 1 h using PtO$_2$ as a catalyst to convert unsaturated compounds into saturated hydrocarbons. The released compounds were analysed by GC and GC-MS [see *Hoefs et al.*, 1997 for details].

Aliquots of the polar fractions spiked with a thiophene standard [2,3-dimethyl-5-(1,1-d$_2$-hexadecyl)thiophene] were also desulfurised with Raney Nickel and subsequently hydrogenated as described by Sinninghe Damsté et al. [*Sinninghe Damsté et al.*, 1990]. The released hydrocarbons were isolated by column chromatography with alumina and analysed by GC and GC-MS. Subsequently, $AgNO_3$ column chromatography was used to obtain relatively simple fractions for irm-GC-MS.

7.2.5 Isolation of macromolecular material. The residues obtained after Soxhlet extraction of the sediments of the SEFB and ODP Site 1049C were decalcified by treatment with 2 M HCl (12 h at 60°C). Subsequently, the decalcified sediments were rinsed with demineralised water (3x) to remove $CaCl_2$ and ultrasonically re-extracted with methanol (3X) and DCM/hexane (1:1) to remove extractable OM. Macromolecular material was isolated from the decalcified and extracted sediments by density centrifugation (at 3700 r.p.m. for 5 min.) using pure DCM (floating fraction).

7.2.6 Ruthenium tetroxide treatment. This treatment was modified from a procedure reported previously [*Blokker et al.*, 1998]. Briefly, *c.* 5 mg of isolated macromolecular material of the SEFB or ODP Site 1049C was ultrasonically suspended in a mixture of 1 ml chloroform, 1 ml acetonitrile and 2 ml of an aqueous solution of $NaIO_4$ (0.2 M, pH 3-4). After addition of 6 mg $Ru(III)Cl_3$, the two phase system was allowed to react in an ultrasonic bath. After 4 h, 3 ml water and 2 ml hexane were added. The organic layer was removed and quenched with methanol (MeOH) (0.5 ml). The aqueous layer was extracted with 2 ml hexane (1x) and 2 ml dichloromethane (2x) and these organic layers were transferred to the first organic extract. The black Ru-salts were precipitated from the organic layer by centrifugation. The remaining supernatant was washed with 0.5 ml $Na_2S_2O_3$ solution (5% in H_2O). The extract was dried over Na_2SO_4, evaporated to dryness under a nitrogen flow and derivatised with BF_3/methanol prior to analysis.

7.2.7 Gas chromatography. GC was performed using a Hewlett-Packard 5890 instrument, equipped with an on-column injector. A fused silica capillary column (25 m x 0.32 mm) coated with CP-Sil 5 (film thickness 0.12 μm) was used with helium as carrier gas. Both a flame ionization detector (FID) and a sulfur-selective flame photometric detector (FPD) were used, applying a stream-splitter with a split ratio of FID:FPD = c. 1:2. The samples were dissolved in ethyl acetate and injected at 70 °C. Subsequently, the oven was programmed to 130 °C at 20 °C/min and then at 4 °C/min to 320 °C at which it was maintained for 20 min.

7.2.8 Curie-point pyrolysis gas chromatography. Pyrolysis (Py)-GC was conducted on a Hewlett Packard 5890 series II gas chromatograph fitted with a 25 m x 0.32 mm CP-Sil 5 (film thickness 0.45 μm) fused silica capillary column and equipped with a FID. Samples of ODP Site 1049C were pressed on flattened ferromagnetic wires with a Curie temperature of 610°C. The wire was inserted into a glass liner, subsequently introduced into a FOM-4LX pyrolysis unit and inductively heated for 10 s. The desorbed fragments were flushed into the capillary column using helium as the carrier gas. The gas chromatograph was equipped with a cryogenic unit and programmed from 0°C (5 min) to 320°C (hold time 10 min) at 3°C/min. Helium was used as a carrier gas and the temperature of the flame ionisation detector (FID) was 320°C.

7.2.9 Gas chromatography-mass spectrometry. GC-MS was performed using a Hewlett-Packard 5890 gas chromatograph interfaced to a VG Autospec Ultima Q mass spectrometer operated at 70 eV with a mass range m/z 50-800 and a cycle time of 1.8 s (resolution 1000). The column

conditions and temperature program were the same as described above for GC and Py-GC analyses, respectively.

7.2.10 Isotope-ratio-monitoring gas chromatography-mass spectrometry. Compound-specific $\delta^{13}C$ analyses were performed for the samples of ODP Site 1049C using an isotope-ratio-monitoring GC-MS (irmGC-MS) system that is in principal similar to the DELTA-S system described by *Hayes et al.* [1990]. A Hewlett-Packard 5890 gas chromatograph was used. The column conditions and temperature program were the same as described above for GC analyses. The $\delta^{13}C$ values for individual compounds are reported in the standard delta notation against VPDB standard and are the means of duplicate runs with a precision of ±0.3 to 0.6‰.

7.2.11 High performance liquid chromatography/atmospheric pressure positive ion chemical ionization mass spectrometry. Intact isoprenoid glycerol dialkyl glycerol tetraethers (GDGTs) in the polar fractions of ODP site 1049C were determined according to Hopmans *et al.* [2000]. Briefly, aliquots of the polar fractions were redissolved in hexane:propanol (99:1) and filtered through 0.45 µm PTFE filters. Analyses were performed using an HP (Palo-Alto, CA, USA) 1100 series LC-MS equipped with an auto-injector and Chemstation chromatography manager software. Separation was achieved on an Econosphere NH_2 column (4.6 x 250 mm, 5 µm; Alltech, Deerfield, IL, USA), maintained at 30°C. GDGTs were eluted with 99% A and 1% B for 5 min, followed by a linear gradient to 1.8% B in 45 min, where A = hexane and B = propanol at a flow rate of 1 ml/min. Detection was achieved using atmospheric pressure positive ion chemical ionization mass spectrometry (APCI-MS) of the eluent. Positive ion spectra were generated by scanning *m/z* 950-1450 in 1.9 s. GDGTs were quantified by comparing their combined $[M+H]^+$ and $[M+H]^+ + 1$ ion intensities to the combined $[M+H]^+$ and $[M+H]^+ + 1$ ion intensity of known amounts of caldarcheol, isolated from Arabian Sea sediments according to Sinninghe Damsté *et al.* [2000].

7.2.12 Fourier transform infrared spectroscopy. Fourier transform infrared spectroscopy was performed for the isolated macromolecular material of ODP Site 1049C on a Bruker IFS28 instrument scanning over a frequency range of 400 cm^{-1} to 4000 cm^{-1} using KBr pellets containing 2 mg of dry macromolecular material.

7.3. Results and discussion

7.3.1 Abundance and stable carbon isotopic composition of organic carbon

While the upper Aptian-lower Albian marls and calcareous marls of ODP site 1049C are characterised by a low (< 0.1 wt%) TOC content, the black shale interval contains up to 6 wt% TOC (Fig. 2a). The sixty-fold increase in TOC content is accompanied by a sharp increase in the $^{13}C/^{12}C$ ratio for bulk OC of approximately 4-5‰ during OAE1b (Fig. 2b). The uppermost sample of the black shale is characterised by the most ^{13}C-enriched OC. Similar increases in $\delta^{13}C$ values have

been observed for marine carbonates and organic matter from other mid Cretaceous OAEs and have been attributed to globally enhanced carbon burial rates [*Arthur et al.*, 1988]. The isotope effect associated with carbon fixation (ε_p) by primary producers causes OC to be enriched in ^{12}C relative to the inorganic carbon source. Therefore, burial of large quantities of OC into black shales could lead to an increase in the ^{13}C content of the remaining oceanic-atmospheric pool of inorganic carbon. However, results obtained from selected specimens of planktic and benthic foraminifers [*Erbacher et al.*, 1999; *Erbacher et al.*, 2001] indicate that there was no significant increase in $\delta^{13}C$ values for inorganic carbon during the OAE1b at ODP site 1049C. Hence the increase in $\delta^{13}C$ values for bulk OC cannot be attributed to globally enhanced OC burial rates.

In order to resolve the origin of the increase in $\delta^{13}C$ values for bulk OC ($\delta^{13}C_{org.}$), both the extractable and insoluble OM was investigated in detail.
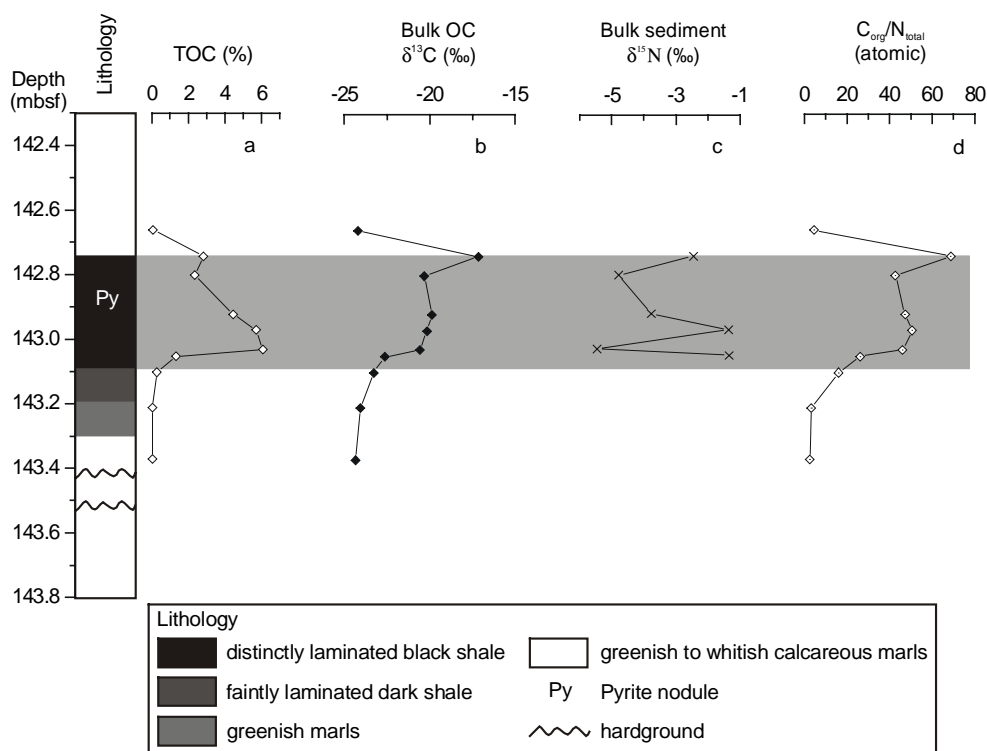
Figure 2. Stratigraphy and bulk sediment data of ODP Site 1049C. TOC content **(a)**, carbon isotope values (in ‰ vs. VPDB) of bulk OC **(b)**, nitrogen isotope values (in ‰ vs. atmospheric N_2) of bulk sediment **(c),** and atomic C_{org}/N_{total} ratios **(d)** of late Aptian/early Albian abyssal sediments from ODP Site 1049C. In all graphs the centre of the bullet corresponds to the top of the ~2 cm thick sediment samples. The OAE1b black shale interval has been indicated as a grey shaded area in the graphs.

7.3.2 Extractable OM

7.3.2.1 Composition of the extractable OM. Only small amounts of total extracts were recovered from the OM-lean sediments outside the black shale interval (below quantification limit), while higher amounts (1.0 to 2.0 mg/g dry sediment) were recovered from the black shales. The extractable OM was separated into apolar and polar fractions. There is approximately 50 times more

polar than apolar material within the black shale interval, which probably indicates a low thermal maturity of the OM. The apolar hydrocarbon fractions within the black shale interval consist mainly of short-chain *n*-alkanes (C_{16}-C_{22}) with no odd-over-even predominance, long-chain (C_{25}-C_{31}) *n*-alkanes with a moderate odd-over-even carbon number predominance (CPI = 2), hopanoids, and acyclic isoprenoids (Fig. 3a). The polar fraction from the black shale interval typically contains sterols, a compound that has tentatively been identified as the ketone of 2,6,15,19-tetramethylicosane (TMI; **I**, see Appendix), biphytane diols [*Schouten et al.*, 1998], and diphytanylglycerol diether (archaeol; **III**, see Appendix) [*Koga et al.*, 1993] and is strongly dominated by an unresolved hump. In addition, HPLC/MS revealed abundant intact isoprenoid glycerol dialkyl glycerol tetraethers (GDGTs) in the polar fraction. Since GDGTs are not GC amenable and relatively simple fractions are needed for irm-GC-MS, the polar fractions were treated with HI/LiAlH$_4$ and subsequently hydrogenated to convert the sterols, archaeol and biphytane diols/GDGTs into steranes, phytane and biphytanes, respectively. HI/LiAlH$_4$ treatment of the polar fractions from the black shale released fractions containing *n*-alkanes with an even-over-odd carbon number predominance, phytane, cholestane, 24-methylcholestane and 24-ethylcholestane, but which are dominated by acyclic (**a**), monocyclic (**b**), bicyclic (**c**) and tricyclic (**d**) biphytanes (C_{40} isoprenoids) (Fig. 3b). HI/LiAlH$_4$ treatment of the polar fractions of the marls mainly released *n*-alkanes with an even-over-odd carbon number predominance of unknown origin, phytane, cholestane and 24-ethylcholestane, while biphytanes are absent.

Since functionalised lipids and carotenoids may become sulfurised during early diagenesis in anoxic, sulfide-rich sediments [*Kok et al.*, 2000], three polar fractions from the black shale interval were also desulfurised. The apolar fractions (Fig. 3c) obtained after desulfurisation of the polar fractions are mainly dominated by phytane and two isomers of a C_{20} monocyclic isoprenoid (**V**, Appendix).

In the following sub-paragraphs the relative abundances and stable carbon isotopic compositions of the various classes of biomarkers encountered in the sediments from site 1049C are discussed.

7.3.2.2 *n*-Alkanes. The apolar fractions from the OAE1b black shales contain short-chain *n*-alkanes (C_{16}-C_{22}) with no odd-over-even carbon number predominance and long-chain (C_{25}-C_{33}) *n*-alkanes with a moderate odd-over-even carbon number predominance (Fig. 3a). The odd-over-even predominance (CPI ~ 2) of the *n*-C_{25} to *n*-C_{33} suggests that leaf waxes of terrestrial plants are a significant source [*Eglinton and Hamilton*, 1967]. A major mode of transport of leaf wax *n*-alkanes is *via* wind, as indicated by the high relative amounts of leaf wax components in aeolian dust collected at remote ocean sites [*Gagosian et al.*, 1981]; consequently, they are common constituents of extractable OM of recent and ancient abyssal plane sediments [*Farrington and Tripp*, 1977]. Taking into account the prevailing wind direction [*Poulsen*, 1999], the most likely candidate for the origin of these aeolian transported terrestrial *n*-alkanes is the nearby North American continent (Fig. 1).

The concentration of leaf-wax *n*-alkanes (normalised to TOC) is enhanced in the faintly laminated dark shale interval and in the less OM-rich black shales (up to ~20 µg/gTOC, Fig. 4b) compared to the underlying marls (5 to 10 µg/gTOC). Concentrations decrease again to well below
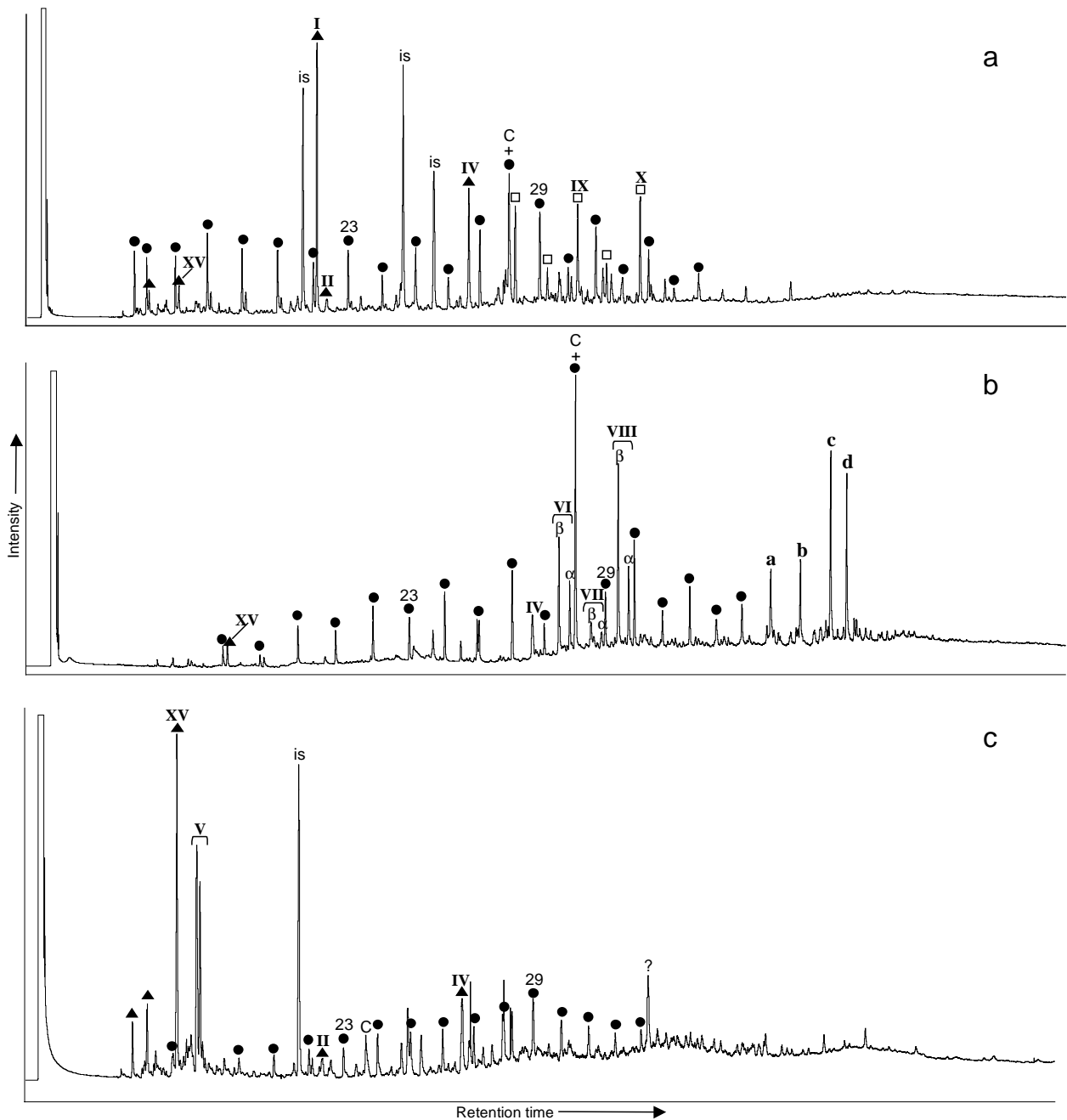
Figure 3. Typical gas chromatograms of apolar fraction (**a**), and hydrocarbon fractions released after HI-LiAlH$_4$ treatment (**b**), and desulfurisation (**c**), of the polar fraction from sediment extracts of the OAE1b black shales of ODP Site 1049C. Filled circles, open squares and filled triangles indicate *n*-alkanes, hopanes and saturated acyclic isoprenoids, respectively. Abbreviations are: is, internal standard; 23, *n*-C$_{23}$; 29, *n*-C$_{29}$; C, contaminant; α, 5α isomers of steranes; β, 5β isomers of steranes; ?, compound of unknown structure. Other letters and roman numbers refer to structures shown in the Appendix.

10 μg/gTOC in the overlying more OM-rich black shales. These trends can not be attributed to changes in redox state of the bottom-waters because *n*-alkanes and bulk marine OM have a similar preservation potential under oxic conditions [*Sinninghe Damsté et al.*, 1997a; Hoefs et al., in prep]. The increase in *n*-alkane concentrations could point to a relatively enhanced terrestrial contribution

to the sediment during the onset of black shale deposition, while the decrease can probably fully be attributed to dilution by marine OM.
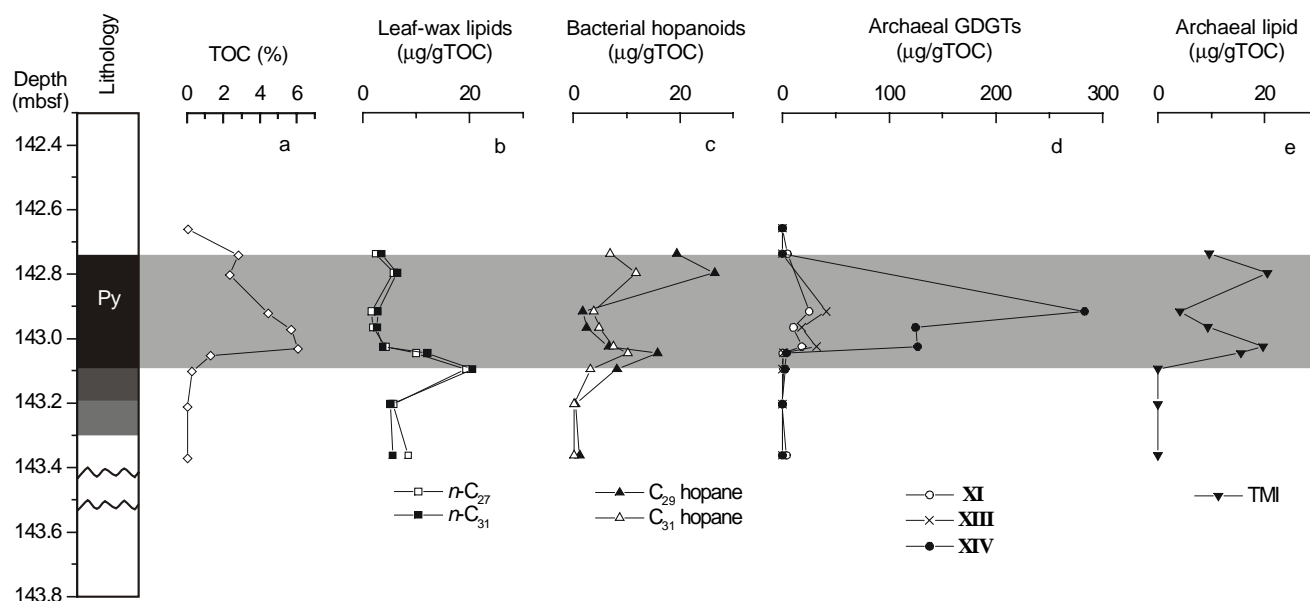
Figure 4. Stratigraphy, bulk and biomarker data of ODP Site 1049C. TOC content **(a)**, and concentrations (μg/gTOC) of *n*-alkanes (*n*-C_{27} and C_{31}) mainly derived from leaf-waxes **(b)**, hopanoids (i.e. C_{27} and C_{29} hopanoids) mainly derived from bacteria **(c)**, GDGTs **XI**, **XIII** and **XIV** derived from archaea **(d)**, and TMI derived from archaea **(e)** of late Aptian/early Albian abyssal sediments from ODP Site 1049C. In all graphs the centre of the bullet corresponds to the top of the ~2 cm thick sediment samples. Roman numbers refer to structures shown in the Appendix. The OAE1b black shale interval has been indicated as a grey shaded area in the graphs. Lithology as in Fig.2.

The $\delta^{13}C$ values of the *n*-C_{27} and *n*-C_{31} range from –28 to –29‰ (Fig. 5b), which is slightly more enriched than the –30 to –37‰ typically observed for extant plants using a C_3 metabolism [*Collister et al.*, 1994; *Lockheart et al.*, 1997]. Since this small offset can fully be attributed to a ^{13}C-enrichment of the inorganic carbon (e.g. CO_2) pool (2-3‰) during the mid-Cretaceous [*Arthur et al.*, 1985b], it seems likely that the *n*-alkanes derive predominantly from a C_3-type vegetation. This fits well with models that predict C_3 domination, even of low-latitude terrestrial vegetation, as a result of the high p_{CO2} levels during the mid-Cretaceous [*Cerling et al.*, 1997].

7.3.2.3 Steroids. Treatment of the polar fractions of extracts from the black shale interval with HI/LiAlH$_4$ to cleave ether bonds and subsequent hydrogenation released significant amounts of steranes (Fig. 3b). Remarkably, some of the samples from the OAE1b black shales contain significantly more 5β than the more commonly occurring 5α isomers of cholestane (**VI**), 24-methylcholestane (**VII**) and 24-ethylcholestane (**VIII**) (Fig. 3b). The polar fractions from the black shale interval are strongly dominated by an unresolved hump, but also contain abundant intact sterols; mainly cholesterol, 24-methylcholesterol and 24-ethylcholesterol. Since HI/LiAlH$_4$ treatment also defunctionalises alcohols, the 5α and 5β steranes are expected to derive predominantly from cholesterol, 24-methylcholesterol and 24-ethylcholesterol, which are predominately biosynthesized by marine algae [*Volkman*, 1986]. 24-Ethylcholestane (**VIII**) may,

however, also have a terrestrial contribution [*Volkman*, 1986]. Cholesterol and other C_{27} sterols are also indirectly formed by dealkylation of ingested C_{28} and C_{29} sterols [*Goad*, 1981] by zooplankton heterotrophically living on algal biomass. The stable carbon isotopic fractionation resulting from such heterotrophy has been shown to be negligible for steroids [*Grice et al.*, 1998] and hence $\delta^{13}C$ values of cholestane released after HI/LiAlH$_4$ should reflect the average stable carbon isotopic composition of algal sterols. Similarly, 24-methylcholestane ($\delta^{13}C$ = -27 to –29‰) and, to a lesser extent, 24-ethylcholestane (Fig. 5c) record changes in the carbon isotopic composition of algae.
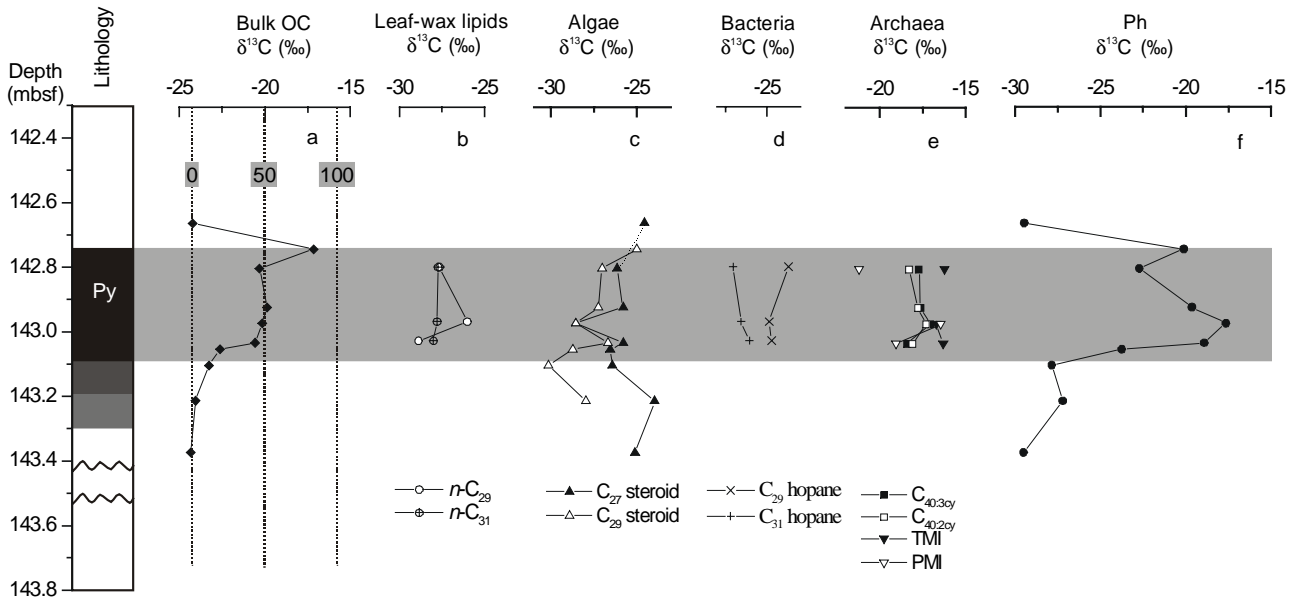
Figure 5. Stratigraphy, bulk and biomarker data of ODP Site 1049C. Carbon isotope values (in ‰ vs. VPDB) of bulk OC (**a**), *n*-alkanes (*n*-C_{27} and C_{31}) mainly derived from leaf-waxes (**b**), oxygen-bound steranes [C_{27} steroid (cholestane) and C_{29} steroid (24-ethyl-cholestane)] mainly derived from marine algae (**c**), hopanoids (i.e. C_{27} and C_{29} hopanoids) mainly derived from bacteria (**d**), bi- ($C_{40:2cy}$) and tricyclic ($C_{40:3cy}$) biphytanes, PMI and TMI derived from archaea (**e**), and oxygen-bound phytane (Ph) derived either from the isotopically 'light' (^{12}C-rich) phytol side-chain (**XVI**) of algal and cyanobacterial chlorophyll or the isotopically 'heavy' (^{13}C-rich) archaeal membrane lipids (**III**) (**f**) of late Aptian/early Albian abyssal sediments from ODP Site 1049C. In all graphs the centre of the bullet corresponds to the top of the ~2 cm thick sediment samples. The OAE1b black shale interval has been indicated as a grey shaded area in the graphs. Dotted lines in graph (**b**) indicate estimated contributions (in %) of archaeal derived insoluble OM to TOC as discussed in text. Lithology as in Fig.2.

The $\delta^{13}C$ values of both C_{27} and C_{29} steranes show significant fluctuations throughout the investigated interval, but there is no clear trend across the black shale interval (Fig. 5c). Since $\delta^{13}C$ values of picked planktonic foraminifers indicate that there is no significant shift in isotopic composition of inorganic carbon [*Erbacher et al.*, 2001], the observed fluctuations for steranes may result from changes in atmospheric CO_2 concentrations and/or algal growth rates/cell sizes [e.g. *Rau et al.*, 1989; *Laws et al.*, 1995; *Pancost et al.*, 1997; *Popp et al.*, 1998; *Burkhardt et al.*, 1999; *Bidigare et al.*, 1999].

7.3.2.4 Hopanes. Considerable amounts of C_{27}-C_{31} hopanes (up to ~30 µg/gTOC for the sum of the stereoisomers of the C_{29}-hopane) were detected in the apolar fractions of samples from the OAE1b black shale interval (Figs. 3a, 4c). Hopanoids were also detected outside the black and dark shale interval, albeit in significantly lower concentrations (below 5 µg/gTOC, Fig. 4c). Sedimentary hopanes are likely diagenetic products of hopanols such as bacteriohopanopolyol derivatives (C_{35}) or diplopterol (hopanes $< C_{30}$) and may derive from numerous bacterial taxa such as cyanobacteria, heterotrophic bacteria and methanotrophic bacteria [*Rohmer et al.*, 1992]. The lower hopane concentrations in the marls could have partly resulted from selective oxic degradation of the hopanol precursors relative to bulk OM. Rates of oxic degradation exceeding those for bulk OM (up to 5 times as fast) have been reported for another triterpenoid [i.e. tetrahymanol, *Sinninghe Damsté et al.*, 1997a; Hoefs et al., in prep]. Part of the observed increase in the black shale could, however, also have resulted from an increase in bacterial production.

Hopanes containing a methyl group at the C2 position are considered reliable biomarkers for cyanobacteria because 2-methylbacteriohopanepolyols occur in a high proportion of cultured cyanobacteria and environments dominated by cyanobacteria [*Summons et al.*, 1999]. No detectable amounts of 2-methyl hopanes were found in the black shale sediments of ODP site 1049C. In fact, only trace amounts of hopanes $>C_{31}$ are present and are restricted to the desulfurised polar fractions. However, a cyanobacterial source for the hopanes from ODP site 1049C cannot be fully excluded because not all cyanobacteria produce 2-methylbacteriohopanepolyols. The strong predominance of the 17β,21β(H)-isomers indicates a low thermal maturity [(ββ/(αβ+βα+ββ)) C_{31} hopane ratio = 0.6] of the organic matter [*Seifert and Moldowan*, 1986] for these sediments.

The stable carbon isotopic composition ($\delta^{13}C$ = –24 to –27‰) of the hopanes (Fig. 5d) extracted from the OAE1b black shales excludes an important contribution of methanotrophic bacteria. $\delta^{13}C$ values for these biomarkers should be significantly more negative if methanotrophs were substantial sources because their lipids are strongly ^{13}C-depleted (up to –120‰) as a result of both the generally strong depletion in ^{13}C of methane and large degree of isotope fractionation associated with the assimilation of methane [*Summons et al.*, 1994; *Pancost et al.*, 2000; *Freeman et al.*, 1990; *Spooner et al.*, 1994].

7.3.2.5 Isorenieratene derivatives. Previous studies have shown that while bottom-waters were well oxygenated before and after OAE 1b, anoxic conditions prevailed at this bathyal sites during the deposition of the black shales [*Erbacher et al.*, 1999]. To investigate whether this anoxia extended into the photic zone, the samples from the black shale interval of hole 1049C were checked for specific pigments (isorenieratene and its derivatives) of the brown coloured strain of green sulfur bacteria (Chlorobiaceae). These photosynthetic bacteria require both light and H₂S for carbon fixation and are, therefore, indicators for photic zone anoxia. At the present day the habitat for green sulfur bacteria is restricted to a few euxinic basins such as the Black Sea [*Repeta et al.*, 1989; *Sinninghe Damsté et al.*, 1993; *van Gemerden and Mas*, 1995]. Sinninghe Damsté and Köster [1998] showed that during the mid Cretaceous C/T OAE these organisms were also present in the proto North Atlantic Ocean. However, no isorenieratene derivatives were found in the black shales

from site 1049C, indicating that, in contrast to the C/T OAE, the specific conditions of overlapping photic and anoxic zone were not present during the lower Albian OAE1b.

7.3.2.6 Isoprenoid glycerol dialkyl glycerol tetraethers. A recently developed technique using HPLC/APCI-MS [*Hopmans et al.*, 2000] revealed abundant intact isoprenoid glycerol dialkyl glycerol tetraethers (GDGTs) in the polar fraction. GDGTs are the main constituents of archaeal membranes [*Koga et al.*, 1993; *De Rosa and Gambacorta*, 1988]. Four different GDGTs (**XI-XIV**) were identified in the extracts from the black shale interval (Fig. 6a).
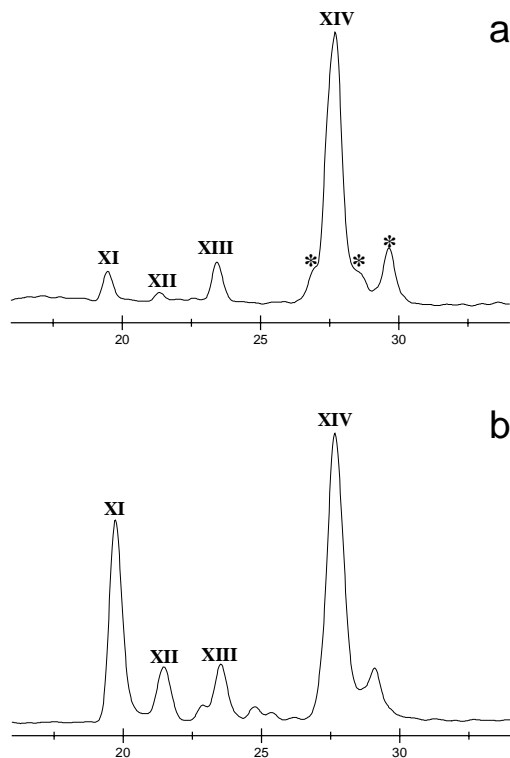
Figure 6. Base peak mass chromatograms of sediment extracts of the OAE1b black shales of ODP Site 1049C **(a)**, and the Arabian Sea (Holocene) [from Sinninghe Damsté et al., in prep.] **(b)**. Asterisks indicate isomers of GDGT **XIV**. Roman numbers refer to structures shown in the Appendix.

These GDGTs have recently also been identified in a wide variety of marine sediment extracts (Schouten et al., 2000) (e.g. Fig. 6b). GDGTs **XI**, **XIII** and **XIV** are the most abundant biomarkers in the extractable OM of the black shale interval, with concentrations of **XIV** of up to 300 µg/gTOC (Fig. 4d). In sharp contrast, both above and below the black shale interval only small amounts of **XI** were detected, while **XII**-**XIV** are absent. The absence of these GDGTs in the marls can not be attributed to preferential loss of the GDGTs under oxic conditions, because GDGTs have a similar oxic degradation rate as other marine biomarkers such as sterols [Sinninghe Damsté et al., in prep]. Therefore, the increase in GDGT concentrations indicates a sharp increase in archaeal production. GDGTs **XII**-**XIII** are characteristic of the archaeal lineage Crenarchaeota containing hyperthermophilic archaea [*De Rosa and Gambacorta*, 1988; *Stetter*, 1998], which thrive at temperatures >60°C. In contrast, **XIV** appears to be highly diagnostic for their non-thermophilic relatives [*Hoefs et al.*, 1997; *DeLong et al.*, 1998], and the dominance of this compound (representing 60% of total GDGTs) indicates an important input of non-thermophilic planktonic

archaea [*Schouten et al.*, 2000; *Hoefs et al.*, 1997]. To the best of our knowledge this is the earliest fossil evidence for marine planktonic archaea, extending their geological record by more than 60 million years [*Hoefs et al.*, 1997].

Treatment of the polar fractions of the extracts of the black shales with $HI/LiAlH_4$ to cleave ether bonds released fractions dominated by acyclic (**a**), monocyclic (**b**), bicyclic (**c**) and tricyclic (**d**) biphytanes (C_{40} isoprenoids) (Fig. 3b). The GDGTs are the source for these biphytanes released upon ether-bond cleavage. In addition, the released biphytanes may partly originate from biphytane diols, which are also present in the polar fraction. Although the biphytane diols have not yet been identified in organisms, their structural similarities with ether-bound biphytanes and their co-occurrence in sediments led Schouten and co-workers [*Schouten et al.*, 1998] to suggest that they are also biosynthesised by planktonic archaea.

The $\delta^{13}C$ values of the archaeal biphytanes **a-d** (Fig. 5e) are significantly enriched in ^{13}C relative to algal steroids **VI-VIII** (Fig. 5c), bacterial derived hopanes **IX-X** (Fig. 5d) and the leaf-wax *n*-alkanes *n*-C_{29} and *n*-C_{31} from higher plants (Fig. 5b). This ^{13}C enrichment indicates a 'heavy' (^{13}C-rich) carbon source (e.g. bicarbonate) for the archaea and/or the utilisation of a pathway of carbon-fixation with a reduced ^{13}C fractionation compared to the Calvin cycle that is used by algae, cyanobacteria and higher plants. The large differences (up to 12 ‰) in $^{13}C/^{12}C$ ratio between the algal steranes and the archaeal biphytanes suggest that the marine planktonic archaea were not living heterotrophically on photoautotrophic biomass, although it has been shown that some extant marine crenarchaeotes can take up amino acids [*Ouverney and Fuhrman*, 2000]. While photoautotrophy within the domain of the Archaea is restricted to only a few species from hypersaline environments, chemoautotrophy is common. Hence it seems likely that the marine archaea present during OAE1b used a chemical energy source for carbon fixation.

Compound-specific radiocarbon analyses of archaeal biphytanes **c** and **d** and algal sterols isolated from marine sediments from the Santa Monica and Santa Barbara Basins deposited before (pre-bomb) and after (post-bomb) the introduction of large quantities of 'nuclear bomb' $^{14}CO_2$ into the atmosphere also indicates a chemoautotroph ecology for marine planktonic archaea [*Pearson*, 2000]. Pearson showed that, in sharp contrast to the sterols, the biphytanes do not show a large increase in ^{14}C content during the transition from the pre-bomb to post-bomb sediments. This indicates that marine planktonic archaea are not living on phytoplanktonic biomass but rather are autotrophs using 'old' ^{14}C depleted dissolved inorganic carbon from below the photic zone [*Pearson*, 2000].

Like the mid-Cretaceous biphytanes, lipids of marine planktonic archaea isolated from recent sediments and suspended particles show a significant ^{13}C enrichment relative to algal steroids [*Hoefs et al.*, 1997], albeit smaller (4-5‰) than for the OAE1b sediments (8-11‰). This enrichment indicates that these non-thermophilic archaea, like related hyperthermophiles, may use a non-Calvin cycle pathway of carbon assimilation such as the 3-hydroxypropionate (3-HP) pathway [*Menendez et al.*, 1999] or the reverse TCA cycle [*Fuchs et al.*, 1992]. The degree of carbon-isotope fractionation during carbon assimilation is much smaller for these pathways than for the Calvin cycle such that prokaryotes using these pathways are expected to be depleted in ^{13}C by only 8-14‰ relative to dissolved CO_2 [*Holo and Sirevåg*, 1986]. Recently, an even smaller ^{13}C-depletion (~3‰) of bulk cell material relative to the inorganic carbon source (bicarbonate) was observed for the

hyperthermophylic crenarchaeon *Metallosphaera sedula*, which uses a 3-HP-like pathway [*van der Meer et al.*, 2001]. The acyclic, mono-, di- and tri-cyclic biphytanes released upon ether bond cleavage from the total lipid fraction of this crenarchaeon were ~2‰ enriched in ^{13}C relative to the bulk cell material. Biphytanes of marine pelagic archaea could be similarly ^{13}C-enriched relative to bulk cell material, if these non-thermophilic archaea also use a 3-HP-like pathway. During the mid-Cretaceous dissolved inorganic carbon (e.g. CO_2) was enriched in ^{13}C by 2-3‰ relative to modern values [*Hayes et al.*, 1999], which could explain the offset between δ^{13}C values for the biphytane **d** in Holocene (-20 to –23‰) [*Hoefs et al.*, 1997] and OAE1b (-17 to –18‰) sediments. Enhanced carbon isotope fractionation by algae during the mid-Cretaceous due to enhanced CO_2 availability [*Arthur et al.*, 1985b] may account for the remainder of the larger (3-7‰) enrichment of biphytane **d** relative to algal steroids. This suggests that mid-Cretaceous marine planktonic archaea occupied a similar niche in the marine environment as their present-day representatives.

Compound-specific radiocarbon analyses of recently deposited lipids derived from marine planktonic archaea indicate that these organisms thrive near the maximum concentration of nitrite, which is the initial product formed upon ammonium oxidation (nitrification), suggesting that these chemoautotrophs are nitrifiers [*Pearson*, 2000]. This is supported by the positive correlation between crenarchaeal rRNA abundance and nitrite observed for marine pelagic sites [*Murray et al.*, 1999]. Ammonium-oxidising planktonic archaea are expected to be strongly depleted in ^{15}N because autotrophic organisms growing at high concentrations of ammonium exhibit large (up to 20‰) isotopic effects during nitrogen fixation [*Pennock et al.*, 1996]. Hence the extreme ^{15}N depletion ($\delta^{15}N_{average}$ = -2.7‰ and $\delta^{15}N_{minimum}$ = -4.9‰) of the OM of the black shale interval of ODP site 1049C (Fig. 2c) is in good agreement with an important input of biomass of nitrifying planktonic marine archaea during OAE1b.

7.3.2.7 Other acyclic and cyclic isoprenoids. The most abundant compound in the apolar fraction isolated from the black shales (Figs. 3a) is the irregular acyclic isoprenoid, TMI (**I**); in contrast this compound is absent in the overlying and underlying units (Fig. 4e). Since there is no reason to assume that TMI or its functionalised derivatives are significantly more labile than other marine biomarkers, it seems unlikely that the absence in the marls resulted from the preferential loss of TMI. Therefore, the increase in TMI points to a sharp increase in abundance of the organism(s) producing this biomarker during black shale deposition. So far, TMI has only been found in the contemporaneous [*Erbacher et al.*, 1999] OAE1b black shales of the Southeast France Basin (SEFB) [*Vink et al.*, 1998]. TMI (**I**) is structurally similar to 2,6,10,15,19-pentamethylicosane (PMI) (**II**), a compound of known archaeal origin [*Brassell et al.*, 1981; *Schouten et al.*, 1998], which is also present in the saturated hydrocarbon fraction, albeit in relatively low amounts. PMI was also released from the polar fraction after Raney-Nickel desulfurisation; the most likely precursors for these sulfur bound (S-bound) compounds are unsaturated archaeal PMIs [*Schouten et al.*, 1998]. Sulfurisation of compounds containing functional groups such as the double bonds present in unsaturated PMI occurs during early diagenesis in sulfide-containing anoxic surface sediments [*Kok et al.*, 2000; *Werne et al.*, 2000].

In some of the apolar fractions from the OAE1b black shales, squalane (**IV**) is present in considerable amounts (Fig. 3a). In addition to TMI (**I**) and squalane (**IV**), other isoprenoids of unknown origin but structurally related to the archaeal lipids are abundant. Amongst them are two isomers (C_{20}) of a tentatively identified cyclic isoprenoid (**V**), which were released from the polar fraction after Raney-Nickel desulfurisation (Fig. 3c). So far, this C_{20} cyclic isoprenoid skeleton has also only been found in the OAE1b black shales from the SEFB [*Vink et al.*, 1998].

The carbon isotopic values of the isoprenoids **I** ($\delta^{13}C$ = -16 to -17‰, Fig. 5e), **IV** ($\delta^{13}C$ = -18 to -23‰) and **V** ($\delta^{13}C$ = -15 to -16‰) is similar to compounds of unambiguous archaeal origin such as **II** ($\delta^{13}C$ = -16 to -21‰, Fig. 5e), and **a-d** ($\delta^{13}C$ = -17 to -20‰, Fig. 5e). The offset of >10‰ between $\delta^{13}C$ profiles for TMI/PMI and the algal biomarkers (Figs. 5c, e) is in agreement with observations for the SEFB [*Vink et al.*, 1998]. The close structural similarity of TMI and PMI and their extreme ^{13}C-enrichment indicates an archaeal origin for TMI [*Vink et al.*, 1998]. For similar reasons an archaeal source is suggested for **IV** and **V** as well.

Pristane and phytane are only minor constituents of the apolar fractions. Phytane (Ph, **XV**) released from the polar fractions upon HI/LiAlH$_4$ treatment (Fig. 3b) derives either from the phytol side-chain (**XVI**) of algal and cyanobacterial chlorophyll or archaeal membrane lipids such as archaeol (**III**). Archaeol, but not phytol, was found in the polar fraction of the black shales, indicating a predominantly archaeal source for the released Ph from the OAE1b sediments. This is also indicated by a similar ^{13}C-enrichment relative to algal steroids for Ph (up to 12‰) and archaeal derived compounds such as PMI and biphytanes **a-d** (Figs.5c, e, f). Before and after the black shale interval $\delta^{13}C$ values for Ph are similar to those of the steranes, consistent with an algal origin for Ph. Hence it seems likely that the ~12‰ positive shift in $\delta^{13}C$ values for Ph (Fig. 5f) resulted from an increase in the contribution of isotopically 'heavy' (^{13}C-rich) archaeal derived Ph relative to the isotopically 'light' (^{12}C-rich) algal or cyanobacterial Ph. The fact that there is no coinciding positive shift in $\delta^{13}C$ values for the algal steranes (Fig. 5c) supports this.

The Ph that dominates the apolar fractions obtained after desulfurisation of the polar fractions of the black shale interval (Fig. 3c) shows a similar ^{13}C-enrichment also indicating an archaeal source.

7.3.3 Insoluble OM

7.3.3.1 Causes for the positive shift in $\delta^{13}C$ values for bulk OC. The positive shift in stable carbon isotope values for bulk OC (Fig. 5a) could have resulted from a decrease in atmospheric CO_2 concentrations as ε_p values for marine phytoplankton show a pronounced dependence on CO_2 concentration [*Rau et al.*, 1989]. In addition, ε_p for marine phytoplankon shows a strong negative correlation with both growth rate and cell size [*Laws et al.*, 1995; *Pancost et al.*, 1997; *Popp et al.*, 1998; *Burkhardt et al.*, 1999; *Bidigare et al.*, 1999] and hence increases in growth rate and/or cell size could also have caused the observed positive shift for bulk OM. However, there is no coinciding positive shift for biomarkers that record changes in the carbon isotopic composition of algae such as cholestane and to a lesser extent 24-ethyl-cholestane (Fig. 5c).

Alternatively and in our view more likely, the shift in $\delta^{13}C$ values for bulk OC could result from a change in the composition of the OM. Similarly as for Ph released from the polar fraction upon

HI/LiAlH$_4$ treatment, an increase in the relative contribution of ^{13}C enriched archaeal biomass to the OM deposited during OAE1b could also explain the shift in δ^{13}C values for bulk OC (Fig. 5a).

7.3.3.2 Nature of the OM from OAE1b. The atomic C$_{org}$/N$_{total}$ ratios show a close correlation (R^2 = 0.97) with the δ^{13}C values for bulk OC. Before and after the OAE1b interval C$_{org}$/N$_{total}$ ratios are between 3 and 16, while the black shale sediments show significantly higher values of 26 to 69 with the maximum value for the uppermost black shale sample (fig. 2d). C/N ratios are commonly used to differentiate between terrestrial and marine OM [e.g. *Prahl et al.*, 1980; *Meyers*, 1994]. The atomic C$_{org}$/N$_{total}$ ratios (Fig. 2d) in the OAE1b interval are significantly higher than C/N Redfield ratios for modern marine plankton (6.6). Since, inorganic nitrogen, in addition to organic-bound nitrogen, contributes to the N$_{total}$, the real C/N ratios for the sedimentary OM (C$_{org}$/N$_{org}$) should be even higher. The values are closer to the ratios observed for modern terrestrial [>20, *Meyers*, 1994] than to modern marine organic matter. C/N ratios exceeding Redfield ratios are common for sedimentary OM (C$_{org}$/N$_{org}$) and have been attributed to the preferential remineralisation of the more labile nitrogen-rich organic compounds such as proteins, during passage through the water column, and during the early stages of OM burial [*Aller*, 1994]. Alternatively the enhanced contribution of nitrogen-poor, ^{13}C-enriched archaeal-derived OM could explain the observed increase in both C$_{org}$/N$_{total}$ and δ^{13}C values for bulk OC during the OAE1b.

While woody debris sporadically occur in the Cretaceous sediments near the black shales, high Rock Eval hydrogen indices (HI) and the extremely low abundance or even absence of vascular plant remains indicate a predominantly marine origin for the OC within the OAE interval [*Shipboard Scientific Party*, 1998]. This is supported by the low abundance of molecular fossils of unambiguous terrestrial origin (e.g. leaf-wax lipids and oleananes) in the extractable OM (Fig. 3a-c).

Products, released upon thermal degradation (flash pyrolysis) can reveal important insights into the sources of insoluble OM [e.g. *Blokker et al.*, 2000]. Pyrolysis of the decalcified black shale sediments predominatly released *n*-alkenes/*n*-alkanes, alkylbenzenes and C$_7$-C$_{15}$ isoprenoidal alkenes/alkanes. The extremely low abundance of lignin thermal degradation (pyrolysis) products generated from the kerogen (Fig. 7a) supports a marine origin for the OM. Remarkably, the C$_8$-C$_{15}$ isoprenoidal alkenes/alkanes are by far the most abundant compounds released (Fig. 7a). These isoprenoidal compounds are also abundant in the flash pyrolysates of the OAE1b sediments of the SEFB [*Höld et al.*, 1998; *Vink et al.*, 1998]. In sharp contrast pyrolysates from the C/T OAE [Kuypers et al., unpublished results] and from ancient marine kerogens in general [e.g. *Sinninghe Damsté et al.*, 1989; *Eglinton et al.*, 1990; *Larter and Horsfield*, 1993; *Hartgers et al.*, 1994a] are dominated by *n*-alkanes/*n*-alkenes, alkylbenzenes and/or alkylthiophenes, while isoprenoidal compounds are only present in relatively low amounts.

Thin laminae of amorphous OM (as revealed by SEM, Fig. 8) that occur throughout the black shale interval make up a significant part of the OM of the OAE1b sediments. The macromolecular OM of the laminae was isolated from the sediments by density centrifugation using pure DCM (floating fraction). This OM can neither be hydrolysed by strong acid nor base and also shows the strong enrichment in ^{13}C (δ^{13}C$_{TOC}$= -15.5‰) typical for the archaeal lipids. Flash pyrolysis of this amorphous OM releases almost exclusively C$_8$-C$_{15}$ isoprenoidal alkenes/alkanes

(Fig. 7b). Small amounts of TMI (**I**) and mono-unsaturated PMI (**II:1**) were also detected in the pyrolysate (Fig. 7b). Absorption bands at 2929, 1458 and 1378 cm^{-1} in the Fourier transform infrared spectrum of the isolated OM are consistent with the aliphatic isoprenoid nature of the macromolecular material.
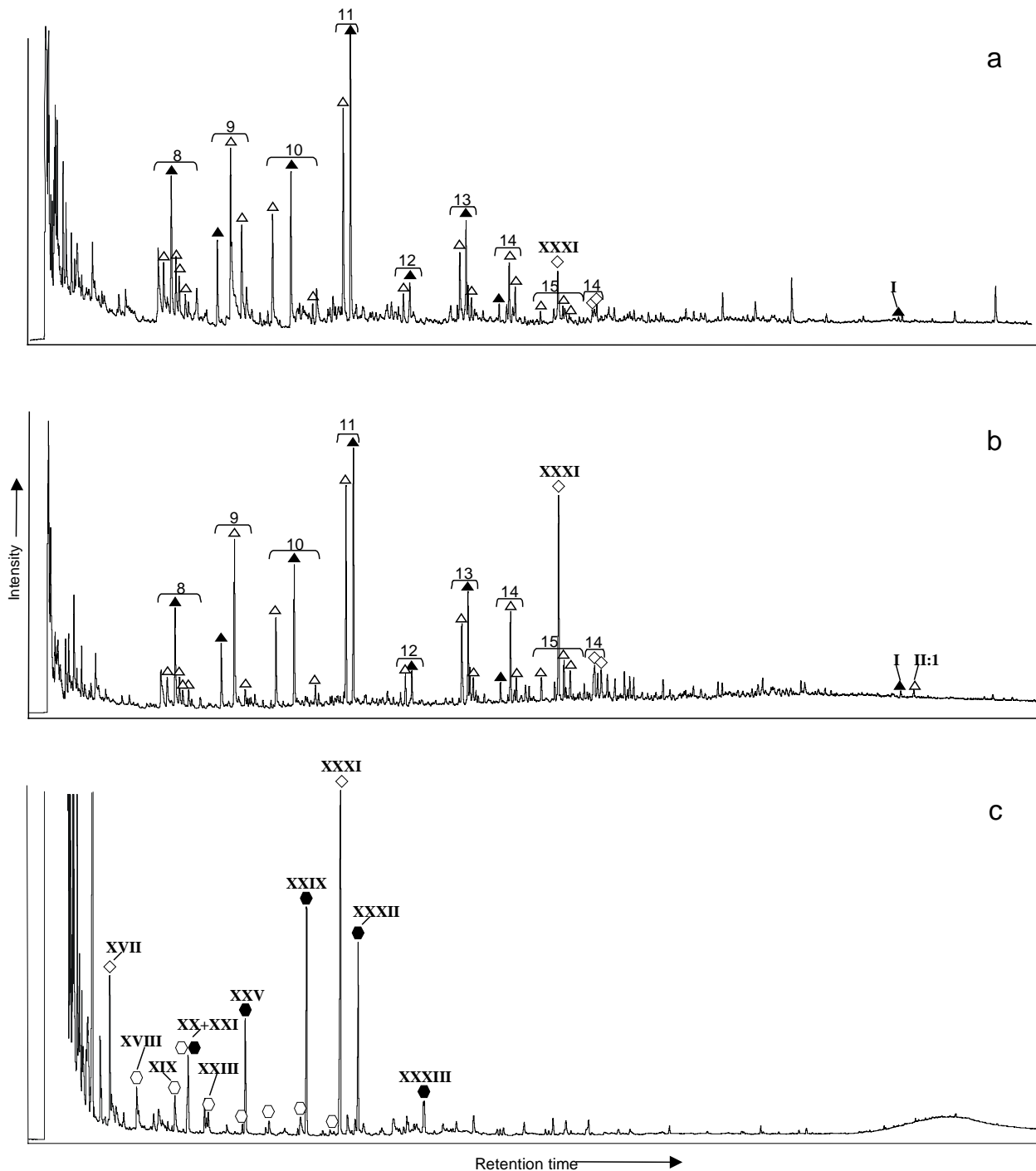

Figure 7. Gas chromatograms of the flash pyrolysates (Curie temperature of 610 °C) of decalcified and extracted sediment **(a)**, and macromolecular material isolated by density centrifugation **(b)**, and gas chromatogram of hydrocarbon fraction released after RuO$_4$ treatment of the isolated macromolecular material **(c)** from the OAE1b black shales of ODP Site 1049C. Filled triangles, open triangles, open diamonds, filled hexagons and open hexagons indicate

acyclic saturated isoprenoids, mono-unsaturated isoprenoids, isoprenoid ketones, branched mono-acids and branched and straight chain diacids, respectively. Brackets with arabic numbers indicate isoprenoid isomers with the same number of carbon atoms (i.e. C_8 to C_{15}). Roman numbers refer to structures shown in the Appendix.
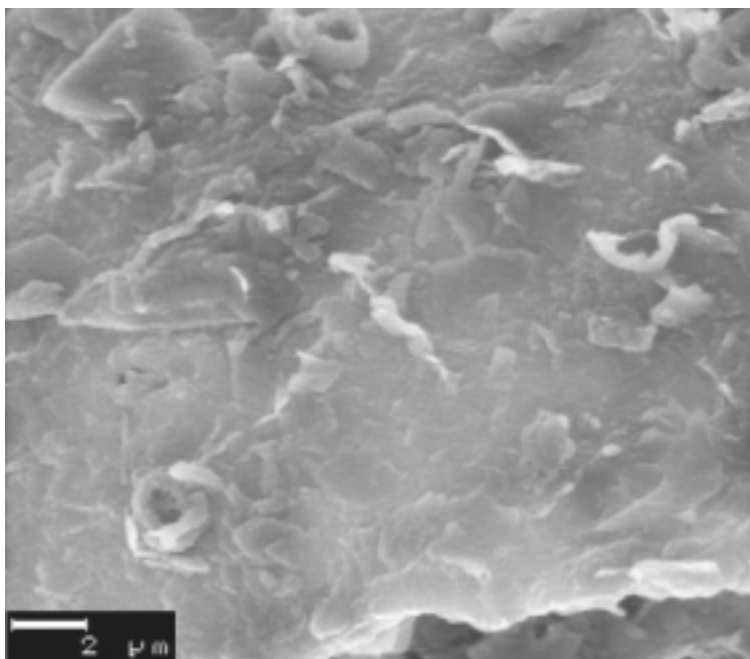
Figure 8. SEM of laminae of amorphous, macromolecular organic matter from the OAE1b black shales of ODP Site 1049C.

Chemical degradation (i.e. RuO_4 oxidation) has been a useful method in the analyses of aliphatic biomacromolecules because it releases characteristic, GC-amenable fragments from the macromolecules [*Blokker et al.*, 1998; *Schouten et al.*, 1998]. Fragments containing either carbonyl or carboxyl functionalities or both are released from the macromolecules upon RuO_4 oxidation depending upon the original functional group and its position (Fig. 9).
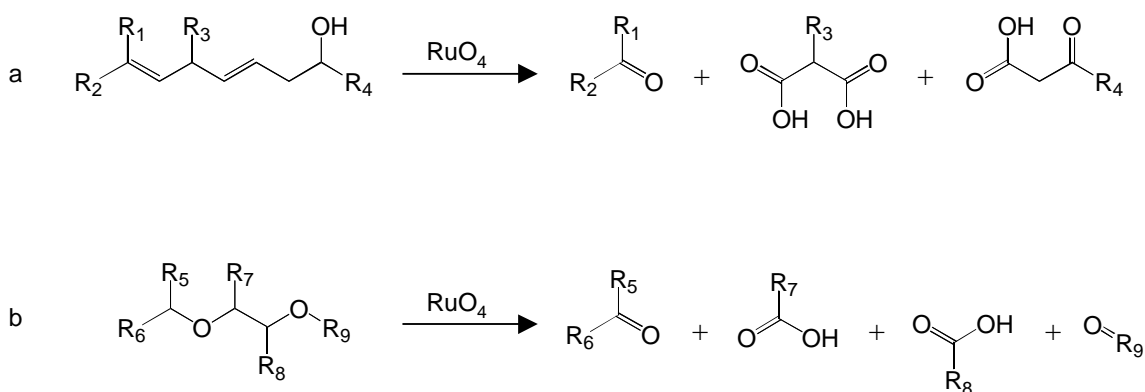
Figure 9. Schematic representation of the main reactions involved in the RuO_4 oxidative degradation of double bonds and alcohols **(a)**, and single and vicinal ether-linkages **(b)**.

RuO_4 oxidation of double bonds and vicinal ether-linkages give similar products; straight-chain compounds yield fragments containing one or more carboxyl groups while some branched compounds yield fragments containing carbonyl groups. Oxidation of alcohols or single ether-bonds

on the other hand releases exclusively compounds containing carbonyl groups [see also *Blokker et al.*, 1999] for a more thorough discussion]. RuO_4 oxidation of the amorphous OM isolated by density centrifugation from the black shales releases almost exclusively compounds with acyclic isoprenoidal carbon skeletons. More specifically, the RuO_4 degradation products (Fig. 7c) are dominated by C_8-C_{14} isoprenoidal mono-acids/ketones and C_4-C_8 straight chain/branched dicarboxylic cids (**XVII-XXXIII**). The $\delta^{13}C$ values of the C_8-C_{14} isoprenoidal mono-acids/ketones are between –12 and –17‰, with a weighted average of -14‰. This weighted average is in good agreement with the bulk isotopic composition of the OC from the laminae, indicating that these degradation products represent the main building blocks of this polymeric OM. RuO_4 oxidation of the amorphous OM of the OAE1b black shales from the SEFB also released mainly compounds with acyclic isoprenoidal carbon skeletons, albeit almost exclusively smaller than C_{10}. Since the isolated organic material of ODP site 1049C is macromolecular, the mono- and dicarboxylic acids and the ketones released upon RuO_4 oxidation can not only derive from hydroxyl-groups and double bonds. Ether-bonds, either vicinal or single, are required to build a macromolecule. The abundance of dicarboxylic acids with both branched and straight-chain carbon skeletons (**XVIII**, **XIX**, **XXI**-**XXIV**, **XXVI**-**XXVIII**, **XXX**) indicates that some of the building blocks contained at least two functional groups; either vicinal ether-linkages or double bonds. In fact the distribution of chemical degradation products is entirely consistent with a polymer consisting of monomers with essentially two different carbon skeletons: TMI (**I**) and PMI (**II**) linked together by vicinal ether-bonds (Fig. 10). The occurrence of compounds containing the TMI and PMI carbon-skeleton in the pyrolysate (i.e **I** and **II:1**, Fig. 7b) of the macromolecular material and their abundance in the extractable OM supports this hypothesis. The lower abundance of dicarboxylic acids relative to monocarboxylic acids in the RuO_4 degradation product mixture could result from either losses of the more water-soluble dicarboxylic acids during the work-up procedure or an incomplete oxidation of the macromolecular material as it is easier to oxidise one than two vicinal bonds. Although no residue was recovered, it can not be excluded that soluble, but non-GC amenable, oligomers were released. This would partly explain the relatively low (~1%) yield of the RuO_4 oxidation as determined by GC. Significant amounts of material may also have been lost by evaporation of volatile short chain products, as highly water-soluble dicarboxylic acids, or as carbon dioxide. In addition, short-chain products formed upon RuO_4 oxidation could remain undetected because they coelute with the solvent peak.

There are no known modern analogues for this TMI/PMI based aliphatic isoprenoidal macromolecular material. In principal this material could either be a biopolymer formed by the archaea themselves, such as a structural component of their cell wall, or a geopolymer formed upon diagenesis after the archaea died. Although aliphatic biopolymers have been identified in cell walls of various organisms such as specific freshwater [e.g. *Blokker et al.*, 1998] and marine [e.g. Gelin et al.,1996], they have never been found in archaea. The absence of a clear cellular structure and the smooth, homogeneous appearance of the thin laminea of macromolecular material are suggestive of a geopolymer rather than a biopolymer. This archaeal-polymer could have formed in a similar way as has been suggested for natural fossil casts of dinoflagellates formed upon polymerisation of unsaturated fatty-acids during early diagenesis [Blokker et al., in prep.]. However, ultralaminae such as those reported in Largeau et al., [1989] and suggestive of cell walls, may have escaped

detection by SEM; thus, based on the available data it is not possible to exclude that the macromolecular OM is actually a biopolymer. On the other hand it is likely that the macromolecular material formed upon cross-linking of PMI and TMI derivatives containing some functional groups such as double bonds. That such functionalities were present in these molecules is indicated by the fact that both a ketone of TMI and sulfur-bound PMI are present in the polar fraction. In any case our data indicate that archaeal macromolecular material is a quantitatively important component of the sedimentary OM of the black shale interval.
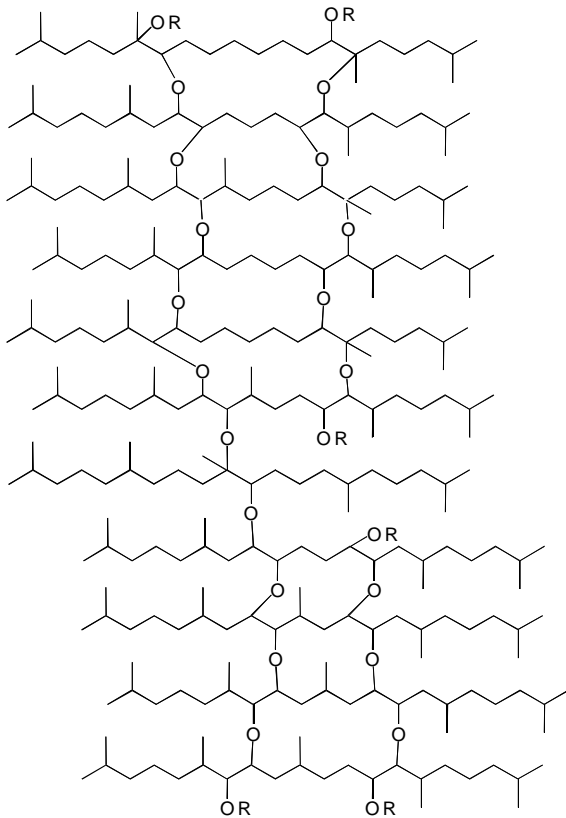
Figure 10. Generalised and simplified reconstruction of the proposed TMI/PMI based macromolecular material isolated from the OAE1b black shales of ODP Site 1049C by density centrifugation (floating fraction).

7.3.3.3 Archaeal contribution to the OM. The relative contribution of the archaeal polymer to the OC can be estimated from $\delta^{13}C_{org}$ using a two end-member mixing model and assuming that the $\delta^{13}C$ value (~ -24‰) for bulk sedimentary OC before the OAE1b represents the non-archaeal endmember and $\delta^{13}C$ = -15.5‰ the archaeal endmember. Based on this, there is on average a very large (~50 wt%) contribution of archaeal OC that even dominates (~80 wt%) in some sections of the black shale interval (Fig. 5a). A significant contribution (up to 40 wt%) of archaeal OC is also estimated from the $\delta^{13}C_{org}$ values of the black shales of the SEFB using the stable carbon isotopic values of *n*-alkanes and isoprenoids obtained after off-line pyrolysis of the bulk OM [*Höld et al.*, 1998] as algal and archaeal endmembers, respectively (Table 1).

The maximum relative contribution of archaeal OC of ~80 wt% for the uppermost part of the black shales of ODP Site 1049C could indicate that environmental conditions were especially favourable for marine pelagic archaea during the latter part of the OAE1b. But this could also be explained by renewed oxygenation of the bottom waters and sediments after OAE1b resulting in the

preferential oxidative removal of labile algal OM relative to the more refractory archaeal polymer from the uppermost part of the black shale interval. Both the observed extreme C_{org}/N_{total} ratios and $\delta^{13}C$ values for bulk OM of the uppermost OAE1b black shale sample could have resulted from such a selective oxidation of OM (Fig.2).

Sample	Thickness (m)	TOC (%)	$\delta^{13}C_{org}$ (‰)	Archaeal OC (%)
3714	0.9	1.7	-24.8	32
3717	1	2.6	-25.0	30
3722	1.25	2.8	-24.6	34
3724	1.37	2.1	-25.2	29
3726	1.42	2.7	-23.9	41

Table 1. Estimated relative archaeal OC contribution to the OAE1b black shales of the Ravel section of the SEFB. TOC content and $\delta^{13}C$ values for bulk OC of these black shales are also indicated. The relative contribution of archaeal OC was estimated from $\delta^{13}C_{org}$ using the $\delta^{13}C$ values of the *n*-alkane ($\delta^{13}C \sim -28‰$) and isoprenoidal ($\delta^{13}C \sim -18‰$) fractions obtained after off line pyrolysis of the bulk OM [*Höld et al.*, 1998] as non-archaeal (e.g. algal) and archaeal endmembers, respectively.

Although prokaryotes can constitute > 70 wt% of carbon biomass in the upper ocean [*Fuhrman et al.*, 1989] and their biomarkers are abundantly present in the sediment [*Ourisson and Albrecht*, 1992], evidence for a substantial (>10 %) prokaryotic contribution to Phanerozoic sedimentary OC is generally lacking [*Hartgers et al.*, 1994b; *Sinninghe Damsté et al.*, 1997b]. Therefore, the abundance of OM derived from archaea at ODP Site 1049C and the SEFB during OAE1b is unexpected.

7.3.4 Sedimentary OM of the early Albian OAE1b and the C/T OAE black shales: a comparison at the molecular level.

The extractable OM of the OAE1b black shales is clearly dominated by archaeal lipids. In sharp contrast, the extractable OM of the C/T OAE black shales is dominated by molecular fossils (e.g. S-bound 2-methylhopanoids) of cyanobacterial membrane lipids and algal biomarkers such as steroids [*Kuypers et al.*, 1999; Kuypers et al., 2000 submitted to Paleoceanography; Kuypers et al., in prep.]. Although archaeal lipids have also been found in the C/T OAE black shales, their contribution to the extractable OM is generally small [Kuypers et al., unpublished data]. While GDGTs **XI**-**XIV** and PMI have been identified, neither TMI nor the tentatively identified cyclic isoprenoid **V** were found in the C/T black shales. In fact, none of these latter components have so far been reported outside the OAE1b black shale interval.

Archaea-derived C_8-C_{15} isoprenoidal alkenes/alkanes are by far the most abundant compounds released upon pyrolysis from the OAE1b black shales. The stable carbon isotopic composition of the bulk OC indicates that black shales from OAE1b contain up to 80% of OC derived from archaea. In contrast, isoprenoidal compounds in general are only present in relatively

low amounts in the C/T OAE black shales with the C_{18} (e.g. pristane, pristene) homologues being most abundant. The C_8-C_{15} isoprenoidal alkenes/alkanes that characterise the OAE1b interval are extremely rare or absent from the C/T OAE black shales [Kuypers et al., unpublished data]. Instead, *n*-alkanes/*n*-alkenes, alkylbenzenes and/or alkylthiophenes [Kuypers et al., unpublished data], generally dominate the pyrolysates from the C/T OAE. This indicates a non-archaeal, probably phytoplanktonic, source for the OM of the C/T black shales. A predominantly phytoplanktonic origin for the sedimentary OM of the C/T black shales is also suggested by the significant co-variation between the carbon isotopic composition of typical algal (e.g. steroids) and cyanobacterial (e.g. extended hopanoids) biomarkers and bulk OM [Kuypers et al., in prep].

The comparison on the molecular level indicates that not only the sources of the sedimentary OM of the OAE1b and C/T OAE black shales are different, but also that the redox conditions of the water column may have been different during deposition. Molecular fossils (e.g. isorenieratane) of a pigment indicative of anoxygenic photosynthetic bacteria recovered from abyssal and shelf sites indicate that anoxic conditions extended into the photic zone of the southern proto-North Atlantic during the C/T OAE [*Sinninghe Damsté et al.*, 1998]. Isorenieratane was recently also recovered from C/T black shales deposited in the northern proto-North Atlantic, albeit in significantly smaller amounts [Kuypers et al., unpublished data]. In contrast, there were no isorenieratene derivatives found in the OAE1b black shales from the SEFB and ODP Site 1049C, indicating that the specific conditions needed by these bacteria, with overlapping photic and anoxic zone, were not present in the northern-proto North Atlantic/western Tethys during the lower Albian OAE1b.

Although various analysis (e.g. Rock Eval, pyrolysis) indicate that there is only a minor contribution of terrestrial biomass to the insoluble sedimentary OM of both black shales, leaf-wax *n*-alkanes were identified in the saturated hydrocarbon fraction of the OAE1b and the C/T OAE black shales [*Kuypers et al.*, 1999]. In sharp contrast to the C/T OAE [*Kuypers et al.*, 1999] the stable carbon isotopic composition of these leaf-wax lipids does not provide evidence of abundant C_4-type vegetation during OAE1b. This could indicate that atmospheric CO_2 concentrations during the early Albian OAE were significantly higher than during the C/T OAE. Alternatively, abundant C_4-type vegetation did occur during OAE1b but was restricted to the equatorial region (e.g. northern Africa). Compound specific biomarker analyses from early Albian equatorial sites are required to clarify this issue.

7.4 Conclusions

1). Archaea-derived isoprenoidal tetraether membrane lipids and free and macromolecularly bound isoprenoid alkanes are abundant in the investigated OAE1b black shales.
2). Up to ~40% of the organic matter of the SEFB and up to ~80% of the organic matter of ODP site 1049C preserved in the black shales is derived from archaea.
3). The abundance of a GDGT containing a bicyclic and a tricyclic biphytane indicates an important contribution of representatives of the marine planktonic archaea (crenarchaeota).
4). To the best of our knowledge this GDGT provides the earliest fossil evidence for marine planktonic archaea, extending their geological record by more than 60 million years.

5).   The large difference (up to 12 ‰) in $^{13}C/^{12}C$ ratio between the algal biomarkers and the much more abundant pelagic archaea-derived biomarkers indicate that the latter were living chemoautotrophically, possibly using ammonium as an energy source.

6).   There seems to be no unifying mechanism for black shale deposition during the mid-Cretaceous OAEs. Although there are apparent similarities (distinct lamination, low abundance or absence of benthic foraminifers, ^{13}C-enrichment of OC) between the black shales of OAE1b and other OAEs, our detailed molecular work shows that the origin of the OM (prokaryotic versus eukaryotic), redox conditions of the photic zone of the ocean and causes for ^{13}C-enrichment of OC are completely different.

7.5 References

Aller, R., Bioturbation and remineralization of sedimentary organic matter: effects of redox oscillation, *Chemical Geology*, 114, 331-345, 1994.

Arthur, M. A., W. A. Dean, and L. M. Pratt, Geochemical and climatic effects of increased marine organic carbon burial at the Cenomanian/Turonian boundary, *Nature*, 335, 714-717, 1988.

Arthur, M. A., W. E. Dean, and G. E. Claypool, Anomalous ^{13}C enrichment in modern marine organic carbon, *Nature*, 315, 216-218, 1985b.

Arthur, M. A., W. E. Dean, and S. O. Schlanger, Variations in the global carbon cycle during the Cretaceous related to climate, volcanism, and changes in atmospheric CO_2, *American Geophysical Union Monograph*, 32, 504-529, 1985a.

Arthur, M. A., S. O. Schlanger , and H. C. Jenkyns, The Cenomanian-Turonian Oceanic anoxic event,II. Palaeoceanographic controls on organic-matter production and preservation, *Geological Society Special Publication*, 26, 401-420, 1987.

Barron, E. J., A warm, equable Cretaceous: the nature of the problem, *Earth-Science Reviews*, 19, 305-338, 1983.

Berner, R. A., Palaeo-CO_2 and climate, *Nature*, 358, 114-114, 1992.

Bidigare, R. R., K. L. Hanson, K. O. Buesseler, S. G. Wakeham, K. F. Freeman, R. D. Pancost, F. J. Millero, P. A. Steinberg, B. N. Popp, M. Latasa, M. R. Landry, and E. A. Laws, Iron-stimulated changes in ^{13}C fractionation and export by equatorial Pacific phytoplankton: Toward a paleogrowth rate proxy, *Paleoceanography*, 14, 589-595, 1999.

Blokker, P., S. Schouten, J. W. De Leeuw, J. S. Sinninghe Damsté, and H. Van den Ende, Molecular structure of the resistant bioploymer in zygospore cell walls of *Chlamydomonas monoica*, *Planta*, 207, 539-543, 1999.

Blokker, P., S. Schouten, J. W. De Leeuw, J. S. Sinninghe Damsté, and H. Van den Ende, A comparative study of fossil- and extant algaenans using ruthenium tetroxide degradation, *Geochim.Cosmochim.Acta*, 64, 2055-2065, 2000.

Blokker, P., S. Schouten, H. Van den Ende, J. W. De Leeuw, P. G. Hatcher, and J. S. Sinninghe Damsté, Chemical structure of algaenans from the fresh water algae T*etraedron minimum*, *Scenedesmus communis* and *Pediastrum boryanum*, *Org.Geochem.* , 29, 1453-1468, 1998.

Brassell, S. C., A. M. K. Wardroper, I. D. Thomson, J. R. Maxwell , and G. Eglinton, Specific acyclic isoprenoids as biological markers of methanogenic bacteria in marine sediments, *Nature*, 290, 693-696, 1981.
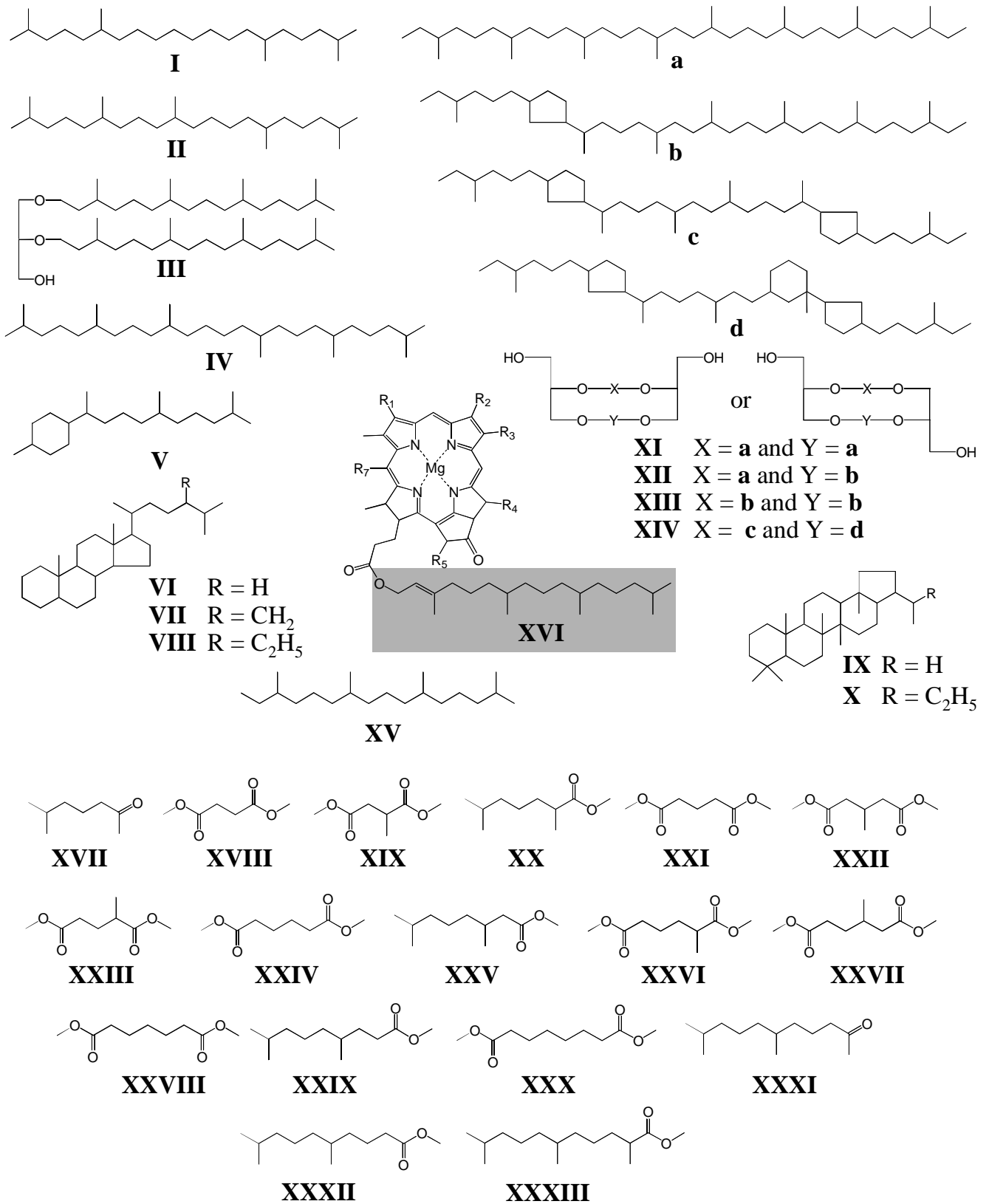
Burkhardt, S., U. Riebesell, and I. Zondervan, Effects of growth rate, CO_2 concentration, and cell size on the stable carbon isotope fractionation in marine phytoplankton, *Geochim.Cosmochim.Acta*, 63, 3729-3741, 1999.

Cerling, T. C., J. M. Harris, B. J. MacFadden, M. G. Leakey, J. Quade, V. Eisenmann, and J. R. Ehleringer, Global vegetation change through the Miocene/Pliocene boundary, *Nature*, 389, 153-158, 1997.

Collister, J. W., G. Rieley, B. Stern, G. Eglinton, and B. Fry, Compound-specific $\delta^{13}C$ analyses of leaf lipids from plants with differing carbon dioxide metabolisms, *Org.Geochem.*, 21, 619-627, 1994.

De Rosa, M. and A. Gambacorta, The lipids of Archaebacteria, *Prog.Lipid Res.*, 27, 153-175, 1988.

DeLong, E. F., L. L. King, R. Massana, H. Cittone, A. Murray, C. Schleper, and S. G. Wakeham, Dibiphytanyl ether lipids in nonthermophilic Crenarchaeotes, *Appl.Environ.Microbiol.*, 64, 1133-1138, 1998.

Eglinton, G. and R. J. Hamilton, Leaf epicuticular waxes, *Science*, 156, 1322-1335, 1967.

Eglinton, T. I., J. S. Sinninghe Damsté, M. E. L. Kohnen, and J. W. De Leeuw, Rapid estimation of the organic sulphur content of kerogens, coals and asphaltenes by pyrolysis-gas chromatography, *Fuel*, 69, 1394-1404, 1990.

Erbacher, J., C. Hemleben, B. T. Huber, and M. Markey, Correlating environmental changes during early Albian oceanic anoxic event 1B using benthic foraminiferal paleoecology, *Mar.Micropal.*, 38, 7-28, 1999.

Erbacher, J., B. T. Huber, R. D. Norris, and M. Markey, Increased thermohaline stratification as a possible cause for a Cretaceous oceanic anoxic event, *Nature*, 409, 325-327, 2001.

Erbacher, J. and J. Thurow, Influence of oceanic anoxic events on the evolution of mid-Cretaceous radiolaria in the North Atlantic and western Tethys, *Mar.Micropal.*, 30, 139-158, 1997.

Farrington, J. W. and B. W. Tripp, Hydrocarbons in western North Atlantic surface sediments, *Geochim.Cosmochim.Acta*, 41, 1627-1641, 1977.

Freeman, K. H., J. M. Hayes, J. M. Trendel, and P. Albrecht, Evidence from carbon isotope measurements for diverse origins of sedimentary hydrocarbons, *Nature*, 343, 254-256, 1990.

Fry, B., W. Brand, F. J. Mensch, K. Tholke, and R. Garritt, Automated analysis system for coupled $\delta^{13}C$ and $d^{15}N$ measurements, *Anal.Chem.*, 64, 288-291, 1992.

Fuchs, G., A. Ecker, and G. Strauss, Bioenergetics and autotrophic carbon metabolism of chemolithotrophic archaebacteria, in *The Archaebacteria: Biochemistry and Biotechnology*, edited by M. J. Danson, D. W. Hough, and G. G. Lunt, p. 23+36-23+37, Portland Press, London, 1992.

Fuhrman, J. A., T. D. Sleeter, C. A. Carlson, and L. M. Proctor, Dominance of bacterial biomass in the Sargasso Sea and its ecological implications, *Marine Ecology Progress Series*, 57, 207-217, 1989.

Gagosian, R. B., E. T. Peltzer, and O. C. Zafiriou, Atmospheric transport of continentally derived lipids to the tropical North Pacific, *Nature*, 291, 312-314, 1981.

Gelin, F., I. Boogers, A. A .M. Noordeloos, J. S. Sinninghe Damsté, P.G. Hatcher and J. W. De Leeuw, Novel, resistant microalgal polyethers: an important sink of organic carbon in the marine environment?, *Geochim.Cosmochim.Acta*, 60, 1275-1280, 1996.

Goad, L. J., Sterol biosynthesis and metabolism in marine invertebrates, *Pure Appl.Chem.*, 51, 837-852, 1981.

Grice, K., W. M. Klein Breteler, S. Schouten, V. Grossi, J. W. De Leeuw, and J. S. Sinninghe Damste, Effects of zooplankton herbivory on biomarker proxy records, *Palaeoceanography*, 13, 686-693, 1998.

Hartgers, W. A., J. S. Sinninghe Damsté, and J. W. De Leeuw, Geochemical significance of alkylbenzene distribution in flash pyrolysates of kerogens, coals, and asphaltenes, *Geochim.Cosmochim.Acta*, 58, 1759-1775, 1994a.

Hartgers, W. A., J. S. Sinninghe Damsté, A. G. Requejo, J. Allan, J. M. Hayes, and J. W. De Leeuw, Evidence for only minor contributions from bacteria to sedimentary organic carbon, *Nature*, 369, 224-227, 1994b.

Hayes, J. M., K. F. Freeman, B. N. Popp, and C. H. Hoham, Compound-specific isotopic analyses: A novel tool for reconstruction of ancient biogeochemical processes, *Org.Geochem.*, 16, 1115-1128, 1990.

Hayes, J. M., H. Strauss, and A. J. Kaufman, The abundance of ^{13}C in marine organic matter and isotopic fractionation in the global biogeochemical cycle of carbon during the past 800 Ma, *Chemical Geology (Isotope Geoscience Section)*, 161, 103-125, 1999.

Hoefs, M. J. L., S. Schouten, J. W. De Leeuw, L. L. King, S. G. Wakeham, and J. S. Sinninghe Damsté, Ether lipids of planktonic Archaea in the marine water column, *Appl.Environ.Microbiol.*, 63, 3090-3095, 1997.

Holo, H. and R. Sirevåg, Autotrophic growth and CO_2 fixation of *Chloroflexus aurantiacus*, *Arch.Microbiol.*, 145, 173-180, 1986.

Hopmans, E. C., S. Schouten, R. D. Pancost, M. T. J. Van der Meer, and J. S. Sinninghe Damsté, Analysis of intact tetraether lipids in archaeal cell material and sediments by high performance liquid chromatography/atmospheric pressure chemical ionization mass spectrometry, *Rapid.Commun.Mass Spectrom.*, 14, 1-5, 2000.

Höld, I. M., S. Schouten, H. M. E. Kaam-Peters, and J. S. Sinninghe Damsté, Recognition of *n*-alkyl and isoprenoid algaenans in marine sediments by stable carbon isotopic analysis of pyrolysis products of kerogens, *Org.Geochem.*, 28, 179-194, 1998.

Koga, Y., M. Nishihara, H. Morii, and M. Akagawa-Matsushita, Ether lipids of methanogenic bacteria: structures, comparative aspects, and biosyntheses, *Microbiol.Rev.*, 57, 164-182, 1993.

Kohnen, M. E. L., J. S. Sinninghe Damsté, W. I. C. Rijpstra, and J. W. Leeuw, Alkylthiophenes as sensitive indicators of palaeoenvironmental changes: A study of a Cretaceous oil shale from Jordan, *ACS Symposium Series*, 429, 444-485, 1990.

Kok, M. D., W. I. C. Rijpstra, L. Robertson, J. K. Volkman, and J. S. Sinninghe Damsté, Early steroid sulfurisation in surface sediments of a permanently stratified lake (Ace Lake, Antarctica), *Geochim.Cosmochim.Acta*, 64, 1425-1436, 2000.

Kuypers, M. M. M., R. D. Pancost, and J. S. Sinninghe Damsté, A large and abrupt fall in atmospheric CO_2 concentration during Cretaceous times, *Nature*, 399, 342-345, 1999.

Largeau, C., S. Derenne, E. Casadevall, C. Berkaloff, M. Corolleur, B. Lugardon, D. Raynaud, and J. Connan, Occurrence and origin of "ultralaminar" structures in "amorphous" kerogens of various source rocks and oil shales, *Org.Geochem.*, 16, 889-895, 1989.

Larson, R. L., Geological consequences of superplumes, *Geology*, 963-966, 1991.

Larter, S. R. and B. Horsfield, Determination of structural components of kerogens by the use of analytical pyrolysis methods, in *Organic geochemistry; principles and applications*, edited by M. H. Engel and S. A. Macko, pp. 271-287, Plenum Press, New York, 1993.

Laws, E. A., B. N. Popp, R. R. Bidigare, M. C. Kennicutt, and S. A. Macko, Dependence of phytoplankton carbon isotopic composition on growth rate and $(CO_{2)aq}$: Theoretical considerations and experimental results, *Geochim.Cosmochim.Acta*, 59, 1131-1138, 1995.

Lockheart, M. J., P. F. Bergen, and R. P. Evershed, Variations in the stable carbon isotope compositions of individual lipids from leaves of modern angiosperms: implications for the study of higher land plant-derived sedimentary organic matter, *Org.Geochem.*, 26, 137-153, 1997.

Menendez, C., Z. Bauer, H. Huber, N. Gad'on, K. O. Stetter, and G. Fuchs, Presence of acetyl coenzyme A (CoA) carboxylase and propionyl-CoA carboxylase in autotrophic *Crenarchaeota* and indication for operation of a 3-hydroxypropionate cycle in autotrophic carbon fixation, *J.Bacteriol.*, 181, 1088-1098, 1999.

Meyers, P. A., Preservation of elemental and isotopic source identification of sedimentary organic matter, *Chemical Geology*, 114, 289-302, 1994.

Murray, A. E., A. Blakis, R. Massana, S. Strawzewski, U. Passow, A. Alldredge, and E. F. DeLong, A time series assessment of planktonic archaeal variability in the Santa Barbara Channel, *Aquat.Microb.Ecol.*, 20, 129-145, 1999.

Ourisson, G. and P. Albrecht, Hopanoids. 1. Geohopanoids: the mosty abundant natural products on earth?, *Acc.Chem.Res.*, 25, 398-402, 1992.

Ouverney, C. C. and J. A. Fuhrman, Marine planktonic archaea take up amino acids, *Appl.Environ.Microbiol.*, 66, 4829-4833, 2000.

Pancost, R. D., K. H. Freeman, S. G. Wakeham, and C. Y. Robertson, Controls on carbon isotope fractionation by diatoms in the Peru upwelling region, *Geochim.Cosmochim.Acta*, 61, 4983-4991, 1997.

Pancost, R. D., J. S. Sinninghe Damsté, S. De Lint, M. J. E. C. Van der Maarel, J. C. Gottschal, and the Medinaut Shipboard Scientific Party, Biomarker evidence for widespread anaerobic methane oxidation in Mediterranean sediments by a consortium of methanogenic Archaea and Bacteria, *Appl.Environ.Microbiol.*, 66, 1126-1132, 2000.

Pearson, A., Biogeochemical applications of compound-specific radiocarbon analysis, Thesis, Woods Hole Oceanographic Institution, 2000.

Pennock, J. R., D. J. Velinsky, J. D. Ludlam, J. H. Sharp, and M. L. Fogel, Isotopic fractionation of ammonium and nitrate during uptake by *Skeletonema costatum*: implications for δ^{15}N dynamics under bloom conditions, *Limnology and Oceanography*, 41, 451-459, 1996.

Popp, B. N., E. A. Laws, R. R. Bridigare, J. E. Dore, K. L. Hanson, and S. G. Wakeham, Effect of phytoplankton cell geometry on carbon isotopic fractionation, *Geochim.Cosmochim.Acta*, 62, 69-77, 1998.

Poulsen, C. J., The mid-Cretaceous ocean circulation and its impact on Greenhouse Climate dynamics, Thesis, Pennsylvania State University, 1999.

Prahl, F. G., J. T. Bennett, and R. Carpenter, The early diagenesis of aliphatic hydrocarbons and organic matter in sedimentary particulates from Dabob Bay, Washington, *Geochim.Cosmochim.Acta*, 44, 1967-1976, 1980.

Rau, G. H., T. Takahashi, and D. J. Des Marais, Latitudinal variations in plankton δ^{13}C: implications for CO_2 and productivity in past oceans, *Nature*, 341, 516-518, 1989.

Repeta, D. J., D. J. Simpson, B. B. Jorgensen, and H. W. Jannasch, Evidence for anoxygenic photosynthesis from the distribution of bacterio-chlorophylls in the Black Sea, *Nature*, 342, 69-72, 1989.

Rohmer, M., P. Bisseret, and S. Neunlist., The hopanoids, prokaryotic triterpenoids and precursors of ubiquitous molecular fossils, in *Biological markers in sediments and petroleum*, edited by J. M. Moldowan, P. Albrecht, and R. P. Philp, pp. 1-17, Prentice Hall, New Jersey, 1992.

Schlanger , S. O. and H. C. Jenkyns, Cretaceous oceanoc anoxic events: causes and consequences, *Geologie en mijnbouw*, 55, 179-184, 1976.

Schouten, S., M. J. L. Hoefs, M. P. Koopmans, H. J. Bosch, and J. S. Sinninghe Damsté, Structural characterization, occurrence and fate of archaeal etherbound acyclic and cyclic biphytanes and corresponding diols in sediments, *Org.Geochem.*, 29, 1305-1319, 1998.

Schouten, S., E. C. Hopmans, R. D. Pancost, and J. S. Sinninghe Damste, Widespread occurrence of structurally diverse tetraether membrane lipids: Evidence for the ubiquitous presence of low-temperature relatives of hyperthermophiles, *Proc.Natl.Acad.Sci.USA*, 97, 14421-14426, 2000.

Seifert, W. K. and J. M. Moldowan, Use of biological markers in petroleum exploration, in *Methods in geochemistry and geophysics Vol. 24* , edited by R. B. Johns, pp. 261-290, Elsevier Science Publishers, Amsterdam, 1986.

Shipboard Scientific Party, Site 1049, *Proc.ODP, Init.Rep.*, 171B, 47-92, 1998.

Sinninghe Damsté, J. S., T. I. Eglinton, and J. W. De Leeuw, Characterisation of sulfur-rich high molecular weight substances by flash pyrolysis and Raney Ni desulfurisation, *ACS Symposium Series*, 429, 486-528, 1990.

Sinninghe Damsté, J. S., T. I. Eglinton, J. W. De Leeuw, and P. A. Schenck, Organic sulphur in macromolecular sedimentary organic matter: I. Structure and origin of sulphur-containing moieties in kerogen, asphalthenes and coal as revealed by flash pyrolysis, *Geochim.Cosmochim.Acta*, 53, 873-889, 1989.

Sinninghe Damsté, J. S., M. J. L. Hoefs, W. I. C. Rijpstra, E. Schefuss, G. J. de Lange, and J. W. De Leeuw, Bias of the sedimentary biomarker record through oxic degradation at different rates, *18th International meeting on organic geochemistry*, Part I, 33-34, 1997a.

Sinninghe Damsté, J. S., E. C. Hopmans, R. D. Pancost, S. Schouten, and J. A. J. Geenevasen, Newly discovered non-isoprenoid dialkyl diglycerol tetraether lipids in sediments, *J.Chem.Soc., Chem.Comm.*, 1683-1684, 2000.

Sinninghe Damsté, J. S., M. D. Kok, J. Köster, and S. Schouten, Sulfurized carbohydrates: an important sedimentary sink for organic carbon?, *Earth and Planetary Science Letters*, 164, 7-13, 1998.

Sinninghe Damsté, J. S., S. Schouten, H. v. Vliet, H. Huber, and J. A. J. Geenevasen, A polyunsaturated irregular acyclic C_{25} isoprenoid in a methanogenic archaeon, *Tetrahedron Letters*, 38, 6881-6884, 1997b.

Sinninghe Damsté, J. S., S. G. Wakeham, M. E. L. Kohnen, J. M. Hayes, and J. W. De Leeuw, A 6,000-year sedimentary molecular record of chemocline excursions in the Black Sea, *Nature*, 362, 827-829, 1993.

Spooner, N., G. Rieley, J. W. Collister, M. Lander, P. Cranwell, and J. R. Maxwell, Stable carbon isotopic correlation of individual biolipids in aquatic organisms and a lake bottom sediment, *Org.Geochem.*, 21, 823-827, 1994.

Stetter, K. O., Hyperthermophiles: isolation, classification and properties, in *Extremophiles: microbial life in extreme environments*, edited by K. Horikoshi and W. D. Grant, pp. 1-24, Wiley-Liss, Inc., New York, 1998.

Summerhayes, C. P., Organic-rich Cretaceous sediments from the North Atlantic, *Geological Society Special Publication*, 26, 301-316, 1987.

Summons, R. E., L. L. Jahnke, J. M. Hope, and G. A. Logan, 2-Methylhopanoids as biomarkers for cyanobacterial oxygenic photosynthesis, *Nature*, 400, 554-557, 1999.

Summons, R. E., L. L. Jahnke, and Z. Roksandic, Carbon isotopic fractionation in lipids from methanotrophic bacteria: Relevance for interpretation of the geochemical record of biomarkers, *Geochim.Cosmochim.Acta*, 58, 2853-2863, 1994.

Tribovillard, N. P. and G. E. Gorin, Organic facies of the Early Albian Niveau Paquier, a key black shales horizon of the Marnes Bleues Formation in the Vocontian Trough (Subalpine Ranges, SE France), *Pal.Geo, Pal.Clim, Pal.Ecol.*, 85, 227-237, 1991.

van der Meer, M. T. J., Schouten, S., Rijpstra, W. I. C., Fuchs, G., and Sinninghe Damsté, J. S. Stable carbon isotope fractionations of the hyperthermophilic crenarchaeon *Metallosphaera sedula*. FEMS Microbiology Letters . 2001.
Ref Type: In Press

van Gemerden, H. and J. Mas, Ecology of phototrophic sulfur bacteria, in *Anoxygenic photosynthetic bacteria*, edited by R. E. Blankenship, M. T. Madigan, and C. E. Bauer, pp. 49-85, Kluwer Academic Publishers, Dordrecht, 1995.

Vink, A., S. Schouten, S. Sephton, and J. S. Sinninghe Damsté, A newly discovered norisoprenoid, 2,6,15,19-tetramethylicosane, in Cretaceous black shales, *Geochim.Cosmochim.Acta*, 62, 965-970, 1998.

Volkman, J. K., A review of sterol markers for marine and terrigenous organic matter, *Org.Geochem.*, 9, 83-99, 1986.

Werne, J. P., D. J. Hollander, A. Behrens, P. Schaeffer, P. Albrecht , and J. S. Sinninghe Damste, Timing of early diagenetic sulfurization of organic matter: A precursor-product relationship in Holocene sediments of the anoxic Cariaco Basin, Venezuela, *Geochim.Cosmochim.Acta*, 64, 1741-1751, 2000.

Appendix. Structures of compounds.

I

a

II

b

III

c

IV

d

V

VI   R = H
VII R = CH$_2$
VIII R = C$_2$H$_5$

XI   X = **a** and Y = **a**
XII X = **a** and Y = **b**
XIII X = **b** and Y = **b**
XIV X = **c** and Y = **d**

or

XVI

IX R = H
X R = C$_2$H$_5$

XV

XVII

XVIII

XIX

XX

XXI

XXII

XXIII

XXIV

XXV

XXVI

XXVII

XXVIII

XXIX

XXX

XXXI

XXXII

XXXIII

Tussen 130 en 90 miljoen jaar geleden, tijdens het Krijt, was de aarde veel warmer dan zij vandaag de dag is. Deze periode is dan ook niet voor niets bekend als de 'broeikas wereld'. Dit warme klimaat met veel kleinere temperatuursverschillen tussen de evenaar en de polen dan nu was waarschijnlijk het gevolg van de vulkanische uitstoot van enorme hoeveelheden van het broeikasgas kooldioxide (CO_2).

Tijdens een aantal geologisch gezien korte periodes (elk duurde slechts enkele honderdduizenden jaren) zou echter het gehalte aan broeikasgas tijdelijk kunnen zijn afgenomen als gevolg van de begraving van grote massa's aan organische koolstof in de zeebodem. Zo'n 'begravings' episode vond plaats circa 90 miljoen jaar geleden, tijdens een periode van het Krijt die het Cenomaan-Turoon word genoemd. Uit geochemisch onderzoek van chemische fossielen van landplanten blijkt dat er tijdens deze periode een drastische verandering in de Noord-Afrikaanse plantengemeenschappen heeft plaatsgevonden (hoofdstuk 2). In ongeveer 30.000 jaar verdrongen planten, die op een actieve manier de hoeveelheid CO_2 in hun bladeren kunnen verhogen (zgn. C_4-planten), de tot dan toe dominante, maar primitievere planten. Bij deze planten is het de passieve diffusiesnelheid die de hoeveelheid CO_2 in het blad bepaalt. Een dergelijke verandering is hoogst opmerkelijk omdat een actieve, energiekostende manier om CO_2 vast te leggen niet past in het broeikasklimaat van het Krijt. In het Krijt milieu met haar hogere atmosferische kooldioxideconcentraties zijn immers de 'actieve' C_4-planten in het nadeel. Wij concluderen dan ook dat de verandering in het Noord-Afrikaanse ecosysteem alleen is te verklaren door een forse (40-80 procent), geologisch gesproken abrupte (in zo'n 60.000 jaar) afname van het broeikasgas.

De oorzaak voor de periodieke begraving van grote hoeveelheden organisch koolstof in de oceaan is nog onduidelijk, maar volgens sommige onderzoekers zijn er aanwijzingen dat veranderingen in oceaanstromingen geleid hebben tot zuurstofloze omstandigheden in bepaalde delen van de zee, waardoor afgestorven algenmateriaal niet werd afgebroken, maar in de bodem begraven werd. Andere onderzoekers denken dat de massale bloei van algen tot de begraving van grote hoeveelheden algenmateriaal heeft geleid onder andere doordat zoveel zuurstof tijdens de bloei aan het oceaanwater onttrokken werd dat minder algenmateriaal kon worden afgebroken. De aanwezigheid van chemische fossielen van fotosynthetische bacteriën die groeien onder zuurstofloze omstandigheden en sporenelementen die aangerijkt worden in het sediment onder dergelijke omstandigheden duiden erop dat ten minste het zuidelijk deel van de Noord Atlantische Oceaan al zuurstofloos was vóór de eigenlijke koolstof-'begravings' episode tijdens het Cenomaan-Turoon (hoofdstuk 3). Dit duidt erop dat vermoedelijk een algenbloei tot de verhoogde begraving van algenmateriaal heeft geleid. De onderzochte zeesedimenten uit het Krijt bevatten hiervoor ook directe chemische bewijzen.

Bewijzen voor een algenbloei als oorzaak voor de begraving van grote massa's aan organisch koolstof komen ook van sedimenten uit het Cenomaan-Turoon van het noordelijke deel van de Noord Atlantische Oceaan (hoofdstuk 4). In dit deel van de Noord Atlantische Oceaan was er echter ook in een tijdsbestek van enkele tienduizenden jaren een sterke fluctuatie in de hoeveelheid organisch koolstof die begraven werd. Dit is waarschijnlijk een gevolg van veranderingen in het klimaat van het Krijt. Deze klimaatsschommelingen vonden plaats in

regelmatige periodes van zo'n 20.000 jaar en waren het gevolg van veranderingen in de hoeveelheid zonnestraling die de aarde bereikte door fluctuaties in de baan die de aarde om de zon maakt.

De oorzaak van de algenbloei is nog niet duidelijk. Vast staat echter dat grote hoeveelheden extra voedingsstoffen nodig zijn voor de massale bloei van algen. Twee van de belangrijkste voedingsstoffen voor algen zijn stikstof en fosfor. In hoofdstuk 5 onderzoeken we de rol van bepaalde blauwgroene algen, die in tegenstelling tot andere algen, uit de atmosfeer stikstof kunnen opnemen en dus alleen afhankelijk zijn van de beschikbaarheid van fosfor in de Noord Atlantische Oceaan tijdens het Cenomaan-Turoon. Het blijkt dat deze blauwgroene algen een belangrijk onderdeel waren van de algengemeenschappen en niet alleen organisch koolstof aan het sediment hebben bijgedragen, maar destijds ook extra stikstof aan het zeewater hebben toegevoegd voor de groei van andere algen. Tijdens de 'begravings' episode in het Cenomaan-Turoon zou het omhoogbrengen van fosforrijk water uit de diepere delen van de Noord Atlantische Oceaan, als gevolg van veranderende oceaanstromingen, tot de massale bloei van blauwgroene algen hebben kunnen geleid. Tevens zou dit ook tot de bloei van andere algen, die de extra stikstof konden benutten, kunnen verklaren. De veranderende oceaanstromingen zouden een gevolg kunnen zijn geweest van de vorming van een diepe zeeverbinding tussen de Noord en Zuid Atlantische Oceaan, als gevolg van het uit elkaar drijven van Afrika en Zuid-Amerika.

In hoofdstukken 6 en 7 hebben we de bron voor het organische materiaal van een organische koolstof-begravings episode, circa 110 miljoen jaar geleden, chemisch en microscopisch onderzocht. Hieruit bleek dat niet algen of landplanten de belangrijkste bron van het organisch materiaal zijn, maar archaea die, naast de bacteriën en de organismen met celkern, de derde grote belangrijke onderverdeling van het leven representeren. Dit toont aan dat de organismen die betrokken waren bij de 'begravings' episodes circa 110 en 90 miljoen jaar geleden, totaal verschilden, ondanks het feit dat in vele andere aspecten deze episodes grote overeenkomsten vertonen.

Marcel Kuijpers werd op 6 juni 1970 geboren in Hunsel. Na de MAVO en HAVO doorlopen te hebben volgde hij een opleiding organische chemie aan het HLO te Sittard waar hij, na stage te hebben gelopen bij Andeno B.V. te Venlo-Blerick, zijn diploma behaalde in 1992. Vervolgens studeerde hij organische chemie aan de Katholieke Universiteit Nijmegen. Deze studie werd in 1995 afgerond. Na driekwart jaar vrijwilligers werk aan het Natuurhistorisch Museum Maastricht en een zeer kortstondig verblijf in militaire dienst is hij in 1996 in dienst getreden van NWO als onderzoeker-in-opleiding aan het Nederlands Instituut voor het Onderzoek der Zee bij de afdeling Mariene Biogeochemie en Toxicologie. Aansluitend op dit promotieonderzoek is hij als Postdoc gestart bij de afdeling Biogeochemie van het Max-Planck-Institut für Marine Mikrobiologie te Bremen.